eman ta zabal zazu

Universidad del País Vasco

Euskal Herriko Unibertsitatea

FILMS AND BIOCOMPOSITES BASED ON AGRO-INDUSTRIAL WASTES AND BY-PRODUCTS

Tania Garrido Díaz

Department of Chemical and Environmental Engineering

Donostia-San Sebastián, 2019

eman ta zabal zazu

Universidad del País Vasco

Euskal Herriko Unibertsitatea

Films and biocomposites based on agro-industrial wastes and by-products

Tania Garrido Díaz

Supervisors:

Koro de la Caba & Pedro Guerrero

Department of Chemical and Environmental Engineering

Donostia-San Sebastián, 2019

Zuri,

ESKERRAK

AGRADECIMIENTOS

ACKNOWLEDGEMENT

Cuando comienzas a escribir estas líneas te das cuenta de que esta etapa, que ha formado parte de tu vida durante estos últimos años, está llegando a su fin, y que durante este camino de más luces que sombras, han pasado muchas personas que han puesto su granito de arena para hacer que todo sea un poquito más fácil.

Para empezar, quería agradecer a mis directores, Koro de la Caba y Pedro Guerrero, por toda la ayuda que me han brindado durante todo este tiempo. Con ellos he aprendido que si a la tercera no va la vencida no hay que tirar la toalla y que si quieres algo es solo cuestión de confiar en ti mismo y en lo que haces.

I wish to thank Paul Kilmartin and Marija Gizdavic-Nikolaidis for their warm welcome in the University of New Zealand. It was a pleasure to shear such a great experience with them and with all my college that introduce me in the interesting world of the winemaking. It was an intense three months experience

in the other part of the world that has boosted my self-confident and independence.

Bestalde, nirekin elkarren ondoan lan egin duten pertsonei eskerrak eman nahi dizkiet. Lankideak baino gehiago lagunak izan direlako, eta lan gogorra egiteaz gain, momentu oso dibertigarriak ere pasatu ditugulako.

No puedo olvidar tampoco a mis amiguis, y por supuesto a mi gran familia, que, aunque no me han podido ayudar en el aspecto más técnico, han hecho algo mucho más importante, estar ahí. Porque su paciencia y comprensión han sido infinitos y porque gracias a sus consejos y sus pequeños empujoncitos hoy puedo estar escribiendo estas lineas dándoles las gracias.

Badago ere espero ez duzunean epeltasuna ematen duen jendea. Udaberriko lehen eguzkia eskertzen duzun bezala eskertzen duzu zure bizitzan agertu izana. Horiei ere, eskerrik asko.

Amaitzeko, Euskara Errektoreordetzari, Biomat ikerketa taldeari eta Gipuzkoako Foru Aldundiari eskerrak eman nahi dizkiet emandako diru-laguntzengatik. Baita UPV/EHU-ko Ikerkuntzarako Zerbitzu Orokorrari (SGIker) ere.

Because nobody said it was easy...eskerrik asko denoi!!

“and suddenly you just know…

…it´s time to start something new and trust the magic of beginnings” ~M.E.~

SUMMARY

The research for new applications and alternative sources of biopolymers has experienced a boom in the last years, mostly due to the growing interest in the valorisation of agro-industrial wastes and by-products as well as their environmentally friendly management. In fact, every year huge amounts of agricultural residues are produced, but the vast majority of them are underutilization. In this context, soy protein is a by-product obtained from soy oil production, which can be purified to obtain soy protein isolate. This protein has been widely used as an alternative to petroleum-derived polymers due to its attractive properties, such as renewability, abundance and biodegradability. Therefore, the combination of soy protein with other compounds that overcome its drawbacks can open new opportunities to employ this material in food and biomedical applications in order to reduce the amount of non-renewable and non-biodegradable materials.

Taking the above into consideration, the objective of this doctoral thesis was to develop soy protein-based films and biocomposites with improved properties, incorporating other biopolymers obtained from different biowastes and employing different processing methods. Thus, this thesis is divided into 11 chapters. **Chapter 1** provides an overview of the current development of films and coatings based on vegetal proteins, giving special emphasis to soy protein-based films. Furthermore, the improvements carry out mainly in protein-based packaging in terms of active materials are intended to be highlighted. **Chapter 2** describes the materials employed in this work, including the extraction methods used to recover valuable products from waste, such as proteins and polysaccharides, as well as the equipment and methods employed to characterize the developed products. In **Chapter 3**, the effect of pH, plasticizer and

processing method is analysed, and also the environmental impact caused by soy protein-based films. Once optimized processing conditions, in **Chapter 4** functional properties and the environmental impact of the films were analysed based on the processing method employed.

In the following chapters, the valorisation of different agro-industrial wastes was carried out in order to improve functional properties of the developed films. In **Chapter 5**, an environmentally friendly and inexpensive method was addressed to obtain hydrolysed keratin from chicken feathers, which can be used to improve the chemical and thermal stability of the films processed by solution casting and compression moulding. After that, in **Chapter 6**, agar extracted from red algae was employed to obtain films based on soy protein and processed by extrusion followed by compression moulding. The waste obtained in the extraction of the agar was used as a filler in **Chapter 7** to manufacture biocomposites by the techniques employed in the plastics industry; soy protein pellets were obtained by extrusion and biocomposites by injection moulding. Afterwards, in **Chapter 8**, β-chitin was extracted from squid pen, a waste from fishery industry, by a simple alkaline hydrolysis. Chitin was employed to reinforce soy protein films in order to obtain a multifunctional material with enhanced physicochemical and mechanical properties, employing compression moulding as processing method to produce chitin-reinforced soy protein films. Besides enhancing functional properties, the improvement of the antioxidant activity of films can increase the variety of applications of the products developed; thus, in **Chapter 9**, grape marc, a waste from the winery industry, was employed to extract polyphenols using microwave-assisted extraction.

Finally, **Chapter 10** summarised the general conclusions extracted from the previous chapters and **Chapter 11** lists the references cited along this thesis work.

OBJECTIVES

The main objective of this doctoral thesis was to develop soy protein-based films and biocomposites with improved properties, incorporating other biopolymers obtained from agro-industrial wastes and employing different processing methods.

The specific objectives can be summarised as follows:

- Analyse the functional properties of soy protein based-materials, in terms of mechanical, barrier, morphological, optical, physicochemical and thermal properties.
- Optimise the pH used and the plasticizer type and content.
- Study the effect of the processing method employed.
- Assess the environmental impact of soy protein-based materials from cradle to grave.
- Valorise different biowastes derived from agro-food, fishery, poultry and wine industries in order to extract proteins, polysaccharides and polyphenols to incorporate them into soy protein-based formulations, enhancing the functional properties of the products developed.

INDEX

1

chapter

INTRODUCTION

Garrido T., Uranga J., Guerrero P., de la Caba K. (2018)

The potential of vegetal and animal proteins to develop more sustainable food packaging. In: Gutiérrez T. (ed.), Polymers for Food Applications. Springer, Cham, 25-59

Etxabide A., Garrido T., Uranga J., Guerrero P., de la Caba K. (2018)

Extraction and incorporation of bioactives into protein formulations for food and biomedical applications. International Journal of Biological Macromolecules, 120, 2094-2105

SUMMARY

Biopolymers are attracting immense attention since they can address growing environmental concerns and consumers' desire for nontoxic and safe products in various applications (Niaounakis, 2015). In this context, interest in natural and active food packaging has been growing in recent years due to consumers' demand for higher quality and safe foods with extended shelf lives along with the desire for natural and biodegradable materials instead of synthetic materials (Cerqueira et al., 2016). In the same way, biodegradable materials have been widely investigated in order to address biomedical applications such as scaffolds for tissue engineering. Unlike most of non-degradable permanent implants used with the aim of replacing the damaged tissue, the biodegradability of biopolymer-based scaffolds allows a more effective regeneration of damaged tissues (Balakrishnan et al., 2018). Therefore, the use of biodegradable and renewable materials to replace petroleum-derived materials has increased the interest of the global market for novel food packaging and biomaterials.

Food packaging technology is a research field that has shown a fast growing in recent years. In fact, a high amount of studies is focused on the improvement of food safety and quality and the preservation and extension of the product shelf life (Ma et al. 2017; Pinheiro et al., 2016; Sousa-Gallagher et al., 2016). The largest part of the materials employed for food packaging finds their origin in the petrochemical industry, which causes serious environmental problems due to non-biodegradability and non-renewability; thus, research efforts are being driven to develop alternative materials derived from bio-resources (Wang et al., 2017a). In that way, unlikeable circumstances, such as hazardous microorganisms (including bacteria and fungi), external physical

forces, chemical compounds, sunlight, permeable volatile compounds, oxygen and moisture, have to be controlled by the use of renewable and biodegradable packaging (Garavand et al., 2017).

Protein films and coatings could be an alternative to synthetic packaging since they can provide a range of barrier attributes that can benefit the packaged food, improving its aroma, taste, texture and stability. Thus, they play an important role in food preservation, as well as in food distribution and marketing (Falguera et al., 2011). Films can be defined as performed thin layers, which can be placed surrounding the food product, between food components, or even sealed into edible pouches; whereas a coating is directly formed onto food surface by dipping, spraying, brushing or panning (Junqueira-Gonçalves et al., 2017; Otoni et al., 2017). Proteins have been considered promising alternatives to develop food packaging films and coatings since they are edible, food compatible, renewable and able to increase the nutritional value of the coated product. Moreover, proteins are generally superior to polysaccharides in their ability to form three-dimensional macromolecular networks, stabilised and strengthened by hydrogen bonds, hydrophobic interactions and disulphide bonds, which contribute to enhance mechanical and barrier properties (Gupta and Nayak, 2015). Apart from providing external protection to food, films and coatings can act as effective carriers of many types of compounds, including antimicrobial and antioxidant additives. The incorporation of antimicrobial agents into films can help to prevent or delay the growth of foodborne pathogens and thus, food spoilage (Aloui and Khwaldia, 2016), while the incorporation of antioxidants can inhibit or retard the oxidation of food, thus, extending food shelf life and improving food safety and quality (Álvarez et al., 2017). Other additives can also be incorporated into films with the purpose of enhancing their functional properties, as well as the organoleptic properties of the packaged product.

Some examples of these additives could be anti-browning agents, nutraceuticals, texture enhancers, flavour and colour ingredients, or even other protein and polysaccharides (Olivas et al., 2007).

Regarding antioxidants, synthetic ones have been traditionally employed in packaging applications. However, these additives are increasingly more challenged due to their potential health risk, resulting from their migration into food products, as well as to the strict statutory controls currently existing in so many countries (Gómez-Estaca et al., 2014). Fortunately, the use of natural antioxidants, such as tocopherol (Córdoba and Sobral, 2017), plants extracts (Saberi et al., 2017) and essential oils (EOs) (Atarés and Chiralt, 2016), among others, is being studied. In fact, obtaining bioactive compounds from vegetal sources, especially from inexpensive waste products from food, forest or agricultural industries, is taking importance in order to add value to an unavoidable amount of waste that grows day-by-day. High amounts of wastes are released during industrial manufacturing of apple, blueberry, olive, raspberry, grape or citrus fruits, among many others. Hence, valuable compounds from wastes, such as anthocyanins, phenolic acids and flavonoids, could be successfully recovered and employed to develop active and intelligent packaging (Socaci et al., 2017). For instance, Luchese et al. (2018) employed blueberry pomace obtained from blueberry juice processing wastes, rich in phenolic compounds such as anthocyanins, to prepare films with the ability to change colour when subjected to different pH values, which could be correlated with the pH changes in some food products. Prietto et al. (2017) and Ma and Wang (2016) also used this antioxidant extracted from other sources, such as black bean seeds, red cabbage leaves and grape skins. Olejar et al. (2017), studied the antioxidant activity of grape tannins extracted from an agro-waste stream from the wine industry and de Moraes Crizel et al. (2018) obtained flour and

microparticles, considered suitable to provide antioxidant activity, from olive pomace generated during olive oil manufacturing.

Concerning antimicrobials, the incorporation of natural antimicrobial agents into films has been also widely studied. EOs, chitosan, extracts of herbs, plants and species have been employed to control the microbial growth into the packaged product (Etxabide et al., 2017, Irkin and Esmer, 2015). Arfat et al. (2014) studied the antimicrobial impact of basil leaf EO and ZnO nanoparticles into fish protein isolate and fish skin gelatin blend. The addition of basil leaf EO, especially in combination with ZnO nanoparticles, exhibited strong antibacterial activity against the evaluated foodborne pathogenic and spoilage bacteria. Other authors have analysed the efficacy of natural antimicrobial agents directly into food; Alparslan and Baygar (2017) studied the antimicrobial effect of chitosan combined with orange peel EO on the shelf life of deepwater pink shrimp, and Kakaei and Shahbazi (2016) analysed the incorporation of ethanolic red grape seed extract and *Ziziphora clinopodioides* EO on fish fillets.

Apart from food packaging applications, bioactive compounds have been also used for biomedical applications in order to design a sustained release of these molecules from the implantable/administered biomaterials and provide a faster and more comfortable recovery of the patients (Ruiz-Ruiz et al., 2017). For instance, Raja and Fathima (2015), synthesised gelatin based formulations with antioxidant properties, through conjugation and physical crosslinking of small antioxidant molecules, as effective drug delivery agent to fight against oxidative stress in blood stream. Patel et al. (2018) prepared lupeol loaded hydrogel films from the blended mixture of chitosan and gelatin, using glutaraldehyde as crosslinker, and concluded that chitosan/gelatin

hydrogel films can be ideal delivery systems for sustained released of lupeol and for enhanced wound healing.

Up to now, a variety of bioactives and other kind of compounds has been successfully incorporated into protein-based films since they are suitable for controlled release of different additives, and can easily create new interactions between the components. Therefore, many research works have been conducted in order to develop films and coatings from various proteins sources, including collagen (Wang et al., 2017b), gelatin (Molinaro et al., 2015), soy (Galus et al., 2012), whey (Cecchini et al., 2017), zein (Pena-Serna et al., 2016), pea (Kowalczyk et al., 2016) or wheat gluten (Sharma et al., 2017), among others. Especially, soy protein has received much attention since it is widely available at a relative low-cost, meets food grade standards and has interesting characteristics such as film forming ability and biodegradability. Moreover, the use of proteins to develop films and coatings not only satisfies the needs of consumers, but also helps to add value to industrial by-products and waste materials from agricultural, meat, poultry and fish processing industries.

Taking the above-mentioned into consideration, the aim of this chapter is to provide an overview of the current development of films and coatings based on vegetal proteins, giving special emphasis to soy protein-based films. Furthermore, the improvements carried out mainly in protein-based packaging in terms of active materials are intended to be highlighted.

1.1 PROTEIN STRUCTURE AND PROPERTIES

A proper study of protein structure, folding and interactions is essential to understand their characteristic properties and functions. Proteins can be defined as biological macromolecules consisting of a linear chain of amino acids that fold into three-dimensional structures composed of different secondary structure elements (Yan et al., 2014); thus, α-amino acids are the basic structural units of proteins. Natural proteins contain up to 20 different primary amino acids, which are linked together by amide bonds. These amino acids are composed of an α-carbon atom covalently attached to a hydrogen atom, an amino group, a carboxyl group and a side chain group. This side chain group is characteristic from each amino acid and have a direct relationship in the solubility, net charge, chemical reactivity and hydrogen bonding potential of the protein (Damodaran, 2007). Each amino acid possesses a range of chemical properties, which collectively endows each protein molecule with a unique set of physicochemical characteristics. Amino acids can be classified according to the chemical properties of their side chain, which provides specific characteristics to each amino acid. In particular, the polarity of the amino acid side chain, can determine the ability the amino acid has to interact with other entities. For instance, polar amino acids are able to interact with other polar amino acids and even with water molecules surrounding the protein, improving its solubility. Moreover, these interactions have an important role in the protein folding (Kessel and Ben-Tal, 2010).

Proteins possess different amino acid compositions, depending on protein source or origin, which influences their interactions with other compounds and their functional properties. As can be seen in **Table 1.1**, fish gelatin contains mostly glycine (31-37%), proline-hydroxiproline (14-20%) and alanine (10-12%); while bovine gelatin contains

higher amounts of proline-hydroxiproline (22%) and alanine (12%). It is worth noting that hydroxyproline is a non-essential amino acid, present mainly in collagen but rarely in other proteins, which is produced by hydroxylation of proline. For most gelatins derived from type I collagen, cysteine and tryptophan are absent, and the content of tyrosine residues is below 1% (Gómez-Guillén et al., 2009; Lassoued et al., 2014).

Table 1.1. Amino acid concentration of some animal and vegetal proteins.

Amino acids	**Composition (%)**				
	Fish gelatin	**Bovine gelatin**	**Soy protein**	**Zein**	**Wheat gluten**
Aspartic acid[a]	5.2	4.4	11.6	4.6	2.8
Threonine	2.5	1.7	3.6	3.5	2.8
Serine	6.4	2.9	5.2	7.05	5.7
Glutamic acid[b]	7.8	7.5	19.8	26.9	31.9
Proline	15.6 [c]	21.9[c]	5.6	10.5	14.1
Glycine	34.4	34.5	4.1	-	5.4
Alanine	9.6	11.6	4.1	10.5	3.5
Cysteine	-	-	1.2	0.8	2.2
Valine	1.8	2.1	4.7	4.0	5.4
Methionine	1.7	0.5	1.3	2.4	1.3
Isoleucine	1.1	1.1	4.8	5.0	4.1
Leucine	2.2	2.5	7.7	21.1	7.2
Tyrosine	0.3	0.1	3.7	5.3	2.8
Phenylalanine	1.6	1.2	5.2	7.3	4.4
Histidine	0.8	0.5	2.6	1.3	1.7
Lysine	2.9	2.6	6.0	-	1.4
Arginine	5.6	4.8	7.6	4.7	3.2
Tryptophan	-	-	1.3	-	-

[a]Value for aspartic acid and asparagine
[b]Value for glutamic acid and glutamine
[c]Value for proline and hydroxyproline

Regarding vegetal proteins, they have a higher amount of cysteine, which helps to promote the formation of disulphide bonds (Garrido et al., 2018). Soy protein contains mainly glutamic acid (20%) and aspartic acid (12%), as well as leucine (8%) and arginine (8%) (Kalman, 2014). Zein is particularly rich in glutamic acid (27%), leucine (21%), proline (10%) and alanine (10%), but deficient in glycine, cysteine, lysine and tryptophan and this high proportion of nonpolar amino acid residues is responsible for the limited solubility of zein, mainly restricted to aqueous alcohols

(Shukla and Cheryan, 2001). With regard to wheat gluten, glutamic acid (32%) and proline (14%) are the main amino acid residues (Rombouts et al., 2009).

Protein structure is stabilized through hydrogen bonding and hydrophobic and electrostatic interactions among the functional groups of amino acid residues in four protein levels (Verbeek and van den Berg, 2010), as shown in **Figure 1.1**. The primary structure refers to the sequence of amino acids linked by the α-carboxyl group of one amino acid to the α-amino group of another one through a peptide bond. The chain size, as along with the amino acid order, defines the physical, chemical, structural, biological and functional properties of the protein. The next level, the secondary structure, is conformed of regular arrangements of the backbone of the polypeptide chain. They can be found mainly in two secondary structures, α-helix and β-sheets, but also in unordered random coil structures. The folding of the secondary structure segments into a compact three-dimensional form results in the tertiary structure. The formation of this structure assumes the optimization of hydrophobic, electrostatic and Van der Waals interactions, and hydrogen bonds between the different available groups of the protein (Rodrigues et al., 2012). Finally, the disposition of more than one peptide chain constitutes the forth level of organization. The protein structure is especially important for film formation since it determines the ability of proteins to interact with themselves and other components.

Protein structure can be modified by physical (heating, shearing, hydrostatic pressure or irradiation), chemical (alkylation, acylation, acetylation or pH alteration) and biochemical methods (enzymes), which result in a structural or conformational change of the native structure, without altering the amino acid sequence (Zink et al., 2016). These structure modifications can improve functional properties of the proteins

in order to adapt them to a specific final application. These modifications induce the protein denaturation, promoting protein unfolding and the exposure of functional groups followed by new chain associations through intermolecular interactions (Cordeiro de Azeredo, 2012; Schmid et al., 2014).

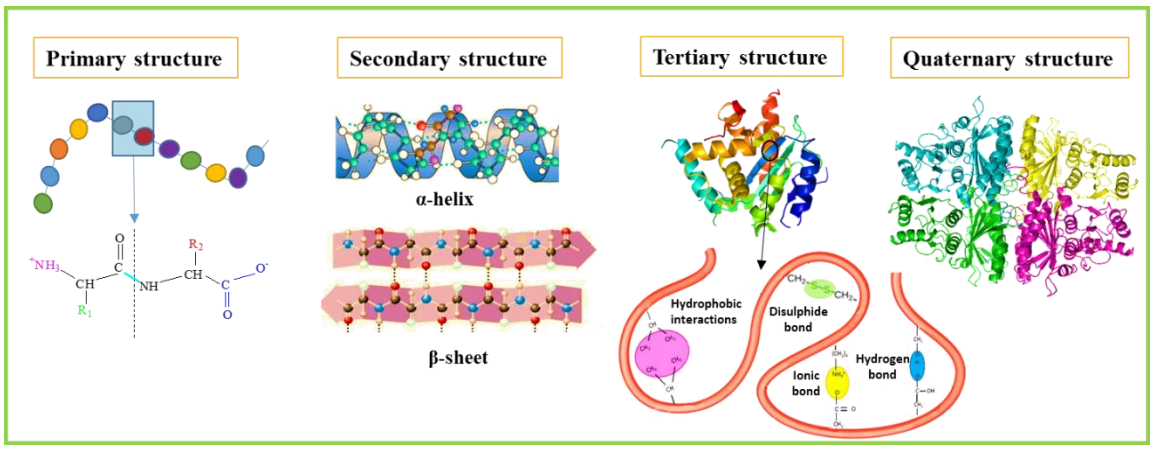

Figure 1.1. The four protein structures: primary, secondary, tertiary and quaternary structures.

pH value is a factor that determines protein structure and therefore, the functional properties of proteins. Intermolecular interactions, such as hydrogen bonds, hydrophobic interactions and disulphide bonds, are especially influenced by a pH shift. Proteins exhibit a net negative charge at a pH higher than their isoelectric point (IP) and a net positive charge at a pH lower than their IP. Thus, when pH is adjusted away from the IP, electrostatic repulsion between protein molecules occurs, increasing protein solubility. In turn, at the IP, protein molecules have no net charge, which results in protein aggregation and precipitation (Wihodo and Moraru, 2013).

In order to change protein-protein interactions, crosslinking have been explored as a viable method to improve the mechanical strength and barrier properties of protein films. In this context, chemicals like aldehydes are used to interact with the functional groups of proteins, such as the amino function in lysine and hydroxylysine or the

carboxyl group in aspartic and glutamic acids (Etxabide et al., 2015). However, aldehydes can be toxic, so natural crosslinkers are preferred for protein modifications. Aragui and Moslehi (2014) crosslinked fish gelatin with caffeic acid, a natural phenolic compound, to improve barrier and physicochemical properties, and Samsalee and Sothornvit (2017) employed rutin, caffeic acid and genipin to crosslink porcine plasma protein. Enzymes, such as transglutaminase, are also used to crosslink proteins (Al-Saadi et al., 2014; Song and Zhao, 2014). In addition to physical, chemical and biochemical modifications, the addition of plasticizers is often used to modify the brittle behaviour of proteins, improving their processability and those properties required to employ proteins for the development of films and coatings. Possible food grade plasticizers are glycerol, mannitol, sorbitol and sucrose, but water also acts as an effective plasticizer (Ustunol, 2009). The effectiveness of a plasticizer depends on the size, shape and compatibility with the protein matrix. Rezaei and Motamedzadegan (2015) studied the effect of plasticizer type in protein films; results showed that glycerol was a better plasticizer than sorbitol since it increased elongation to the breaking point, besides imparting suitable tensile strength to the films.

Finally, regarding protein classification, these macromolecules can be classified depending on their shape as globular or fibrous proteins. The globular proteins fold into spherical- or ellipsoidal-shaped structures, resulting from the enrolling on itself, holding mutually by an arrangement of hydrogen, ionic, hydrophobic and disulphide bonds; while the fibrous proteins are stem-like shaped, coupled in parallel constructions by hydrogen bonds to form fibres (Gupta and Nayak, 2015). Vegetal proteins such as soy protein are an example of globular proteins. They are composed of a mixture of albumins and globulins, 90% of which are storage proteins with globular structure. According to the sedimentation rate, soy protein consists of four major fractions, 2S, 7S,

11S and 15S, being 7S (β-conglycinin) and 11S (glycinin) more than 80% of the total protein (Acosta-Dominguez et al., 2016). On the other hand, collagen can be an example of a fibrous structured protein. Collagen is composed of three crosslinked α-chains intertwined in the so-called collagen triple-helix. Likewise, this structure is mainly stabilized by intra- and inter-chain hydrogen bonding that varies according to animal species, age, tissue and other factors (Alfaro et al., 2015). Collagen fibres are hardly soluble, so they are chemically denaturated to obtain gelatin. During this process, hydrogen and covalent bonds are cleaved, leading to a destabilization of the triple-helix as a result of the helix-to coil transition and thus, the conversion into soluble gelatin. The structure of gelatin can change under the influence of some parameters, such as extraction temperature, pH, drying temperature and relative humidity (Duconseille et al., 2017). Overall, these structural differences reflect the specific characteristics and functionality of each protein. As shown in **Table 1.1**, each protein shows different amino acid profile and, consequently, different thermal, rheological, viscoelastic and mechanical properties (Díaz-Calderón et al., 2017). Although the functional properties may vary, all proteins have in common some properties that make them suitable for food packaging. Their mayor advantages can be attributed to the excellent film forming ability, good transparency, excellent barrier properties against fat and oxygen, heat sealability, as well as odourless and tasteless characteristics (Song and Zheng, 2014; Tongnuanchan et al., 2012; Tongnuanchan et al., 2016). However, proteins possess great sensitivity to water and moderate mechanical properties and thus, the improvement of those properties is needed in order to develop new active packaging based on proteins (Lin and Zhao, 2007; Park et al., 2014).

1.2 MANUFACTURE OF PROTEIN FILMS AND COATINGS

Different production techniques are used to manufacture protein films, mainly wet and dry processing. The wet process, also called solution casting, is the most widely used at laboratory scale owing to its simplicity (Kashiri et al., 2017a; Liu et al. 2017a), but at larger scale films can be produced by extrusion, compression moulding or injection moulding (Ciannamea et al., 2017). Therefore, the technology used in the plastic industry can be also used for the production of renewable and biodegradable films. A scheme of these manufacturing methods is shown in **Figure 1.2**.

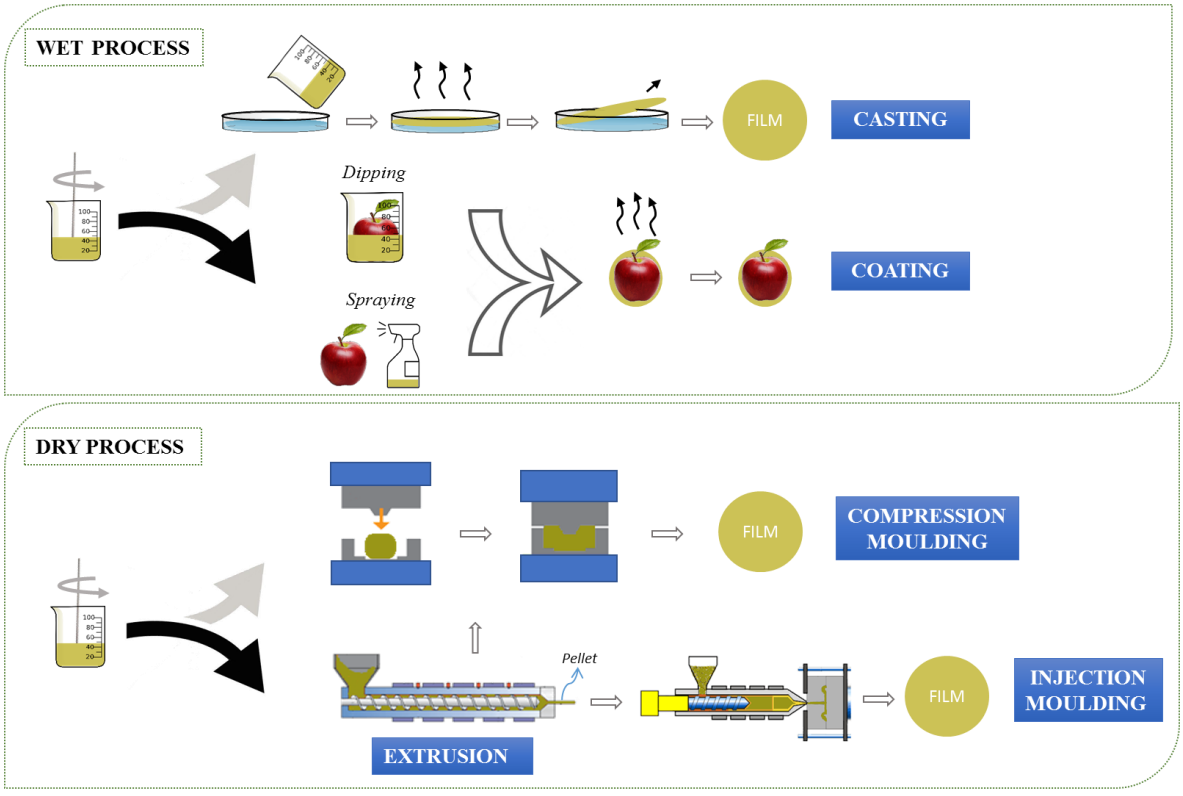

Figure 1.2. Manufacture of films and coatings by wet and dry processes.

Traditionally, protein films and coatings are manufactured by solution casting. Although water is the main solvent employed, water-alcohol solutions can also be used for some proteins such as zein. Heating, stirring and pH adjustment are the parameters

under control in order to obtain homogenous films and coatings, since those processing conditions affect protein denaturation, promoting or hindering interactions. Once the film forming solution is prepared, it is poured into Petri dishes and allowed to dry to form the film (Liu et al., 2016; Qazanfarzadeh and Kadivar, 2016) or it is applied directly onto food surface by dipping or spraying (Zhong et al., 2014). Drying processes can be carried out at room conditions or under controlled temperature and relative humidity, which may affect the film properties (Cerqueira et al., 2016). In order to scale-up production of protein films, tape casting, also known as spread casting or knife-coating, has been used in plastic and paper industries. This technique consists on spreading the film forming solution on a tape and drying it by heat conduction, convection, infrared radiation or a combination of them. This technique requires more concentrated protein solutions than the traditional solution casting (Ortiz et al., 2017). Continuous processes can be carried out by this technique, although the measurement of rheological properties is needed in order to ensure appropriate flow conditions and minimize undesired sedimentation (de Moraes et al., 2013).

Regarding dry processes, when extrusion, compression or injection moulding are employed, proteins must be heated above their glass transition temperature to make them flow (Ghanbarzadeh and Oromiehi, 2008). Additionally, pressure is also applied and plasticizers are added to decrease glass transition temperature and promote the thermoplasticity of the protein (Hernandez-Izquierdo and Krochta, 2008; Visakh and Nazarenko, 2017). Plasticizers such as polyols are usually used, but also water can act as a plasticizer (Bertuzzi and Slavutsky, 2016; Nur Hanani et al., 2013). Concerning extrusion, this technique is a continuous, efficient, high-performance and low-cost process, advantageous for large-scale productions. Proteins are fed to the extruder where they are mixed with the incorporated additives (Koch et al., 2017). In the feeding

zone, the mixture is slightly compressed, but compression increases in the kneading zone, where higher pressures are applied. In the heating zone, the highest shear rates, temperatures and pressures are achieved and, finally, the product exits from the die and is pulled away at constant velocity (Bertuzzi and Slavutsky, 2016). Single-screw extruders or twin-screw extruders can be used to push forward and mix the components of the film forming formulations (Bouvier and Campanella, 2014). Extrusion is a complex multi-input-output process in which some parameters must be mastered (Emin et al., 2017), mainly extruder parameters (screw speed, barrel temperature, screw configuration, die dimension) and process parameters (moisture content, specific mechanical energy, residence time) (Guerrero et al., 2012). In the case of compression, the film forming components are mixed and a specific quantity of the mixture is placed between the two halves of a heated mould, applying pressure to obtain the film under the effect of the mould temperature (Tatara, 2017; Türe et al., 2012). The parameters (pressure, temperature and time) for each step of the process depend on the protein used, even so, protein films are successfully prepared in short times by this process. Injection moulding is another manufacturing technique useful to modify extruded protein materials for obtaining films. This versatile dry process consists in the injection under high-pressure conditions, of heat-induced softened material into a mould where protein mixtures are shaped. Different type of moulds can be used, such as rectangular-shaped specimen and dumb-bell-type specimen (Bourny et al., 2017). It is a potentially automated cyclic process and a single cycle can last few seconds (Zema et al., 2012). Thereby, it can be easily transferred to industrial scale by the use of larger equipments and moulds. However, this technique, which is among the most common processing methods used with synthetic polymers, has not been widely used for protein-based materials.

1.3 ACTIVE FILMS BASED ON VEGETAL PROTEINS

1.3.1 BIOACTIVE EXTRACTION TECHNIQUES

During the last years, the research works that have studied the optimization of bioactive compounds extraction from natural resources have increased exponentially. The benefits that these compounds provide for human health have opened new opportunities for developing new biopolymeric materials, manufactured by different techniques, with great potential in food packaging and biomedical applications. In fact, these bioactive compounds are able to interact efficiently with different biopolymers, such as proteins, providing desired outcomes in the developed material, including antioxidant or antimicrobial effects (Chen et al., 2017; Lau et al., 2017; Yu et al., 2018). In the approach of bioactives' recovery, five-stages have been described in literature: macroscopic pretreatment, micro- and macromolecules separation, extraction, purification and isolation, and product formation (Galanakis, 2015), and the extraction has been considered one of the most important steps. For that reason, many different extraction processes have been evaluated towards the recovery of the targeted compounds. The conventional solvent extraction has been the most employed technology for bioactive compounds recovery (Ballesteros et al., 2014; da Silva Haas et al., 2018; Gullón et al., 2017; Maniglia et al., 2014). This technique is based on the extracting power of different solvents and the application of high temperatures, promoting the mass transfer between different phases of the system (Daso and Okonkwo, 2015). However, the main drawbacks rely on the use of large amounts of organic solvents that can be toxic for human health and the environment, and the high energy and time consumption of the process. Moreover, the severe conditions used can result in the degradation of the desired compounds (Khuwijitjaru et al., 2014;

Setyaningsih et al., 2015). Therefore, a new search for eco-friendly, safe and low operational cost techniques is being carried out in order to overcome the disadvantages of conventional methods. In this aspect, subcritical and supercritical, pressurized liquid, microwave-assisted and ultrasound-assisted extractions can be highlighted, among others.

1.3.1.1 Supercritical fluid extraction (SFE)

SFE is one of the most employed techniques based on the use of compressed fluids. SFE is a green technique, which allows the processing of the extraction at low temperatures, limiting the thermal degradation, and avoiding harmful toxic solvents. Other main advantages are shorter extraction times and reduced use of organic solvents with a potential risk of storage. Moreover, it can be suitable for the recovery of lower volatility solid/liquid compounds (Ameer et al., 2017; Santos et al., 2017). This extraction process occurs in two steps. In the first one, the solvent flows through the packed bed to solubilise the existing compounds present in the matrix, while in the second one, the solvent exits the extractor to carry the solubilised compounds and the extract becomes solvent free by pressure reduction and/or temperature increase (da Silva et al., 2016). SFE is characterised for employing supercritical fluids, which above their critical point exhibit liquid-like properties (insignificant surface tension) as well as gas-like properties (elevated diffusivity and low viscosity) (Bubalo et al., 2018). One of the most employed supercritical fluids is CO_2. CO_2 can typically dissolve non-polar and medium polar compounds like oils, fats and waxes because of its non-polar character (Al-Bulushi et al., 2018; da Silva et al., 2017; de Zordi et al., 2017). This fluid is also able to replace organic solvents such as hexane or heptanes (Al-Hamimi et al., 2016). In this context, the extraction of quinoa oil was carried out by using hexane and CO_2, and the authors determined that the extraction with CO_2 presented higher

tocopherol content and, therefore, better antioxidant capacity (Benito-Román et al., 2018).

With the aim of improving the extraction efficiency and modifying the selectivity of the main solvent, co-solvents can be employed. In this regard, the extraction of oleic and linoleic acids was carried out by the combination of supercritical CO_2 and eight organic co-solvents used in food and pharmaceutical productions (Tirado et al., 2018). The authors found out that the best co-solvents for the solubilisation of both fatty acids were short-chain alcohols, such as ethanol and methanol. Other authors determined that the main influential factors in SFE were the co-solvents percentage and pressure (Salazar et al., 2018).

1.3.1.2 Pressurized liquid extraction (PLE)

Along with SFE, PLE, known as accelerated solvent extraction as well, is also one of the most employed techniques for extracting phytochemicals such as flavonoids (Leyva-Jiménez et al., 2018), phenolic acids (Sánchez-Camargo et al., 2016), or anthocyanins (Feuereisen et al., 2017) from a great variety of vegetal sources. Overall, samples are packed in an extraction cell with a dispersant and then, the extraction can be carried out in a short time (5-20 min) employing temperature (40-200 ºC), pressure (5-20 MPa) and a suitable solvent (water, ethanol, ethyl lactate, ethyl acetate) (de Oliveira et al., 2018; Kovačević et al., 2018; Lores et al., 2015; Otero et al., 2018).

The efficiency of this method was studied by extracting polyphenols and anthocyanins from residues of the industrial processing of blackberry pulp and evaluating the influence of temperature and solvent type (Machado et al., 2015). It was found out that a mixture of ethanol/water at 100 °C was the best PLE condition for recovering the highest amount of bioactives. With the same mixture of solvents, but

increasing the temperature up to 137 ºC, phenolic compounds from myrtle leaves were obtained (Díaz-de-Cerio et al., 2018). The presence of high concentrations of gallic acid and ellagic acid derivatives was reported, demonstrating that PLE improved the extraction of phenolic compounds for nutraceutical formulations.

The comparison of PLE to other methods has also been carried out. In this regard, the antioxidant activity of *Thymus munbyanus* extracts was higher with PLE rather than with the SFE-CO_2 technique (Monteiro et al., 2018), and the pressure extraction was the one that provided the highest yield of lipids rich in ω3 polyunsaturated fatty acids from fish canning industry liquid by-products. Moreover, the Life Cycle Assessment (LCA) validated this process as the most adequate due to its minor environmental impact and lower production cost.

When the extraction solvent is only water, PLE can be subcritical water extraction, pressurized hot water extraction, or superheated water extraction. In these methods, the temperature of water is increased from 200 to 350 °C, so the dielectric constant decreases to around 20-30, similar to some solvents used in conventional extractions, such as methanol, ethanol and acetone at room temperature (Bodoira et al., 2017). A wide range of medium and low polarity compounds can be dissolved employing these techniques (Erşan et al., 2018; Luo et al., 2018a; Vardanega et al., 2017). Subcritical water extraction comprises a high-pressure pump to push the solvent into an extraction cell, which is maintained in an oven to control the extraction temperature, and different valves and restrictors to control the extraction pressure. Solvent-controller valves, nitrogen-purging lines, extraction cells, and vial trays for automation can be some other additional parts (Herrero et al., 2015).

1.3.1.3 Ultrasound-assisted extraction (UAE)

UAE is another widely used technique since it is relatively easy to use, versatile and requires low investment compared to other extraction techniques, such as the above-mentioned PLE. The acoustic cavitation phenomena produced by the ultrasound and mechanical mixing effects are the main mechanisms in UAE. All these processes cause cellular disruption, high solvent penetration and particle size reduction, increasing extraction efficiency and reducing the extraction time (Pena-Pereira et al., 2017). Physical effects of ultrasound are associated with lower frequencies (20-100 kHz), while chemical effects dominate the higher frequencies (200-500 kHz) (Tiwari et al., 2015).

The biological activity of the bioactive compounds is strongly dependent on the UAE conditions, such as temperature, type of solvent and extraction time (Alonso-Carrillo et al., 2017). Regarding the solvent choice, parameters such as solubility of the target metabolites, as well as the viscosity, surface tension and vapour pressure of the solvent, play an important role. Those parameters can affect the acoustic cavitation phenomenon, thus, a solvent with low vapour pressure is preferred in UAE, as the collapse of cavitation bubble is more intense compared to solvents with high vapour pressure (Chemat et al., 2017).

This technique has been successfully employed for the extraction of different compounds (Al-Dhabi et al., 2017; Luo et al., 2018b; Pudziuvelyte et al., 2018). On this matter, the ultrasound extraction technique was chosen to optimize the extraction yield of okra polysaccharide (Wang et al., 2018a). Under optimal extraction conditions (59 °C, 30 min, and 522 W), the extraction yield of the polysaccharide was 10.35 ± 0.11%, which strongly agreed with the predicted value. Water-soluble

polysaccharides were also extracted from dried and milled mushroom production by-products employing UAE as extraction method (Aguiló-Aguayo et al., 2017). Natural antioxidants from the flowers of *Limonium sinuatum* were also recovered with this technique (Xu et al., 2017), as well as curcumin, a phytochemical widely used in biomedical applications, which was isolated from *Curcuma amada* (Shirsath et al., 2017).

In the application of this technique, UAE protocols with different energy inputs can be applied for extracting components, and the dependency of the selectivity of extraction of catechin upon applied UAE protocol can be proved (Wang et al., 2018b). In fact, it was determined that the increase in ultrasound specific energy input resulted in the increase in the final concentration of catechin and so, in total phenolic content. It was suggested that the extraction mechanism induced by ultrasound may include combination of many effects related to fragmentation, erosion, sonocapillarity, and detexturation. Moreover, the manifestation of these effects could be quite different in dependence on structures of flesh and peel tissues, ability of their swelling and rehydration, and distribution of phenolic compounds inside these tissues.

1.3.1.4 Microwave-assisted extraction (MAE)

MAE can be another suitable option for extracting bioactives from food matrices (Ho et al., 2015; Valdés et al., 2015). This technique uses directly the microwave energy to heat the molecules within the material structure, increasing the internal pressure and facilitating partition of analytes from the sample into the solvent (Ince et al., 2014). Comparing to traditional extraction techniques, a significant reduction in the extraction time can be obtained. Water, ethanol, methanol or a combination of these solvents is usually used for extraction (Alara et al., 2018; Setyaningsih et al., 2015).

A number of recent works have confirmed the advantages of MAE. Recently, it was shown that the yield of phenolic compounds extraction from *Thymus algeriensis* herb by MAE significantly increased comparing to SFE and hydroalcoholic extraction and fractionation (Boutaoui et al., 2018). Furthermore, the effectiveness of MAE for the extraction of biologically active β-glucans from *Pleurotus ostreatus* and *Ganoderma lucidum* fruiting was reported (Smiderle et al., 2017), as it was the polyphenols extraction from apple tree wood residues (Moreira et al., 2017). Moreover, it was found that the employment of MAE for extraction of polyphenols from *Myrtus communis* leaves required extraction times about 14 and 15 times lower than the UAE and the traditional extraction method, respectively (Dahmoune et al., 2015).

Microwave hydrodiffusion and gravity method uses only the internal water of the plant material, without employing any other solvent, and is an alternative method to the traditional MAE. This technique consists of heating the material internal water, which induces the breaking of the plant cell and improves the release of bioactive compounds. It has been demonstrated that microwave hydrodiffusion and gravity is a valuable tool for the preparation of non-degraded polyphenol extract from fresh *Lettuce sativa* on a laboratory scale, as well as its larger production in a pilot reactor, which allows a massive reduction in biomass wastes (Périno et al., 2016). This method was also used to extract essential oils from citrus peels (Boukroufa et al., 2015). The authors obtained high added value compounds in shorter time and they managed to make a closed loop using only the resources provided by the plant, which is better in terms of time and energy saving, cleanliness and reduced waste water.

Microwave-assisted hydro-distillation and solvent-free microwave extraction are other two derivatives from the traditional MAE that have been proven to be fast and efficient for extracting essential oils (Jeyaratnam et al., 2016; Kusuma et al., 2018).

Moreover, it was shown that these two methods could be termed as “green” from an energy point of view and were proposed to be employed for large-scale productions of essential oils (Golmakani et al., 2015).

1.3.1.5 Combination of techniques

Taking the advantage of the benefits of each method, the combination of different techniques has also been studied for a more effective extraction of the targeted bioactives. The employment of both UAE and MAE by means of simultaneous irradiations is one of the most promising combined techniques (Albuquerque et al., 2017; Chan et al., 2017; Liew et al., 2016; Lu et al., 2017; Pongmalai et al., 2015; Wang et al., 2018c). For instance, a sequential microwave-ultrasound-assisted extraction approach was designed for isolation of piperine from black pepper, being the extraction yield (46.6 mg piperine/g pepper) higher than those obtained separately by Soxhlet (39.1 mg/g), microwave-assisted (38.8 mg/g) and ultrasound-assisted (37.0 mg/g) extractions (Gorgani et al., 2017).

Ultrasound technique has also been employed along with PLE. This combination was used to increase the extraction of phenolic compounds from pomegranate peels (Sumere et al., 2018). The authors demonstrated that this combination could be an efficient and a green alternative due to the replacement of an organic solvent for water, the reduction of extraction time, the use of relatively low temperature and no clogging problems. This technique was also employed for recovering anthocyanins from blackberry, blueberry and grumixama residues (Machado et al., 2017). Combination of PLE and microwave techniques can also show several advantages, such as the effective extraction of bioactive carbohydrates (inositols and inulin) from artichoke external bracts (Ruiz-Aceituno et al., 2017).

Customised multi-task equipment, combining SFE-CO_2 and PLE with ethanol, was developed to recover selectively antioxidant compounds from cocoa bean hulls (Mazzutti et al., 2018). A study using PLE technology on the extraction of fucoxanthin from *Phaeodactylum tricornutum* algae, which is an oxygenated carotenoid with several biological activities, including antioxidant, antiobesity, antidiabetic, anti-inflammatory, antiphotoaging and anticancer, was conducted (del Pilar Sánchez-Camargo et al., 2017). The recovery of fucoxanthin was approximately the 50% of the amount of this carotenoid present in the biomass, enforcing to design a continuous extraction aided by supercritical CO_2 to obtain a higher recovery.

Apart from all the advantages that these new technologies can provide to the bioactive extraction processes, these methods still need a scale-up study to evaluate the economic viability in order to be considered among other extraction technologies for industrial applications when bioactive extracts are produced on a large scale and sold at the current market price. For that reason, an economic evaluation of sequential multi-stage and single-stage processes was carried out (Viganó et al., 2017). The results demonstrated that both processes seem to be economically applicable at large production scale since scaling up increased the process productivity and decreased the cost of manufacturing. An economic analysis of oleoresin production from malagueta peppers by SFE was also carried out (de Aguiar et al., 2017). The manufacturing cost (125 US$/kg) under the proposed conditions (15 MPa and 40 °C) was lower than the estimated commercialization price of the extract (223 US$/kg). This assessment suggested that the production of malagueta oleoresin on a large scale by SFE could also be economically applicable. Therefore, protein-based products can act as excellent vehicles of bioactive compounds, developing a new opportunity to the manufacturing of new protein-based materials for food packaging and biomedical application.

1.3.2 VEGETAL PROTEINS FOR ACTIVE FILMS DEVELOPMENT

The incorporation of these biologically active compounds, or other compounds such as proteins or polysaccharides, into protein-based film forming formulations manufactured via different processing methods, promotes the improvement of films properties. Proteins from different vegetal sources have been employed along with these compounds for a variety of applications, and have become promising alternatives to synthetic polymers. Among them, soy protein, zein and wheat gluten can be highlighted.

1.3.2.1 Soy protein

Soy protein is extracted from soybeans used to obtain soy oil. According to USDA (United States Department of Agriculture), the soybean production in 2018/2019 has been around 370 million metric tons worldwide (USDA, 2018), which makes this resource abundant, accessible and low-cost. During soy oil extraction, secondary products such as soy flour (SF), soy protein concentrate (SPC) and soy protein isolate (SPI) are obtained (Preece et al., 2017). These three products differ in the protein concentration: SF has the less protein content, around 40-60% protein, combined with fats and carbohydrates; SPC contains around 60-70% protein, a polysaccharide fraction of around 8-15%, mainly composed of cellulose and pectic polysaccharides, and a minor content of fats (1%), fibres (1-3%) and ashes (3-5%); and SPI contains about 90% protein (Ciannamea et al., 2014). Due to this high amount of protein, its renewability, biodegradability and abundance, SPI has become a potential candidate in the polymer industry for food packaging applications (Božič et al. 2015; Garrido et al., 2014). These bio-based materials must fulfil certain conditions to maintain food sensory quality and safety by serving selective barriers to moisture transfer, oxygen uptake, lipid

oxidation and losses of volatile aromas and flavours, without forgetting the requirement of having an adequate mechanical behaviour (González et al., 2015). For that reason, a high amount of research works has been published focused on meeting all these requirements.

SPI films have inferior mechanical properties and lower resistance to moisture than synthetic plastics; thus, different methods have been studied in order to modify SPI with the aim of overcoming these drawbacks. Among these methods, blending with natural substances (Pan et al., 2014; Wang et al., 2014), chemical crosslinking (Jiang et al., 2017; Xu et al., 2015), employment of different processing methods (Garrido et al., 2016), and enzyme treatment (Meinlschmidt et al., 2016) can be highlighted.

The incorporation of additives, such as other proteins, polysaccharides, lipids or other natural substances, has been widely considered in order to take advantage of the properties of each compound and the synergy between them. In that way, the properties of SPI-based films and coatings can be enhanced and new functionalities can be provided. Bai et al. (2013) studied the incorporation of gelatin into SPI-based films. Results showed an increase in tensile strength, elongation at break and contact angle and a decrease in water vapour transmission rate. The addition of polysaccharides has also been considered. Sui et al. (2016) incorporated guar gum into SPI films and results indicated that guar gum induced increased network compactness, resulted from strong intermolecular interactions. Consequently, SPI-based films were more tensile-resistant, water-resistant and had better barrier properties to light. The addition of starch into SPI films has also been used. Starch nanocrystals improved the tensile strength and elastic modulus of SPI films, which became more rigid due to the interactions and the high cohesion between the two components; additionally, the solubility, swelling and water

vapour permeability decreased (González and Igarzabal, 2015). Regarding mechanical properties, similar trend was observed when cassava starch (Chinma et al., 2012) or oxidized potato starch was incorporated into SPI films (Galus et al., 2013). In a similar vein, taking advance of the good properties of lipids, Hopkins et al. (2015) combined SPI with flaxseed oil to perform films with lower moisture content and swelling but with higher strength.

The added compounds can act also as crosslinkers and contribute to the enhancement of the film network. Xia et al. (2015) employed an epoxidized soybean oil, an environmentally friendly crosslinking agent derived from soybean, which effectively improved tensile strength values in a 140% and the modulus in a 696% in comparison to the untreated SPI-based films, whereas Friesen et al. (2015) determined that the incorporation of rutin into SPI films decreased the water vapour permeability and increased the film strength.

In addition, the efficiency of soy protein films to work as carriers of antioxidants, such as chestnut bur extract (Wang et al., 2016), tannins (Wang and Wang 2017) or catechin (Han et al., 2015), and antimicrobial agents, such as thymol (antibacterial) and natamycin (antifungal) (González and Igarzabal, 2013), has been proved by many authors. Natural extracts or bioactives, such as anthocyanin-rich red raspberry (Wang et al., 2012), mango kernel extract (Adilah et al., 2018) or licorice residue extract (Han et al., 2018), can also have influence on the functional properties of films, apart from improving the antioxidant or antimicrobial activity inherent of each additive. For instance, it was determined that the incorporation of mango kernel extract increased the tensile strength of SPI-based films and reduced the water solubility and elongation at break; whereas, licorice residue extract improved the mechanical, water,

oxygen and light barrier properties when its content was lower than 70 g per kg of protein. Moreover, total phenolic content was measured in aqueous (10 % ethanol) and fatty (95% ethanol) food simulants, and the results showed that the extract incorporation notably increased the phenolic compound release, giving values of 4.0-5.6 mg gallic acid/g film in the alcoholic simulant and 2.2-5.5 mg gallic acid/g film in the fatty food simulant. Echeverría et al. (2016) carried out the addition of clove EO into SPI films reinforced with montmorillonite. Besides the important antioxidant and antimicrobial properties provided by the EO, a plasticizing effect was exerted. Furthermore, the nanoclay had a further strengthening effect on films containing clove EO; whilst nanocomposite films containing 10 g montmorillonite/100 g SPI reached an increase of 105 and 200% in tensile strength and Young's modulus, respectively, those that also contained clove reached higher variations (230 and 345%, respectively). Phenolic compounds, such as carvacrol, ferulic, caffeic and gallic acids, have also been successfully employed in SPI films. In general, the effect of phenolic acids incorporated into protein-based films is controlled by two different features: their ability to form hydrogen bonds or other interactions between the carboxyl groups and the amino groups of proteins, and their affinity towards water that results in high water absorption (Ganiari et al., 2017). Otoni et al. (2016) incorporated carvacrol and cinnamaldehyde and promoted an increase in the rigidity of films, while Insaward et al. (2015) studied the influence of ferulic, caffeic and gallic acids and their oxidized products. Results determined that gallic acid-containing films exhibited the highest tensile strength and elongation at break, and oxidized phenolic acids were shown to produce films with higher tensile strength and elongation at break than their unoxidized counterparts. Moreover, phenolic-containing films showed reduced water vapour permeability and water solubility and increased contact angles. Finally, Ciannamea et al. (2016) added

different amounts of red grape extract (0-10% w/w) and thermo-compressed the mixture in a three-step operation: 150 ºC for 5 min at 10 kg/cm^2, 150 ºC for 2 min at 100 kg/cm^2, and cooling up to 30 ºC at 100 kg/cm^2 for about 30 min. The results showed that the incorporation of the extract into soy protein resulted in lower elongation at break and higher elastic modulus values. Furthermore, the addition of 5% of the extract improved the antioxidant activity of the film since DPPH radical scavenging activity increased from 58 to 81% due to the presence of polyphenolic compounds, such as catechin, epicatechin and procyanidin, in the red grape extract. It was observed that higher concentrations of the extract (10% w/w) did not affect the antioxidant activity of films.

Some research studies have demonstrated that films and coatings based on soy protein have multiple benefits regarding the extension of food shelf life; in particular, reduction of oxidation and discoloration, retardation of rancidity processes, inhibition or reduction of the microbial contamination, prevention of moisture loss and diminution of the loss of flavour compounds, standing out as the most significant ones. Some studies that demonstrated the potential of SPI-based films and coatings for food products, such as meat, fish, fruits, vegetables and others are outlined in **Table 1.2**.

Strategies to extend the quality of fruits and vegetables need to target several key challenges, such as minimizing dehydration, reducing or avoiding microbial growth and extending maturation and senescence periods. The incorporation of chitosan and stearic acid (Wu et al., 2017c) and ferulic acid (Alves et al., 2017) into SPI films extended the shelf life of apples and improved film properties, including gas permeability and tensile strength. In another study, Arancibia et al. (2014) showed that the addition of 3% w/v citronella EO to SPI films blended with lignin had good antifungal activity against

pathogen microorganisms (*Fusariun oxysporum*) in bananas. Also the application of SPI coatings with citral and limonene preserved postharvest quality of lime and provided antifungal activity against *Penicillium italicum* in inoculated limes (González-Estrada et al., 2017). Other additives, such as cysteine (Ghidelli et al., 2014; Ghidelli et al. 2015), lauric acid and propylenglycol alginate (Zeng et al., 2013), incorporated into SPI coatings have shown to reduce enzymatic browning and improve the quality of artichokes, eggplant and jujubes. The prevention of other effects indicative of quality loss, such as shrinkage, oxidative off-flavours, microbial contamination and discoloration in meat, fish and poultry products, is also of great importance. Echeverría et al. (2017) applied soy protein/montmorillonite/clove EO films for the preservation of refrigerated tuna fillets. It was observed that SPI-based films decreased *Pseudomonas* growth and lipid oxidation; furthermore, montmorillonite favoured the release of clove EO, extending the tuna shelf life. Also SPI coatings have been found to be effective for meat preservation by delaying lipid oxidation and colour deterioration and maintaining textural parameters in beef patties (Guerrero et al., 2015). Beef has also been coated employing SPI with thyme and oregano EOs. According to Yemiş and Candoğan (2017), these soy protein coatings exhibited antimicrobial activity against *E. coli* O157:H7, *Listeria monocytogenes* and *S. aureus*. Moreover, Coşkun et al. (2014) confirmed that the addition of these two EOs controlled lipid oxidation in SPI-coated beef patties. Other bioactives, such as cinnamaldehyde and eugenol (Zhang et al., 2013) or nisin, sodium lactate and EDTA (Liu et al., 2017b) have also showed a significant inhibitory effect on the growth of *S. aureus*, *Pseudomonas* and *yeast*, being cinnamaldehyde-containing SPI films the most effective ones. The films containing 6% EOs showed the preservation effect on pork. Besides that, films showed a significant antimicrobial effect on three food pathogens, *E. coli*, *Salmonella* and *Bacillus cereus*,

when nisin, sodium lactate and EDTA were incorporated into SPI films, extending pork shelf life up to 3-6 days.

Table 1.2. SPI-based films or coatings for food packaging.

Active agent	Additive role*	Food tested	Processing	Reference
Clove EO	AM AO	Tuna	Casting	Echeverría et al., 2017
Nisin Sodium lactate EDTA	AM	Pork	Casting	Liu et al., 2017b
Cinnamaldehyde Eugenol	AM	Pork	Casting	Zhang et al., 2013
Thyme EO Oregano EO	AM	Beef	Casting	Yemiş and Candoğan, 2017
Thyme EO Oregano EO	AO	Beef	Casting	Coşkun et al., 2014
Citral Limonene	AM	Persian lime	Coating	González-Estrada et al., 2017
Ferulic acid	AO	Apple	Casting	Alves et al., 2017
Citronella EO	AM	Banana	Casting	Arancibia et al., 2014
Cinnamon oil	AM	Dry tofu	Casting	Liu et al., 2014
Catechin	AO	Walnut	Coating	Kang et al., 2013

*AO = antioxidant
*AM = antimicrobial

1.3.2.2 Zein

Zein is a protein used for food packaging applications, since it exerts better barrier against transmission of water vapour and volatile compounds in comparison to other types of protein films (Ozcalik and Tihminlioglu, 2013). Moreover, zein has an excellent film forming ability since it is believed to involve the development of hydrophobic, hydrogen and limited disulphide bonds between zein chains in the film matrix (Bourtoom, 2008). This biopolymer can be defined as a water-insoluble hydrophobic storage protein found in corn and maize. Based on solubility and sequence homology, it can be separated into α-zein (19 and 22 kDa), β-zein (14 kDa), γ-zein (16 and 27 kDa) and δ-zein (10 kDa). α-zein, which consists of highly homologous repeat units with a high content of α-helix (Zhang et al., 2015b), composes around 70-

85% of the total fraction of zein mass, while γ-zein is the second most abundant fraction (10-20%).

In the manner of other proteins, the brittleness is the major disadvantage of zein. It is known that the incorporation of plasticizers helps to reduce the brittleness (Xu et al., 2012), but blending or mixing with other natural compounds can be also a solution due to the benefits that these components can provide to the film. Since zein and gliadin are both readily dissolved in aqueous ethanol and have a good film-forming property, Gu et al. (2013) prepared films with these two proteins. The results showed that the addition of gliadin enhanced the strain at break of zein films as a result of the increase in the content of α-helix and β-turn structures and the decrease in the level of β-sheet structure. Cheng et al. (2015) prepared active zein films with chitosan and phenolic compounds (ferulic acid or gallic acid) and dicarboxylic acids (adipic acid or succinic acid). The antimicrobial properties against *S. aureus* and *E. coli* were determined and the antioxidant activity was confirmed by DPPH and ABTS free radical scavenging tests. Additionally, zein glycosylated with chitosan by transglutaminase has resulted effective in retarding lipid oxidation of ground pork, indicating that enzymatic glycosylation might be a new approach to modify the functional properties of zein (Wang et al., 2017c).

Other authors have also employed the crosslinking strategy to obtain zein films with enhanced properties. Succinic anhydride, eugenol and citric acid were employed by Khalil et al. (2015) as natural crosslinking agents. All crosslinked films showed remarkable antibacterial activities against *B. cereus* ATCC 49064 and *Salmonella enterica* ATCC 25566. However, these crosslinkers were also added to chemically modify zein in order to improve the functional properties of the films; thus, the addition

of these compounds resulted in 2- to 3-fold increases in tensile strength values. On the other hand, Santos et al. (2017) assessed the addition of tannic acid, especially in its oxidized form, to crosslink zein and concluded that higher tannic acid contents and pH values resulted in films with better physical properties.

In general, one of the advantages of working with zein comes from its hydrophobicity, which makes it compatible with natural antimicrobials (Yemenicioğlu, 2016). Naturally occurring antimicrobial compounds are an alternative to synthetic preservatives and their use is increasingly growing. In this context, many natural antimicrobial agents have been employed to develop zein films with antimicrobial effects. *Z. multiflora* Boiss. is a thyme-like plant belonging to the *Lamiaceae* family, being carvacrol and thymol its main antimicrobial components. The addition of these two EOs into zein films was studied by Kashiri et al. (2017a) and Moradi et al. (2016). These authors confirmed the good antimicrobial properties of *Z. multiflora* Boiss. against *L. monocytogenes* and *E. coli,* as well as the good antioxidant properties of these substances. Moreover, Kashiri et al. (2017b) demonstrated that the addition of *Z. multiflora* Boiss. EO caused an increase in the percent of elongation at break of the films. Alkan and Yemenicioğlu (2016) not only evaluated the employment of carvacrol and thymol EOs into zein films, but also studied other EOs, such as eugenol and citral, some phenolic acids like gallic, vanillic and cinnamic acids, and phenolic extracts from clove, oregano, artichocke stem and walnut shells. The incorporation of these antimicrobial compounds into zein films show positive results against bacterial plant pathogens, such as *Erwinia amylovora*, *Erwinia carotovora*, *Xanthomonas vesicatoria* and *Pseudomonas syringae*. Moreover, these authors concluded that phenolic-containing zein coatings could provide an additional post-harvest benefit by delaying bacterial spoilage of coated fresh fruits and vegetables.

A limited number of studies have investigated the effectiveness of zein-based films in fresh products. Ünalan et al. (2013) determined the release profiles of lysozyme and mixtures of lysozyme and phenolic compounds (catechin and gallic acid) from zein and zein-wax composite films to cold-stored fresh Kashar cheese. They concluded that all lysozyme-containing films prevented the increase in *L. monocytogenes* counts in the cheese stored at 4 °C for 8 weeks. However, only zein-wax films with sustained lysozyme-release rates caused a significant reduction of initial microbial load of inoculated cheese samples. The mixture of catechin and gallic acid improved the *in vitro* antimicrobial effect of films against *L. monocytogenes*, but showed no considerable antimicrobial effect on cheese. In another study (Chen et al., 2016), grass carp fish balls were coated by zein containing a polymeric chelator based on hexadentate 3-hydroxypyridinones. The study demonstrated that this coating could effectively improve the sensory properties of fish balls and maintain their freshness due to the inhibition of microbial growth and the delay of protein decomposition and lipid oxidation during storage. Mehyar et al. (2014) coated Berhi date palm fruits, harvested at the khalal stage, with different edible materials, including zein protein. Results confirmed that zein coatings were one of the most effective coatings in retarding fruit maturation by extending the khalal stage from 7 to more than 14 days.

1.3.2.3 Wheat gluten

Wheat gluten is a storage protein obtained as a by-product of the isolation process of starch from wheat flour (Day, 2011). This protein consists of a mixture of two main proteins, gliadins and glutenins, which differ in their solubility in aqueous alcohols and their propensity to form intermolecular disulphide bonds (Zubeldía et al., 2015). Gliadins are monomers, while glutenins are composed of discrete polypeptide

subunits linked together by interchain disulphide bonds to form high molecular weight polymers. Therefore, gluten proteins cover a broad range of molecular masses up to several million daltons. The amount of disulphide bonds, as well as the hydrogen bonds present in wheat gluten, plays an important role in the structure and properties of this protein (Pommet et al., 2005). Zein and wheat gluten share many similarities, including the solubility in aqueous alcohols, the high amount of proline, low-cost and availability (Dahesh et al., 2016). Moreover, since these two proteins are insoluble in water, they produce insoluble coatings. However, wheat gluten, in comparison to zein, exhibits remarkable viscoelastic properties, which promote largely the film forming ability. As other proteins, wheat gluten films have limited resistance to water vapour and weak mechanical properties, but the chief advantage of using gluten as a raw material is its low oxygen permeability rates (Mojumdar et al., 2011; Tanada-Palmu et al., 2000).

Regarding film forming techniques, many authors have used thermo-mechanical processing to manufacture wheat gluten films (Ansorena et al., 2016; Thammahiwes et al., 2017). Exposing wheat gluten to high temperatures results in important changes in the type and degree of covalent crosslinking within the molecular network, which leads to brittle wheat gluten films in the absence of plasticizers (Jansens et al., 2013). Thus, incorporation of plasticizers in wheat gluten film forming solutions is required to promote film flexibility, being glycerol the most used plasticizer (Duval et al., 2015; Sharma et al., 2017). As in the case of the previously mentioned proteins, blending or mixing with other biopolymers can be also a way to enhance wheat gluten film properties. In this regard, the influence of adding some polysaccharides, such as locust bean gum, methyl cellulose, carboxymethyl cellulose (Zárate-Ramírez et al., 2014), starch (Basiak et al., 2015; Basiak et al., 2017) and chitosan (Chen et al., 2014), has been analysed.

During the last few years, a number of studies have aimed to evaluate the effectiveness of wheat gluten films against food-contaminating fungi and microbes in order to provide evidence of their applicability in different food products. *E. coli*, *Salmonella Typhimurium*, *S. aureus*, *B. cereus* and *L. monocytogenes* are common pathogens that can damage the foodstuffs; thus, Barazi and Osman (2017) evaluated the antimicrobial activity of gluten films with different concentrations of *Origanum vulgare* EO against these pathogens. Other antimicrobial agents, such as clove, red thyme, carvacrol, cinnamaldehyde and white thyme also showed antimicrobial effectiveness against *Aspergillus niger*, *Candida albicans, E. coli* and *S. aureus* (Gómez-Heincke, 2016). Also the incorporation of formic acid and oregano EO into wheat gluten films has demonstrated antimicrobial activity against *A. niger*, *Candida kefyr*, *B. cereus* and *E. coli*. (Martínez et al., 2013). Pomegranate peel and curry leaf extracts have been also employed in the development of wheat gluten-based films in order to extend the life of cherry tomatoes and mangoes (Kumari et al., 2017). It was observed that pomegranate peel extract showed significantly higher antibacterial activity than curry leaves powder against tested pathogens, *S. aureus* and *Micrococcus luteus*. The antimicrobial performance of wheat gluten films was tested on meat products (Massani et al., 2014). Wheat gluten-containing *Lactobacillus curvatus* CRL705 was employed to assess the release properties in contact with substances commonly used as food simulants (sunflower oil and water). According to the results, it should be expected that in the timescale of vacuum-packaged cooked sausages (approximately 30-40 days), the film could provide an efficient antimicrobial effect on these products.

Although the research interest has mainly been focused on manufacturing active films for packaging applications, intelligent packaging development is growing gradually (Ghaani et al., 2016). According to Biji et al. (2015), an intelligent packaging

material can be defined as a material that monitors the condition of packaged food or the environment surrounding of food to give information regarding the quality of the packaged food during transportation and storage. Therefore, monitoring carbon dioxide as well as controlling the variation of relative humidity in food packages could be interesting so as to give a better control on the evolution of food metabolism and to meet the consumers demand for higher quality food products. With regard to wheat gluten, this is considered a polarisable material having dielectric properties (Sharma et al., 2010); thus, this protein could be suitable to manufacture intelligent packaging. In fact, Bibi et al. (2017) mentioned that the electric and dielectric properties of wheat gluten are known to be sensitive to carbon dioxide. For that reason, gluten-based films could be used for monitoring packaging headspace in intelligent packaging systems. In that context, the authors were able to determine the potential use of wheat gluten as a carbon dioxide sensor, showing interesting results particularly at high relative humidity values (90% RH). Moreover, Bibi et al. (2016) investigated wheat gluten protein to monitor relative humidity, confirming the good sensitivity of wheat gluten at high relative humidity values, ideal for foreseen applications related to the control of packaged food products.

1.3.2.4 Other vegetal proteins

Although soy protein, zein and wheat gluten are widely studied and employed proteins, other vegetal proteins have also been considered to develop active films and coatings. Sunflower protein films with clove EO were used for the preservation of refrigerated sardine patties, retarding lipid oxidation and delaying the growth of total mesophiles. The viability of canola for food packaging applications has also been studied. Canola is mostly obtained as a by-product from the oil industry, but it is

underutilized in the marketplace since it is sold traditionally for its use as livestock feed. The protein content within the meal can be up to 50% (on a dry weight basis) and has a well-balanced amino acid profile and thus, it has been used for the preparation of films plasticized with glycerol (Chang and Nickerson, 2015), sorbitol or polyethylenglycol (Chang and Nickerson, 2014). Other vegetal proteins such as bitter vetch seeds, which contain up to 25% protein, are also an inexpensive source of protein and thus, could be an affordable raw material to produce films for food applications; however, bitter vetch protein films do not satisfy mechanical requirements (Arabestani et al., 2013). Hence, different additives, such as oxidized ferulic acid (Arabestani et al., 2016a) or pomegranate juice (Arabestani et al., 2016b) have been incorporated into film forming formulations to enhance properties, obtaining markedly higher tensile strength and elongation at break values. Recently, edible oil production from hazelnuts has become increasingly important since hazelnut oil has similar fatty acid profile to olive oil, so due to its nutritive value and high protein content, the hazelnut meal obtained from oil extraction is gaining success. Aydemir et al. (2014) demonstrated that hazelnut protein isolate shows antioxidant, anticancerogenic and antihypertensive activity, but poor emulsifying, gelling and water absorption capacities. However, hazelnut proteins form transparent, flexible, and light to brown coloured films. Sesame protein can also be obtained as a by-product of oil extraction. Sesame meal contains 35-40% protein and can be used for film formation. Sharma and Singh (2016) employed sesame protein isolate, extracted from defatted sesame meal, to prepare films. Although further research is required to improve the mechanical and optical properties of those films, this protein can be used for food packaging of fruits and vegetables since it provides barrier to moisture.

1.4 FUTURE TRENDS AND OPPORTUNITIES

Films and coatings based on vegetal proteins are promising systems to be mainly used for food applications but also for biomedical applications. In the case of food packaging, the proper understanding of the role of each component of the packaging, is a key issue in order to develop films and coatings with the suitable functional properties to control the mechanism of food deterioration, and consequently, improve food quality and extend food shelf life, fulfilling all the specifications required for those materials in contact with food. Several studies have been focused on optimizing the composition, functional properties and processing methods of protein-based films and coatings in order to develop economically and environmentally sustainable materials able to compete against synthetic plastics and reduce their use as food packaging. Therefore, the employment of protein along with bioactive compounds, which can be extracted from wastes or by-products from agriculture, meat, poultry and fish processing industries, could contribute to the cost-effective production of this environmentally friendly packaging, as well as to the promotion of new desirable functionalities. There is a growing number of research works that apply protein films and coatings onto fresh food, demonstrating that these proteins are able to improve the quality, safety, functionality and shelf life of food products, consequently, new market opportunities are opened for the commercial implementation of these protein-based food packaging systems.

Regarding the employment of these types of materials in the biomedical field, it has been considered the function of protein-based products as vehicles of bioactives; thus, these biologically active compounds have been added into protein-based formulations to develop active materials suitable, for instance, as wound healing.

Although for this kind of application manufacture processes such as solution casting and compression moulding have been widely studied, some other techniques are being taking into consideration in order increase the opportunities that these materials possess. For instance, scaffolds produced by freeze-drying or 3D printing are starting to be used for tissue engineering. However, an in-depth research work is needed to maximise the benefits of bioactive addition into protein-based biomaterials.

Generally, a technological innovation has been carried out in terms of bioactive extraction and protein-based products development for both food and biomedical applications, but more research is needed to overcome some engineering limitations of the extraction and manufacturing techniques in order to scale-up the production of bioactives and protein products from proto-type to volume manufacturing.

2

chapter

MATERIALS AND METHODS

2.1 MATERIALS AND REAGENTS

Soy protein isolate (SPI), PROFAM 974, was obtained from ADM Protein Specialties Division. According to the information provided by the supplier, SPI has a minimum of 90% protein content on a dry basis, a maximum of 5% moisture, 4% fat, 5% ash, and its isoelectric point is 4.6. SPI amino acid content was also supplied by ADM Protein Specialties Division, while SPI amino acid analysis was performed with a Biochrom 30+ amino acid analyser physiological system.

Glycerol (Gly) and sorbitol (Sor), supplied by Panreac, were used as plasticizers. Glycerol (92 g/mol) is a colourless and viscous liquid, whilst sorbitol (182 g/mol) is a fine white powder.

Reagents such as gallic acid, Folin-Ciocalteu reagent, 2,2-diphenyl-1-picryhydrazyl (DPPH) and enkephalin hydrated leucine acetate (95% purity), were purchased from Sigma Aldrich; sodium carbonate, copper sulphate, sodium hydroxide, sodium thiosulphate and potassium iodide were purchased from ECP; sulphuric acid and Rochelle salt were purchased from JT Baker; acetic acid came from Merck; methanol, acetonitrile and formic acid were purchased from Fisher Scientific. Distilled water was used in all films preparation.

2.2 EXTRACTED MATERIALS FROM BIOWASTES

2.2.1 Keratin extraction and characterization

Hydrolysed keratin (HK) was extracted from chicken feathers, kindly supplied by Lumagorri S.L. Feathers were washed with water and dried at room temperature; then, the quills and the barbs were cut into small pieces and grinded. Afterwards, the

grinded feathers were treated in a Soxhlet with methanol during 3 h and, finally, they were dried and stored at room temperature in a closed container before use. These pre-treated chicken feathers (CF) were mixed with NaOH (1 M) in a CF/NaOH ratio of 1:20 (w/v) and the mixture was stirred during 8 h at room temperature (Lavall et al., 2007). After that, 100 mL of distilled water were added and the solution was filtered (HK). If necessary, HK solution was freeze-dried using Alpha 1-4 LD freeze dryer to obtain freeze-dried powder.

The analysis of protein fractions with different molecular weights was carried out by sodium dodecyl sulphate-polyacrylamide gel electrophoresis (SDS-PAGE), according to the method of Laemmli (Laemmli, 1970) on SPI. Different amounts of samples were dissolved in a buffer containing SDS, tris-HCl buffer (pH 6.8), dithiothreitol (DTT), glycerol and bromophenol blue. The stacking and the separating gels were 12% polyacrylamide. Electrophoresis voltage used was 200 V. After electrophoresis, the gel was washed with water and then, stained with a staining solution (Coomassie Brilliant Blue R-250, BIO-RAD). Subsequently, the sample was distained with a mixed solution (water, methanol, glacial acetic acid). The protein standard (Precision plus protein all blue standards, BIO-RAD) was used for calibration.

2.2.2 Agar extraction and characterization

Agar (AG) was extracted from the red algae *Gelidium sesquipedale (Rodophyta)*, collected on the northern coast of Spain (Hondarribia beach: 43º23’50N, 01º47’50W) in autumn (September). The dried red algae (30 g) were immersed in boiling water (900 mL) for 4 h and the solution was separated from the residue by filtration on 50 μm blutex nylon. Then, the solution was gelled at room temperature and freeze-dried to obtain the powder. In addition, the insoluble residue was extracted twice

in boiling water for 3 h, separated from the solution by filtration on 25 μm blutex cheesecloth and dried. After that, the residue was extracted in a Soxhlet with boiling ethanol to remove the chlorophyll pigments, and subsequently dried, milled and sieved to obtain the powder used as filler, designated as alga waste (AW). AW is mainly composed of cellulose, proteins and agarose (Guerrero et al., 2014; Vignon et al., 1994).

^{1}H and ^{13}C nuclear magnetic resonance (NMR) spectra of agar were recorded with a Bruker Avance, equipped with BBO z-gradient probe. Agar solutions, 5% (w/v) in D_2O, were prepared and data were recorded at 90 ºC. Experimental conditions for ^{1}H NMR were as follows: 500 MHz, 64 scans, spectral window of 5000 Hz, and recovery delay of 1 s. For ^{13}C NMR, the conditions used were 125.75 MHz, 14000 scans, spectral window of 25000 Hz, and recovery delay of 2 s.

2.2.3 Chitin extraction and characterization

β-Chitin (CH) was extracted from fresh squid pens (*Loligo* sp.), kindly supplied by a local fish market. The squids were fished in the Cantabrian Sea (Spain) during the fishing season (March-August). Prior to the chitin isolation procedure, pens were collected and washed with abundant tap water in order to remove soluble organics and impurities. Then, pens were frozen and preserved at -20 ºC until processing. Prior to use, the pens were defrosted and cut into pieces of 1×2 cm^2 and allowed to dry at room temperature. Squid pens were treated with NaOH (1 M) in a relation of 1:20 (w/v) at room temperature for 24 h under continuous stirring to avoid possible degradation and deacetylation of native chitin (Chaussard and Domand, 2004). Subsequently, the sample was filtered and the solid fraction (β-chitin) was washed several times with distilled water until neutral pH was obtained. Finally, the β-chitin was freeze-dried and milled to obtain the powder to be blended with SPI.

Ash content of squid pens was estimated by heating 1 g of sample in a muffle furnace at 525 ºC for 3 h according to TAPPI T211-02 (TAPPI, 2002). Ash content was calculated as follows:

$$\text{Ash content (\%)} = \frac{m_a}{m_s} \times 100$$

where m_a was the weight of ash (g) and m_s was the weight of the moisture-free specimen (g).

Elemental analysis (EA) was carried out using a Euro EA Elemental Analyser. Carbon (C) and nitrogen (N) contents were employed to determine the average degree of acetylation (DA) of chitin, calculated by the following equation (Xu et al., 1996):

$$\overline{DA}(\%) = \frac{(C/N)-5.14}{1.72} \times 100$$

where C/N is the carbon/nitrogen ratio.

2.2.4 Polyphenols extraction and characterization

Polyphenols were extracted from winery grape marc (GM) from the Chardonnay variety, which was obtained from the Marlborough region, New Zealand, during the 2015 vintage. The GM was composed of seeds, grape skin and stems and was maintained at -18 ºC prior to utilization. Before polyphenols extraction, grape marc was defrosted at room temperature and grounded for 1 min using a blender (Model 219706) in order to obtain a fine powder and facilitate the extraction process (Muhamad et al., 2017). Phenolic compounds from grape marc were extracted using the microwave-assisted extraction procedure in a single mode focused CEM reactor (Model Discover, CEM) operating at 2.45 GHz with the ability to control the output power. The temperature in the system was measured using a fibre optic temperature sensor

preventing interaction with the microwaves and their impact on the temperature reading (Gizdavic-Nikolaidis et al., 2010). An external cooling circuit maintained a constant temperature for the mixture and constant irradiation power. All the experiments were run under the same conditions regarding power (93 W), temperature (24 ± 1 °C) and solvent volume (10 mL). Ethanol at different concentrations was employed as a safe and efficient solvent for the extraction of phenolic compounds and the solvent was removed by centrifugation at 60 ºC (Dahmoune et al., 2015; Kerton and Marriot, 2013).

Sugar content of grape marc extract was determined using the Rebelein method (Zoecklein et al., 1995). Firstly, a 2 mg/mL solution was prepared by diluting the grape marc extract in water. Then, 10 mL of copper sulphate (0.168 M) in sulphuric acid (0.005 M), 10 mL of Rochelle salt (0.886 M) in sodium hydroxide (2 M) and 2 mL of the extract solution were combined into a 200 mL Erlenmeyer flask. The mixture was heated until steam was derived and maintained for 1.5 min, after which it was rapidly cooled down in an ice bath. Afterwards, a mixture of 10 mL of potassium iodide (1.81 M) in sodium hydroxide (0.1 M), 10 mL of 16% sulphuric acid, and 10 mL of a 1% starch solution in potassium iodide (0.120 M) added into sodium hydroxide (0.01 M) was incorporated to the solution prepared as abovementioned. The resulting solution was titrated using sodium thiosulphate (0.056 M) in sodium hydroxide (0.05 M) until a creamy white solution was obtained. The amount of sugars was calculated using the following equation:

$$\mathrm{RS}\left(\frac{\mathrm{mg}}{\mathrm{g}}\right) = \frac{\left(28\text{-}28\times\left(\frac{V_S}{V_B}\right)\right)\times 1000}{S}$$

where V_s is the amount of titrant used for the sample in mL, V_B is the amount of titrant used for the blank in mL, and S is the sample concentration in mg/mL.

High performance liquid chromatography (HPLC) was used to determine monosaccharides in grape marc extract. A Jasco LC Net II/ADC chromatograph equipped with a refractive index detector was employed. The analysis was accomplished using a 300 × 7.8 mm CARBOSep CHO-628 LEAD column operated at 80 ºC (mobile phase: deionised water eluted at 0.4 mL/min). The injection volume was 20 µL.

On the other hand, the determination of the phenolic compounds was carried out by Ultrahigh performance liquid chromatography (UHPLC) with an ACQUITY UPLC™ system from Waters, equipped with a binary solvent delivery pump, an autosampler, a column compartment and a PDA detector. A reverse phase column (Acquity UPLC BEH C18 1.7 µm, 2.1 mm × 100 mm) and a precolumn (Acquity UPLC BEH C18 1.7 µm VanGuard™) from Waters were used at 40 °C for the separation. The flow rate was 0.35 mL/min and the injection volume was 2.0 µL. Mobile phases consisted of 0.1% acetic acid in water (A) and 0.1% acetic acid in acetonitrile (B). Separation was carried out under the following conditions: 0.00-1.60 min, 2% B; 1.60-2.11 min, 15% B; 2.11-8.88 min, 8% B; 8.88-9.80 min, linear gradient from 8.00 to 10% B; 9.80-17.00 min, 10% B; 17.00-22.00 min, linear gradient from 10.00 to 20.00% B; 22.00-23.40 min, linear gradient from 20.00 to 23.00% B; 23.40-54.20 min, linear gradient from 23.00 to 60.00% B; 54.20-55.20 min, linear gradient from 60.00 to 100% and finally, washing and re-equilibration of the column prior to the next injection. All samples were kept at 4 °C during the analysis. The wavelength range of the PDA detector was 210-500 nm (20 Hz, 1.2 nm resolution). Benzoic acids were recorded at 240 nm, the flavanols at 280 nm, hydroxycinamic acids at 320 nm and the flavonols and dihidroflavonols at 370 nm.

All mass spectrometry (MS) data acquisitions were performed on a SYNAPT™ G2 HDMS with a quadrupole time of flight (Q-TOF) configuration, equipped with an electro-spray ionization (ESI) source operating in positive and negative mode. The capillary voltage was set to 1.0 kV for both ESI+ and ESI-. Nitrogen was used as the desolvation and cone gas at flow rates of 1000 L/h and 10 L/h, respectively. The source temperature was 120 °C, and the desolvation temperature was 400 °C. A leucine-enkephalin solution (2 ng/μL) in acetonitrile:water (50:50 (v/v) + 0.1% formic acid) was utilized for the lock mass correction and the ions at mass-to-charge ratio (m/z) 556.2771 and 278.1141 in the positive ionization mode from this solution were monitored (0.3 s scan time, 10 s interval, 3 average scans, ± 0.5 Da mass window, 30 V cone voltage, 10 μL/min flow rate). Data acquisition took place over the 50-1200 m/z mass range in resolution mode (FWHM ≈ 20,000) with a scan time of 0.1 s and an interscan delay of 0.024 s. All the acquired spectra were automatically corrected during acquisition based on the lock mass. Before analysis, the mass spectrometer was calibrated with a sodium iodide solution.

To perform MS^E mode analysis, the cone voltage was set to 20 V and the first quadrupole (Q1) operated in a wide band RF mode only. Two discrete and independent interleaved acquisition functions were automatically created. The first function, typically set at 6 eV in trap cell of the T-Wave, collected low energy or unfragmented data, while the second function collected high energy or fragmented data, using 6 eV in trap cell and a collision ramp of 10-40 eV in transfer cell. In both cases, argon gas was used for collision-induced dissociation (CID) and data were recorded in centroid mode.

MS^2 product ion spectra was performed using the protonated molecule $[M+H]^+$ as precursor ion at a cone voltage of 20 V. A collision energy ramp from 10 to 40 eV in trap cell and of 6 eV in transfer cell was used with the aim of acquiring spectra with

different fragmentation degrees from the precursor ion and, thus, obtaining as much structural information as possible. MS/MS data were collected at a range of 50-2000 m/z in centroid mode in the same conditions as described above.

The identification of the phenolic compounds was carried out using the UV-Vis spectrum to assign the phenolic class (Abad-García et al., 2009), the low collision energy MS^E spectrum in positive mode to determine the molecular weight, the high collision energy MS^E and MS^2 product ion spectra to assign the protonated aglycone $[Y0]^+$ and observed fragmentations in order to elucidate other structural details.

2.3 SOY PROTEIN PRODUCTS PREPARATION

2.3.1 Films by solution casting and compression moulding

5 g of SPI and 100 mL of distilled water were mixed and dispersions were heated at 80 ºC for 30 min under magnetic stirring. After that, plasticizer was added, dispersions were maintained at 80 ºC for other 30 min, and the pH was adjusted using NaOH (1 M). Dispersions were poured onto Petri dishes and dried at room temperature for 48 h to obtain SPI-W films.

SPI and plasticizer were blended and the mixture was thermally compacted using a caver laboratory press. The powder was placed between two aluminium plates and it was introduced into the press, previously heated up to 150 °C, and pressed at 12 MPa for 2 min to obtain SPI-D films.

All films were conditioned in a climatic chamber (ACS SU700V) at 25 ºC and 50% relative humidity for 48 h before testing.

Films thickness was measured to the nearest 0.001 mm with a QuantuMike Mitutoyo hand-held digimatic micrometer. The values obtained for each sample at five different locations were averaged. All the films had values between 80 and 100 µm.

2.3.2 Extrusion

First of all, all the components of the mixtures were blended in a Stephan UMC 5 mixer for 5 min at 1500 rpm in order to obtain a good blend. Blends were added into the feed hopper and mixed with water in the barrel of a twin-screw extruder. The MPF 19/25 APV Baker extruder used in this study had 19 mm diameter-barrel and a length/barrel diameter ratio of 25:1. Barrel temperatures were set at 70, 80, 95, and 100 ºC for the four zones from input to output, and die temperature was set at 100 ºC, based on a previous work (Guerrero et al., 2012). Water was pumped directly into the extruder barrel at a constant speed of 250 rpm using a peristaltic 504U MK pump. All trials were carried out using a water speed of 2.68 g/min (0.16 kg/h). The feed rate of extruder was adjusted to 1 kg/h and a single die of 3 mm diameter was used, giving a throughput per unit area of 0.141 kg/h mm^2. The pellets obtained by extrusion were used to obtain films by compression or sheets by injection.

Piece densitiy (PD) of each extrudate was obtained by dividing the mass of the extrudate piece (W_{piece}) by its volume (V_{piece}), which was calculated from its dimensions (diameter, d; and length, l). The dimensions of ten pieces (2 cm long) were measured and PD value was calculated as follows:

$$PD = \frac{W_{piece}}{V_{piece}} = \frac{4 \times W_{piece}}{\pi \times d^2 \times l}$$

Measurements were taken ten times for each composition.

Expansion ratio (ER) is the ratio of the extrudate cross-sectional area to the die orifice cross-sectional area, and was calculated as:

$$ER = \frac{d^2}{d_{die}^2}$$

where d_{die} is the die diameter and d is the extrudate diameter (average of 10 samples).

Specific mechanical energy (SME) of the extrudate samples was determined using the following expression (Hernández-Izquierdo and Krochta, 2008; Hu et al., 1993):

$$SME\ \left(\frac{kJ}{kg}\right) = \frac{\text{Screw speed} \times \text{Power (kW)} \times \text{Torque (\%)}}{\text{Max. screw speed} \times \text{Throughput}\ \left(\frac{kg}{h}\right) \times 100}$$

2.3.3 Injection

The pellets obtained by extrusion were injection-moulded into Type I ASTM tensile specimens by using a Haake MiniJet II injection-moulding machine. The injection moulded specimens were obtained at 120 ºC using a pressure of 450 bar. All samples were conditioned in a biochamber (ACS Sunrise 700V) at 25 ºC and 50% relative humidity for 48 h before testing.

2.4 PHYSICOCHEMICAL CHARACTERIZATION

2.4.1 Moisture content (MC), water uptake (WU) and total soluble matter (TSM)

In order to calculate MC, three samples of each composition were weighed (m_w), dried in an air circulating oven at 105 ºC for 24 h and reweighed (m_0). MC was calculated as:

$$MC\ (\%) = \frac{m_w - m_0}{m_w} \times 100$$

Then, samples were immersed into 30 mL distilled water at room temperature. After 1-8 and 24 h, the samples were taken out, wiped, weighed (m_t) and immersed into water again. WU values were calculated as:

$$WU\ (\%) = \frac{m_t - m_0}{m_0} \times 100$$

After the immersion in distilled water for 24 h, the samples were dried in an air circulating oven at 105 ºC for 24 h and weighed (m_f). TSM values were calculated by the following expression:

$$TSM\ (\%) = \frac{m_0 - m_f}{m_0} \times 100$$

All values were calculated by triplicate for each composition.

2.4.2 Fourier transform infrared (FTIR) spectroscopy

FTIR spectra of samples were collected on a Nicolet Nexus spectrometer using an ATR Golden Gate (Specac) accessory. A total of 32 scans were performed at 4 cm^{-1} resolution. Measurements were recorded between 4000 and 800 cm^{-1}.

2.5 THERMAL CHARACTERIZATION

2.5.1 Differential scanning calorimetry (DSC)

DSC experiments were performed using a Mettler Toledo DSC 822. About 4 mg of sample were heated from -50 ºC to 250 ºC at a rate of 10 ºC/min under nitrogen

atmosphere to avoid oxidation reactions. Sealed aluminium pans were used to prevent mass loss during the experiment.

2.5.2 Thermogravimetric analysis (TGA)

TGA was carried out using a Mettler Toledo SDTA 851 equipment. All specimens were scanned from room temperature to 800 ºC at a heating rate of 10 ºC/min. All TGA tests were carried out in a nitrogen environment to avoid thermo-oxidative reactions.

2.5.3 Dynamic mechanical analysis (DMA)

Thermo-mechanical measurements were performed using a DMA Explexor 100N, Gabo Qualimeter. Experiments were performed in a temperature range from -100 ºC to 120 ºC at a heating rate of 2 ºC/min. The measurements were carried out under tension at a constant frequency of 1 Hz and the strain applied was fixed at 0.05%.

2.6 OPTICAL PROPERTIES

2.6.1 Colour measurement

Colour was determined with the colorimeter Konica-Minolta CR-400 Croma Meter. Specimens were placed on the surface of a white standard plate (calibration plate values L^*= 97.39, a^*= 0.03 and b^*= 1.77) and L^*, a^*, b^* colour parameters were measured using the CIELAB colour scale: L^*= 0 (black) to L^*= 100 (white), -a^* (greenness) to +a^* (redness), and –b^* (blueness) to +b^* (yellowness).

Measurements were taken 10 times for each sample and total colour difference (ΔE^*) was referred to a pattern sample and calculated by the following equation (Francis and Clydesdale, 1975):

$$\Delta E^{*} = \sqrt{\left(\Delta L^{*}\right)^{2} + \left(\Delta a^{*}\right)^{2} + \left(\Delta b^{*}\right)^{2}}$$

2.6.2 Gloss measurement

Gloss was measured at 60 º incidence angle according to the ASTM D523-14 (ASTM, 2014), using a Multi Gloss 268 plus gloss meter (Konica-Minolta). Measurements were taken 10 times for each sample.

2.6.3 Ultraviolet-visible (UV-vis) spectroscopy and transparency

The spectrophotometer UV-Jasco (Model V-630) was used to determine light barrier properties of samples. The light absorption was measured at wavelengths from 200 nm to 800 nm and film transparency (T) was calculated by the following equation:

$$T = \frac{A_{600}}{L}$$

where, A_{600} is the absorbance at 600 nm and L is the film thickness (mm). For this, a rectangular sample was cut and directly clamped between two spectrophotometer cells. Three specimens were tested for each composition.

2.7 BARRIER PROPERTIES

2.7.1 Water contact angle (WCA)

WCA measurements were performed at room temperature using a contact angle system (model OCA 20). A sample was laid on a movable sample stage and about 3 µL of distilled water was placed onto the film surface to estimate the hydrophobic character. The contact angle images were recorded immediately or after 5 and 10 min of

dropping the water on the sample, using SCA20 software. Five measurements were made for each composition.

2.7.2 Water vapour permeability (WVP)

WVP was determined in a controlled humidity environment chamber (PERME^{TM} W3/0120), according to ASTM E96-00 (ASTM, 2000). Circles of 7.40 cm diameter, with a test area of 33 cm^2, were cut for each sample. The set up was subjected to a temperature of 38 ºC and a relative humidity of 90%. Water vapour transmission rate (WVTR) was calculated by the following expression:

$$\text{WVTR}\left(\frac{\text{g}}{\text{s cm}^2}\right) = \frac{\text{G}}{\text{t} \times \text{A}}$$

where G is the change in weight (g), t is time (s), and A is the test area (cm^2). WVP was calculated as:

$$\text{WVP}\left(\frac{\text{g}}{\text{cm s Pa}}\right) = \frac{\text{WVTR} \times \text{L}}{\Delta\text{P}}$$

where L is the thickness of the test specimen (cm) and ΔP is the partial pressure difference of the water vapour across the sample (Pa). WVP was calculated and reported for three specimens of each sample.

2.7.3 Oil permeability (OP)

The measurement of OP for each sample was based on the method described by Hanani et al. (2012). Briefly, filter papers (70 mm diameter) were conditioned at 25 ºC and 50% relative humidity and weighed. Samples were placed on a filter paper and sunflower oil was spread onto the sample without exceeding the edge of the sample.

After 24 h, the sample was removed and the filter was reweighed. Measurements were carried out in triplicate for each composition.

2.7.4 Oxygen transmission rate (OTR)

OTR was analysed with a MOCON OX-TRAN Model 2/21 gas permeability tester, according to ASTM D3985 (ASTM, 2010). Samples were tested at 23 °C, 760 mm Hg and 50% relative humidity. Measurements were carried out in triplicate for each composition.

2.8 MECHANICAL PROPERTIES

Elastic modulus (EM), tensile strength (TS) and elongation at break (EB) were measured according to ASTM D638-03 (ASTM, 2003), using an electromechanical testing system (MTS Insight 10). The samples were cut into strips of 4.75 mm × 22.25 mm and the crosshead rate was 1 mm/min. Five samples were tested for each composition.

2.9 MORPHOLOGICAL CHARACTERIZATION

2.9.1 Optical microscopy (OM)

OM was carried out using a Nikon Eclipse E600 microscope with a magnification of ×500 to observe the morphology of the cross-section of each sample.

2.9.2 Scanning electron microscopy (SEM)

The morphology of the cross-section of the films was analysed using a Hitachi S-4800 scanning electron microscopy. The cross-section was prepared using mechanical means like conventional cutter. Then, samples were mounted on a metal stub with

double-side adhesive tape and coated under vacuum with gold, using a JEOL fine-coat ion sputter JFC-1100 in an argon atmosphere prior to observation. All samples were examined using an accelerating voltage of 15 kV.

2.10 X-RAY ANALYSES

2.10.1 X-ray diffraction (XRD)

XRD was performed with a diffraction unit PANalytical Xpert PRO, operating at 40 kV and 40 mA. The radiation was generated from Cu-Kα (λ=1.5418 Å) source. The diffraction data were collected from 2θ values from 2 º to 50 º, where θ is the angle of incidence of the X-ray beam on the sample. The crystalline index (CrI) of samples was calculated with the following equation:

$$Cr_I = \frac{I_{110}\text{-}I_{am}}{I_{110}} \times 100$$

where I_{110} was the maximum intensity of the (1 1 0) plane at 2θ ≅ 20 º and I_{am} was the intensity of the amorphous region at 2θ ≅ 16 º.

2.10.2 X-ray photoelectron spectroscopy (XPS)

XPS was performed in a SPECS spectrometer using a monochromatic radiation equipped with Al Kα (1486.6 eV). The binding energy was calibrated by Ag 3d5/2 peak at 368.28 eV. All spectra were recorded at 90 º take-off angle. Survey spectra were recorded with 1.0 eV step and 40.0 eV analyser pass energy and the high resolution regions with 0.1 eV step and 20.0 eV pass energy. All core level spectra were referred to the C 1s peak at 284.6 eV. Spectra were analysed using the CasaXPS 2.3.16 software, and peak areas were quantified with a Gaussian-Lorentzian fitting procedure.

2.11 ANTIOXIDANT ACTIVITY

2.11.1 Total phenolic content (TPC)

TPC was measured by Folin-Ciocalteu method. In a 4 mL cuvette, 3.16 mL of deionised water was added to 20 µL of the extract. Then, 200 µL of Folin-Ciocalteu reagent was incorporated, mixed well and left to react for 3 min. After that time, 600 µL of 20% sodium carbonate solution was added. The resulting solutions were shielded from light and left at room temperature for 90 min before the absorbance was measured at 765 nm. Gallic acid was employed to create a standard curve, thus the results were obtained as mg of gallic acid equivalents per mL of extract (mg GAE/mL extract).

2.11.2 Determination of antioxidant activity

The antioxidant activity of the extract was measured using the DPPH radical scavenging assay, as describied by Liu et al. (2015) with some modifications. Firstly, a solution of DPPH in ethanol at a concentration of 63.4 µmol/L was prepared. In a 4 mL cuvette, 3.9 mL of the DPPH solution and 0.1 mL of extract were added, mixed well and protected from light at room temperature for 30 min. After that time, the absorbance of each sample was measured at 515 nm using a spectrophotometer (Shimadzu 1700 UV/Vis). The percentage of free radicals scavenged by DPPH was calculated using the following equation:

$$\text{DPPH(\% inhibition)} = \frac{(A_{DPPH} - A_{sample})}{A_{DPPH}} \times 100$$

where A_{DPPH} is the absorbance of the DPPH solution at 515 nm, and A_{sample} is the absorbance of each extract at 515 nm.

2.12 RESPONSE SURFACE METHODOLOGY (RSM)

2.12.1 Experimental design for formulation optimization

With a view to maximizing the extraction of phenolic compounds, the effect of three independent factors on TPC and DPPH radical scavenging responses was studied under a RSM scheme. The three inputs were ethanol content, solid content, and time, coded at three levels: low (-1), medium (0) and high (+1). The selected values were based on a preliminary study: 30, 45 and 60% for the ethanol concentration, 1.0, 1.5 and 2.0 g for the solid mass, and 5, 10 and 15 min for the extraction time. A Box-Behnken design was applied due to its economy regarding the number of necessary experimental runs. The design variables selected in this study are shown in **Table 9.1 (Chapter 9)** with actual and coded levels along with response variables. The corresponding Box-Behnken design comprises 12 runs, and 4 additional runs were included at the centre of the design to evaluate the pure error. All runs were made in random order. For each response variable, a full-quadratic polynomial model was created by multiple regression technique in order to determine subsequently the optimal formulation that maximizes both responses:

$$y=b_0+\sum_{i=1}^{n} b_i x_i+\sum_{i=1}^{n} b_{ii} x_i^2+\sum\sum_{i<j=2}^{n} b_{ij} x_i\, x_j$$

where, b_0 was the constant coefficient or intercept, b_i were the first order linear coefficients, b_{ii} were the quadratic coefficients, and b_{ij} (with $i \neq j$) were the second order interaction coefficients.

2.12.2 Statistical analysis and response optimization

An analysis of variance (ANOVA) was conducted to evaluate the quality of the fitted quadratic models. The significance ($p < 0.05$) of the regression coefficients was evaluated by determining the F value. For the validation of the model, the coefficient of determination, R^2, as well as the significance values of the model and of the lack of fit were calculated. To be reliable, the model must be statistically significant to a 95% confidence level ($p < 0.05$), while the lack of fit should be non-significant ($p \geq 0.05$). An optimization of the two response variables was then carried out to determine the optimal maximum responses, allowing the same weighting for both. The desirability function approach introduced by Derringer and Suich (1980) was used for this purpose.

Data analysis, ANOVA, and linear regression, including responses optimization, were performed by using Minitab 17 software.

2.13 ENVIRONMENTAL ASSESSMENT

The environmental analysis was carried out according to ISO 14040 guidelines and recommendations (ISO, 2006). The software used was SimaPro. On one hand, the data relating to polypropylene (PP) films were obtained from Ecoinvent database, developed by Swiss Centre of Life Cycle Inventories, available in SimaPro. On the other hand, the inventory analysis of soy protein films was carried out taking into account the materials used in the laboratory and the energy consumption regarding the manufacture step, although the database of the software was also used for data relating to the raw materials and their conversion processes. The glycerol employed as plasticizer was considered as a co-product of the production of soybean oil to obtain biodiesel and esterification process of soybean oil to methyl ester and glycerol in the

process of biodiesel production was considered. Data were obtained from Ecoinvent database. The functional unit considered in this study was 1 m^2 of film of 80 μm.

Based on inventory data, environmental impacts were evaluated according to the Hierarchist version of Eco-Indicator 99. The impact categories are classified in three damage categories: human health, ecosystem quality, and resources. Human health category groups six impact categories: carcinogens, respiratory organics, respiratory inorganics, climate change, radiation, and ozone layer. Ecosystem quality considers three impact categories: ecotoxicity, acidification/eutrophication, and land use. Finally, the damage category of resources considers minerals and fossil fuels. Normalisation was performed on European level with updates for the most important emission (Goedkoop and Spriensma, 2011). Normalised values were determined by dividing characterization factors by a magnitude for each impact category.

2.14 STATISTICAL ANALYSIS

Data were subjected to one-way analysis of variant (ANOVA) by means of a SPSS computer program (SPSS Statistic 23.0). Post hoc multiple comparisons were determined by the Tukey's or Duncan´s test with the level of significance set at $p < 0.05$. Data is presented as mean values ± the standard error of the mean.

3

chapter

EFFECT OF PLASTICIZER, pH AND PROCESSING METHOD IN SOY PROTEIN-BASED FILMS

Garrido T., Etxabide A., Leceta I., Cabezudo S., de la Caba K, Guerrero P. (2014)

Valorization of soya by-products for sustainable packaging. Journal of Cleaner Production, 64, 228-233

Garrido T., Etxabide A., Peñalba M., de la Caba K, Guerrero P. (2013)

Preparation and characterization of soy protein thin films: Processing-properties correlation. Materials Letters, 105, 110-112

SUMMARY

Biopolymers produced from natural resources such as soy proteins are regarded as attractive alternatives since they are renewable and biodegradable; moreover, they are abundant, available and have excellent film forming abilities. However, soy protein films without any additive have a brittle behaviour, which makes processing difficult; thus, addition of plasticizers is an effective way to obtain flexible SPI-based films. In this chapter, the final properties of plasticized soy protein films prepared by solution casting or compression were analysed, and the effects of plasticizer content and processing conditions were studied. Furthermore, designing biobased packaging films involves many considerations to manufacture sustainable packaging, including environmental aspects; therefore, Life Cycle Assessment (LCA) was employed as a key tool to measure environmental impact from the extraction of raw materials to ultimate disposal.

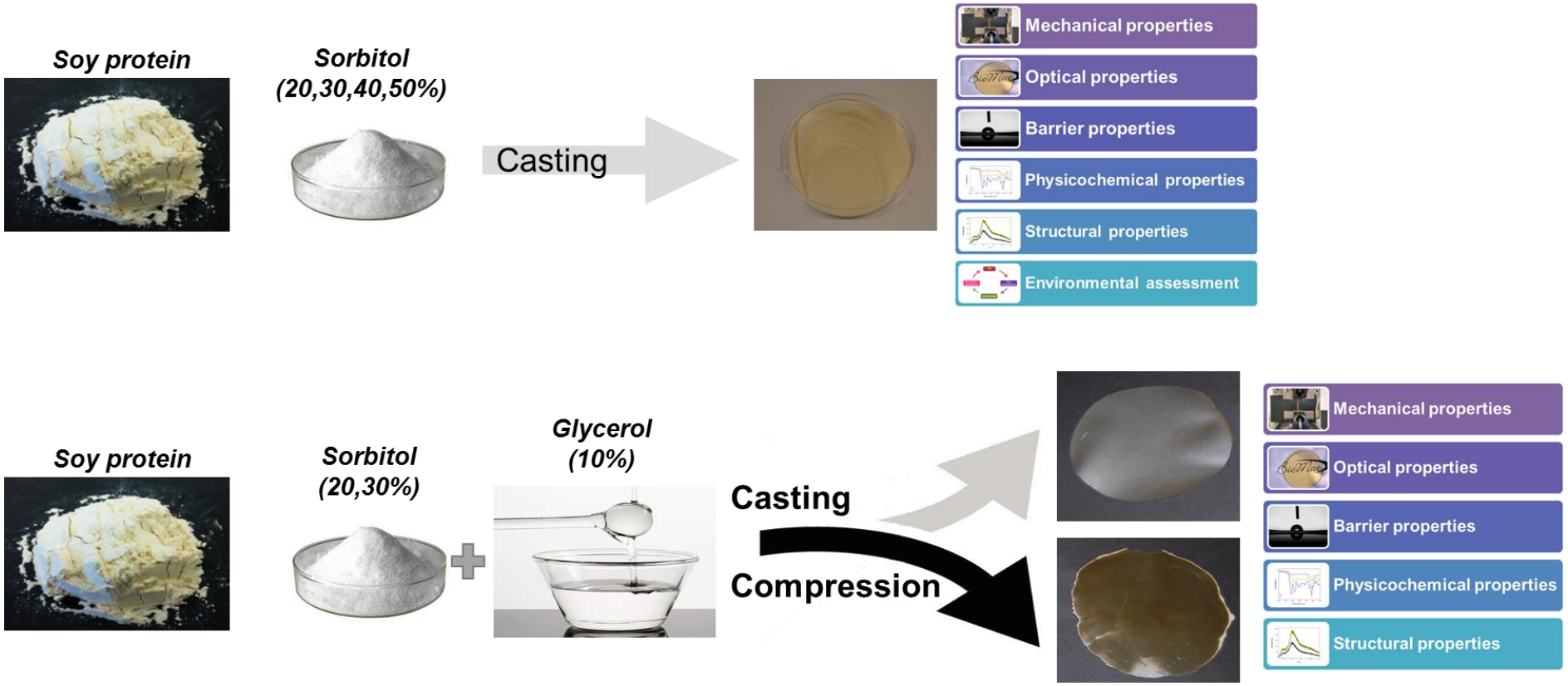

Figure I. Graphical abstract of Chapter 3.

3.1 FILM PREPARATION

On the one hand, 5 g of SPI and 100 mL of distilled water were mixed and dispersions were heated at 80 ºC for 30 min under magnetic stirring. Then, 20, 30, 40 and 50 wt % sorbitol (Sor) (based on SPI dry basis) was added, dispersions were maintained at 80 ºC for other 30 min, and the pH was adjusted to 7 and 10 with NaOH (1 M). Dispersions were poured into Petri dishes and dried at room temperature for 48 h to obtain films. These films prepared with 20, 30, 40 and 50 wt % sorbitol were designated as Sor20, Sor30, Sor40, and Sor50, respectively.

On the other hand, 5 g of SPI and 100 mL of distilled water were mixed and dispersions were heated at 80 ºC for 30 min under magnetic stirring. Then, 20 or 30 wt % sorbitol and 10 wt % glycerol (Gly) were added to SPI dispersions and maintained at 80 ºC for other 30 min. Dispersions were poured into Petri dishes, dried at room temperature, and peeled from the dishes to obtain casting films (W). In addition, 20 or 30 wt % sorbitol and 10 wt % glycerol were mixed with SPI and thermally compacted using a caver laboratory press (Atlas^{TM}). The powder was deposited between two aluminium sheets and was introduced into the press previously heated at 150 ºC, and pressed at 12 MPa for 2 min to obtain compression films (D). Films were designated as Sor20Gly10-W, Sor30Gly10-W, Sor20Gly10-D, and Sor30Gly10-D as a function of sorbitol content and preparation method employed.

3.2 RESULTS AND DISCUSSION

3.2.1 Film characterization

First of all, functional properties of soy protein-based films plasticized only with sorbitol and manufactured via solution casting were assessed.

The measurement of optical properties is very relevant due to the direct influence in the appearance of films (Monedero et al., 2009). It is well known that soy protein provides a characteristic yellowish colour to the films (Su et al., 2012), which was measured by the b^* parameter displayed in **Table 3.1**. This parameter increased with pH and sorbitol content. Moreover, ΔE^* showed that there was an increase ($p < 0.05$) of colour difference between the films with 20 wt % sorbitol prepared at pH 7, taken as the reference film, and the rest of the films, especially with those prepared at pH 10.

Table 3.1. Colour parameters of SPI films prepared with different sorbitol contents at pH 7 and pH 10.

pH	Film	L^*	a^*	b^*	ΔE^*
7	**Sor20**	92.58 ± 0.11^{c}	0.05 ± 0.05^{d}	14.87 ± 0.31^{a}	
	Sor30	93.22 ± 0.45^{c}	-0.42 ± 0.07^{c}	14.27 ± 1.02^{a}	0.99^{a}
	Sor40	92.03 ± 0.14^{bc}	-0.01 ± 0.04^{d}	15.61 ± 0.54^{b}	0.92^{a}
	Sor50	88.83 ± 0.18^{a}	0.36 ± 0.13^{e}	19.46 ± 1.41^{c}	5.94^{c}
10	**Sor20**	90.75 ± 0.18^{b}	-0.56 ± 0.13^{c}	17.85 ± 0.70^{c}	3.55^{b}
	Sor30	89.07 ± 0.16^{a}	-0.96 ± 0.04^{b}	22.98 ± 0.12^{d}	8.89^{d}
	Sor40	90.36 ± 0.12^{b}	-1.44 ± 0.09^{a}	21.25 ± 0.47^{c}	6.92^{c}
	Sor50	89.31 ± 0.13^{a}	-1.11 ± 0.07^{b}	22.71 ± 0.44^{d}	8.57^{d}

[ad]Two means followed by the same letter in the same column and in the same section are not significantly ($p > 0.05$) different thought the Tukey's multiple range test.

Another parameter often used to evaluate the appearance of films is gloss, which describes the capacity of a surface to reflect direct light. Gloss values were measured at 60 º incidence angle and are shown in **Figure 3.1**. As can be seen, the gloss of the films

was independent of pH ($p < 0.05$). It is worth noting that all values were around 10, which is considered low gloss, indicating the surface roughness.

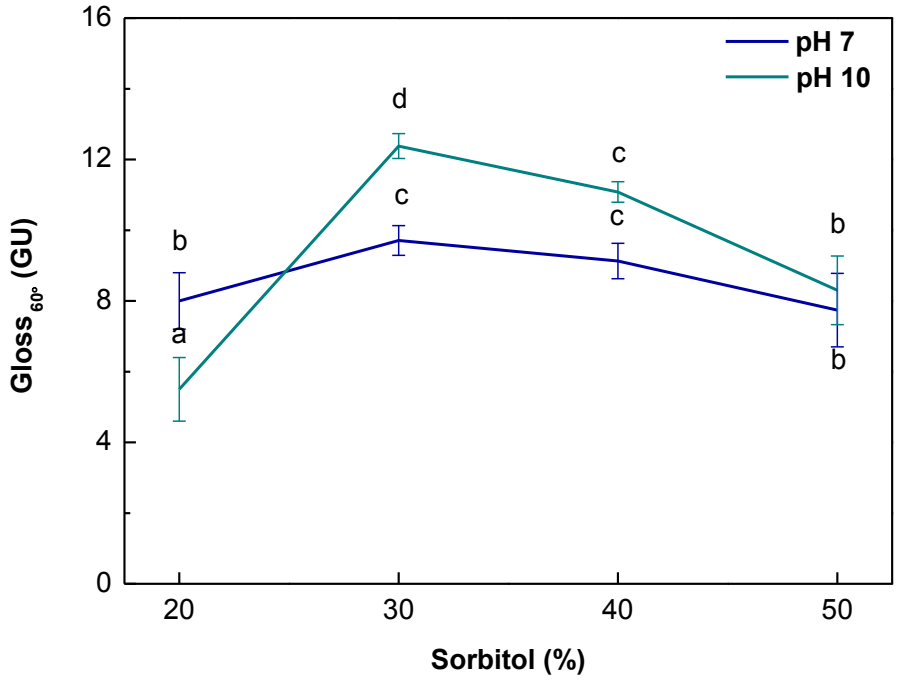

Figure 3.1. Gloss values measured at 60 º as a function of sorbitol content and pH. [ad]Two means followed by the same letter in the same column are not significantly ($p > 0.05$) different thought the Tukey's multiple range test.

Additionally, UV-vis spectroscopy was used to measure the film transparency. These values are shown in **Table 3.2**. It can be observed that all films exhibited high transparency ($p < 0.05$), especially the films prepared with higher content of sorbitol, at both pH 7 and 10, showing similar transparency values to those of low density polyethylene (LDPE), a commercial film widely used for packaging.

UV spectroscopy was also used to measure barrier properties against UV light. **Table 3.2** shows light transmission values of the films prepared with different sorbitol contents at different pHs. All films showed low transmission values between 200 and 280 nm. Hence, the films have excellent barrier properties in the UV region probably owning to tyrosine (Tyr 3.79% in SPI), phenylalanine (Phe 5.18% in SPI) and tryptophan

(Trp 1.10% in SPI), which are well known chromophores that can absorb the light at wavelength below 300 nm (Li et al., 2004). These results suggest that soy protein films might be able to retard the oxidation of the packaged product better than synthetic films such as LDPE or orientated polypropylene (OPP).

Table 3.2. Light transmission (%) and transparency (T) (A_{600}/mm) values of SPI films prepared with different sorbitol contents at pH 7 and pH 10, in comparison with films based on synthetic polymers.

pH	Film	Wavelength (nm)								T
		200	**280**	**350**	**400**	**500**	**600**	**700**	**800**	
7	**Sor20**	0.007	0.013	2.153	7.549	10.485	11.604	12.199	12.497	6.93[d]
	Sor30	0.011	0.030	2.473	7.250	9.877	10.992	11.681	12.109	6.80[d]
	Sor40	0.016	0.026	3.084	10.661	15.653	18.178	20.029	21.403	3.94[a]
	Sor50	0.005	0.010	0.896	4.442	6.995	8.064	8.730	9.171	4.17[a]
10	**Sor20**	0.006	0.014	1.772	6.089	12.578	14.260	15.167	15.592	5.75[c]
	Sor30	0.008	0.018	1.582	6.296	13.657	15.397	16.274	16.626	5.08[c]
	Sor40	0.004	0.019	1.477	6.033	13.660	15.418	16.291	16.654	4.56[b]
	Sor50	0.017	0.019	1.023	4.167	9.355	10.572	11.197	11.471	4.49[b]
	OPP	4.216	71.789	81.088	83.330	86.097	87.507	88.253	88.714	1.57
	LDPE	0.452	27.645	35.760	39.976	45.530	49.807	53.237	56.329	4.26

[ad]Two values followed by the same letter in the same column are not significantly ($p > 0.05$) different thought the Tukey's multiple range test.

Apart from optical properties, water resistance is also an important functional property for packaging films. Water resistance was evaluated by measuring the contact angle of water on the film surfaces. Water contact angle values are good indicators of the degree of hydrophobic character of films, being higher when hydrophobic character is higher, thus the final state of the water drop on the film surface can be taken as an indication of surface wettability. It is accepted that protein films with contact angle values higher than 65 º exhibit hydrophobic character (Vogles, 1998). The contact angle values for SPI films are shown in **Table 3.3**. At both pH 7 and 10 contact angle values were higher than 65 º, in fact, higher than 80 º, so that all films showed high hydrophobicity. Moreover, the hydrophobic character increased with sorbitol content ($p < 0.05$) and pH

($p < 0.05$), indicating a better protein-sorbitol interaction at basic pH and therefore, less exposure of the polar groups toward the surface.

Table 3.3. Contact angle values as a function of sorbitol contents and pH.

pH	Film	Contact Angle (º)
7	**Sor20**	84.41 ± 3.65^{ab}
	Sor30	89.05 ± 6.01^{abc}
	Sor40	96.27 ± 3.60^{bc}
	Sor50	99.73 ± 1.44^{cd}
10	**Sor20**	80.68 ± 7.68^{a}
	Sor30	92.68 ± 4.12^{abc}
	Sor40	101.33 ± 3.02^{cd}
	Sor50	112.03 ± 2.78^{d}

[ad]Two values followed by the same letter in the same column are not significantly ($p > 0.05$) different thought the Tukey's multiple range test.

In order to evaluate protein-plasticizer interactions, FTIR analysis was carried out. **Figure 3.2** shows FTIR spectra of the films prepared with 30 wt % sorbitol at different pHs. The main absorption bands are located in the spectral range from 800 cm^{-1} to 1630 cm^{-1}. The bands of the protein are related to C=O stretching at 1630 cm^{-1} (amide I), N-H bending at 1530 cm^{-1} (amide II) and C-N stretching at 1230 cm^{-1} (amide III) (Schmidt et al., 2005). The main absorption bands of sorbitol are related to the five bands corresponding to the vibrations of C-C and C-O bonds. The bands at 850 cm^{-1}, 940 cm^{-1}, and 1000 cm^{-1} are attributed to C-C bonds, whilst the ones at 1050 cm^{-1} and 1100 cm^{-1} correspond to C-O (Basu et al., 2011). It can be seen that the region corresponding to the three amide bands did not show any change as a function of the pH employed, indicating that sorbitol did not react with the protein through covalent linkages. However, the relative intensity between the bands at 1050 cm^{-1} and 1100 cm^{-1}, attributed to C-O bonds, changed, indicating that sorbitol would interact with the protein through hydrogen bonding.

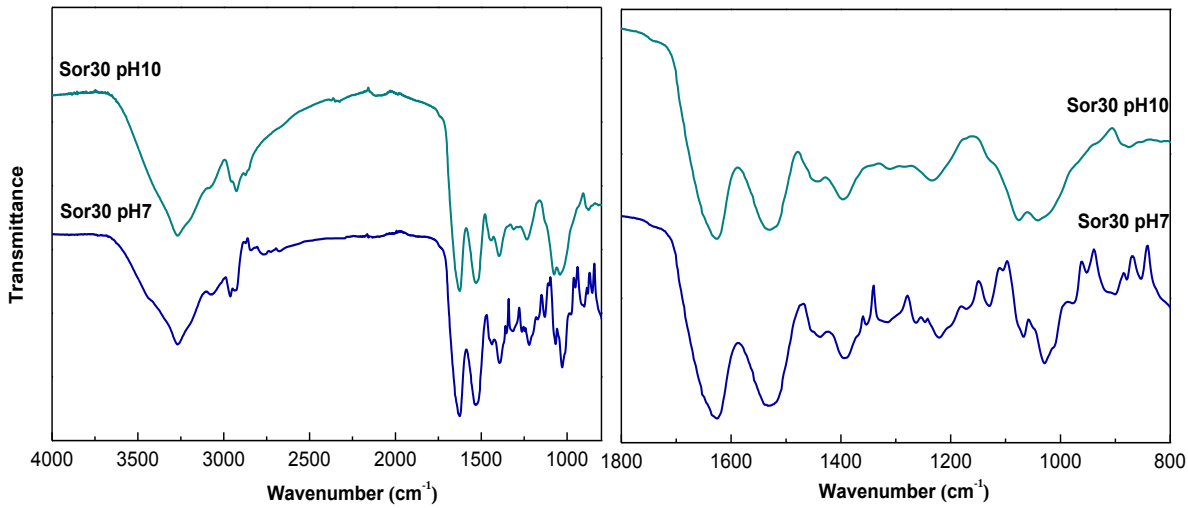

Figure 3.2. FTIR spectra of soy protein films prepared with 30 wt % sorbitol as a function of pH.

To determine the change in the structure of the films prepared with different contents of sorbitol at different pHs, XRD was carried out. **Figure 3.3** shows that all samples exhibited a peak with a maximum at $2\theta = 21$ º, characteristic of SPI and related to the slight order in the protein, as also shown by Guerrero et al. (2011) for soy protein films plasticized with glycerol. It can be observed that at basic pH and when the sorbitol content was higher, the intensity of the band increased, which means that the degree of structural order also increased, which would be indicative of SPI-sorbitol interactions.

Finally, mechanical properties of the films are shown in **Table 3.4**. The films with 20 wt % sorbitol were brittle and it was no possible to cut samples for mechanical analysis. The results for the rest of the films showed that an increase in sorbitol content yielded a decrease ($p < 0.05$) in tensile strength at both pH 7 and 10.

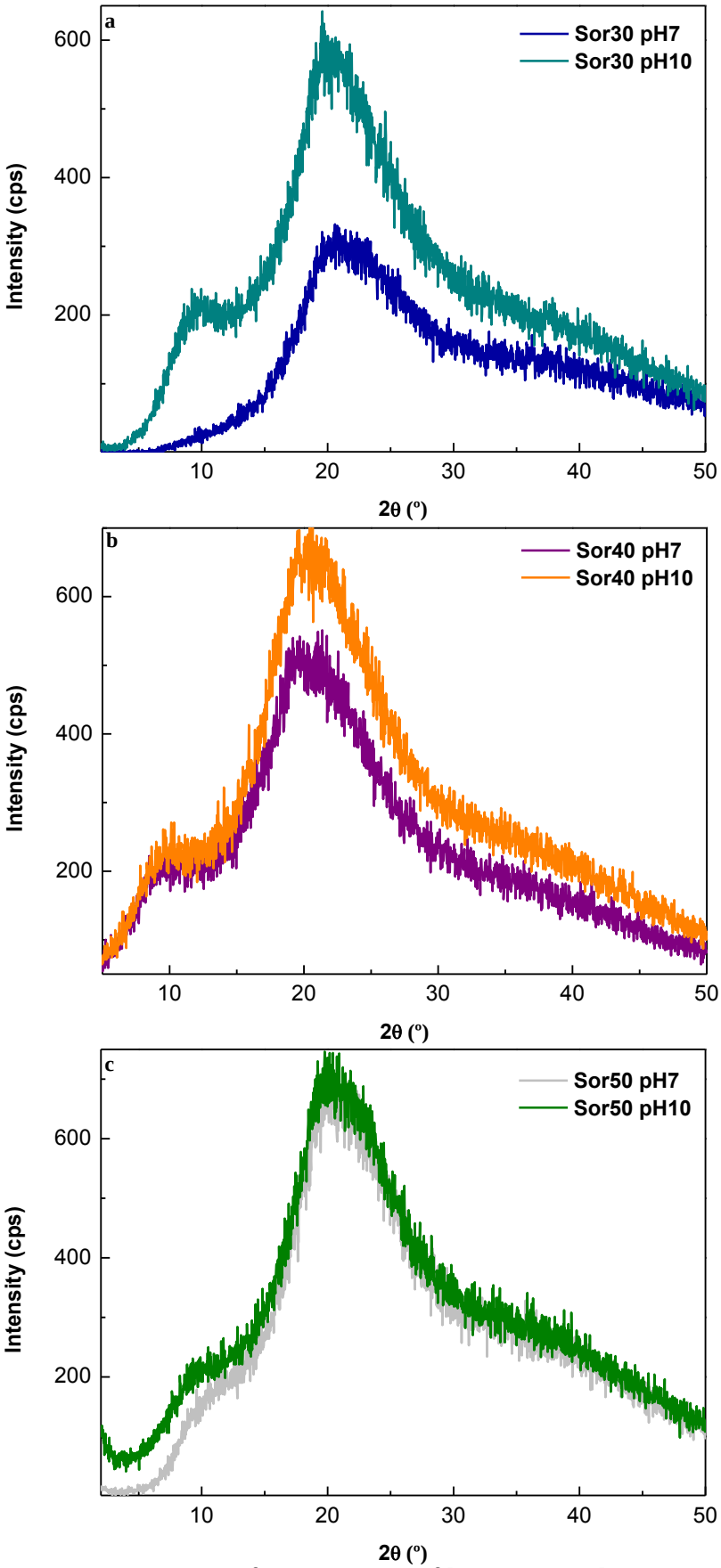

Figure 3.3. XRD patterns of soy protein films prepared at pH 7 and 10 with a) 30 wt % sorbitol, b) 40 wt % sorbitol, and c) 50 wt % sorbitol.

The strong interactions among the chains of soy protein molecules restrict segment rotation and molecular mobility, which lead to an increase in tensile strength. However, when sorbitol was added, these interactions were disrupted and molecular mobility was increased, decreasing tensile strength but increasing elongation at break. The elongation at break increased ($p < 0.05$) with the percentage of sorbitol, mainly at pH 10, due to the higher unfolding of the protein, which permitted higher interaction between hydroxyl groups of sorbitol and polar groups of soy protein, as shown by FTIR results, thus decreasing intermolecular interactions between protein chains, increasing the free volume and improving the flexibility of the material. Moreover, the increase in the plasticizer content increased moisture content of the film, which also contributes to the reduction of the forces between chains, as shown by Guerrero and de la Caba (2010) for soy protein films processed at different pHs.

Table 3.4. Tensile strength (TS) and elongation at break (EB) of SPI films prepared with different sorbitol contents at pH 7 and pH 10.

pH	Film	EB (%)	TS (MPa)
7	**30Sor**	3.95 ± 0.63^{a}	5.91 ± 0.27^{cd}
	40Sor	48.79 ± 7.64^{c}	6.34 ± 0.53^{d}
	50Sor	24.91 ± 10.62^{b}	1.55 ± 0.08^{a}
10	**30Sor**	29.66 ± 9.11^{b}	7.50 ± 1.00^{e}
	40Sor	105.61 ± 5.21^{c}	5.31 ± 0.61^{c}
	50Sor	117.83 ± 22.92^{d}	2.90 ± 0.32^{b}

[ad]Two values followed by the same letter in the same column are not significantly ($p > 0.05$) different thought the Tukey's multiple range test.

After the assessment of the functional properties of SPI-based films prepared at pH 7 and 10 with different contents of sorbitol, it was concluded that the best results were obtained at pH 10, at which the protein unfolding is better in order to promote protein-plasticizer interactions. Moreover, a total amount of 30 or 40 wt % of plasticizer could be an optimal quantity to obtain films with suitable properties. Taking the above into

consideration, SPI films were prepared at pH 10, employing 20 or 30 wt % sorbitol and adding 10 wt % glycerol.

Apart from the plasticizer, the processing of the polymer is also an important factor to consider to improve the properties of the films. Although the characterization of SPI films obtained by solution casting has been published in the literature (Lee and Kim, 2010; Rhim et al., 2006; Wang et al., 2012), the comparison of the properties achieved between solution casting and compression moulding has not been widely analysed. Thus, in this chapter, films prepared using these processing methods were analysed and the differences observed in optical, barrier, and mechanical properties were evaluated.

Firstly, optical properties of the films were analysed, and colour, gloss and transparency values of the films are shown in **Table 3.5**. It is worth noting that temperature affected the colour of the films. The films processed by compression exhibited higher b^* ($p < 0.05$) and ΔE^* values ($p < 0.05$) than casting films, indicating a significant increase in the typical yellowish of SPI. Moreover, films processed by compression were glossier ($p < 0.05$), indicating the formation of a smoother surface due to the application of pressure in the manufacture process. Regarding transparency, the films prepared by compression showed higher transparency ($p < 0.05$) and the values obtained were similar to the values of commercial films such as OPP.

Table 3.5. Optical properties of SPI films prepared by casting and compression.

Film	L^*	a^*	b^*	ΔE^*	$Gloss_{60^o}$ (GU)	T
Sor20Gly10-W	88.81 ± 1.37^a	-0.89 ± 0.06^a	20.24 ± 0.49^a	3.09^a	10.42 ± 0.61^a	6.57^a
Sor30Gly10-W	90.01 ± 0.75^a	-1.78 ± 0.12^b	21.43 ± 1.95^a	3.86^a	9.36 ± 0.32^a	3.44^b
Sor20Gly10-D	82.02 ± 0.56^b	1.42 ± 0.61^b	45.20 ± 1.80^b	28.77^b	18.10 ± 3.83^b	2.06^c
Sor30Gly10-D	79.53 ± 0.22^b	2.93 ± 0.77^c	47.73 ± 1.89^b	32.11^b	17.40 ± 2.94^b	1.51^c

[ac]Two means followed by the same letter in the same column are not significantly ($p > 0.05$) different thought the Tukey's multiple range test.

The resistance against water was evaluated by measuring the water contact angle on the film surfaces. The water contact angle values for SPI films are shown in **Figure 3.4**. As can be seen, the contact angle values of the films prepared by casting were higher ($p < 0.05$) than 90 º, so that these films showed high hydrophobicity probably due to the fact that both components have more time to rearrange during film formation, promoting protein-sorbitol interactions. Moreover, the hydrophobic character increased ($p < 0.05$) with sorbitol content, indicating less exposure of polar groups toward the surface.

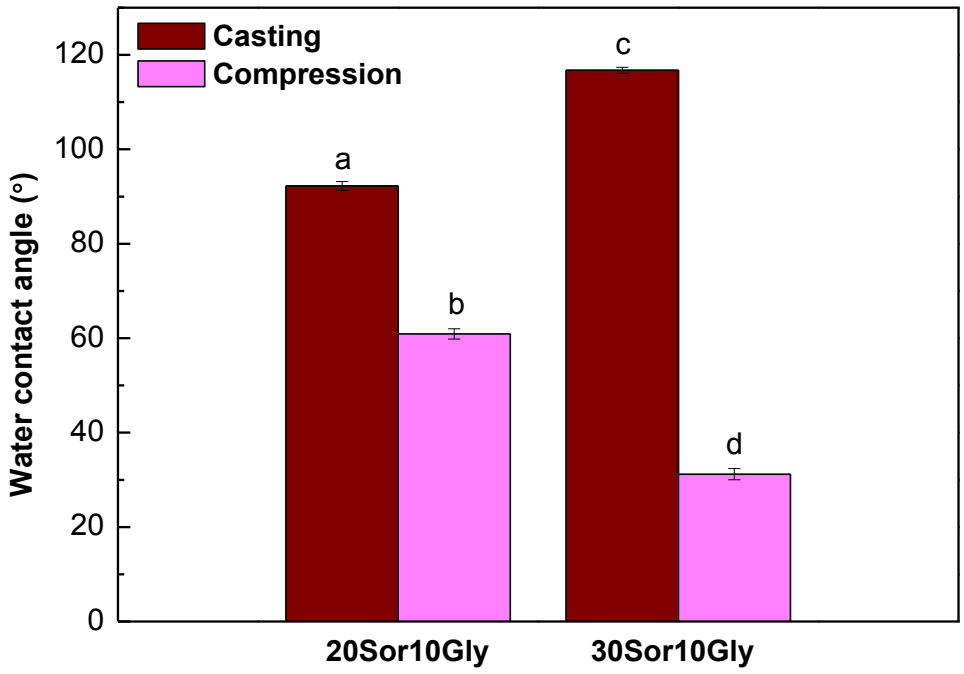

Figure 3.4. Water contact angle values for SPI films processed by casting and compression. [ad]Two means followed by the same letter in the same line are not significantly ($p > 0.05$) different thought the Tukey's multiple range test.

In addition, the films prepared by casting showed better mechanical properties than the films prepared by compression, higher elongation at break with similar tensile strength ($p < 0.05$), as can be seen in **Table 3.6**. Furthermore, results showed that the elongation at break increased ($p < 0.05$) with the content of sorbitol, indicating that the increase in sorbitol content caused a decrease in intermolecular interactions between protein chains and an increase in the free volume, improving the flexibility of the material.

Table 3.6. Elongation at break (EB) and tensile strength (TS) of SPI films processed by casting and compression.

Film	EB (%)	TS (MPa)
Sor20Gly10-W	76.37 ± 5.40^{b}	8.49 ± 0.21^{a}
Sor30Gly10-W	105.80 ± 6.74^{a}	5.39 ± 0.96^{b}
Sor20Gly10-D	11.61 ± 1.03^{d}	8.06 ± 0.70^{a}
Sor30Gly10-D	34.55 ± 4.73^{c}	5.46 ± 1.46^{b}

[ad]Two values followed by the same letter in the same column are not significantly ($p > 0.05$) different thought the Tukey's multiple range test.

Finally, in order to determine the change in the structure of the films prepared by different processing methods, XRD was carried out. **Figure 3.5** shows that all samples exhibited a peak with a maximum at $2\theta = 21$ º, characteristic of SPI and related to the slight order in the protein (Guerrero et al., 2012). It can be observed that both samples showed the amorphous structure associated to soy protein and, although quantitative analysis by XRD has not been carried out in this chapter, higher intensity of the peak for the films prepared by compression could indicate a higher degree of structural arrangement that would inherit protein-plasticizer interactions and explain the poorer mechanical properties found in this study.

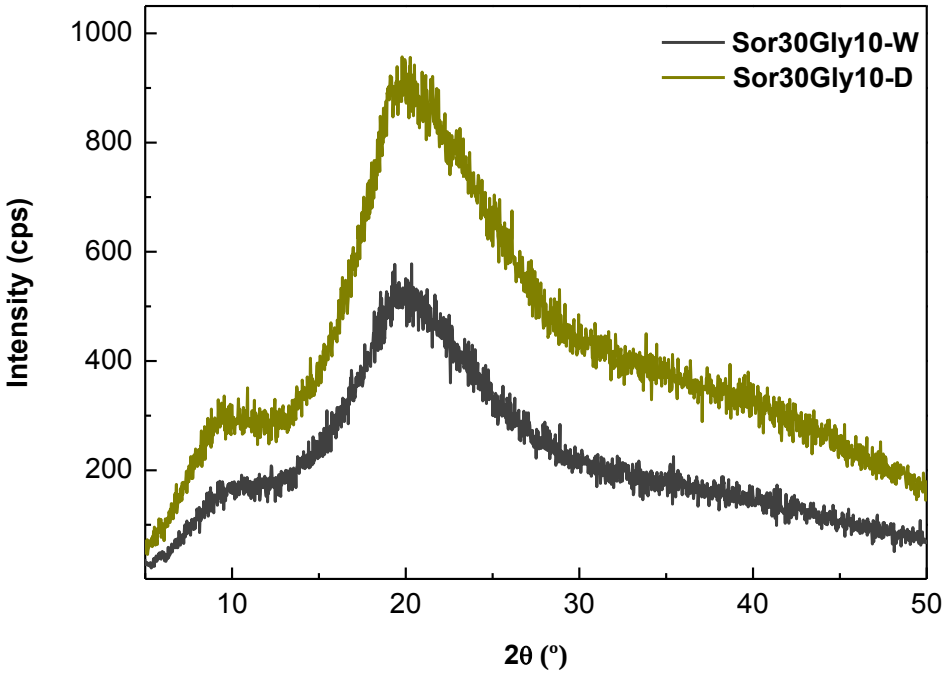

Figure 3.5. XRD patterns of SPI films with 30 wt % sorbitol and 10 wt % glycerol processed by casting and compression.

3.2.2 Environmental assessment

The Eco-indicator 99 was the method used to make an environmental assessment of the films derived from soya by-products, plasticized with sorbitol and manufactured by solution casting, in comparison with conventional PP films. The impact categories considered were carcinogens, respiratory organics, respiratory inorganics, climate change, radiation, ozone layer, ecotoxicity, acidification-eutrophication, land use, minerals, and fossil fuels. In order to simplify the system and delimit the research boundary, three main stages were considered: resource extraction, film manufacture, and waste disposal. The SPI film obtained in this study is biodegradable, so that the waste disposal chosen was composting. Regarding PP film disposal, 58% of municipal solid waste in the Basque Country was managed by landfilling, 21% was recycled, and remaining 21% was incinerated (Department of environment and regional planning of the Basque Government, 2008), thus these data were used in this study. To consider the

relative importance of the impact categories studied, normalised impact values are shown in **Table 3.7**.

In the normalisation step, the characterization factors were divided by a magnitude for each impact category. Although the International Organization for Standardisation (ISO) does not consider normalisation as a compulsory step, this is recommended by the Society of Environmental Toxicology and Chemistry (SETAC) due to the fact that the values obtained in the characterization step are in different units while normalised values have no unit, which allows comparison, as shown in the work carried out by Leceta et al. (2013) for chitosan-based films.

Table 3.7. Normalised environmental impacts of SPI films in comparison with PP films using different disposal scenarios.

Impact Category	**PP landfill**	**PP recycling**	**PP incineration**	**SPI composting**
Carcinogens	$4.50 \cdot 10^{-6}$	$0.13 \cdot 10^{-6}$	$0.38 \cdot 10^{-6}$	$3.68 \cdot 10^{-6}$
Respiratory organics	$1.12 \cdot 10^{-8}$	$0.19 \cdot 10^{-8}$	$1.12 \cdot 10^{-8}$	$2.87 \cdot 10^{-8}$
Respiratory inorganics	$2.08 \cdot 10^{-6}$	$1.34 \cdot 10^{-6}$	$2.14 \cdot 10^{-6}$	$19.2 \cdot 10^{-6}$
Climate change	$1.10 \cdot 10^{-6}$	$0.44 \cdot 10^{-6}$	$2.17 \cdot 10^{-6}$	$2.03 \cdot 10^{-6}$
Radiation	$1.32 \cdot 10^{-8}$	$2.12 \cdot 10^{-8}$	$1.32 \cdot 10^{-8}$	$10.9 \cdot 10^{-8}$
Ozone layer	$0.73 \cdot 10^{-10}$	$1.02 \cdot 10^{-10}$	$0.69 \cdot 10^{-10}$	$6.14 \cdot 10^{-10}$
Ecotoxicity	$2.19 \cdot 10^{-7}$	$0.83 \cdot 10^{-7}$	$1.05 \cdot 10^{-7}$	$3.09 \cdot 10^{-7}$
Acidification/Eutrophication	$1.94 \cdot 10^{-7}$	$1.13 \cdot 10^{-7}$	$2.05 \cdot 10^{-7}$	$9.95 \cdot 10^{-7}$
Land use	$1.69 \cdot 10^{-7}$	$1.73 \cdot 10^{-7}$	$1.59 \cdot 10^{-7}$	$730 \cdot 10^{-7}$
Minerals	$5.61 \cdot 10^{-8}$	$6.34 \cdot 10^{-8}$	$5.71 \cdot 10^{-8}$	$19.4 \cdot 10^{-8}$
Fossil fuels	$3.84 \cdot 10^{-5}$	$0.73 \cdot 10^{-5}$	$3.84 \cdot 10^{-5}$	$1.65 \cdot 10^{-5}$

PP films caused the main environmental damages in respiratory inorganics, climate change, and fossil fuels. The main process that contributed to the high value of these impact categories was the raw material extraction until its delivery at plant. In the case of recycling as waste scenario, the values obtained in the majority of the impact categories were lower.

The most critical process for soy protein films was cultivation of soybeans, which takes into account the use of diesel, machines, fertilizers, and pesticides. In addition, the provision of the land, its transformation, and the emissions from the machinery used represent the main source of impact.

CONCLUSIONS

Films plasticized with sorbitol were successfully prepared and transparent films with excellent UV barrier properties were obtained. The best results were obtained at pH 10, at which the protein unfolding is better to promote protein-plasticizer interactions, as shown by changes in the relative intensity of the bands corresponding to amides in FTIR spectra. Moreover, gloss was low and contact angle high, indicating that the surface is rough and hydrophobic, respectively.

Once evaluated the proper amount of plasticizer, thin films based on soy protein and plasticized with sorbitol and glycerol were prepared by casting and compression. It was observed that the processing method employed influenced the functional properties of the films. Regarding optical properties, the films prepared by compression showed higher transparency and gloss, while the films prepared by casting were more flexible and hydrophobic; thus, depending on the desired application, the processing method can be chosen.

According to the environmental assessment, results revealed that environmental burden associated to soy protein films should be reduced. Therefore, future improvements in the extraction processes together with an optimization of the manufacture would help to increase environmental advantages of these materials that could be sustainable alternatives to petroleum-based films.

4

chapter

CASTING VS COMPRESSION: DEVELOPING SUSTAINABLE FILMS

Garrido T., Leceta I., Cabezudo S., Guerrero P., de la Caba K. (2016)

Tailoring soy protein film properties by selecting casting or compression as processing methods. European Polymer Journal, 85, 499-507

SUMMARY

Once analysed the effect of the plasticizer content, type and processing conditions, SPI films plasticized with 30 wt % glycerol were selected in this chapter for a further analysis of the chosen manufacturing process effect on both film properties and environmental impacts. In fact, the changes that are observed in thermal, optical, barrier and mechanical properties are related to changes in the film structure and the intermolecular forces involved during the film formation. In this regard, films manufactured by two different processing methods, solution casting and compression moulding, were assessed. Besides the film properties, the comparison of the environmental impacts caused by the films as a function of the manufacture process used was carried out, since it can be complementary information in order to select the best option(s).

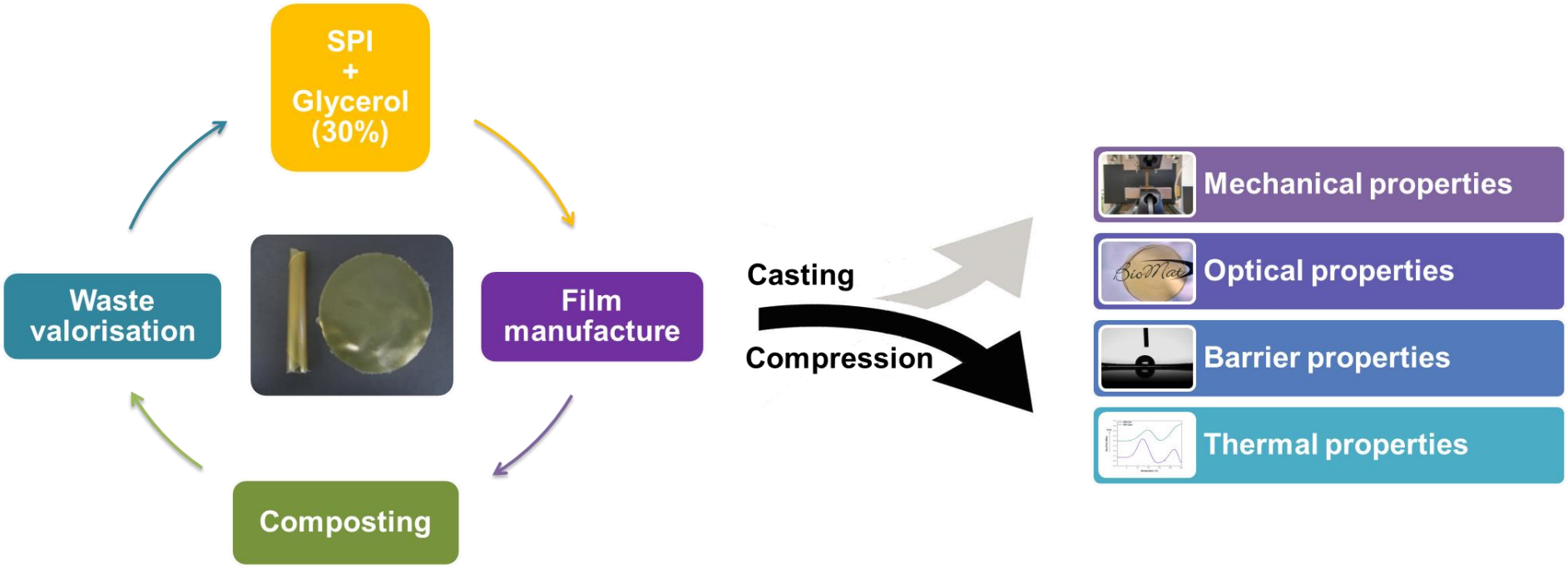

Figure I. Graphical abstract of Chapter 4.

4.1 FILM PREPARATION

Two processing methods were analysed for manufacturing SPI films. On the one hand, the wet (W) process was used, in which SPI film forming dispersions were prepared by mixing 5 g of SPI and 100 mL of distilled water. Dispersions were heated at 80 °C for 30 min under magnetic stirring. Then, 30 wt % glycerol (based on SPI dry basis) was added and dispersions were maintained at 80 °C for other 30 min under stirring. Subsequently, dispersions were poured into Petri dishes and dried at room temperature to obtain SPI-W films.

On the other hand, the dry (D) process was analysed. In this case, SPI and glycerol were blended in a Stephan UMC 5 mixer for 5 min at 1500 rpm and the blend was thermally compacted using a caver laboratory press. The powder was placed between two aluminium plates and it was introduced into the press, previously heated up to 150 °C, and pressed at 12 MPa for 2 min to obtain SPI-D films.

4.2. RESULTS AND DISCUSSION

Film properties vary when different processing methods are employed due to a different rearrangement of protein chains during the film forming process because of the different processing temperatures and times employed. These processing parameters affect intra- and inter-molecular interactions among protein chains and, thus, film properties.

4.2.1 Film characterization

Since intra- and inter-molecular interactions among protein chains are responsible for protein unfolding and denaturation, the knowledge of denaturation degree is a relevant aspect in order to analyse the effect of processing methods on film properties. The denaturation degree is related to the intensity of the peaks observed by DSC, so this analysis was carried out and the thermograms of the SPI films processed by casting and compression are shown in **Figure 4.1**.

The soy protein fractions, classified according to their ultracentrifugation sedimentation rate, are 2S, 7S, 11S and 15S, with 7S (conglycinin) and 11S (glycinin) making up about 70% of the total protein (Tansaz and Boccaccini, 2016). As shown in **Figure 4.1**, there is an endothermic peak corresponding to the denaturation of the fraction of lower molecular weight (7S) at 90 ºC and another one at 225 ºC, associated to the thermal denaturation of the fraction of higher molecular weight (11S) (Mo and Sun, 2012). Since denaturation temperatures are strongly dependant on moisture content and shift to higher values at lower moisture contents, the two peaks observed for SPI-D films appeared at higher temperatures than the peaks for SPI-W films due to a lower moisture content, as shown in **Table 4.1**.

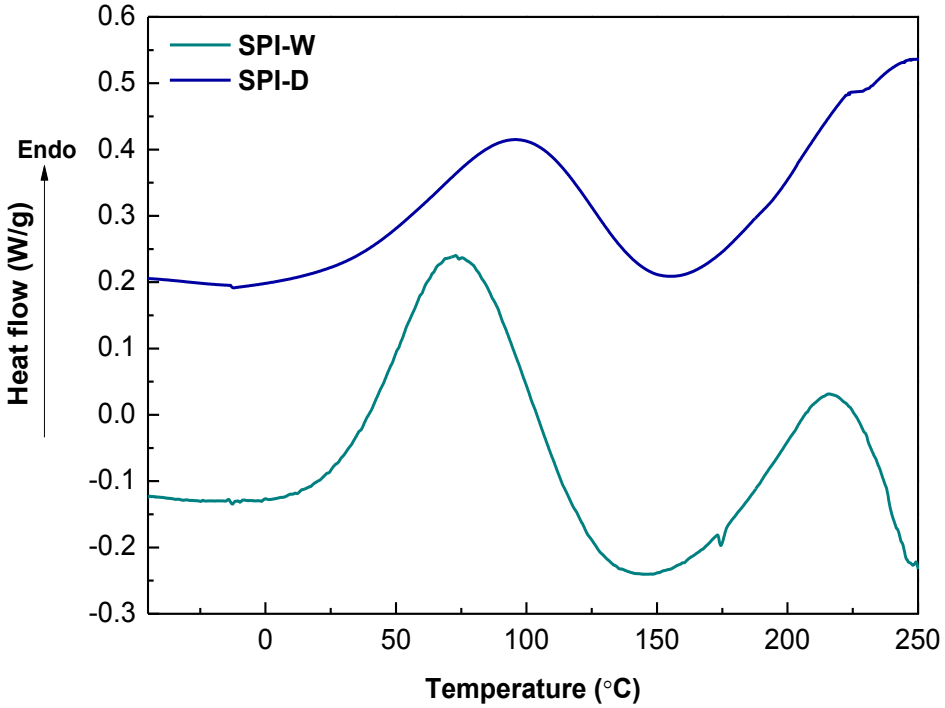

Figure 4.1. DSC thermograms of SPI films processed by casting (SPI-W) and compression (SPI-D).

In the case of SPI-D films, the use of a higher temperature during processing caused a higher degree of denaturation, as observed by DSC, which may facilitate the interactions between protein and plasticizer, increasing physical crosslinking, reducing moisture absorption and leading to lower MC values (Carpiné et al., 2015; Qu et al., 2015). As also shown in **Table 4.1**, SPI-W films showed higher WCA values than SPI-D films, suggesting that the use of longer times during processing promoted the rearrangement of protein chains and the exposure of the hydrophobic groups from non-polar residues toward the surface.

Table 4.1. Moisture content (MC) and water contact angle (WCA) of SPI films processed by casting (SPI-W) and compression (SPI-D).

Film	MC (%)	WCA (º)
SPI-W	17.5 ± 0.8	99 ± 2
SPI-D	11.6 ± 0.1	35 ± 4

In relation to water uptake (WU), the equilibrium state was reached relatively fast regardless of the manufacturing process employed, as can be observed in **Figure 4.2**. This state of swelling occurs when the chemical potential of the solvent in the dispersion equals the chemical potential of the free solvent (Hamman and Schmid, 2014). During 8 h of immersion, SPI-W films maintained a relatively constant WU value around 250%. However, in the case of SPI-D films, the percentage of water uptake increased in the first 4 h until a maximum of 225% and then, remained constant up to 8h. These results can be related to the crosslinking of the network formed. In fact, when the crosslinking degree is higher, the film structure is more compact and the swelling capacity of the film is reduced, as also described by other authors (Jerez et al., 2007).

Optical properties such as colour, gloss and transparency were also analysed and displayed in **Table 4.2**. As can be seen, SPI-W films showed a high L^* value (lightness). The decrease in lightness for SPI-D films coincided with the increase in a^* and b^* values. Regarding a^* parameter, the increase in this value showed the change from a greenish colour for SPI-W films to a more reddish tonality for SPI-D films. As mentioned in the previous chapter, soy protein provides a characteristic yellowish colour to the films. The films processed by compression showed a higher b^* parameter value, probably due to the use of a higher processing temperature for SPI-D films. Moreover, SPI-D films were glossier.

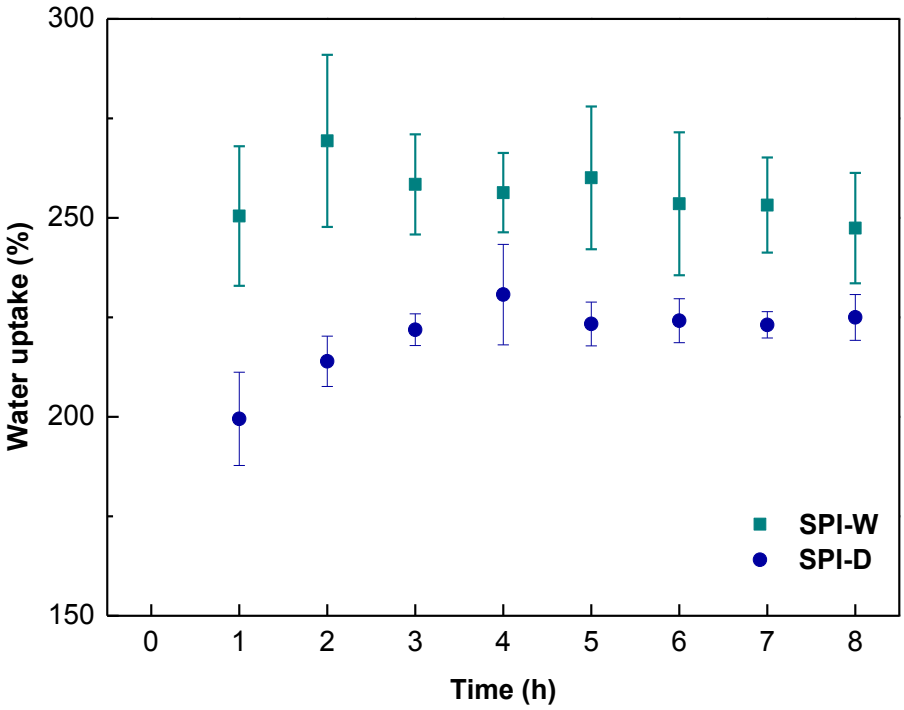

Figure 4.2. Water uptake (WU) of the films processed by casting (SPI-W) and compression (SPI-D).

Table 4.2. Colour (L*, a* and b*), gloss and transparency (T) of SPI films processed by casting (SPI-W) and compression (SPI-D).

Film	L^*	a^*	b^*	$Gloss_{60^o}$ (GU)	T (A_{600}/mm)
SPI-W	90.78 ± 0.37	-1.26 ± 0.06	20.98 ± 0.27	10.50 ± 0.09	8.71
SPI-D	78.94 ± 0.80	2.84 ± 0.60	46.53 ± 1.20	33.60 ± 1.23	1.16

Considering the linear relationship between gloss and surface roughness (Villalobos et al., 2005), SEM images were obtained for both SPI-W and SPI-D films and the images are shown in **Figure 4.3**. As can be seen, SPI-D films presented a smoother surface due to the application of pressure during the film formation process.

Also transparency can be an indication of film homogeneity and compatibility between the components of the composite film. Both SPI-W and SPI-D films were transparent, but lower values for SPI-D films indicated that these films were more

transparent, suggesting a better interaction between the protein and the plasticizer, as confirmed by the results obtained by mechanical testing and shown in **Table 4.3**.

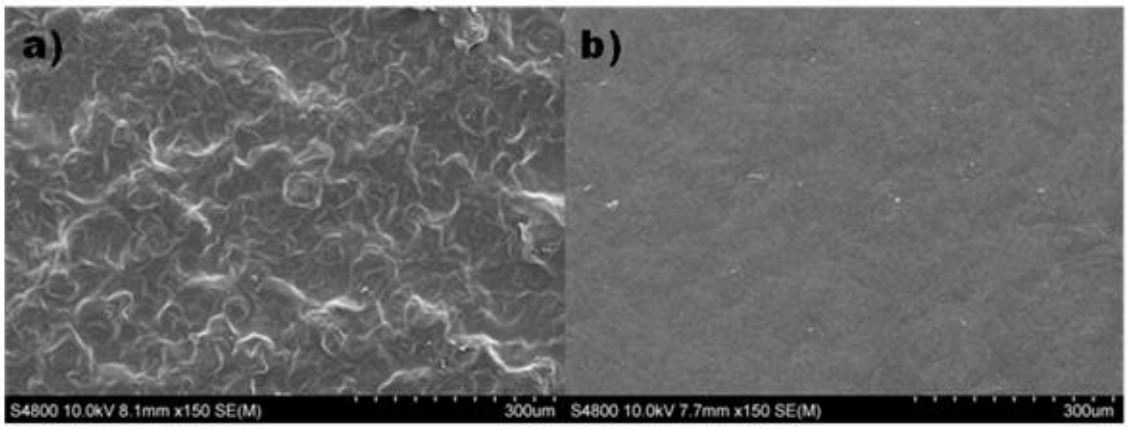

Figure 4.3. SEM images of the surface for a) SPI-W and b) SPI-D films.

The mechanical response of SPI films were explored by analysing their elongation at break (EB), tensile strength (TS) and elastic modulus (EM). It is well known that the mechanical properties of the films are highly related to the nature of film-forming materials as well as to the interactions between the components; therefore, these properties can be affected by the processing method employed (Tian et al., 2011). As can be seen, SPI-D films achieved higher values for EB, TS and EM, since a higher processing temperature in the case of compression moulding could promote further protein denaturation, as shown by DSC, and so facilitate SPI-glycerol interactions and physical crosslinking, resulting in a three dimensional network with improved mechanical properties.

Table 4.3. Elongation at break (EB), tensile strength (TS) and elastic modulus (EM) values of SPI-based films processed by casting (SPI-W) and compression (SPI-D).

Film	EB (%)	TS (MPa)	EM (MPa)
SPI-W	105.4 ± 13.3	4.1 ± 0.4	112.4 ± 5.3
SPI-D	140.6 ± 13.3	7.7 ± 0.6	120.5 ± 5.3

The storage modulus (E'), loss modulus (E'') and loss tangent (tan δ) curves of SPI films as a function of temperature are presented in **Figure 4.4**. Overall, samples exhibited a predominantly elastic character since E' was higher than E'' in all the temperature range, regardless of the method used to process the films. As the temperature increased, the storage modulus values decreased until reaching a minimum value around 25 ºC for SPI-W films and 40 ºC for SPI-D films. As also shown by other authors (Bengoechea et al., 2007), at higher temperatures there was a moduli increase for SPI-W films since these samples were processed at lower temperatures and, thus, they showed some thermosetting potential due to disulphide bonds. The slight increase in SPI-D films could be associated with moisture loss.

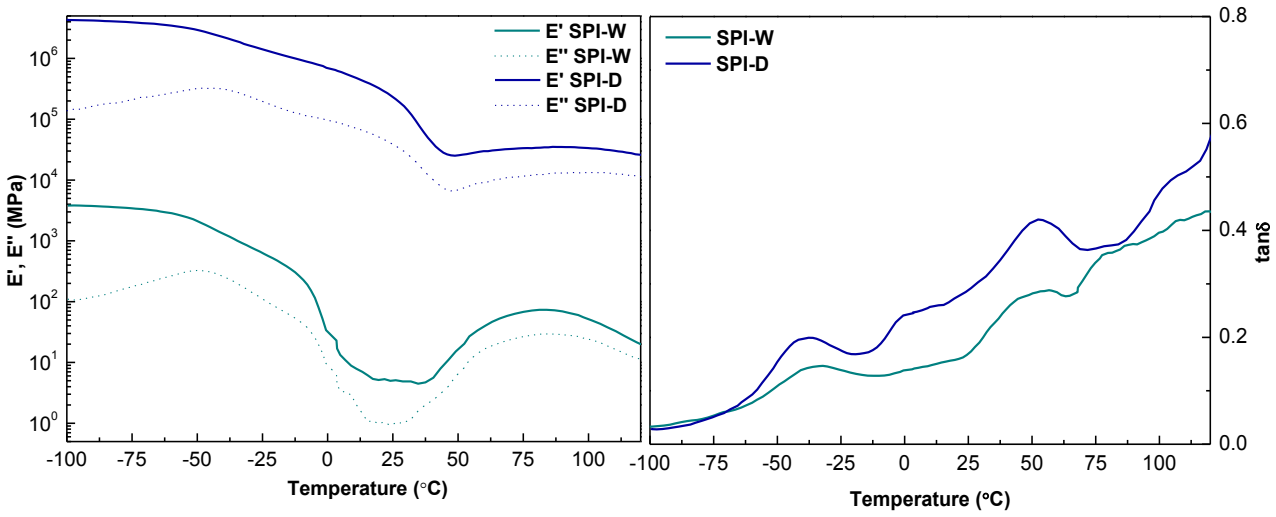

Figure 4.4. Temperature dependence of the storage modulus (E'), loss modulus (E'') and loss tangent (tanδ) for the films processed by casting (SPI-W) and compression (SPI-D).

SPI-D films showed an enhancement of viscoelastic properties, as can be observed by higher moduli values. The curves related to tanδ showed the glass transition temperature (T_g) of glycerol. A T_g value around -40 ºC was obtained for both SPI-W and SPI-D films. This temperature was higher than the T_g of pure glycerol,

-75 ºC, indicating the good interaction between SPI and glycerol (Mathew and Dufresne, 2002; Ogale et al., 2000). Additionally, those interactions depressed the T_g of soy protein. For SPI-D films, this decrease was more significant suggesting that lower moisture contents might enhance the interactions between SPI and glycerol (Chen and Zhang, 2005a; Chen et al., 2005; Mo and Sun, 2002).

4.2.2 Environmental assessment

When choosing a processing technique, the environmental point of view is an aspect to be considered. In this work, only the manufacture stage was consider since extraction of raw materials and the end of life scenario were the same regardless of the processing method employed. However, it is worth noting that agro-industrial by-products were valorised for film production, contributing to resources' efficiency. Furthermore, composting can be selected as the disposal scenario for SPI films, reducing the environmental and economic problems associated with the waste treatment of films after disposal. A schematic diagram of the system boundaries considered in this work is shown in **Figure 4.5.**

The manufacture stage considers the environmental load related to the process of turning raw materials into films. For each processing method, the environmental burden related to the additives employed and the energy consumed was considered. As shown in **Figure 4.6**, results revealed that both methods showed similar impact values, although compression moulding showed lower environmental impacts due to a considerable shorter processing time. Since the energy consumption in the casting process is related to heating during mixing and solvent evaporation, it is worth noting that film forming dispersions were dried at room temperature, so reducing the environmental impact associated with this processing method. As can be seen in **Figure 4.6**, results showed that

the impact categories with higher impact values were land use, respiratory inorganics and fossil fuels.

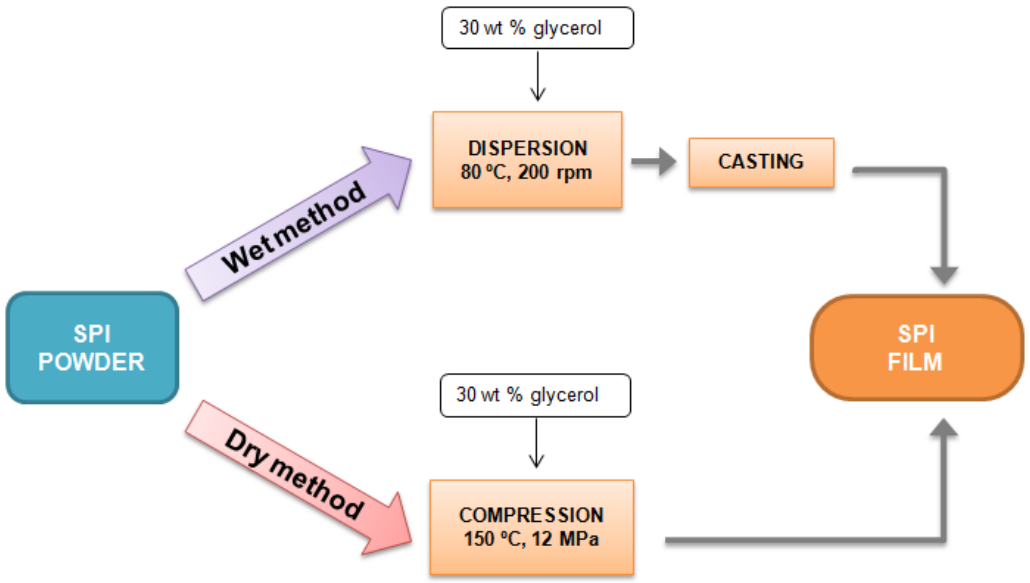

Figure 4.5. System boundaries considered for the films processed by casting (SPI-W) and compression (SPI-D).

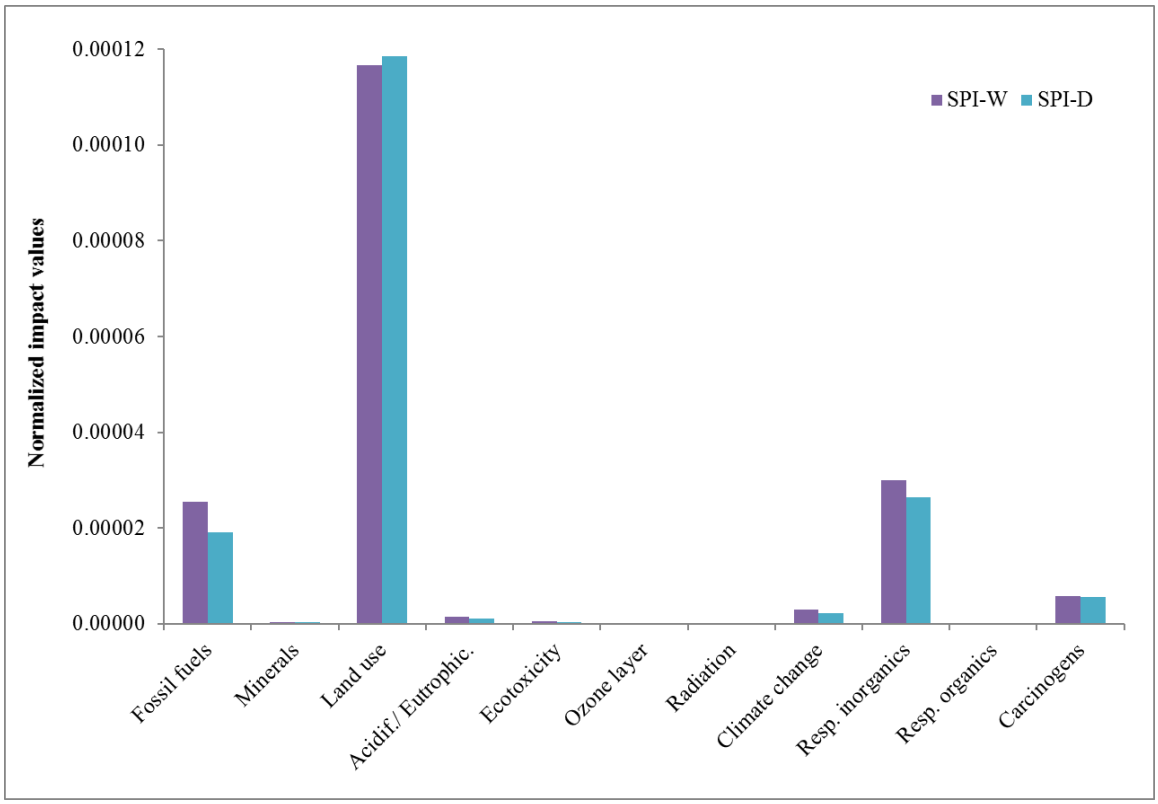

Figure 4.6. Normalised results of the environmental assessment of the films processed by casting (SPI-W) and compression (SPI-D).

Regarding the impact observed in land use category, it was attributed to the glycerol used in the manufacture stage. Glycerol is a co-product in the esterification process to obtain soybean oil and produce biodiesel. In this process, the transformation of the land and soybean cultivation are considered, including diesel, machines, fertilizers and pesticides, which give rise to a high environmental impact in land use category.

Concerning respiratory inorganics, the electricity used for film production and emissions associated to the production of glycerol were responsible for the environmental burden. The energy consumed in the manufacture stage was also responsible for the environmental charge in fossil fuels. Since the processing time is higher for the wet process, these impact categories were higher for SPI-W films, pointing out the importance of reducing manufacturing times to reduce not only costs, but also environmental impacts.

CONCLUSIONS

In this chapter, SPI films were successfully developed by casting and compression. The films processed by compression were thermally and mechanically more stable and showed higher tensile strength and elongation at break values. Moreover, compressed films were more transparent and had a smoother surface, since the use of a higher processing temperature by compression caused a higher denaturation degree and, thus, a better interaction between SPI and glycerol. Furthermore, compression method could be considered a more appropriate process for industrial applications due to the use of shorter processing times.

This aspect had also a great influence on the environmental impacts assessed in this chapter. Results revealed that the impact categories that showed higher environmental impacts were land use, respiratory inorganics and fossil fuels. Films moulded by compression showed lower impact values due to a lower energy consumption, associated with a lower processing time. It is worth noting that both casting and compression films were produced at laboratory scale and, thus, further optimization of manufacture stages is expected to provide energy savings that could increase the environmental benefits of SPI films. Considering the abundance and high availability of soy protein as by-product from some industries, such as food processing or biodiesel production, the improvement of the manufacturing process sustainability could increase the commercial feasibility of soy protein films.

5

chapter

VALORISATION OF CHICKEN FEATHERS AS A SOURCE OF SULPHUR TO ENHANCE FILMS PROPERTIES

Garrido T., Peñalba M., de la Caba K., Guerrero P. (2019)

A more efficient process to develop protein films derived from agro-industrial by-products. Food Hydrocolloids, 86, 11-17

Garrido T., Leceta I., de la Caba K., Guerrero P. (2018)

Chicken feathers as a natural source of sulphur to develop sustainable protein films with enhanced properties. International Journal of Biological Macromolecules, 106, 523-531

SUMMARY

In previous chapters, SPI was employed to develop sustainable materials with good physicochemical properties. However, it is well known that the application of SPI is limited due to its low strength and high moisture absorption. Therefore, adding other biodegradable polymers to soy protein can be an effective way to overcome these drawbacks. In this context, the valorisation of agro-industrial waste to improve functional properties of films has experienced a huge increase in the last years. For instance, chicken feathers, waste from the poultry industry, can be employed as a source of raw materials for applications such as packaging, tissue engineering, water purification, or fuel storage. Feathers are mainly composed of a structural protein, keratin (> 90%), rich in hydrophobic residues and cysteine, which promotes crosslinking by disulphide bonds, enhancing film stability and strength. In contrast to other studies, in which toxic chemicals or expensive methods are employed to hydrolyse feather keratin, in this chapter a simple, environmentally friendly and inexpensive method was addressed.

Furthermore, this hydrolysed keratin (HK) was used along with SPI in order to develop casting and compression films and the physicochemical, thermal, mechanical, optical and morphological properties of these films were analysed. Therefore, in addition to the valorisation of agro-industrial waste, the main aim of the incorporation of hydrolysed keratin into film forming formulations was to increase the sulphur content and, thus, the ability to form disulphide bonds, improving the chemical and thermal stability of the resulting films.

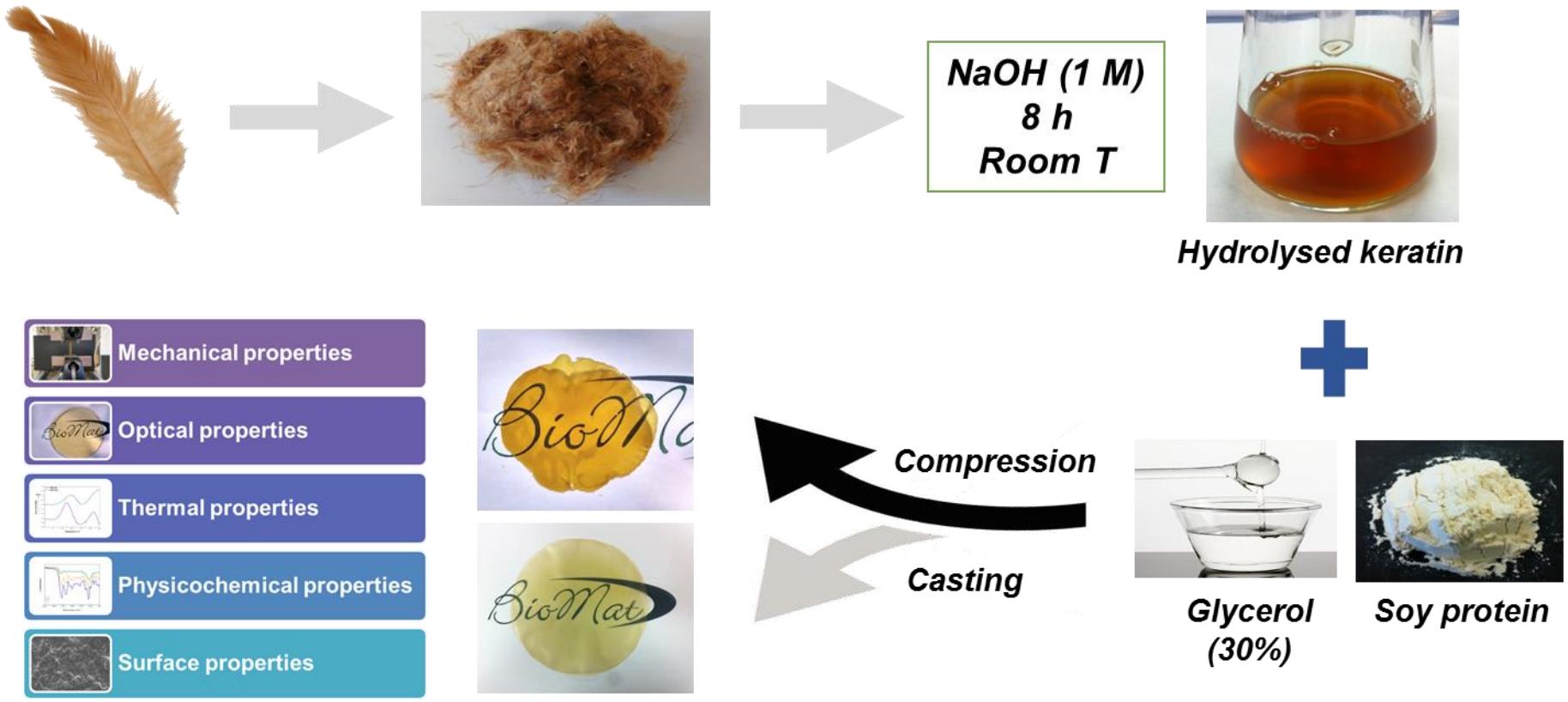

Figure I. Graphical abstract of Chapter 5.

5.1 FILM PREPARATION

Films were prepared by solution casting (wet method, W) or compression moulding (dry method, D). 5 g of SPI were dispersed in 100 mL of HK solution prepared as described in Chapter 2. The concentration of chicken feathers (CF) in HK solutions was fixed at 3, 6 or 9 wt % (based on SPI dry basis). The pH was appropriately adjusted to 10 before heating the dispersion at 80 ºC for 30 min under magnetic stirring. After that, 30 wt % glycerol (based on SPI dry basis) was added and the dispersion was maintained at the same temperature for 30 min. On the one hand, the dispersion was poured into Petri dishes, dried at room temperature and films were peeled from the dishes. These films were designated as HK0-W (control sample for casting), HK3-W, HK6-W and HK9-W. On the other hand, the dispersion was freeze-dried using an Alpha 1-4 LD freeze dryer. The powder obtained was thermally compacted by applying a pressure of 12 MPa for 2 min, using a caver laboratory press, previously heated up to 150 ºC. The films were designated as HK0-D (control sample for compression), HK3-D, HK6-D and HK9-D.

5.2 RESULTS AND DISCUSSION

Conversion of chicken feathers into valuable products is a very challenging process due to the rigid structure of keratin, which is extensively crosslinked by disulphide bonds. Therefore, an efficient treatment is necessary to reduce those disulphide bonds and achieve the feather keratin solubilisation. Reducing agents such as sodium hydroxide, cheaper than potassium hydroxide, are effective in breaking disulphide bonds and, thus, dissolving feather keratins at pH 10-13. Since solubilisation increases as the residence time and temperature increase, it is postulated that feathers are broken down into soluble polypeptides and amino acids (Ji et al., 2014). In this work, the alkali treatment was carried out at room temperature in order to develop a less invasive and an environmentally friendlier method to solubilise keratin. Specifically, the use of a 1 M NaOH solution at room temperature for 8 h was enough to disrupt disulphide bonds and solubilise keratin, as shown in **Figure 5.1**.

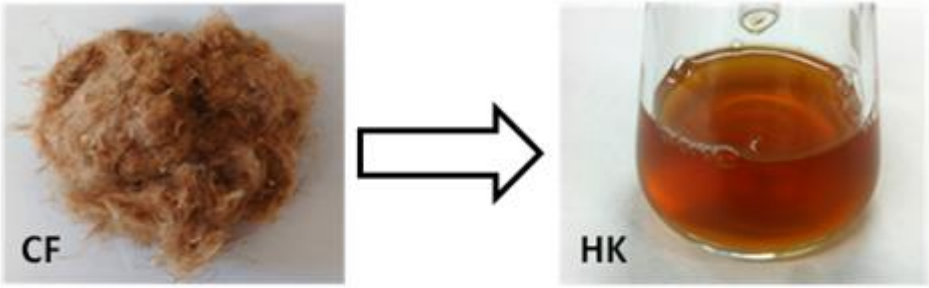

Figure 5.1. Pre-treated chicken feathers (CF) and hydrolysed keratin (HK) solution.

5.2.1 Hydrolysed keratin characterization

The chemical changes caused by alkali treatment in chicken feathers were studied by ATR-FTIR and spectra of pre-treated CF and HK are displayed in **Figure 5.2.** It is well known that chicken feathers are mostly constituted by protein, up to 90% (Cheung et al., 2009); therefore, the ATR-FTIR spectrum of CF shows the

characteristic bands of proteins. These absorption bands appeared at 1629, 1518 and 1238 cm^{-1}, and are related to amide I, amide II and amide III, respectively. Amide I corresponds to C=O stretching; amide II is related to N-H bending; and amide III resulted from C-N stretching and N-H bending. By comparing the ATR-FTIR spectra of CF and HK in this region, it can be clearly observed that the alkali treatment caused a remarkable change in the intensity of those characteristic bands, but also in the frequency at which those bands appeared, indicating a significant change in the protein structure. In fact, the alkali treatment caused the breakdown of peptide bonds. These results are in accordance with the solubilisation of keratin shown in **Figure 5.1**.

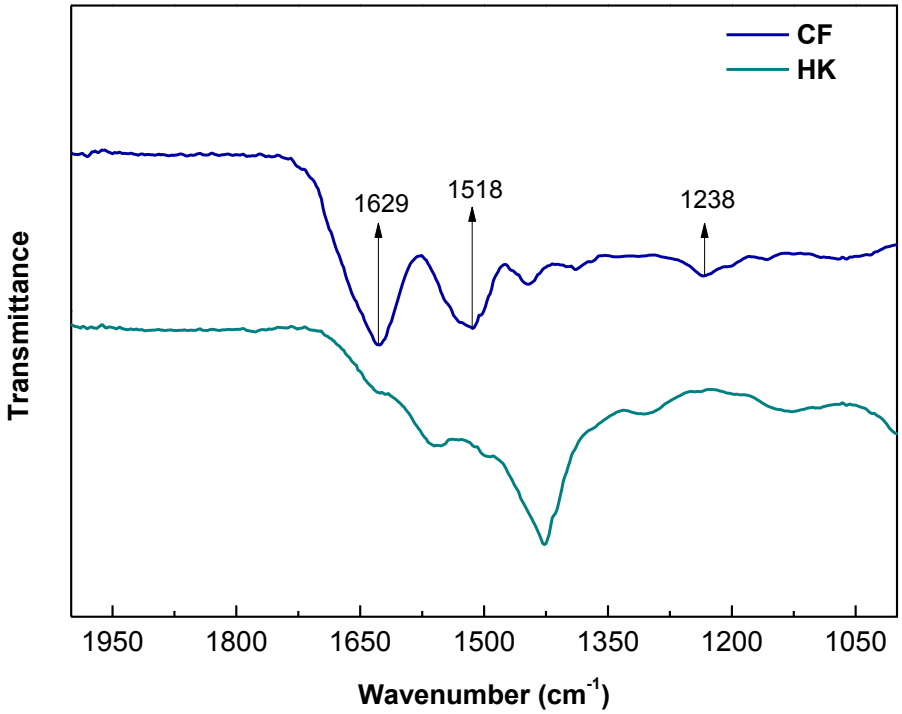

Figure 5.2. ATR-FTIR spectra of pre-treated chicken feathers (CF) and hydrolysed keratin (HK).

In order to study the effect of the treatment conditions on the molecular weight of HK, SDS-PAGE electrophoresis was carried out. **Figure 5.3** shows the electrophoretic profiles of HK samples in comparison to a protein standard (the

electrophoregram on the right). Since no protein fraction with molecular weight higher than 10 kDa was found when the amount of HK sample applied into the gel was 10 μg, the analysis was repeated applying 25 and 100 μg. As can be seen in **Figure 5.3**, no band was found regardless of the amount of HK sample employed, indicating that HK consisted mainly of peptides or amino acids.

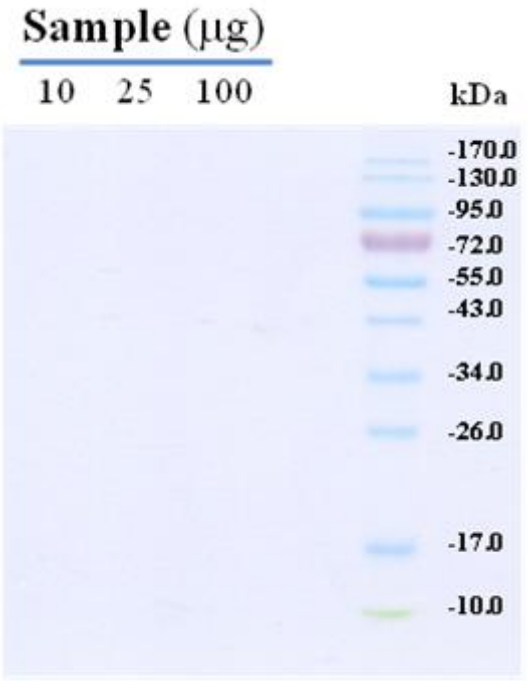

Figure 5.3. Electrophoretic separation patterns (SDS-PAGE) of samples: lane 1, 10 μg of HK; lane 2, 25 μg of HK; lane 3, 100 μg of HK; and lane 4, protein standard.

In order to identify the amino acids present in hydrolysed keratin and their content, elemental analysis was performed and the amino acid composition of hydrolysed keratin (HK) is shown in **Table 5.1**, in which the amino acid composition of soy protein isolate (SPI) is also provided for comparison. Cysteine (10.8%), responsible for the sulphur groups present in keratin, proline (12.4%), serine (11.7%) and glutamic acid (10.3%) were the most abundant amino acids present in the hydrolysed feather keratin, whilst the lowest contents of amino acids were related to histidine (0.2%),

methionine (0.2%) and lysine (0.8%). However, there were considerable contents of alanine (9.9%) and glycine (9.8%), critical components of peptide binding domains, similarly to the extracellular matrix (Yin, et al., 2013). Furthermore, the high content of glycine and proline suggested that feather keratin was rich in β-sheet structures (Tsuda et al., 2014). In contrast, tryptophan was irreversible destroyed in the hydrolysis step (Hill et al., 2010). The amino acid concentrations determined in this work were similar to the ones obtained by Reddy (2015).

Table 5.1. Amino acid composition of hydrolysed keratin (HK) and soy protein isolate (SPI).

Amino acids	**Concentration (%)**	
	HK	**SPI**
Aspartic acid	7.67[a]	11.5
Threonine	1.8	3.8
Serine	11.7	5.4
Glutamic acid	10.3[b]	19.2
Proline	12.4	5.2
Glycine	9.8	4.2
Alanine	9.9	4.2
Cysteine	10.8	1.3
Valine	5.8	4.8
Methionine	0.2	1.3
Isoleucine	2.2	4.8
Leucine	7.0	8.0
Tyrosine	1.7	3.8
Phenylalanine	4.7	5.4
Histidine	0.17	2.7
Lysine	0.78	6.4
Arginine	2.92	7.8

[a]Value for aspartic acid and asparagine
[b]Value for glutamic acid and glutamine

Regarding the elemental analysis carried out, this revealed that the sulphur content in hydrolysed keratin and in soy protein was approximately 4.2 and 0.3%, respectively. These percentages were related to the disulphide linkages mainly derived from cysteine. Consequently, the incorporation of hydrolysed keratin into the film forming formulations may produce an increment of the sulphur content, promoting the

interactions among the mixture components and, thus, leading to a crosslinked material with enhanced properties since thiol groups (-SH) in cysteine are able to form disulphide bonds, providing structural stability to the materials developed.

5.2.2 Film characterization

5.2.2.1 Physical properties

The study of the behaviour of the films in presence of water can provide information about the film integrity and stability in humid environments. Therefore, properties such as moisture content (MC), total soluble matter (TSM), water vapour permeability (WVP), water uptake (WU) and water contact angle (WCA) were analysed. Firstly, MC, TSM and WVP values are presented in **Table 5.2**. Moisture content is important as far as it can act as a plasticizer in the polymeric matrix. As can be observed, moisture content values were higher for the films processed by casting. However, these values showed no significant difference ($p > 0.05$) when hydrolysed keratin was incorporated. Regarding TSM, an upward trend was followed for the films processed by both methods, and the values increased with HK addition. This trend may be due to the presence of free amino acids or low molecular weight peptides that are not connected by covalent crosslinkages with other film components. Therefore, the rise in HK content resulted in an increase of the film solubility. In relation to WVP, an improvement was observed when solution casting was employed. This improvement could be due to the reorganization of protein chains since a longer drying period is provided when the wet process is used. Concerning HK incorporation, WVP values did not change significantly ($p > 0.05$) in HK-W films; however, the addition of HK into HK-D formulations resulted in the increase of the water vapour permeability.

Table 5.2. Moisture content (MC), total soluble matter (TSM), and water vapour permeability (WVP) of the films processed by casting (W) and compression (D) as a function of HK content.

Film	MC (%)	TSM (%)	WVP (10^{-12} g cm/cm^2 s Pa)
HK0-W	17.45 ± 0.77^{a}	29.06 ± 0.92^{a}	3.74 ± 0.24^{a}
HK3-W	17.32 ± 1.57^{a}	31.13 ± 3.02^{a}	3.45 ± 0.34^{a}
HK6-W	17.03 ± 0.43^{a}	32.11 ± 3.74^{ab}	3.55 ± 0.17^{a}
HK9-W	15.84 ± 1.44^{a}	36.87 ± 2.47^{b}	3.54 ± 0.47^{a}
HK0-D	11.58 ± 0.11^{b}	28.57 ± 0.38^{a}	5.62 ± 0.14^{a}
HK3-D	11.07 ± 0.02^{a}	31.02 ± 0.29^{b}	5.82 ± 0.39^{b}
HK6-D	11.67 ± 0.12^{b}	33.03 ± 0.14^{c}	6.74 ± 0.15^{b}
HK9-D	12.88 ± 0.25^{c}	34.74 ± 0.04^{d}	6.76 ± 0.33^{b}

^{ad}Two means followed by the same letter in the same column and in the same section are not significantly ($p > 0.05$) different through the Duncan's multiple range test.

The water resistance can be expressed in terms of water uptake. WU is related to the diffusion process in which small molecules are transported randomly from one side to the other, which is influenced by crosslinking, molecular interactions, crystallinity, as well as the presence of fillers in the film (Tanase and Spiridon, 2014). For all films, the rate of water absorption was fast in the first hour and then, the equilibrium was reached after few hours (**Figure 5.4**).

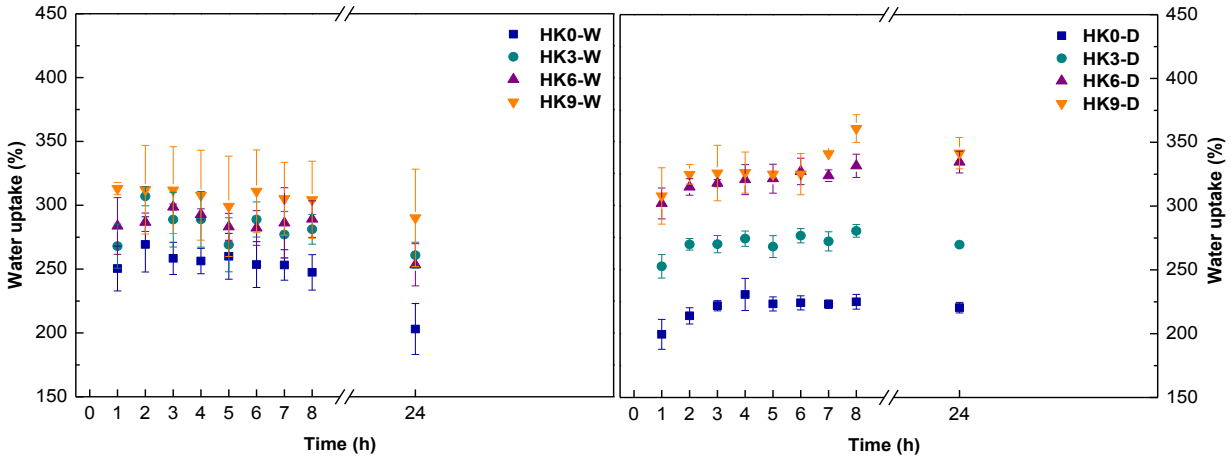

Figure 5.4. Water uptake of SPI films processed by casting (W) and compression (D) as a function of HK content.

In the case of HK-W films, the WU values started to decrease within 24 h of immersion due to the beginning of the film disintegration. In contrast, the films processed by compression moulding maintained the water uptake values constant after 24 h, indicating the major stability of these films. Furthermore, it was observed that the incorporation of hydrolysed keratin affected the uptake capacity, allowing a higher water uptake, obtaining 2-fold values when 9 wt % HK was added.

The knowledge of the hydrophobicity of the films allows for the detection of changes in the orientation of hydrophobic groups toward the surface, caused by changes in the molecular structure of the protein upon denaturation (Timilsena et al., 2016). The hydrophilic or hydrophobic character of the films was evaluated by measuring the water contact angle on the film surface as a function of time and the values are displayed in **Figure 5.5**. Overall, WCA values higher than 90 º correspond to a hydrophobic character or low wettability of films (Karbowiak et al., 2006). In this instance, the films processed by casting showed higher values than those processed by compression and HK0-W films showed values around 90 º, confirming their hydrophobicity. This behaviour can be attributed to a lower concentration of polar groups toward the surface because of a longer period of time for the interactions between the blend components in the case of processing by casting. On the other hand, the hydrophilic character of the films was promoted by the addition of hydrolysed keratin due to the incorporation of the hydrophilic amino acids present in HK. Furthermore, WCA values decreased with time, indicating the wettability of the films.

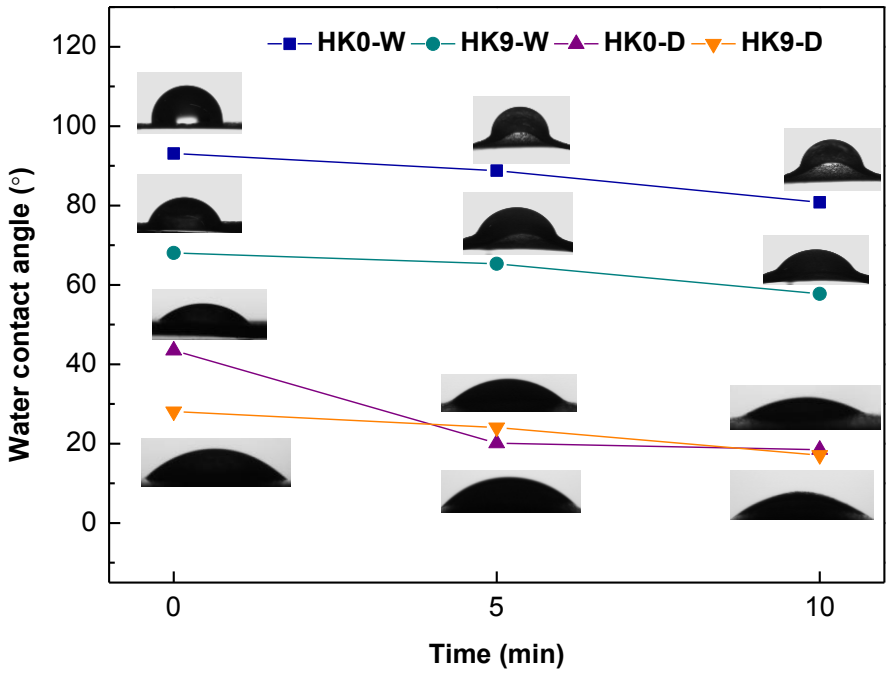

Figure 5.5. Water contact angle values (º) of the control films and the films with 9 wt % HK processed by casting (W) and compression (D) and recorded at 0, 5 and 10 min.

Regarding optical properties, colour and transparency of the SPI-based films were assessed and the results are displayed in **Table 5.3**. The films processed by casting had higher L^* values, resulting in brighter films. However, the addition of HK darkened the films significantly ($p < 0.05$) to the detriment of lightness in comparison to the control film. An opposite trend was found for a^* and b^* parameters. In fact, it was observed that b^* parameter showed high values mainly due to the characteristic yellowish colour that soy protein provides to the film. This parameter increased with the addition of HK, which provided a higher yellowish colour to the films. Furthermore, HK content strengthened significantly ($p < 0.05$) the redness of the films (a^*), as well as the colour difference (ΔE^*). Meanwhile, the employment of compression moulding as processing method increased the values of the above mentioned parameters due to the application of a higher temperature.

Table 5.3. Colour and transparency values of SPI films processed by casting (W) and compression (D) as a function of HK content.

Film	L^*	a^*	b^*	ΔE^*	T (A_{600}/mm)
HK0-W	90.78 ± 0.37^{a}	-1.26 ± 0.06^{a}	20.98 ± 0.27^{a}		8.71^{a}
HK3-W	86.03 ± 0.37^{b}	1.09 ± 0.15^{b}	27.84 ± 0.75^{b}	8.67 ± 0.82^{a}	7.81^{b}
HK6-W	80.07 ± 0.32^{c}	4.26 ± 0.17^{c}	36.70 ± 0.49^{c}	19.81 ± 0.54^{b}	7.02^{c}
HK9-W	76.43 ± 0.20^{d}	6.36 ± 0.10^{d}	40.11 ± 0.14^{d}	25.17 ± 0.25^{c}	6.83^{c}
HK0-D	78.94 ± 0.80^{a}	2.84 ± 0.60^{a}	46.53 ± 1.20^{a}		1.16^{a}
HK3-D	71.19 ± 0.79^{b}	9.87 ± 0.28^{b}	53.37 ± 0.72^{b}	12.54 ± 0.88^{a}	1.17^{a}
HK6-D	68.11 ± 0.83^{c}	11.72 ± 0.42^{c}	52.67 ± 0.84^{bc}	15.35 ± 0.52^{b}	1.25^{ab}
HK9-D	66.65 ± 0.24^{d}	14.63 ± 0.36^{d}	54.42 ± 0.37^{c}	18.79 ± 0.37^{c}	1.35^{b}

[ad]Two means followed by the same letter in the same column and in the same section are not significantly ($p > 0.05$) different through the Duncan's multiple range test.

Besides colour, transparency values of the films are also shown in **Table 5.3**. As can be seen, the processing method also affected the transparency of the films. Although all films were transparent (**Figure 5.6**), transparency values indicated that the films processed by compression moulding were more transparent, since the lower the T value, the higher the transparency (Nawab et al., 2017). However, these values did not change regardless of the amount of HK incorporated. These transparency values for compression films were similar to the values obtained for oriented polypropylene (OPP) (Guerrero et al., 2011). The difference between the two methods employed in this study could be related to the use of a higher temperature by compression moulding, which favoured the denaturation of SPI and, thus, the interactions with HK, increasing the compatibility between both components.

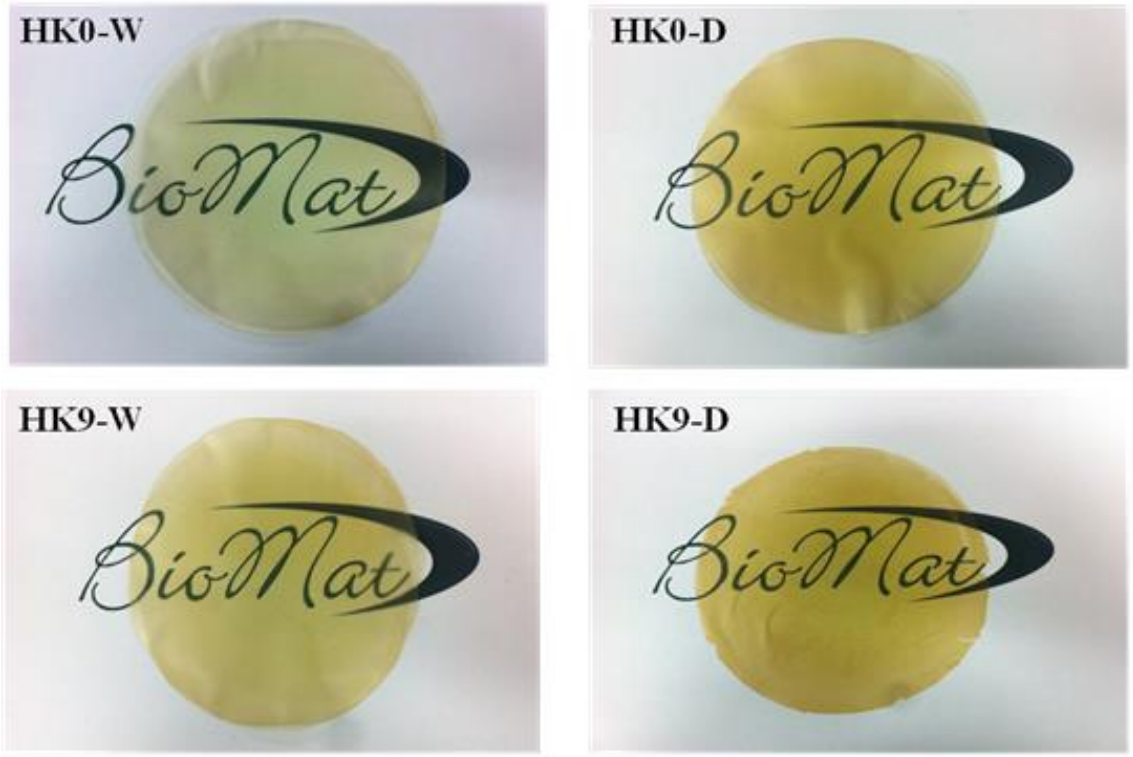

Figure 5.6. Images of the films containing 0 and 9 wt % of hydrolysed keratin processed by casting (HK0-W and HK9-W) and compression moulding (HK0-D and HK9-D).

5.2.2.2 Thermal properties

The thermal behaviour of the developed films was evaluated by differential scanning calorimetry (DSC) and thermogravimetric analysis (TGA) and results are presented in **Figure 5.7** and **Figure 5.8**, respectively. In all the DSC thermograms, one endothermic peak was detected. This peak represents the denaturation of one of the major globular proteins in SPI, β-conglycinin (7S) (Denavi et al., 2009). In the case of the films processed by casting, this thermal transition was observed around 80 ºC, but this temperature increased up to 100 ºC for compression films. It is well known that denaturation temperature of 7S globulin is strongly dependant on moisture content, thus, higher temperature values were obtained at lower moisture content (Koshy et al., 2015). As shown in **Table 5.2**, MC values for compression films were lower than those for casting films, in agreement with DSC results. Additionally, the incorporation of

hydrolysed keratin caused a shift of the peak attributed to 7S globulin to higher temperatures, increasing the thermal stability of films.

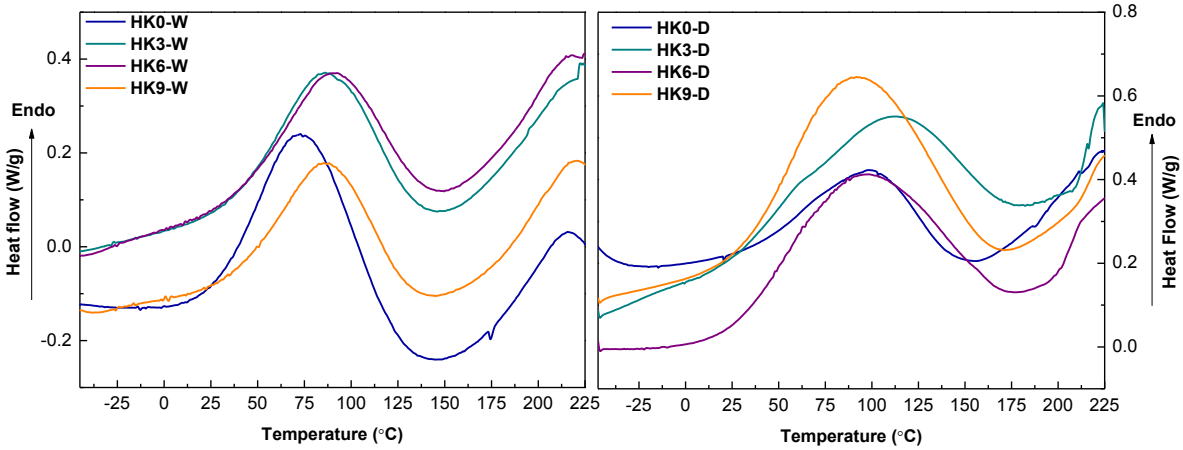

Figure 5.7. DSC thermograms of SPI films processed by casting (W) and compression (D) as a function of HK content.

As can be seen in **Figure 5.8**, TGA curves showed that thermal degradation occurred in three steps. The first stage (< 100 ºC) corresponded to the loss of absorbed moisture. In this step, casting films had a weight loss of 10%, whereas the weight loss of compression films was around 5%. The point of this behaviour was a lower MC in HK-D films. The second stage, starting around 210 ºC, was related to the evaporation of the glycerol used as plasticizer. As shown in other works (Mo and Sun, 2002; Tian et al., 2012), the good compatibility between protein and glycerol induced the increased of the boiling temperature of glycerol, which is 182 ºC. The third stage appeared at around 300 ºC and it was related to the thermal degradation of soy protein. It was observed that both control films (HK0-W and HK0-D) experienced higher weight loss above 300 ºC than the rest of the films, suggesting that the incorporation of hydrolysed keratin enhanced the thermal stability of the films due to a higher amount of disulphide bonds.

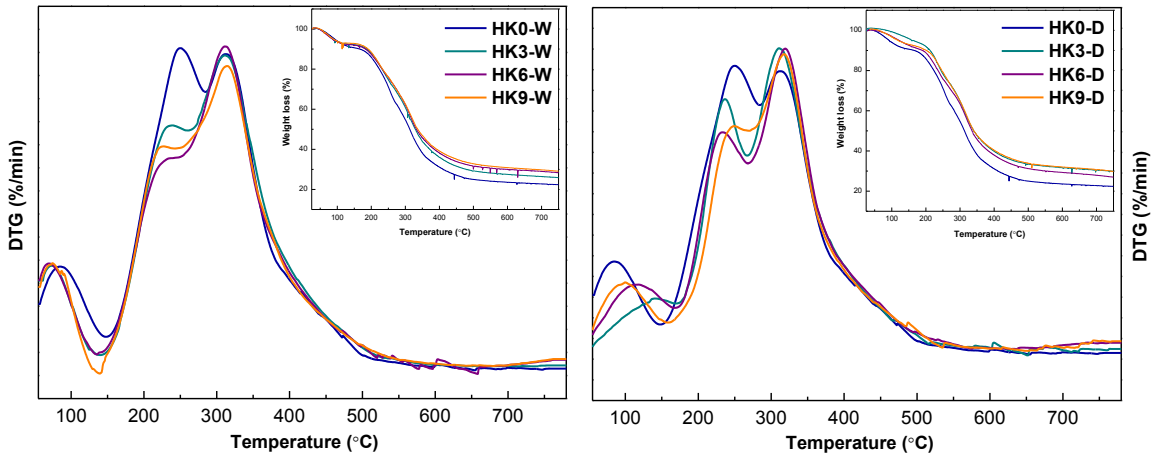

Figure 5.8. TGA and DTG curves of SPI films processed by casting (W) and compression (D) as a function of HK content.

5.2.2.3 Tensile and dynamic mechanical properties

Mechanical properties of SPI-based films with different HK contents were evaluated by measuring the tensile strength (TS), elongation at break (EB) and elastic modulus (EM) and the results are set out in **Table 5.4**. The films prepared by compression moulding possessed an enhanced tensile strength in comparison to those processed by casting. Moreover, the incorporation of HK increased significantly ($p < 0.05$) TS values from 7.47 to 9.52 MPa for HK9-D. At the same time, compression films also exhibited higher EB values, but the addition of HK caused a decrease of EB from 131% to 94% as the HK content increased from 0 to 9 wt %. Regarding the elastic modulus, these values were slightly higher for the films prepared by compression moulding; however, no change was observed when hydrolysed keratin was incorporated. This change in the mechanical behaviour of the films can be related to the increase of sulphur content in film forming formulations by the incorporation of HK. As reported in the literature (Visschers and de Jongh, 2005), the crosslinking by disulphide bonds in proteins is favoured at basic pH, the pH used in this work, and it is promoted by heating due to a higher degree of protein denaturation, which would explain higher

TS values for compression films. Since crosslinking restricts chain mobility, increasing stress and decreasing deformation, this is in accordance with the values shown in **Table 5.4**.

Table 5.4. Tensile strength (TS), elongation at break (EB) and elastic modulus (EM) of SPI films processed by casting (W) and compression (D) as a function of HK content.

Film	TS (MPa)	EB (%)	EM (MPa)
HK0-W	4.03 ± 0.14^{a}	103.92 ± 10.10^{a}	113.79 ± 4.42^{a}
HK3-W	4.83 ± 0.27^{b}	97.80 ± 7.44^{a}	104.25 ± 13.19^{a}
HK6-W	5.12 ± 0.66^{bc}	98.03 ± 8.49^{a}	99.28 ± 10.06^{a}
HK9-W	5.59 ± 0.53^{c}	97.68 ± 8.99^{a}	97.29 ± 10.87^{a}
HK0-D	7.47 ± 1.01^{a}	131.37 ± 7.83^{a}	112.68 ± 9.62^{a}
HK3-D	8.09 ± 0.83^{ab}	110.44 ± 8.23^{b}	109.40 ± 10.04^{a}
HK6-D	8.92 ± 0.56^{bc}	101.34 ± 2.65^{bc}	104.19 ± 5.99^{a}
HK9-D	9.52 ± 0.90^{c}	94.27 ± 9.78^{c}	101.58 ± 8.95^{a}

[ac]Two means followed by the same letter in the same column and in the same section are not significantly ($p > 0.05$) different through the Duncan's multiple range test.

In order to support the above mentioned effects on chain mobility, the temperature dependence of storage modulus (E'), loss modulus (E''), and loss tangent (tanδ) for SPI-based films processed with different HK contents by casting and compression is shown in **Figure 5.9**. As noticed in **Figure 5.9a** and **5.9c**, E' and E'' values were higher for films processed by compression moulding, confirming a higher thermal stability, as shown by DSC analysis. For all samples, the storage modulus was always higher than the loss modulus in the whole temperature range. However, the increase of temperature affected the thermo-mechanical behaviour of the films. As the temperature increased, the moduli values dropped sharply and a minimum value was obtained at around 45 ºC for compression films and at 30 ºC for casting films. Afterwards, and up to 80 ºC, an increase was observed. As reported in the literature, this increase in moduli can be related to the crosslinking by disulphide bonds in proteins (Fernández-Espada et al., 2016). From that temperature on, moduli values for casting

films started to decrease, while those for compression films remained stable until 120 ºC.

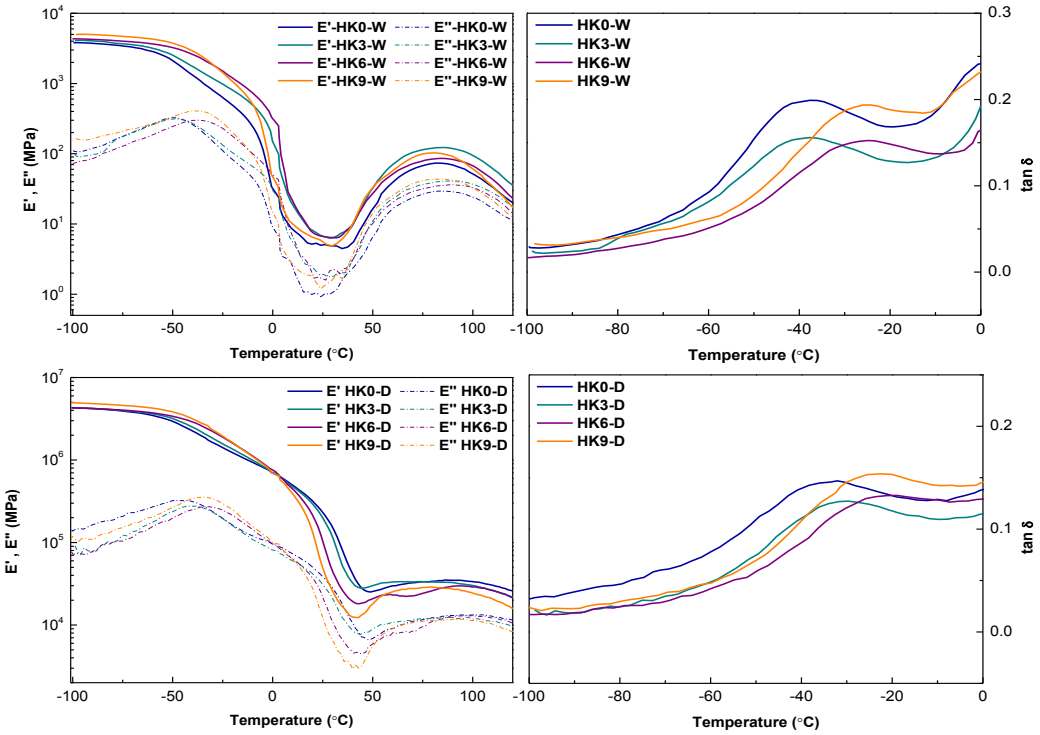

Figure 5.9. Temperature dependence of the storage modulus (E'), loss modulus (E'') and loss tangent (tanδ) curves for SPI films processed by casting (a and b) and compression (c and d) as a function of HK content.

The mechanical properties can also be related to tanδ whose maximum defines the glass transition temperature (T_g). It is worth noting that the increase of T_g resulted in the increase of the resistance of the films (Moore et al., 2006). In this context, **Figure 5.9b** and **5.9d** showed the curves related to tanδ where two transitions were observed. The first one, at around -45 ºC for HK0-W and -40 ºC for HK0-D, was attributed to the glass transition of glycerol (T_{g1}) where glycerol is loosely bound to proteins. The second one, at around 50 ºC for HK0-W and 45 ºC for HK0-D, corresponded to the glass transition of protein (T_{g2}) where glycerol forms a hydrogen-bound structure with proteins (Chen and Zhang, 2005; Dou et al., 2016). The addition of HK contributed to the increase of T_{g1} and T_{g2} not only for casting films but also for

compression films. This increase resulted in higher TS values and lower EB values, in accordance with the values displayed in **Table 5.4**.

5.2.2.4 Surface properties

The effect of the hydrolysed keratin incorporation in soy protein films in terms of the chemical modification of the surface was analysed by XPS. **Figure 5.10** showed four different peaks related to C 1s, N 1s, Na 1s and O 1s.

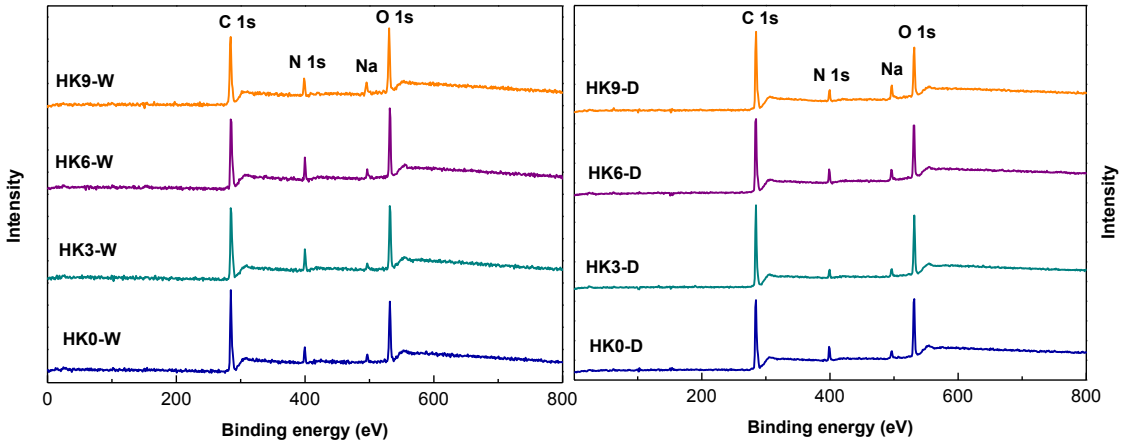

Figure 5.10. XPS survey spectra of SPI-based films processed by casting and compression as a function of HK content.

Sodium was related to the amount of NaOH employed in the chicken feather hydrolysis; thus, an increase of the peak intensity was observed when a higher amount of HK was added. It is known that the band frequency of C and O atoms changes depending on the interactions between the blend components, hence, a change in the intensity of the peaks was expected to occur when different processing methods were employed, as well as when different amount of hydrolysed keratin was added (Guerrero et al., 2013). In the case of HK0-W, the intensity of C 1s was higher than that related to O 1s. However, the intensity of both bands equalled with the HK incorporation. The

opposite occurred for compression films, in which the peak intensity of C and O atoms was similar when no hydrolysed keratin was incorporated.

In order to complete the information appeared in **Figure 5.10**, the concentration of C 1s, O 1s and N 1s atoms on the film surface, as well as the O/C and N/C ratios, are provided in **Table 5.5**. As above mentioned, the surface composition differed from one film to another depending not only on the processing method employed but also on the amount of hydrolysed keratin incorporated. In the case of the films processed by compression moulding, the changes were more remarkable. With the addition of HK, the concentration of C increased whilst the concentration of O decreased, as shown in **Figure 5.10**; therefore, the O/C ratio changed from 0.34 to 0.23 as the amount of HK increased from 0 to 9 wt %. Regarding N content, its concentration increased with the incorporation of HK content for casting films, while decreased for compression films; thus, the N/C ratio increased in the case of the films processed by casting and decreased for the ones processed by compression moulding. This fact could indicate that the content of amino groups on the film surface was higher in the films processed by casting.

Table 5.5. Compositional information by XPS of the SPI-based films processed by casting (W) and compression (D) as a function of HK content.

Film	C (%)	O (%)	N (%)	O/C	N/C
HK0-W	72.29	20.91	6.45	0.29	0.09
HK3-W	68.81	21.61	9.26	0.31	0.13
HK6-W	70.22	21.09	8.16	0.30	0.12
HK9-W	70.47	20.86	8.03	0.29	0.11
HK0-D	69.08	23.41	6.95	0.34	0.10
HK3-D	72.16	22.89	4.33	0.32	0.06
HK6-D	73.88	19.80	5.49	0.27	0.07
HK9-D	75.85	17.26	5.14	0.23	0.07

C 1s peak was divided into three peaks designated as C1 (C-C and C-H), C2 (C-O and C-N) and C3 (C=O) functions. C1 indicates the hydrophobic character of the film surface, whereas C2 and C3 correspond to those functional groups which benefit the wettability of the surface (Li et al., 2015; Zhao et al., 2011). As can be seen in **Table 5.6**, C1 content was higher for compression films. Moreover, C1 values increased with HK incorporation, increasing the hydrophobic character of the films, as confirmed by WCA values. This fact could evidence the reorganization of the chemical groups at the surface upon hydrolysed keratin incorporation, which might promote the change in surface hydrophobicity.

Table 5.6. Content of C1, C2 and C3 determined by XPS for SPI-based films processed by casting (W) and compression (D) as a function of HK content.

Film	C1 (%)	C2 (%)	C3 (%)
HK0-W	52.82	12.66	6.78
HK3-W	45.78	13.31	9.69
HK6-W	46.76	15.43	8.02
HK9-W	48.68	14.08	7.71
HK0-D	44.75	16.61	7.72
HK3-D	50.65	15.96	5.55
HK6-D	51.91	15.20	6.76
HK9-D	55.09	14.49	6.27

In order to provide further information about the surface properties of the films, the assessment of gloss was carried out. In fact, gloss is directly related to the surface roughness, being lower when surface is rougher (Ward and Nussinovitch, 2017). **Table 5.7** shows gloss values for the films with different HK contents processed by casting and compression. Gloss values higher than 70 º were taken as frame of reference to define the film as a glossy material with smooth surface (Trezza and Krochta, 2000). Films prepared by compression moulding showed higher values of gloss than those prepared by casting due to a smoother surface, in accordance with SEM images shown in **Figure 5.11**, as a consequence of the application of pressure during processing.

Furthermore, the incorporation of hydrolysed keratin into the films decreased significantly ($p < 0.05$) the gloss values. For instance, with the addition of 9 wt % HK, the gloss values of casting films decreased from 10.60 º to 4.40 º and, in the case of compression films, from 33.60 º to 23.40 º. These results indicated that the films processed with HK were glossier, in agreement with their smoother surface observed in **Figure 5.11**.

Table 5.7. Gloss values of the SPI-based films processed by casting (W) and compression (D) as a function of HK content.

Film	**Gloss$_{60º}$ (GU)**
HK0-W	10.60 ± 0.11[a]
HK3-W	8.20 ± 0.05[b]
HK6-W	5.50 ± 0.04[c]
HK9-W	4.40 ± 0.11[d]
HK0-D	33.60 ± 1.23[a]
HK3-D	6.60 ± 0.36[d]
HK6-D	10.60 ± 2.61[c]
HK9-D	23.40 ± 1.17[b]

[ad]Two means followed by the same letter in the same column and in the same section are not significantly ($p > 0.05$) different through the Duncan's multiple range test.

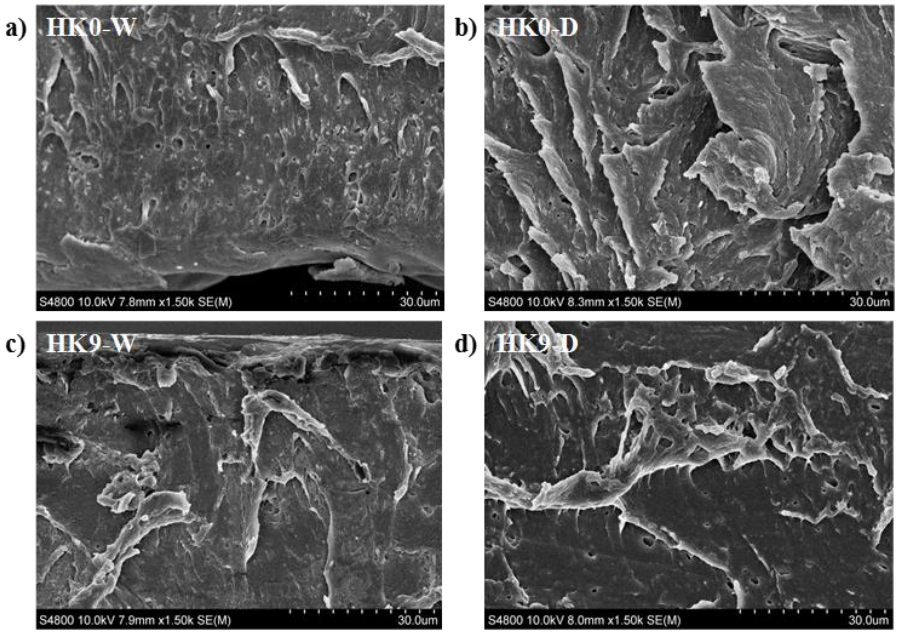

Figure 5.11. SEM micrographs of the cross-section of films containing 0 and 9 wt % of hydrolysed keratin processed by casting (HK0-W and HK9-W) and compression moulding (HK0-D and HK9-D).

CONCLUSIONS

Totally renewable protein-based films were prepared by casting and compression by using only raw materials derived from agro-industrial wastes or by-products, such as keratin from chicken feathers and soy protein from the production of soy oil. The employment of alkaline treatment at room temperature was an appropriate method to obtain hydrolysed keratin, soluble in water and a natural source of sulphur to promote disulphide bonds and, thus, crosslinking in protein-based formulations.

The chemical characterization of the keratin extracted from chicken feathers confirmed the high content of cysteine and also the significant changes produced in the protein structure, leading to the protein solubilisation. Further analyses of the soy protein/hydrolysed keratin films showed the good compatibility among the components, resulting in transparent films. Films processed by compression achieved better mechanical properties in terms of tensile strength, which increased with the incorporation of hydrolysed keratin. Interestingly, it was observed that the water uptake of the films remained constant after 24 h, indicating a high stability and structural integrity of the manufactured films.

Consequently, the incorporation of hydrolysed keratin into soy protein formulations opens up new opportunities to develop sustainable films with higher stability that could be potentially used to develop active and biodegradable films for food or pharmaceutical purposes.

6

chapter

EFFECT OF AGAR ON THE EXTRUDED PELLETS AND COMPRESSION MOULDED FILMS

Garrido T., Etxabide A., Guerrero P., de la Caba K. (2016)

Characterization of agar/soy protein biocomposite films: effect of agar on the extruded pellets and compression moulded films. Carbohydrate Polymers, 151, 408-416

SUMMARY

Renewable and biodegradable films can be also prepared from mixtures of polysaccharides and proteins. Blending process changes physical and chemical properties of the final product as a function of the compatibility between blend components. This compatibility is subjected to some characteristics of the macromolecules, such as the chemical structure and conformation, among others. In this context, agar is a cell-wall polysaccharide extracted from certain red seaweeds (*Gracilaria, Gelidium* and *Pterocladia*) and consists of a mixture of agarose and agaropectin, a sulphated polymer that varies according to the species of seaweed, but the main components of the chains are β-1,3-linked-D-galactose and α-1,4-linked 3,6-anhydro-L-galactose. This polysaccharide can interact with soy protein to form an interconnected network with enhanced physicochemical properties. The synergistic effects resulting from blending these biopolymers are of great importance to create new functional structures and promote new applications.

Regarding processing method, although extrusion has become a common technique to produce pellets from some polysaccharides, there are few reports related to blends of proteins and polysaccharides processed by this technique. It is worth noting that during extrusion the viscous dissipation of mechanical energy predominates, especially at low moisture contents, thus making this process highly energy efficient and cost effective. The effect of extrusion is to disassemble proteins and then reassemble them by disulphide bonds, hydrogen bonds and non-covalent interactions, forming fibrous structures in the extrudates. It is generally accepted that proteins are denatured during the

extrusion process, so these reactive unfolded protein chains can interact with other polymers.

Therefore, in this chapter agar/soy protein films were prepared by extrusion and compression moulding. Since few data are available about the molecular events occurred during blending, it is intended to describe the conformational changes during the extrusion process and the effect of agar on the final structure. Moreover, the functional properties of the films, such as physicochemical, optical, morphological and mechanical properties were measured.

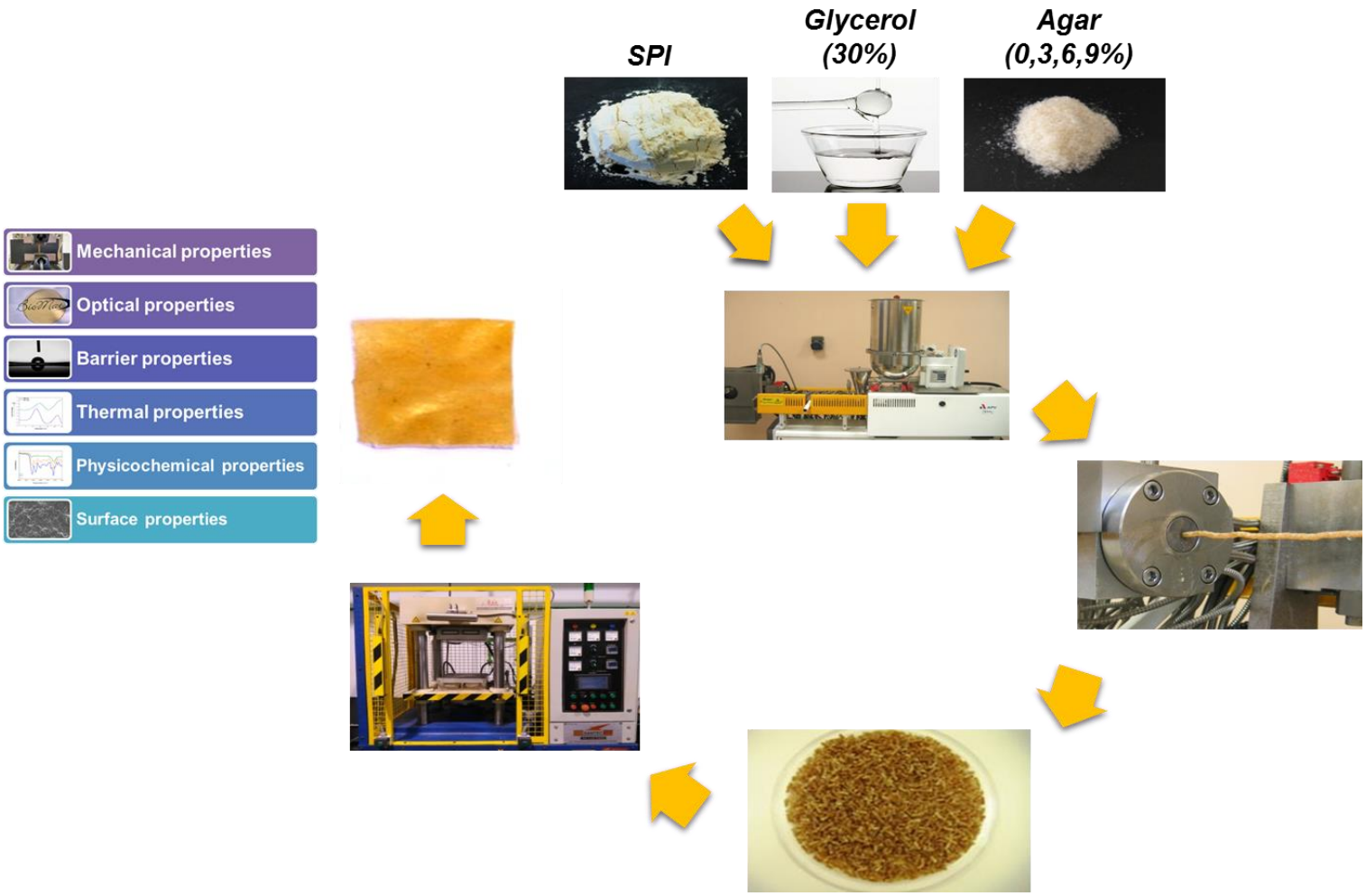

Figure I. Graphical abstract of Chapter 6.

6.1 PELLET AND FILM PREPARATION

6.1.1 Pellet preparation

Agar (AG), soy protein isolate (SPI), and glycerol (Gly) were blended in a Stephan UMC 5 mixer for 5 min at 1500 rpm in order to obtain a good blend. Control films were prepared with SPI and 30 wt % Gly on SPI dry basis and were designated as AG0. SPI was replaced by 3, 6 and 9 wt % AG to prepare the films designated as AG3, AG6 and AG9, respectively.

Blends were added into the feed hopper and mixed with water in the barrel of a twin-screw extruder. Barrel temperatures were set at 70, 80, 95, and 100 ºC for the four zones from input to output, and die temperature was set at 100 ºC. Water was pumped directly into the extruder barrel at a constant speed of 250 rpm using a peristaltic 504U MK pump. All trials were carried out using a water speed of 0.16 kg/h. The feed rate of extruder was adjusted to 1 kg/h and a single die of 3 mm diameter was used, giving a throughput per unit area of 0.141 kg/h mm^2.

6.1.2 Film preparation

The pellets obtained by extrusion were placed between two aluminium sheets and introduced into a caver laboratory press, previously heated at 150 ºC. The pellets were pressed at 130 bar for 2 min to obtain compression-moulded films.

6.2 RESULTS AND DISCUSSION

6.2.1 Agar characterization

NMR analysis was performed to characterize agar extracted from *Gelidium sesquipedale*. ^{1}H NMR spectrum of agar is shown in **Figure 6.1a**. The signal at 1.43 ppm is attributed to the methyl protons (Barros et al., 2013) and the signal at 5.69 ppm is associated with the H-1 of the l-galactose residue linked to a pyruvated D-galactose residue (Murano et al., 1992). The signal due to methylation, assigned at 3.41 ppm, was not observed.

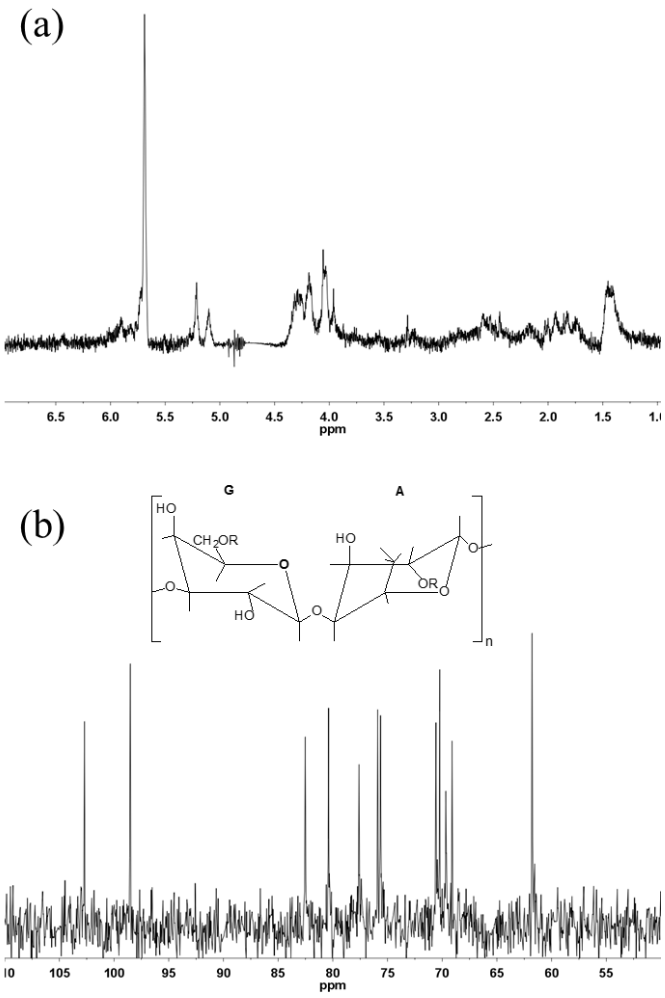

Figure 6.1. (a) ^{1}H NMR and (b) ^{13}C NMR spectra of the agar extracted *from Gelidium sesquipedale*.

The ^{13}C NMR spectrum of agar is shown in **Figure 6.1b** and shows 12 signals, 6 signals related to β-D-galactopyranose (G) and 6 signals related to 3,6 anhydro-α-L-galactopyranose (A). Each residue contains six chemically different carbon atoms, designated as G1-G6 for the galactopyranosyl and A1-A6 for the anhydro galactopyranosyl. As can be seen in **Figure 6.1b**, the signals for each carbon atom in galactose are G1 at 102.7 ppm, G2 at 70.6 ppm, G3 at 82.5 ppm, G4 at 69.1 ppm, G5 at 75.6 ppm and G6 at 61.8 ppm. The carbon atoms in anhydro galactose are A1 at 98.5 ppm, A2 at 70.2 ppm, A3 at 80.4 ppm, A4 at 77.6 ppm, A5 at 75.9 ppm and A6 at 69.7 ppm (Usov et al., 1980). The signals at 98.5 ppm and 69.1 ppm are related to 4-O-sulfate-D-galactopyranose, indicating a sulphated structure (Rochas and Lahaye, 1989), while the absence of the peak at 59.1 ppm related to O-methyl group indicated a low methylated agarose structure (Usov et al., 1983).

6.2.2 Physicochemical properties

The specific mechanical energy (SME), piece density (PD) and expansion ratio (ER) are important factors to be considered due to their direct effect on the final properties (Guerrero et al., 2014). SME, PD and ER values are shown in **Table 6.1** as a function of the agar content. The SME is the amount of work input from the driver motor into the raw material extruded and its value indicates the extent of molecular breakdown the material undergoes during the extrusion process (Zhang et al., 2015). The incorporation of agar caused a more viscous melt due to agar-protein interactions (Rocha et al., 2014). Therefore, a higher torque was required due to a frictional increase in the extruder barrel, thereby resulting in an increase of SME, from 972 to 1044 kJ/kg, and in a better protein denaturation, corroborated by DSC results. Regarding PD and ER, it was found that there was no dependence on the agar content, since no significant ($p > 0.05$) change occurred. This was due to the fact that agar-protein interactions did not cause bubble formation

during the process and thus, the volume of the pellets did not vary and the density was maintained constant. As a result, the product obtained at the extruder die was continuous and homogeneous for all compositions.

Table 6.1. Extruder specific mechanical energy (SME), pellet piece density (PD), pellet expansion ratio (ER) as a function of agar content.

Pellet	SME (kJ/kg)	PD (g/cm^3)	ER
AG0	972 ± 12^{a}	1.63 ± 0.13^{a}	3.37 ± 0.14^{a}
AG3	972 ± 9^{a}	1.59 ± 0.10^{a}	3.32 ± 0.08^{a}
AG6	1008 ± 18^{b}	1.55 ± 0.09^{a}	3.35 ± 0.10^{a}
AG9	1044 ± 16^{c}	1.53 ± 0.15^{a}	3.35 ± 0.12^{a}

[ac]Two means followed by the same letter in the same column are not significantly ($p > 0.05$) different through the Tukey´s multiple range test.

Regarding agar/soy protein films, MC values were measured as a function of agar content and are shown in **Table 6.2**. As can be seen, MC slightly increased ($p < 0.05$) with agar addition due to the hygroscopic character of agar. Due to this fact, WVP values significantly ($p < 0.05$) decreased. It must be considered that three mechanisms contribute to WVP: water vapour absorption at the surface of the film, water vapour diffusion through the film and finally, water vapour desorption from the surface of the film. In the agar-protein biocomposite films, the hygroscopic character of agar caused the retention of water vapour molecules inside the film, resulting in the decrease of the WVP values observed.

Table 6.2. Moisture content (MC), total soluble matter (TSM) and water vapour permeability (WVP) of the films as a function of agar content.

Film	MC (%)	TSM (%)	WVP (10^{-12} g cm/cm^2 s Pa)
AG0	17.32 ± 0.43^{a}	30.45 ± 0.29^{a}	8.57 ± 0.58^{a}
AG3	18.42 ± 0.27^{b}	28.84 ± 0.25^{b}	2.29 ± 0.18^{c}
AG6	20.49 ± 0.55^{c}	27.74 ± 0.35^{b}	2.95 ± 0.20^{bc}
AG9	21.51 ± 0.13^{d}	26.91 ± 0.32^{c}	3.88 ± 0.75^{b}

[ad]Two means followed by the same letter in the same column are not significantly ($p > 0.05$) different through the Tukey´s multiple range test.

As shown in **Table 6.2**, TSM values decreased with the incorporation of agar. This increase of the water resistance of the films was related to the interactions among AG, SPI and Gly. In contrast, WU of the films, shown as a function of time in **Figure 6.2**, increased with agar content, although the equilibrium of the water uptake was reached at the same time in all cases. WU process is developed during the initial stage of film hydration, in which water molecules may form water-polymer hydrogen bonds, thereby reducing inter-chain interactions and facilitating WU (Madera-Santana et al., 2014). Besides, the interactions occurred during the film formation also played a fundamental role in the changes of film structure (Phan The et al., 2009). In order to study these interactions, FTIR analysis was carried out.

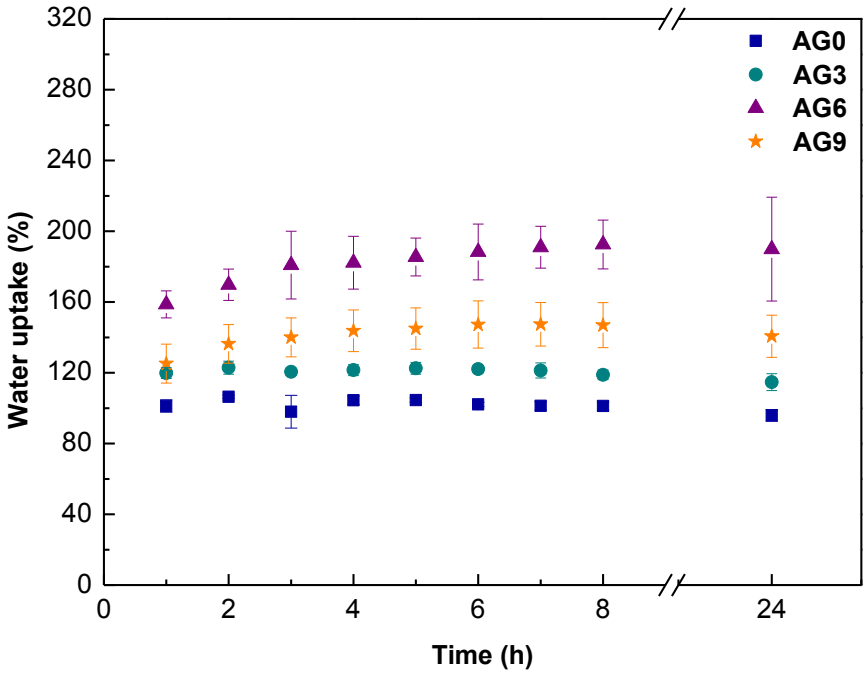

Figure 6.2. Water uptake (WU) of the films prepared with different agar contents.

FTIR spectra of SPI, AG, AG0 and AG9 films are shown in **Figure 6.3.** The FTIR spectrum of SPI exhibited three characteristic peaks common to proteins: amide I band at 1630 cm^{-1}, associated with the carbonyl group; amide II band at 1530 cm^{-1}, corresponding to N-H bending; and amide III band at 1230 cm^{-1}, related to C-N stretching and N-H bending (Su et al., 2008). The broad band observed in the 3500-3000 cm^{-1} range is related to free and bound O-H and N-H groups, able to form hydrogen bonding with the carbonyl group of the peptide linkage in the protein. The main absorption bands of glycerol, located in the region from 800 cm^{-1} to 1150 cm^{-1}, are observed in AG0 and AG9 spectra. The peaks at 850 cm^{-1}, 925 cm^{-1} and 995 cm^{-1} are assigned to the vibration of the C-C skeleton, the band at 1045 cm^{-1} is associated to the stretching of the C-O linkage in C1 and C3, and the one at 1117 cm^{-1} is related to the stretching of C-O in C2. In the case of AG, its spectrum showed a broad band at 3300 cm^{-1} associated with O-H stretching, indicating a high potential for intermolecular hydrogen bonds among hydroxyl groups of agar and protein, as well as between hydroxyl groups in agar and amino groups in protein. Moreover, the typical absorption bands of agar were observed at 930 cm^{-1} for 3,6-anhydrogalactose bridges and at 890 cm^{-1} for C-H of β-galactose (Freile-Pelegrín et al., 2007). The broad band at 1038 cm^{-1}, common to all polysaccharides, was related to the coupling of the C-O or the C-C stretching modes with the C-O-H bending modes, and the band at 1617 cm^{-1} was assigned to amide I vibrations, attributed to the presence of residual protein in agar. The incorporation of agar showed that the band at 1038 cm^{-1} shifted to higher frequencies and that the peaks at 930 and 890 cm^{-1}, related to the pure AG, disappeared, indicating the interactions between AG and SPI.

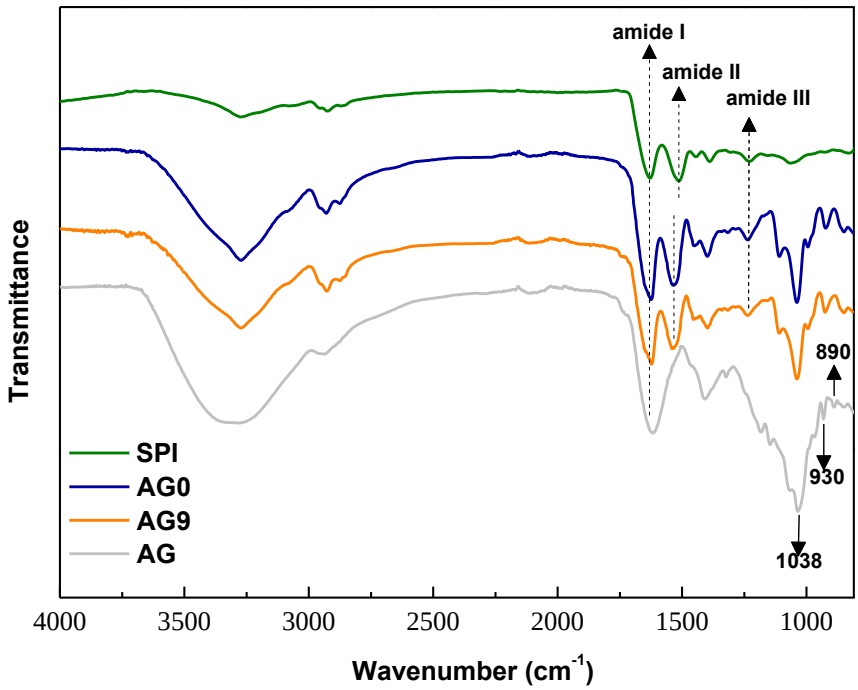

Figure 6.3. FTIR spectra of the films prepared with different agar contents (AG0 and AG9) and of pure compounds (SPI and AG).

The shape of the amide I band is representative of the protein secondary structure and it is used to determine the number and positions of the bands corresponding to the different components in the amide I profile. A curve fitting treatment was carried out to estimate quantitatively the relative proportion of each component representing a type of secondary structure. According to this band decomposition, the amide I profile contains four major components that can be linked, in analogy to other protein models, with aromatic ring vibrations, β-sheets (two components), α-helix/random coils, and β-turns. The second derivatives of the bands appeared in FTIR spectra for the films with different concentrations of agar are listed in **Table 6.3** and correspond to the amount of different types of secondary structures present in the protein. As can be observed, all spectra are dominated by α-helix/random coils (1649 cm^{-1}) and β-sheet (1620 and 1675 cm^{-1}) secondary structures, whereas β-turn structure, located approximately at 1690 cm^{-1}, is less

prominent (Bonwell and Wetzel, 2009). It is worth noting that the quantitative analysis of the amide I band showed a slightly increase of the α-helix/random coil area with the incorporation of agar, as well as a decrease of the β-sheet area, which could confirm that the polysaccharide incorporation modified the secondary structure of the protein due to the interactions between the two biopolymers.

Table 6.3. Secondary structure determination from the amide I band for the films prepared with different agar contents.

Film	Area (%)			
	1620 cm^{-1}	**1649 cm^{-1}**	**1675 cm^{-1}**	**1690 cm^{-1}**
AG0	35	45	19	1
AG3	30	50	19	1
AG6	29	52	17	2
AG9	29	53	16	2

6.2.3 Thermal properties

DSC thermograms of the films processed with different agar contents are shown in **Figure 6.4**. A pronounced endothermic peak was observed at 90-100 ºC, corresponding to the water evaporation, facilitated by the denaturation of 7S globulins present in SPI (Kumar et al., 2002). This thermal denaturation involved the disruption of intramolecular bonding and the unfolding and aggregation of protein molecules. It is worth noting that this peak area decreased in a more pronounced way for the AG9 film than for the rest of the films, resulting in a higher degree of denaturation in the protein and causing an increase in the denaturation temperature from 100 ºC to 125 ºC. This fact could be related to the presence of residual protein in agar, as shown by FTIR results and corroborated by the film colour analysis. Regarding the processing method used, it is generally accepted that proteins are denatured during the extrusion process, so that the more reactive unfolded protein chains can interact with the components incorporated into the

formulations, changing the structure of the polymeric network formed (Guerrero et al., 2014).

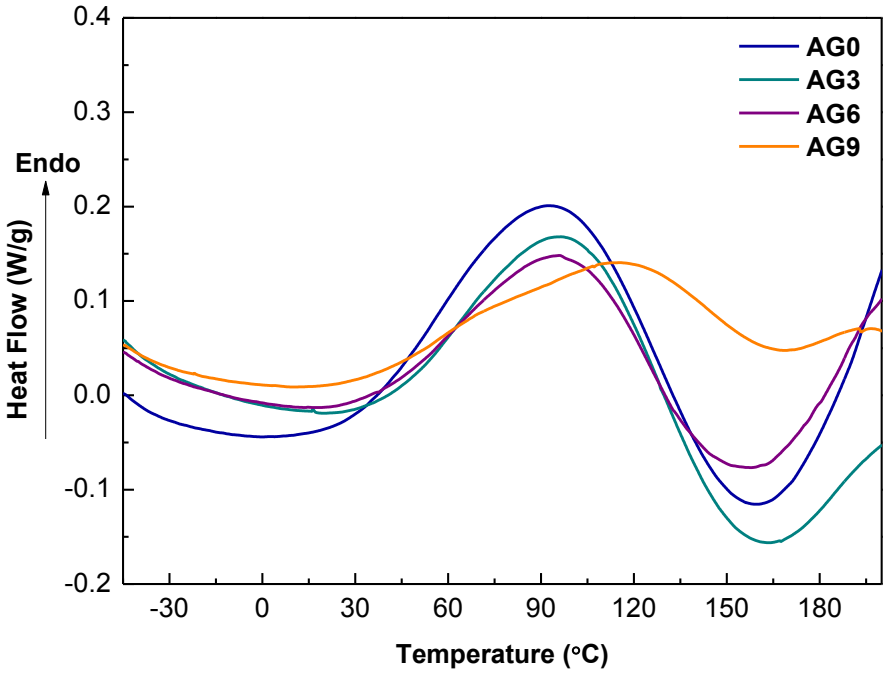

Figure 6.4. DSC thermograms of the films prepared with different agar contents.

TGA was carried out to evaluate the thermal stability of the films with different agar contents. TGA and DTG curves are displayed in **Figure 6.5**. All films showed similar behaviour with three main stages. The first stage around 90 ºC was related to the moisture evaporation. The second stage was associated to the glycerol evaporation (Rhim et al., 2013), and appeared around 220 ºC, higher temperature than the boiling point of glycerol (182 ºC), indicating an interaction between the biopolymers and Gly. It is worth noting that the intensity of this peak became higher as AG content increased, which would corroborate AG-Gly interactions. The third stage above 300 ºC was attributed to the thermal degradation of SPI and AG (El-Hefian et al., 2012).

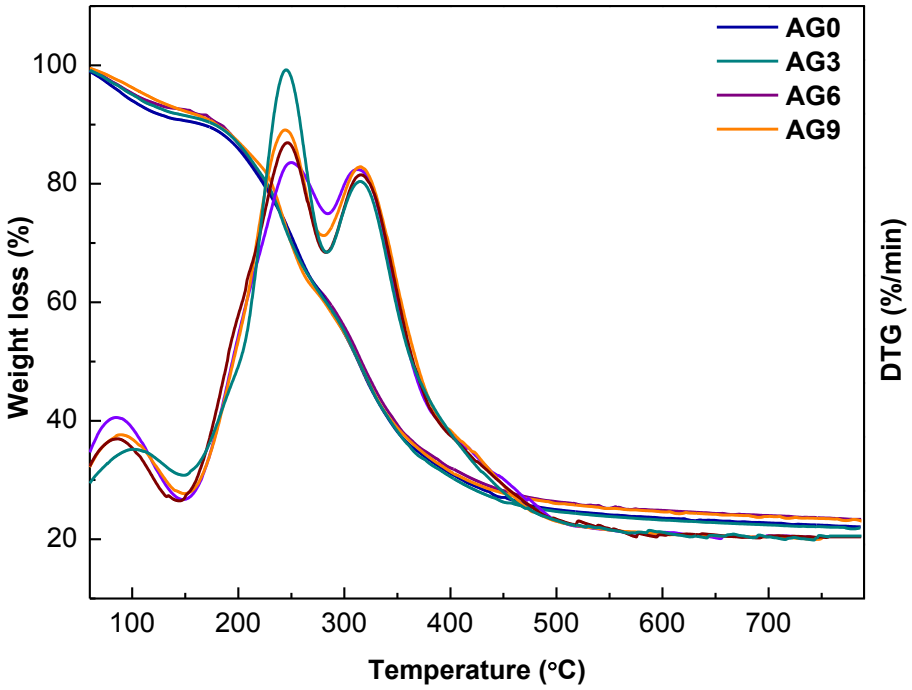

Figure 6.5. TGA thermograms of the films prepared with different agar contents.

6.2.4 Optical and morphological properties

Appearance is the most quickly identifiable quality responsible for acceptance or rejection of a product, so the measurement of the optical properties is a relevant task. All films were transparent, although the films prepared with 9 wt % agar showed a more yellowish colour, as can be observed in **Figure 6.6a-b**. Nevertheless, all films showed a homogeneous surface, as can be seen in **Figure 6.6c-d.**

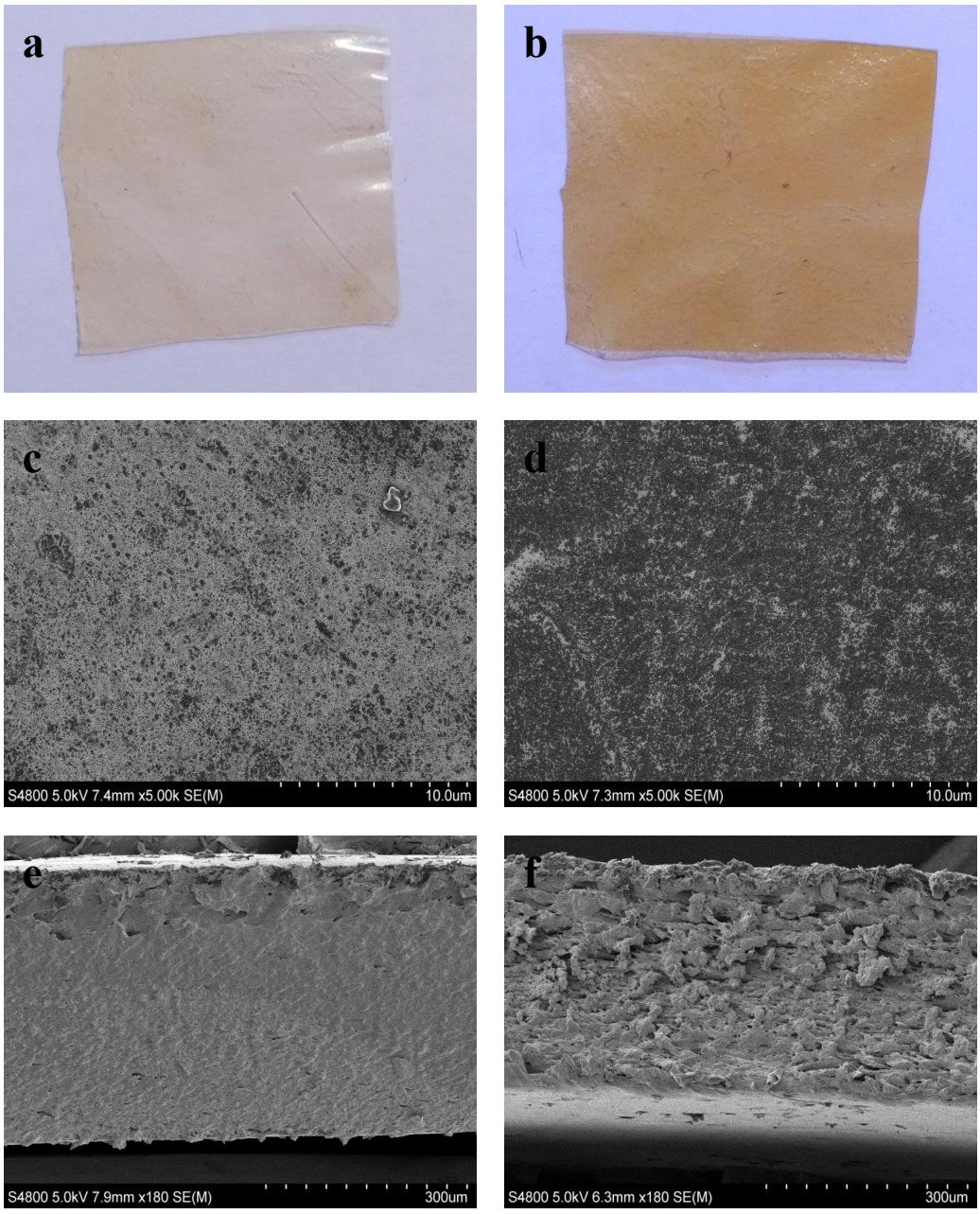

Figure 6.6. Visual aspect (a-b) and SEM images of the surface (c-d) and cross-section (e-f) for AG0 and AG9 films, respectively.

The values of colour and gloss for the films processed with different agar contents are shown in **Table 6.4**. The characteristic yellowish colour of SPI is related to b^* value. This parameter increased significantly ($p < 0.05$) with the agar content due to the gold tonality that the agar provided to the biocomposites. Regarding a^* parameter, the control biocomposite showed a more greenish colour than the biocomposites with agar, which became more reddish with the agar incorporation. This reddish tonality was attributed to

the residual protein present in the agar, as shown by FTIR (López-Simeon et al., 2012). The colour difference (ΔE^*) increased significantly ($p < 0.05$) with the addition of the agar, whereas L^* significantly ($p < 0.05$) decreased. This behaviour could be related to the increase of SME, suggesting that higher SME values resulted in darker products (Fang et al., 2014). Interestingly, this fact did not imply thermal degradation, as shown by TGA.

Regarding the gloss of the film, this is related to the surface morphology, influenced by the compression moulding process, so the higher the surface roughness, the lower the gloss (Ward and Nussinovitch, 1997). All samples had values lower than 70, considered as the standard of a glossy material, which means that all films were slightly glossy and had a high surface roughness (Trezza and Krochta, 2000). It is worth noting that the decrease of the gloss values with the addition of the agar promoted changes in the morphology and caused a direct influence in the surface of the films, obtaining a rougher surface. These changes in the surface characteristics would indicate interactions between the blend components, as shown by FTIR.

Table 6.4. Colour and gloss parameters of the films prepared with different agar content.

Film	L^*	a^*	b^*	ΔE^*	$Gloss_{60^o}$ (GU)
AG0	89.30 ± 0.45^a	-0.26 ± 0.16^a	19.54 ± 0.66^a		39.70 ± 9.15^a
AG3	88.63 ± 0.21^b	0.09 ± 0.03^b	24.95 ± 0.05^b	5.47 ± 0.07^a	49.80 ± 9.23^a
AG6	86.92 ± 0.37^c	0.80 ± 0.07^c	29.36 ± 0.28^c	10.16 ± 0.35^b	27.70 ± 9.79^b
AG9	81.57 ± 0.16^d	3.47 ± 0.07^d	38.94 ± 0.17^d	21.21 ± 0.19^c	25.90 ± 6.81^b

[ad]Two means followed by the same letter in the same column are not significantly ($p > 0.05$) different through the Tukey´s multiple range test.

Light barrier properties, such as transparency and light transmission, are shown in **Table 6.5**. On the one hand, the films showed excellent barrier properties against UV light in the range from 200 to 280 nm. The reason for this high UV light absorbance is the presence of sensitive chromophores in soy protein (tyrosine, phenylalanine and tryptophan), which can absorb the light at the wavelength below 300 nm (Li et al., 2004).

On the other hand, the transparency is an indicator of the compatibility of the components (Liu and Zhang, 2006), so the high transparency in all samples evidenced the good compatibility among agar, protein and glycerol, resulting in a homogeneous structure at macroscopic scale. However, the decrease in transparency as agar content increased suggested that the agar probably formed some agglomerations, as observed by SEM images.

Table 6.5. Optical properties of the films prepared with different agar contents: light transmission (%), and transparency (T) (A_{600}/mm).

Film	200 nm	280 nm	500 nm	600 nm	T
AG0	0.0026	0.0088	65.5362	72.5163	1.11[a]
AG3	0.0077	0.0100	54.0951	64.4303	1.64[b]
AG6	0.0162	0.0116	51.0084	60.8420	1.72[b]
AG9	0.0183	0.0164	46.4457	59.4931	1.56[b]

[ab]Two means followed by the same letter in the same column are not significantly ($p > 0.05$) different through the Tukey´s multiple range test.

In order to study the compatibility among the blend components, the cross sections of the films were analysed by SEM and images are shown in **Figure 6.6e-f**. As can be seen, the cross-sections of the films were rough and became more irregular when adding agar. This fact evidenced significant molecular rearrangements within the blend when increasing the AG content due to AG-SPI interactions, as shown by FTIR results, since both SPI and AG chains have available hydroxyl groups able to promote intermolecular interactions by hydrogen bonds.

6.2.5 Mechanical properties

All films were mechanically resistant when manipulating and showed stability upon storage. Elastic modulus (EM), tensile strength (TS), and elongation at break (EB) values are shown in **Table 6.6**. The significant increase ($p < 0.05$) of the EM for AG9 films resulted in an increase of stiffness, possibly due to the aggregation of agar, as shown

by SEM images. As a consequence, both TS and EB decreased. However, the values obtained in this work are higher than the values obtained for other protein/polysaccharide systems reported by other authors (Coughlan et al., 2004; Zárate-Ramírez et al., 2014). It is worth noting that the processing method also affects mechanical properties, as shown by Tian et al. (2011). These authors compared mechanical properties of soy protein/agar films prepared by solution casting and compression and observed that better mechanical properties were achieved for the films prepared by solution casting due to the formation of a more homogeneous structure. Since thermo-moulding processing is more appropriate to scale up production, further research is required to optimize processing methods and conditions that could lead to a further improvement of mechanical properties.

Table 6.6. Elongation at break (EB), tensile strength (TS) and elastic modulus (EM) of the films prepared with different agar contents.

Film	EB (%)	TS (MPa)	EM (MPa)
AG0	65.1 ± 5.6^{a}	5.8 ± 0.4^{a}	75.0 ± 6.3^{a}
AG3	48.4 ± 5.3^{ab}	5.9 ± 1.0^{a}	83.0 ± 3.5^{a}
AG6	48.7 ± 6.8^{ab}	5.1 ± 0.8^{ab}	87.5 ± 2.7^{a}
AG9	28.6 ± 2.4^{b}	4.3 ± 0.5^{b}	100.2 ± 5.4^{b}

[ab]Two means followed by the same letter in the same column are not significantly ($p > 0.05$) different through the Tukey´s multiple range test.

CONCLUSIONS

Agar/soy protein films were successfully manufactured by extrusion and compression moulding, technological processes used at industrial scale but not usually employed for biopolymers such as agar and soy protein. During these processes, agar-protein interactions occurred and caused conformational changes in the secondary structure of the protein. Furthermore, agar and soy protein showed good compatibility, resulting in transparent and homogeneous films. The incorporation of agar decreased the film solubility while increasing the water uptake, which could be used for a controlled delivery of active substances in both food and pharmaceutical applications.

7

chapter

SOY PROTEIN BIOCOMPOSITES WITH ALGAE WASTE AS A FILLER

Garrido T., Peñalba M., de la Caba K., Guerrero P. (2016)

Injection-manufactured biocomposites from extruded soy protein with algae waste as a filler. Composites Part B, 86, 197-202

SUMMARY

The commercial feasibility of protein-based biocomposites is highly associated with the employment of industrial processing techniques. In the previous chapter, it was shown that extrusion can be successfully employed for the manufacturing of soy-protein based biocomposites. In this chapter, another technique actually used for synthetic composites was employed: injection moulding. The employment of this processing method would greatly promote the application of protein-based biocomposites at an industrial scale.

Besides the processing methods, soy protein biocomposites were prepared with a natural waste from the agar-agar industry as a filler, which has not been used before to the best of our knowledge. The use of this waste can have a double benefit: wastes can be valorised and value-added products can be obtained with lower cost, so bringing both environmental and economic benefits to the development of more sustainable composites. In this context, the aim of this chapter is (i) to investigate the potential of extrusion and injection processes to manufacture soy protein biocomposites with algae waste as a filler, and (ii) to carry out the characterization of the biocomposites prepared by extrusion and injection processes.

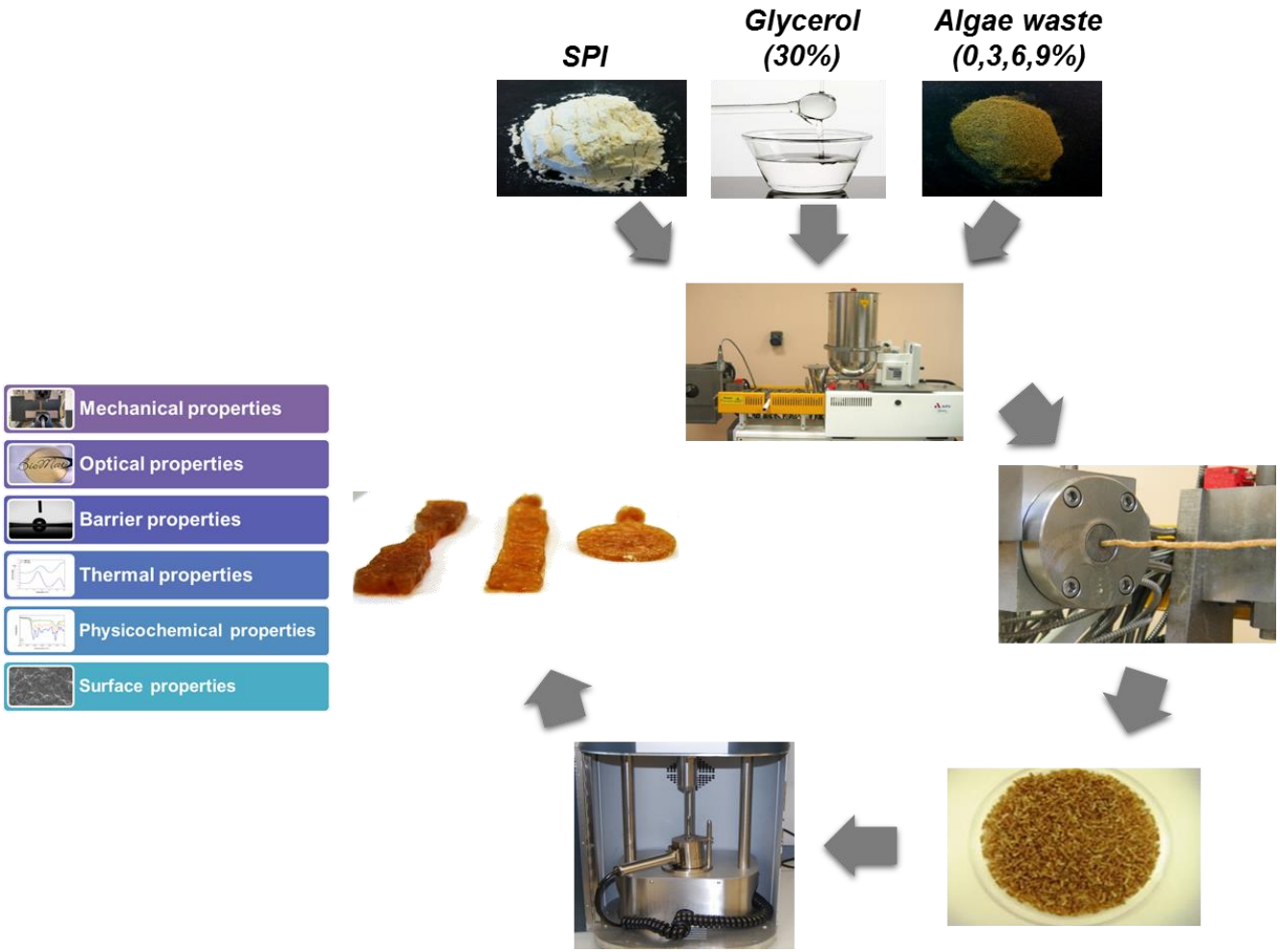

Figure I. Graphical abstract of Chapter 7.

7.1 BIOCOMPOSITE PREPARATION

The required soy protein isolate (SPI), glycerol (Gly) and algae waste (AW) contents to obtain the desired blend composition were mixed in a variable speed Stephan mixer, model UMC 5, for 5 min at 1500 rpm. SPI was replaced by 3, 6 and 9 wt % AW to obtain the blends designated as AW3, AW6 and AW9. The glycerol content selected was 30 wt %, based on the results obtained in a previous work (Guerrero et al., 2013), where this glycerol percentage was observed to be the minimum content needed to process soy protein materials by thermo-mechanical processing. The sample without AW was designated as the control AW0.

Blends were added into the feed hopper and mixed with water in the barrel of a twin-screw extruder. The extruder used in this study has 19 mm diameter barrel and a length/barrel diameter ratio of 25:1. The temperatures in the barrel were set at 70, 80, 95, and 100 ºC for the four zones from input to output, and the die was set at 100 ºC. All trials were carried out using a water speed of 0.15 kg/h and water was pumped directly into the extruder barrel zone 1 using a peristaltic pump. The extruder was operated at a constant speed of 250 rpm. The feed rate of extruder was adjusted to 1 kg/h and had a 2 kW/h motor power in practice. Dies were scaled up by maintaining a constant throughput per unit of orifice area. The extruder was equipped with a single die of 3 mm diameter, giving a throughput per unit area of 0.141 kg/h mm^2.

The pellets obtained by extrusion were injection-moulded into Type I ASTM tensile specimens by using a Haake MiniJet II injection-moulding machine. The injection moulded specimens were obtained at 120 ºC using a pressure of 450 bar.

7.2 RESULTS AND DISCUSSION

7.2.1 Extrusion process

First of all, thermogravimetric analysis (TGA) was carried out in order to estimate the thermal behaviour of the samples. TGA and DTG curves are shown in **Figure 7.1**, where four stages can be distinguished. The first stage, up to 100 ºC, was attributed to the loss of absorbed moisture, which indicates the existence of residual moisture. The second stage at 240 ºC was related to the loss of glycerol. This temperature is higher than the boiling temperature of the plasticizer, around 182 ºC, so this increase of temperature would indicate an interaction between SPI and glycerol (Guerrero et al., 2011).The third stage, around 315 ºC, was associated not only with the soy protein degradation but also with the protein present in AW. Finally, the last stage, between 450 and 600 ºC, was related to the decomposition of volatile metals and carbonates belonging to the filler (Liu et al., 2007).

Once determined that no degradation occurred at the temperatures used for the processing of soy protein biocomposites, the mechanical energy needed to produce the flow of the material through the extruder was measured, and SME values are shown in **Table 7.1**. To produce thermoplastic materials from proteins, non-covalent interactions and crosslinking have to be controlled. Plasticizers improve processability by interposing themselves among protein chains and alter the forces holding the chains together. This plasticizing effect occurs through two mechanisms: lubrication and increase of free volume.

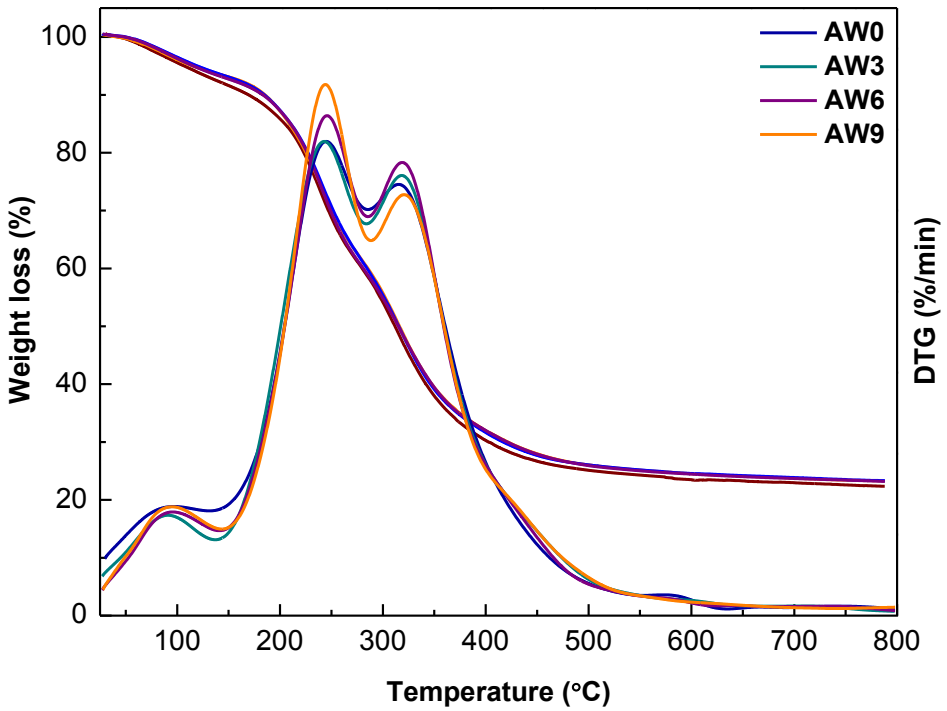

Figure 7.1. TGA and DTG curves of the blends as a function of AW.

In this chapter, water and glycerol were used as plasticizers. These small molecules were easily incorporated into the protein matrix, interacting by hydrogen bonding with the accessible side chains of the polar amino acid residues in protein chains and thus, preventing protein-protein interactions and leading to plasticization. Sufficiently plasticized proteins can be extruded using low SME, as observed in previous works (Guerrero et al., 2012; Harper, 1989). As can be seen in **Table 7.1**, the incorporation of AW in formulations led to an increase ($p < 0.05$) of SME values due to a higher degree of protein denaturation. The use of water and glycerol as plasticizers reduce protein-protein interactions (Guerrero et al., 2012), so enhancing AW diffusion and slowing down the rate of aggregation induced by heat-processing and acting as a good denaturant for soy proteins.

Table 7.1. Specific mechanical energy (SME) for the biocomposites processed with different AW contents.

Film	SME (kJ/kg)
AW0	972 ± 18^{a}
AW3	990 ± 21^{b}
AW6	1008 ± 24^{c}
AW9	1044 ± 17^{d}

[ad]Two means followed by the same letter in the same column are not significantly ($p > 0.05$) different through the Tukey's multiple range test.

The denaturation process was analysed by DSC, and thermograms are shown in **Figure 7.2**. As can be seen, extrusion process did not denature the protein completely and one endothermic peak was observed at 100-125 ºC, corresponding to the thermal denaturation of 7S globulins (Liu et al., 2007). As denaturation is associated with the disruption of intramolecular bonds, changes in denaturation enthalpies could be associated with changes in the bonding pattern, where a protein conformational state with fewer or weaker bonds would require less energy to unfold and, as a consequence, a reduction in enthalpy would be observed. In the case of the soy protein biocomposites prepared in this work, water and glycerol reduced protein-protein interactions and facilitated the diffusion of the algae waste, promoting a good interaction between SPI and AW. As shown in **Figure 7.2**, the addition of the filler caused a decrease of the peak, supporting the denaturation effect of the filler observed by the increase of SME values.

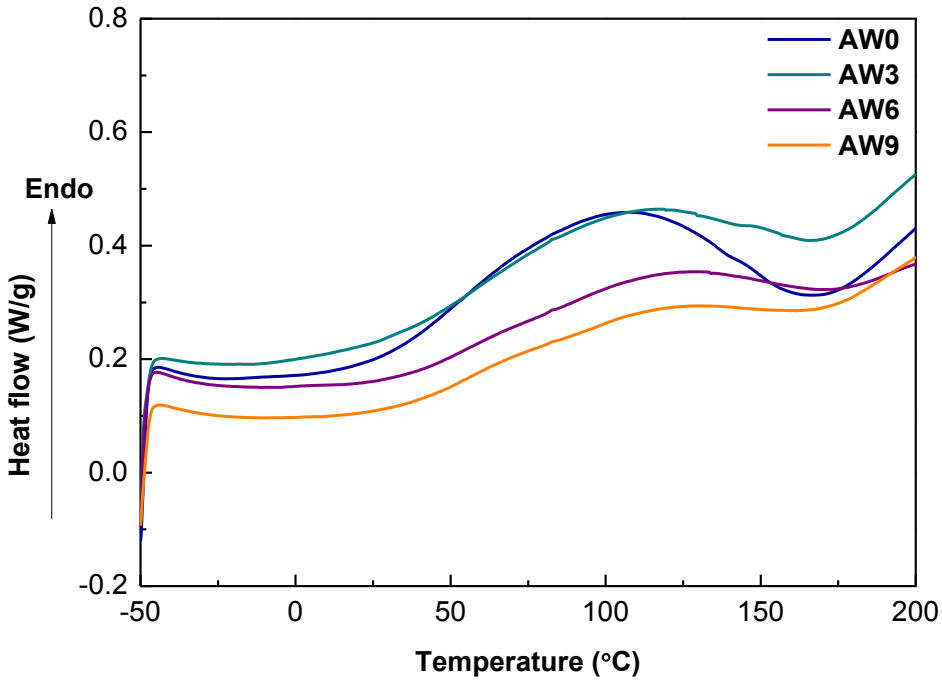

Figure 7.2. DSC thermograms of the biocomposites processed with different AW contents.

The good compatibility among the components of the biocomposites was analysed by FTIR spectroscopy and spectra are shown in **Figure 7.3**. Proteins exhibited three characteristic bands in relation to the peptide bond: amide I band at cm^{-1} associated with C=O stretching, amide II band at 1530 cm^{-1} corresponding to N-H bending, and amide III band at 1230 cm^{-1} related to C-N stretching and N-H bending (Lodha and Netravalli, 2005). Since AW is composed of proteins, it shows the three characteristic bands mentioned above. Additionally, the broad band at 1038 cm^{-1}, associated with the C-O stretching mode in polysaccharides (Guerrero et al., 2014), is related to the cellulose presence in AW. It is worth noting that this band was shifted to higher frequencies (1045 cm^{-1}) in the biocomposites with AW, indicating the interaction between soy protein and AW. This fact is due to the hydrogen bonding interactions formed between SPI and the cellulose in AW, as also shown in other works (Guerrero et al., 2013; Tian et al., 2011).

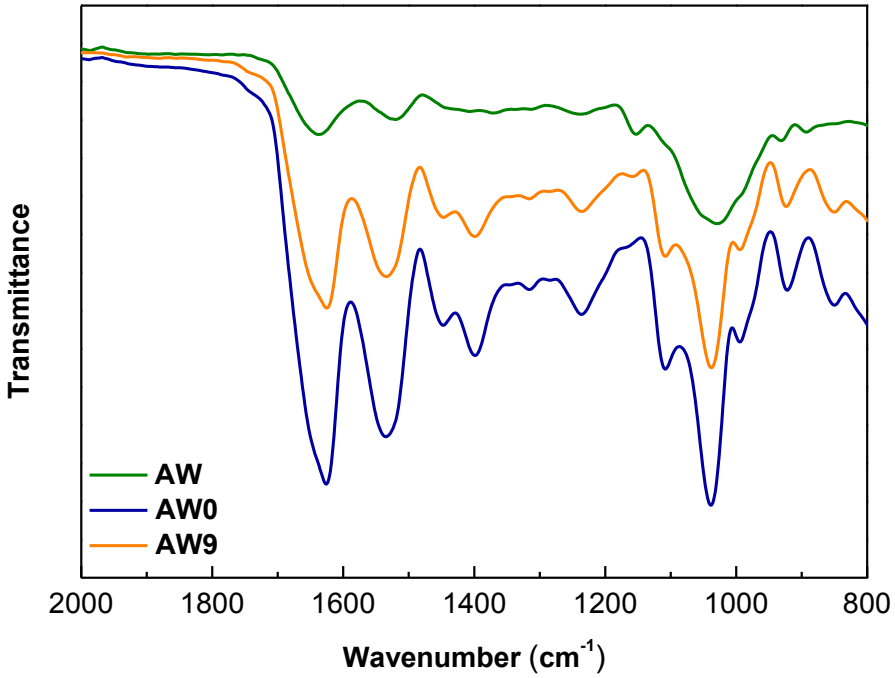

Figure 7.3. FTIR spectra of pure algae waste (AW), control sample (AW0) and the biocomposite with 9 wt % agar (AW9).

7.2.2 Barrier properties

The knowledge of barrier properties is important as far as the biocomposite stability is concerned. Oil permeability, oxygen transmission rate and water vapour permeability were measured and are shown in **Table 7.2**. As can be seen, soy protein-based biocomposites showed excellent barrier properties against lipids and oxygen due to the hydrophilic character of SPI, which contains 58% of polar amino acids and prevents the absorption of non-polar molecules. It is worth noting that the oxygen barrier properties of the SPI biocomposites prepared in this work were notably higher than the ones measured for synthetic polymers, such as polyethylene (PE) or polyethylene terephthalate (PET), used as commercial packaging materials nowadays (Norrahim et al.; 2013 Siró et al., 2010). Regarding water vapour permeability, the hydrophilic character of SPI also caused high WVP values. However, the barrier properties were not significantly

($p > 0.05$) affected by the addition of the algae waste, indicating the good compatibility between the components of the biocomposites, as shown by FTIR analysis.

Table 7.2. Oil permeability (OP), oxygen transmission rate (OTR) and water vapour permeability (WVP) values for the biocomposites processed with different AW contents.

Film	OP (%)	OTR (cm^3/m^2 day)	WVP (10^{-12}g cm/cm^2 s Pa)
AW0	0.38 ± 0.02^a	< 0.005	8.2 ± 0.3^a
AW3	0.37 ± 0.03^a	< 0.005	8.6 ± 0.5^a
AW6	0.38 ± 0.01^a	< 0.005	8.6 ± 0.4^a
AW9	0.37 ± 0.02^a	< 0.005	8.6 ± 0.3^a

[ad]Two means followed by the same letter in the same column are not significantly ($p > 0.05$) different through the Tukey's multiple range test.

In order to measure the resistance against UV light of SPI biocomposites, UV spectroscopy was carried out and absorbance values are shown in **Figure 7.4**. SPI biocomposites showed high absorbance values from 200 to 280 nm due to some chromophores present in soy proteins, such as tyrosine, phenylalanine and tryptophan, which can absorb the light at wavelengths below 300 nm (Li et al., 2004). This excellent UV light resistance was maintained when soy protein was replaced by different contents of algae waste, showing higher absorbance values than synthetic polymers such as PE or polypropylene (PP) (Guerrero et al., 2011b; Jakobsen et al., 2005). These results highlight the potential of SPI biocomposites to retard the oxidation caused by light when used as packaging materials.

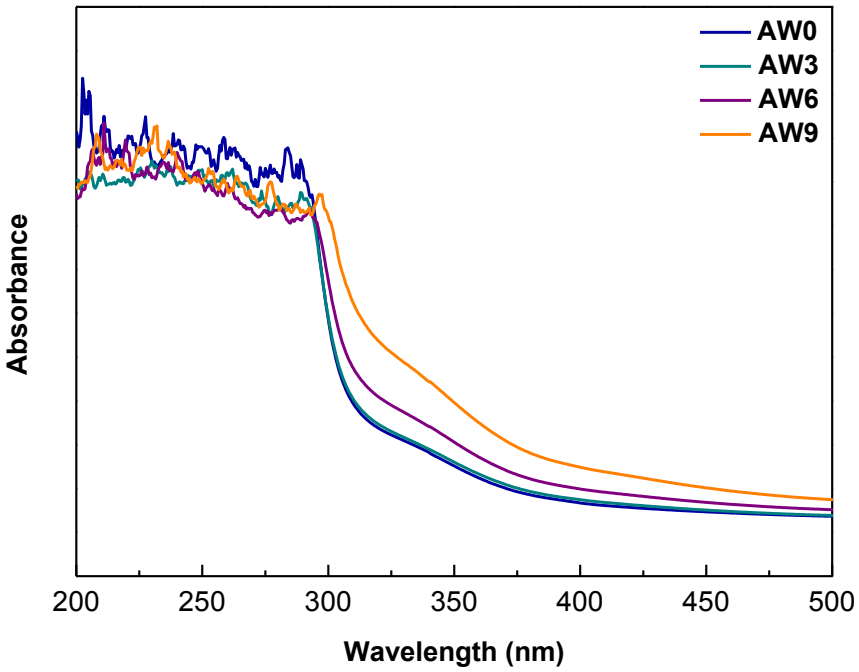

Figure 7.4. UV absorbance curves of the biocomposites processed with different AW contents.

7.2.3 Optical properties

Optical properties have an important effect in external appearance and thus, colour and gloss of SPI biocomposites were measured and are shown in **Table 7.2.** As can be observed, gloss values were lower than 30 GU in all cases, indicating that the surface of the biocomposites was not glossy (Kible-Boeckler, 1996). Gloss and surface roughness share a linear relationship, hence, the lower the gloss, the higher the roughness (Villalobos et al., 2005). Therefore, the high roughness of the biocomposites prepared in this work provides a suitable surface for printing.

Regarding colour values, a^* and b^* parameters have special significance due to the characteristic greenish and yellowish colour of algae waste and soy protein, respectively. Both parameters increased ($p < 0.05$) with AW content and the colour difference (ΔE^*)

related to the control biocomposite also increased ($p < 0.05$) due to the addition of the filler.

Table 7.3. Optical properties of the biocomposites processed with different AW contents.

Film	Gloss$_{60^\circ}$ (GU)	L*	a*	b*	ΔE*
AW0	29.2 ± 2.3^{a}	72.2 ± 0.8^{a}	6.3 ± 0.2^{a}	39.1 ± 0.7^{a}	
AW3	28.6 ± 1.9^{a}	69.4 ± 0.3^{b}	7.1 ± 0.1^{b}	42.2 ± 0.7^{b}	4.3 ± 0.6^{a}
AW6	27.9 ± 2.4^{a}	64.5 ± 1.2^{c}	8.1 ± 0.4^{c}	45.1 ± 0.7^{c}	9.9 ± 1.0^{b}
AW9	26.9 ± 1.8^{a}	62.6 ± 0.7^{d}	8.4 ± 0.2^{c}	45.7 ± 0.9^{c}	11.9 ± 0.3^{c}

^{ad}Two means followed by the same letter in the same column are not significantly ($p > 0.05$) different through the Tukey's multiple range test.

7.2.4 Mechanical properties and morphology

The mechanical properties of SPI biocomposites moulded by injection were measured, and elastic modulus, tensile strength and elongation at break values are shown in **Table 7.4**. When increasing filler content, elastic modulus increased ($p < 0.05$) and elongation at break decreased ($p < 0.05$), suggesting that the interaction between SPI and AW, shown by FTIR analysis, restricted the motion of protein chains. Despite the detrimental effect of AW addition in tensile strength and elongation at break, the incorporation of the filler involved a positive effect in tensile modulus. Similar results have also been evidenced by other authors for other biopolymers reinforced with natural fillers (Fiore et al., 2014).

Table 7.4. Elastic modulus (EM), tensile strength (TS) and elongation at break (EB) of the biocomposites processed with different AW content.

Film	EM (MPa)	TS (MPa)	EB (%)
AW0	73.6 ± 2.3^{a}	5.2 ± 0.4^{a}	71.9 ± 4.6^{a}
AW3	74.2 ± 2.0^{a}	4.7 ± 0.6^{ab}	72.6 ± 6.9^{a}
AW6	86.4 ± 3.6^{b}	4.7 ± 0.7^{ab}	41.3 ± 7.1^{b}
AW9	95.2 ± 1.6^{c}	4.0 ± 0.5^{b}	30.2 ± 5.2^{b}

^{ac}Two means followed by the same letter in the same column are not significantly ($p > 0.05$) different through the Tukey's multiple range test.

In order to explain the mechanical properties shown above, the morphology of SPI biocomposites was analysed by optical microscopy. As can be seen in **Figure 7.5**, biocomposites showed pores in the network microstructure. The addition of AW caused changes in the microstructure and a less porous structure was observed. AW-incorporated biocomposites showed well-defined pores with higher size and more irregular shape than the control biocomposite. This morphology would explain the decrease in TS values since biocomposites with more heterogeneous morphology are more liable to suffer damage with the application of an external force. It is also worth noting that no AW agglomeration was observed, indicating the good compatibility between the protein and the filler.

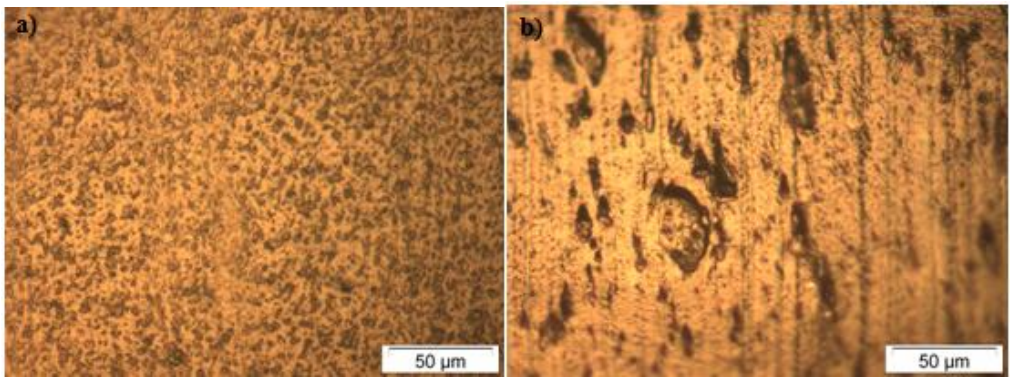

Figure 7.5. Optical microscopy of a) the control biocomposite and b) the biocomposite with 9 wt% AW.

CONCLUSIONS

The results obtained in this chapter showed that the replacement of soy protein by algae waste did not significantly affect the excellent barrier properties of SPI biocomposites, maintaining adequate optical and mechanical properties. These results highlight the potential reduction in the biocomposite costs through the replacement of biopolymers by the use of wastes as fillers, as well as the reduction of waste amounts by the valorisation of algae waste to produce value-added products. At the same time, the request of manufacturing biocomposites by the techniques employed in the plastics industry has been also achieved by obtaining soy protein pellets by extrusion and biocomposites by injection moulding, increasing the commercial potential of these materials.

8

chapter

INCORPORATION OF β-CHITIN TO DEVELOP FILMS AND HYDROGELS

Garrido T., Etxabide A., de la Caba K., Guerrero P. (2017)

Versatile soy protein films and hydrogels by the incorporation of β-chitin from squid pens (Loligo sp.). Green Chemistry, 19, 5923-5931

SUMMARY

The recovery of marketable products from fishery wastes (heads, skins, scales, shells or backbones) could lead to an important waste reduction strategy for industries. In this sense, squid pens have been regarded as an unattractive refuse from squid processing industry for many years. Fortunately, some authors have highlighted the squid pen feasibility to become a β-chitin source since it is composed of around 31-49% β-chitin on dry basis, depending on the squid species. In fact, several interesting properties of chitin have been discovered, such as biocompatibility, non-toxicity and biological activities, which make it attractive for a variety of applications such as biomedical, cosmetic, agriculture, food technology, paper technology, wastewater treatment and textile industry, among others.

Chitin can be extracted from the gladius of the squid, which is defined as a feather-shape internal structure that supports the squid's mantle and serves as a site for muscle attachment, being constituted mainly of proteoglycans and β-chitin. Chitin, in turn, it is composed of linear repeating units of N-acetyl-β-D-glucosamine and it chemically resembles cellulose, in which the hydroxyl group at C-2 has been substituted by acetamide groups.

Depending on its source, chitin occurs as three allomorphs: α-chitin, the most stable form of the three crystalline variations and whose chains arrange in microcrystalline structures of antiparrallel chains; β-chitin, whose chains arrange in microcrystalline structures of parallel chains; and γ-chitin, a combination of both α and β-chitin. In these three structures, the chains are organized in sheets and held by intra-sheet hydrogen bonds. Since up to now the main commercial sources for the production

of chitin have been various crustaceans, principally crab and shrimp shells, α-form has been the most studied polymorph, leaving β-form as a secondary type of chitin.

Nonetheless, the fact that β-chitin is composed of parallel strands conforms it with a less compact or less crystalline structure, which makes easier the interactions with proteins compared with α-chitin. This characteristic could be useful in order to employ chitin as a reinforcement of other biopolymers such as soy protein. Moreover, chitin from squid pens has a more open structure and, therefore, it shows higher swelling grade than α-form, due to less intermolecular hydrogen bonding attributed to the parallel arrangement of the main chains.

The chemical method for chitin isolation from crustacean wastes follows various steps. Firstly, a demineralization step is carried out in order to eliminate the inorganic matter using dilute acidic medium, which, in most cases, is the responsible for decreasing the molecular weight of chitin. Secondly, a deproteinization step is accomplished in an alkaline medium for the extraction of the protein matter. Finally, a decolouration step is performed for sample depigmentation. The employment of squid pens as a source of β-chitin requires neither demineralization nor decolouration steps due to the low content of inorganic components and the absence of pigments in squid pens. Thus, the processing time, the employment of acid pollutants, the voluminous wastewater discharge and the production costs can be considerably reduced.

Regarding the processes followed to isolate chitin, NaOH is usually employed. However, harsher conditions, in terms of NaOH concentrations and the temperatures used, are involved in comparison to those analysed in this chapter. This is a novel point in the extraction of chitin, which might provide relevant benefits, such as greater process simplicity, lower environmental load and lower costs.

Taking into account the characteristics above mentioned, in this chapter β-chitin was employed to reinforce soy protein films in order to obtain a multifunctional material with enhanced physicochemical and mechanical properties, employing compression moulding as processing method. β-Chitin was extracted from squid pens (*Loligo* sp.) by a simple alkaline hydrolysis, avoiding the demineralization and decolouration steps used in the chitin extraction from other sources and, thus, reducing the processing time and the production costs of the films. The initial crystalline structure of chitin influences the reactivity for chemical modification as well as the functional properties of the material; thus, the characterization of the soy protein films with different contents of β-chitin was carried out.

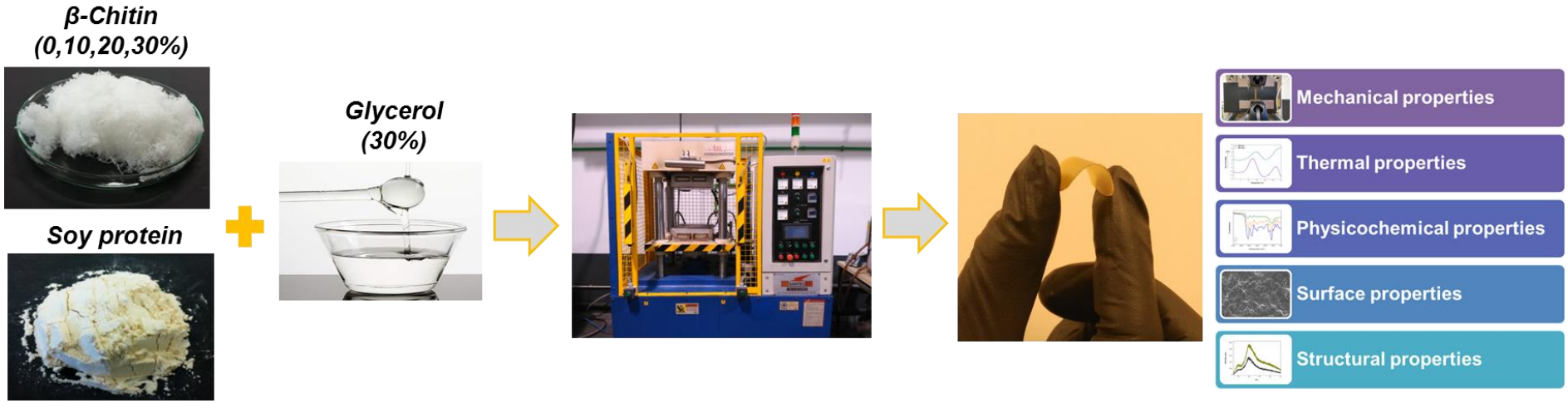

Figure I. Graphical abstract of Chapter 8.

8.1 FILMS PREPARATION

Firstly, 5 g of soy protein isolate (SPI) were mixed with 10, 20 and 30 wt % chitin (CH) (based on SPI dry basis) and 125 mL of distilled water were added. Then, the pH was adjusted to 10 before heating the mixture at 80 ºC for 30 min under magnetic stirring. Afterwards, 30 wt % glycerol (based on SPI dry basis) was added to the mixture, which was heated for other 30 min at the same conditions. Finally, the mixture was poured into Petri dishes and freeze-dried in order to obtain the powder, which was thermally compacted in a laboratory press for 2 min at 150 ºC and 12 MPa. SPI films were designated as CH0, CH10, CH20 and CH30 as a function of CH content.

8.2 RESULTS AND DISCUSSION

8.2.1 β-Chitin characterization

As determined by the analysis of ash content, the squid pens had around 0.66% ashes. This value confirmed the low mineralization level of squid pens, especially by the absence of calcium carbonate, so demineralization step could be avoided (Chandumpai et al., 2004). Furthermore, due to the pen location in endoskeletons, squid pens have low pigmentation, which allows the elimination of the decolouration step. Therefore, the separation of the chitin from the protein present in the gladii by means of deproteinization was the only process required to isolate β-chitin. This simple alkaline treatment employed to extract β-chitin from squid pens was able to recover 41.23% of its initial mass. The yield obtained was in agreement with the values reported for other species (Lavall et al., 2007). Regarding the average degree of acetylation (DA), this was determined from the elemental analysis data. By this analysis, the amounts of C and N present in β-chitin were determined as 42.6 and 6.3%, respectively; thus, the average degree of acetylation of β-chitin was estimated to be 95.6%, which was higher than that obtained in other works (Nata et al., 2012). Since the nitrogen content is also an indicative of the residual protein present in chitin, the low value obtained implied the minimum amount of protein left (Majtán et al., 2007).

The deproteinization caused by alkaline treatment was analysed by UV spectroscopy and the results are shown in **Figure 8.1**. It is well known that the broad band between 200 and 280 nm is related to some chromophores present in proteins, such as tyrosine, phenylalanine and tryptophan (Balestrieri et al., 1978), which are able to absorb the light at wavelengths below 300 nm. As can be observed, the UV absorbance capacity

of the squid pen notably decreased after the alkaline treatment to obtain β-chitin due to the successful protein extraction (Ianiro et al., 2014).

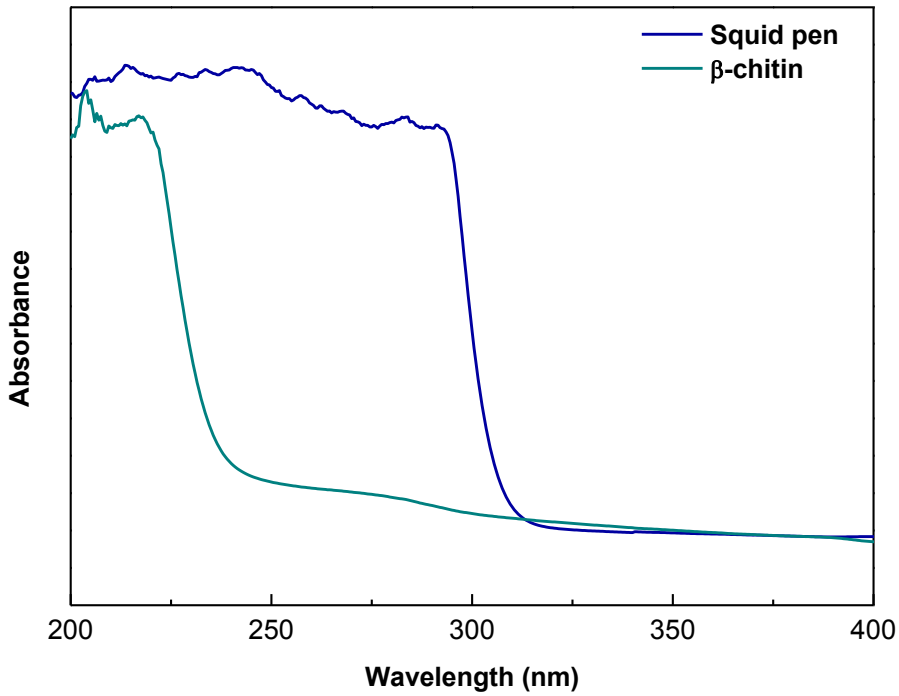

Figure 8.1. UV spectra of the squid pen and the extracted β-chitin.

In the hierarchical structure of the gladius, β-chitin remains wrapped in a protein layer and forms nanofibrils (Kurita, 2001), therefore, when deproteinization step is carried out, changes in the structure of β-chitin happen. In order to evaluate the effect of the protein extraction on the secondary structure of the protein present in the squid pen, FTIR analysis was performed. The spectra of the untreated squid pen and the β-chitin are shown in **Figure 8.2**. The spectra exhibited a broad band at 3271 cm^{-1} that corresponded to the H-bonded NH stretching (Focher et al., 1992), which became more intense and showed sharper shoulders after the alkaline treatment. The bands at 2917 and 2867 cm^{-1} corresponded to the aliphatic CH stretching. Regarding amide I (1629 cm^{-1}), a single band was observed, characteristic of the β-chitin polymorphic form. In contrast to α-chitin,

β-chitin has only intra-sheet hydrogen bonding in its crystalline structure; thus, a single band appears related to the hydrogen bonding between carbonyl and amine groups (Jang et al., 2004). This band became narrower for chitin in comparison to that of squid pen. Additionally, the two bands observed around 1535 cm^{-1} for the squid pen became a single one at 1549 cm^{-1} (amide II) in the chitin spectrum. These two bands related to amide I and amide II confirmed the high acetylation degree in chitin samples, as supported by elemental analysis, which provided an acetylation degree of 95.6%. Regarding the polysaccharide band between 1180 and 953cm^{-1}, no change in the relative intensity between this band and the amide I band was found. The increase of the FTIR band intensities after the alkaline treatment could be due to the strong water dipoles couple with local dipoles of the bonds (Snyder et al., 1982).

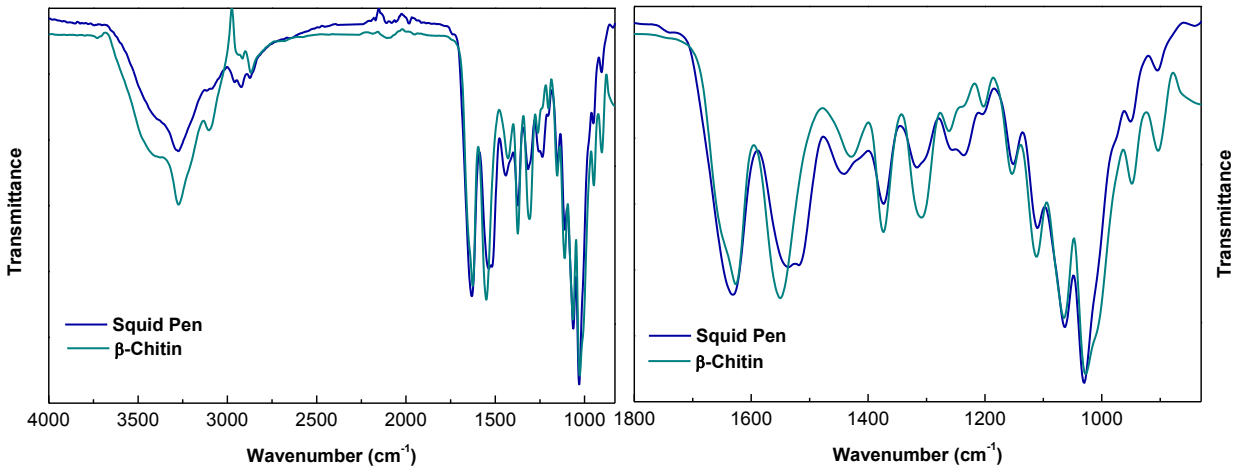

Figure 8.2. FTIR spectra of the squid pen and the extracted β-chitin.

The tertiary structure of proteins can be assessed by XRD, so the crystalline structure of the squid pen and the extracted β-chitin was analysed and the corresponding diffractograms are exhibited in **Figure 8.3**. It is well known that β-chitin has a high crystallinity due to its extensive intra-molecular hydrogen bonding but, after the alkaline

treatment of squid pen, the crystallinity of β-chitin suffered a modification due to the intercalation of water molecules between β-chitin sheets. Two broad crystalline reflections at 2θ = 8.1º and 2θ = 19.4º are observed in **Figure 8.3**. The position of these two peaks confirmed that β-chitin showed a parallel structure (Jung et al., 2014). It can be observed that the width of the peak at 19.4º related to squid pen was wider than that of β-chitin; thus, the higher crystallinity of β-chitin was confirmed. This may happen due to the protein removal after the deproteinization treatment. The crystallinity index (CrI) of the samples was calculated from the diffractogram. As mentioned above, the crystallinity index for β-chitin seems to be higher than that for squid pen. According to the CrI equation, the crystallinity was 80.9% and 87.5% for squid pen and β-chitin, respectively.

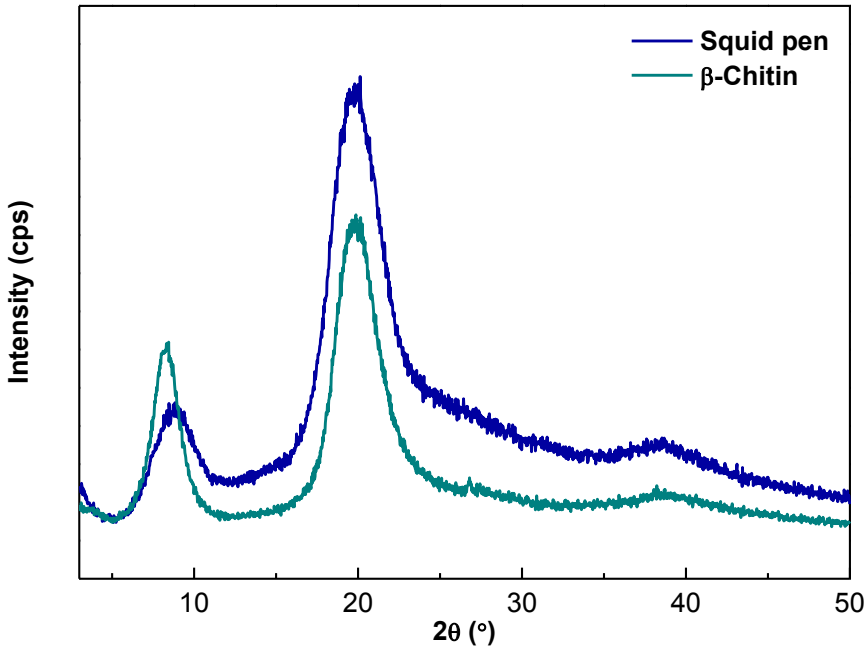

Figure 8.3. XRD pattern of the squid pen and the extracted β-chitin.

The ^{13}C NMR spectra of the squid pen and the extracted β-chitin are shown in **Figure 8.4**. Seven signals are observed in the spectra, corresponding to the eight carbon

atoms of the N-acetyl-β-D-glucosamine repetitive chain. The signals are assigned to C=O at 173.6 ppm, C1 at 103.6 ppm, C4 at 83.6 ppm, C3 and C5 at 74.5 ppm, C6 at 60.7 ppm, C2 at 55.2 and CH3 at 22.7 ppm. The peak related to C3 and C5 appeared as a single peak which is typical of β-chitin and indicates the difference between the two polymorphous, α and β-chitin, due to the differences in hydrogen-bonding (Cortizo et al., 2008). As shown in **Figure 8.4**, the peaks corresponding to methyl and carbonyl groups decreased in the β-chitin spectrum due to the increase of the deacetylation degree. Additionally, the disappearance of the peaks that contribute to ^{13}C resonances from 170 to 105 ppm and from 50 to 25 ppm and indicate protein levels (Schaefer et al., 1987) supported the fact that protein extraction was attained.

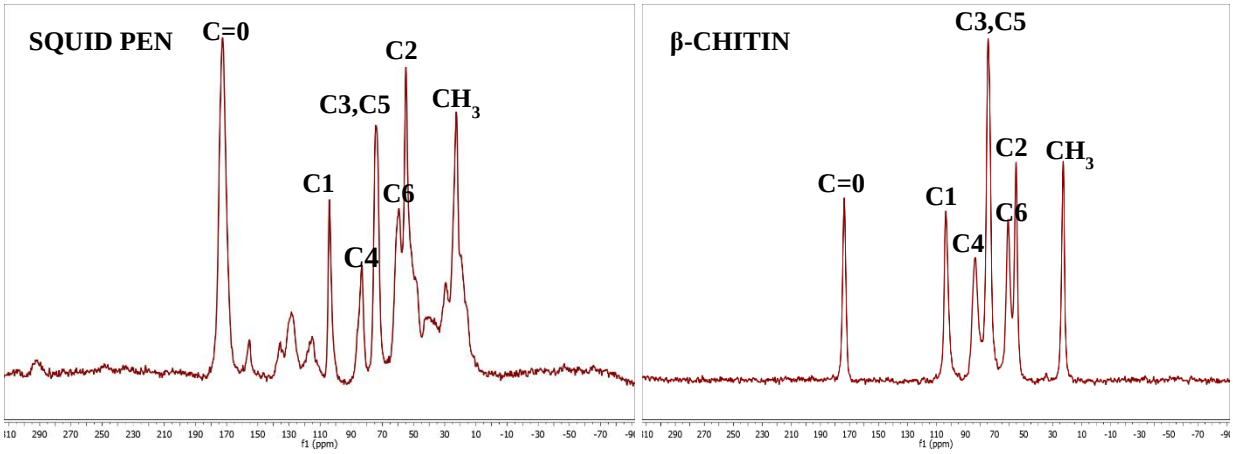

Figure 8.4. ^{13}C NMR spectra of the squid pen and the extracted β-chitin.

8.2.2 Film characterization

The physicochemical properties of SPI/CH films are supposed to be affected by the CH amount incorporated into the film forming formulation; thus, the characterization of the films as a function of β-chitin content was carried out. It is worth noting that the transparency of SPI films was maintained after the incorporation of CH, even when the content added was 30% (**Figure 8.5**). Regarding the film moisture content, MC values

were slightly affected by CH addition, as can be observed in **Table 8.1**. Moisture content significantly ($p < 0.05$) increased for SPI/CH films regardless of CH concentration. This increase in moisture content could be attributed to the amount of moisture absorbed by chitin during the film preparation process (Darmato et al., 2002). With regard to TSM, the film solubility was around 22-24%, mainly related to the migration of glycerol into water. Nonetheless, a significant ($p < 0.05$) decrease of TSM was noticed when CH was added due to the interactions among the film forming components.

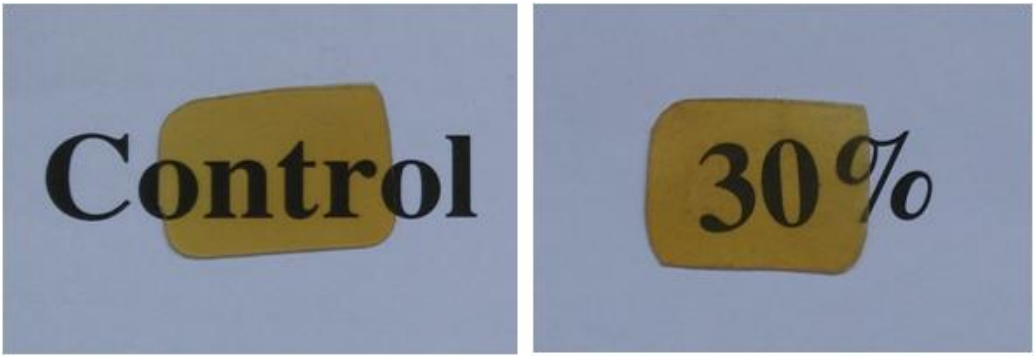

Figure 8.5. Photographs of the control film (CH0) and the film prepared with 30% chitin (CH30).

Table 8.1. Moisture content (MC) and total soluble matter (TSM) of SPI/CH films.

Film	MC (%)	TSM (%)
CH0	11.58 ± 0.11^{a}	24.45 ± 0.14^{a}
CH10	13.51 ± 0.21^{b}	22.99 ± 0.27^{b}
CH20	13.38 ± 0.62^{b}	22.47 ± 0.68^{b}
CH30	13.24 ± 0.49^{b}	21.46 ± 0.55^{c}

[ac]Two means followed by the same letter in the same column are not significantly ($p > 0.05$) different through the Duncan´s multiple range test.

In order to analyse these interactions, FTIR analysis was carried out and spectra are shown in **Figure 8.6**. SPI exhibited three characteristic bands common to proteins: amide I band at 1630 cm^{-1} associated with C=O stretching, amide II band at 1530 cm^{-1} corresponding to N-H bending, and amide III band at 1230 cm^{-1} related to C-N stretching and N-H bending (Su et al., 2008). The main absorption bands of glycerol were related to

five bands corresponding to the vibrations of C-C bonds at 850, 940 and 1000 cm^{-1}, and those related to C-O bonds at 1050 and 1100 cm^{-1} (Ren et al., 2016). For the films with CH, the band corresponding to amide II (1530 cm^{-1}) showed a shift toward higher frequencies (1537 cm^{-1}), attributed to the hydrogen bonding between the hydroxyl groups of CH and the amino groups of SPI. These interactions agree with the decrease of water uptake observed for SPI/CH films.

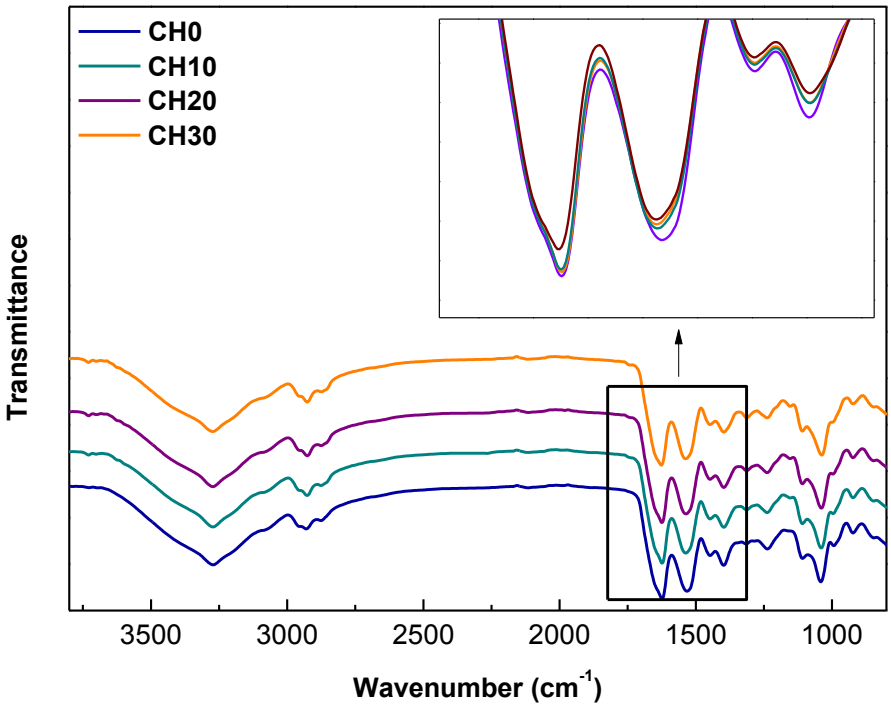

Figure 8.6. FTIR spectra of SPI/CH films.

It is known that the surface composition could change with the incorporation of a new component; therefore, the composition of the film surface was examined by XPS in order to study the effect of the CH addition. The compositional information related to C, O and N content is shown in **Table 8.2**, where O/C and N/C ratios are also provided. Results revealed that C is predominant on the film surface, although the amount of C

slightly decreased from 73% to 71% with the addition of 30 wt % CH while the oxygen content increased from 20% to 23%.

Table 8.2. Compositional information of SPI/CH determined by XPS.

Film	C (%)	O (%)	N (%)	O/C	N/C
CH0	73	20	7	0.27	0.09
CH10	72	22	6	0.30	0.08
CH20	71	22	7	0.31	0.09
CH30	71	23	6	0.32	0.08

The deconvolution of the C peak resulted in three peaks, whose contents are displayed in **Table 8.3**. C1 was attributed to C-C and C-H, C2 was related to carbon bound to nitrogen (C-N) and to oxygen (C-O), and C3 corresponded to C=O. It was noticed that C2 content remained constant, while C1 decreased and C3 increased with the addition of CH, suggesting the interactions among the film forming components.

Table 8.3. C1, C2 and C3 contents of SPI/CH films determined by XPS.

Film	C1 (%)	C2 (%)	C3 (%)
CH0	44	20	9
CH10	39	20	13
CH20	36	20	15
CH30	36	20	15

The crystalline structure of the films with different CH contents was analysed by X-ray diffraction. According to Noishiki et al. (2003), β-chitin can be transformed into the α-chitin crystalline structure by some treatments at harsh conditions, when 50% NaOH or 8 N HCl solutions are used. In this research work, mild conditions (1 M NaOH) were employed to separate chitin and protein and thus, the transformation into α-chitin did not occur. **Figure 8.7** shows two crystalline planes (0 2 0 and 1 1 0) at reflections of 8.6 and 20.0. These two peaks increased with β-chitin content indicating a higher crystallinity. The films obtained by hot pressing from the solid SPI/CH blend maintained

chitin crystallinity after film processing and film crystallinity increased as CH content increased and thus, amorphous SPI films turned into more crystalline films (72.3% crystallinity). The sharper peaks observed when CH concentration increased indicate that more rigid and stable films are obtained when CH was employed as reinforcement. Therefore, mechanical testing was carried out in order to relate film structure and mechanical properties.

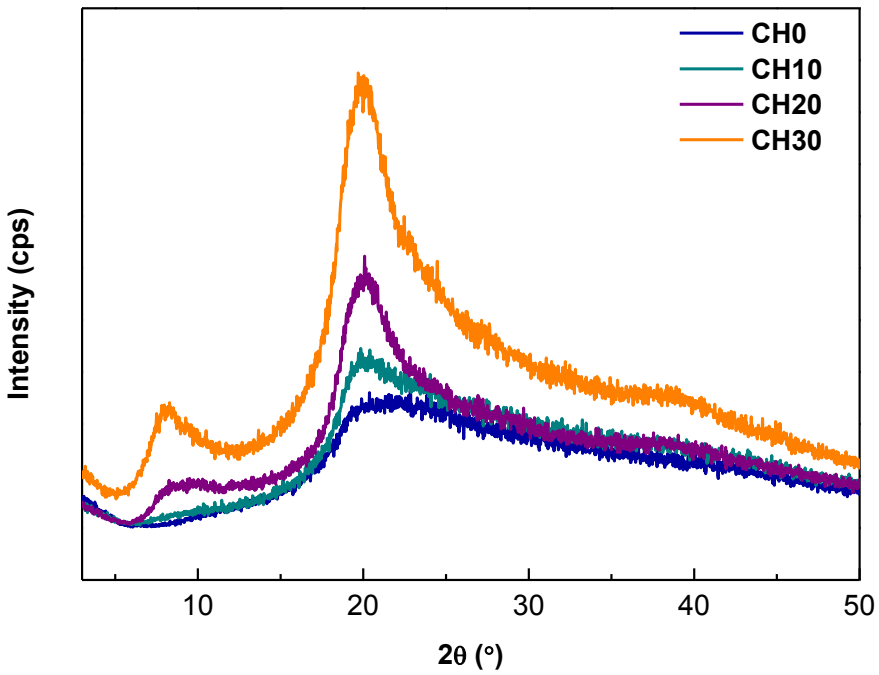

Figure 8.7. XRD pattern of SPI/CH films.

The mechanical properties of SPI/CH films are displayed in **Table 8.4**. When CH content varied from 0 to 30 wt %, tensile strength (TS) significantly ($p < 0.05$) increased from 7.47 to 11.25 MPa, while elongation at break (EB) significantly ($p < 0.05$) decreased from 131.37 to 6.08%. Moreover, the addition of CH significantly ($p < 0.05$) increased the elastic modulus, which resulted in a stiffer material due to the motion restriction caused by the presence of β-chitin in the matrix. This is in agreement

with XRD results in which a higher crystallinity was obtained when CH content increased and, therefore, an enhancement of the mechanical properties in terms of tensile strength and elastic modulus (Shraee et al., 2017).

Table 8.4. Elongation at break (EB), tensile strength (TS) and elastic modulus (EM) of SPI/CH films.

Film	EB (%)	TS (MPa)	EM (MPa)
CH0	102.62 ± 4.29^{a}	7.05 ± 0.52^{a}	105.18 ± 6.09^{a}
CH10	13.86 ± 0.74^{b}	8.11 ± 0.59^{ab}	299.25 ± 10.60^{b}
CH20	7.57 ± 0.55^{c}	10.22 ± 1.69^{ab}	538.84 ± 13.13^{c}
CH30	6.12 ± 0.19^{c}	11.52 ± 0.99^{b}	716.67 ± 7.76^{d}

[ad]Two means followed by the same letter in the same column are not significantly ($p > 0.05$) different through the Duncan´s multiple range test.

In accordance with mechanical properties, SPI/CH film cross section showed a compact structure. SEM micrographs of the fractured cross section of the SPI films with 0, 10, 20 and 30 wt % CH at a magnification of x200 are shown in **Figure 8.8**. This compactness could be attributed to the interactions among the components of the film forming formulations. It is well known that glycerol can migrate when the films are immersed into water. However, as shown in **Table 8.1**, the TSM value for the CH0 film was lower than the glycerol content used in this work (30%), indicating the formation of interactions between SPI and glycerol. When CH was added, these interactions increased and a more compact structure was achieved, preventing the entrance of water molecules into the structure. Consequently, a decrease of film solubility from 24.4% to 21.4% was observed, as shown in **Table 8.1**.

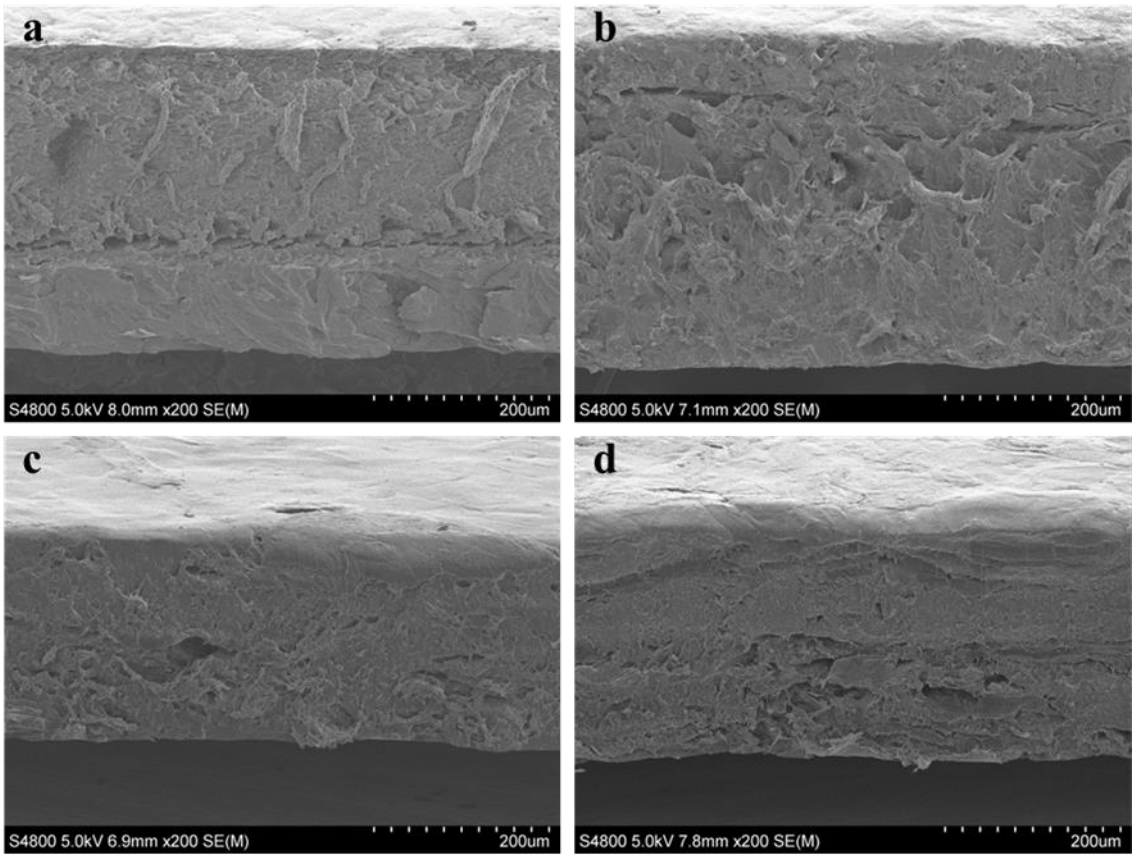

Figure 8.8. SEM micrographs of the cross section of the films a) with 0 wt % CH, b) 10 wt % CH, c) 20 wt % CH and d) 30 wt % CH.

8.2.3 Hydrogel characterization

Finally, the swelling behaviour of the films and their mechanical properties after the water immersion test were analysed. The water uptake capacity of the films as a function of time is shown in **Figure 8.9**. It should be noted that a slight mass loss occurs when samples were immersed into water, mainly due to glycerol migration. Since the migration occurs at the initial time and the values are lower than 30%, as shown by TSM values in **Table 8.1**, this fact has not a significant effect in the swelling behaviour shown by WU curves, where the reduction of the film water uptake can be observed due to CH hydrophobicity (Kumar et al., 2000). Moreover, the films with CH reached the

equilibrium in the first 4 h and maintained their integrity during the 24 h of water immersion, whereas the film without chitin started to dissolve.

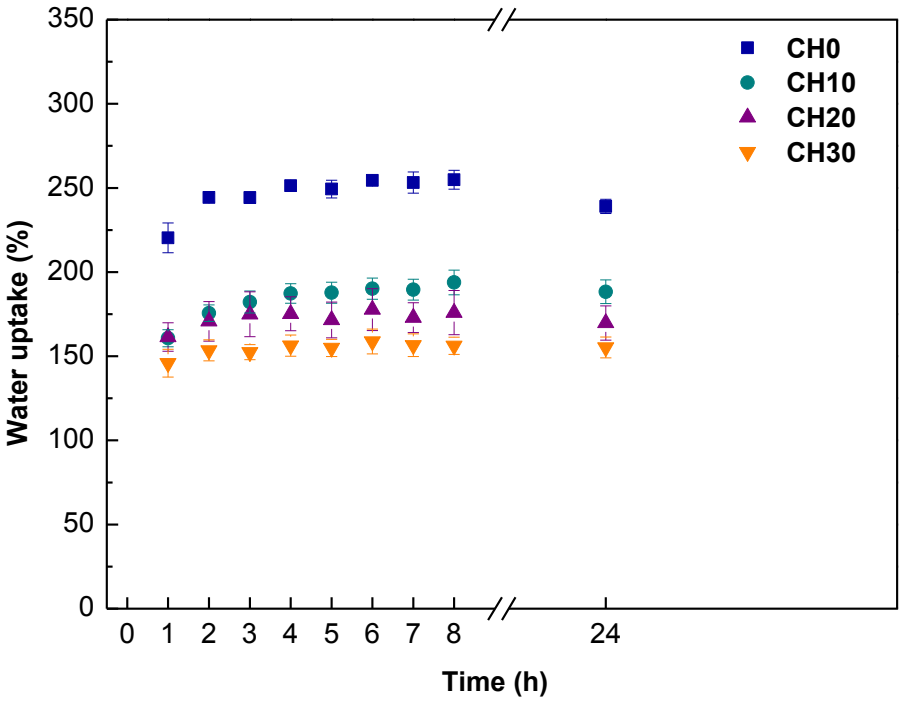

Figure 8.9. Water uptake of SPI/CH films.

Films with 0 and 30 wt % CH before and after 4 h of water immersion are exhibited in **Figure 8.10**. As can be observed, the films maintained their integrity and were easy to handle, probably due to the fact that β-chitin has no inter-sheet hydrogen bonds in the crystal structure, providing high stability (Younes and Rinaudo, 2015). Comparing to other SPI systems (Barkay-Olami and Zilberman, 2016), the SPI/CH films showed lower water uptake, attributed to the interactions among the film forming components.

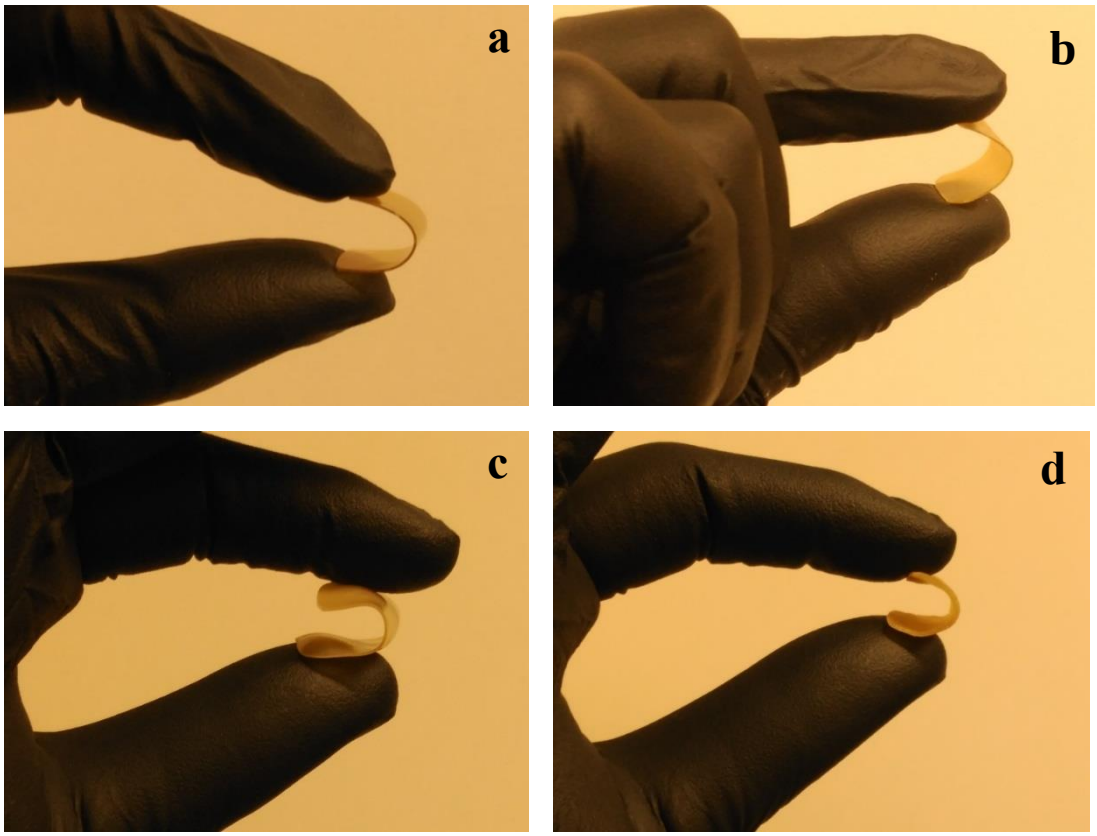

Figure 8.10. SPI/CH films with a) 0 wt % CH and b) 30 wt % CH, and SPI/CH hydrogels with c) 0 wt % CH and d) 30 wt % CH.

Mechanical properties were measured after the water immersion of the film during 4 h (**Table 8.5**) since SPI/CH films reached the equilibrium swelling at this time. As expected, EB, TS and EM values of the hydrogels were lower than those of the films (**Table 8.4**). These values were similar to those obtained for other SPI hydrogels (Cuadri et al., 2016). It was noticed that TS and EM values of SPI/CH hydrogels increased with CH content, while EB decreased. This behaviour was a consequence of the water uptake capacity of the films, since CH0 films were able to uptake more water than the films with CH, increasing the plasticizing effect and, thus, elongation at break.

Table 8.5. Elongation at break (EB), tensile strength (TS) and elastic modulus (EM) of SPI/CH hydrogels.

Film	EB (%)	TS (MPa)	EM (MPa)
CH0	56.75 ± 1.53^{a}	0.50 ± 0.03^{a}	1.01 ± 0.11^{a}
CH10	19.75 ± 1.19^{b}	0.61 ± 0.03^{b}	3.40 ± 0.51^{b}
CH20	15.93 ± 2.78^{b}	0.61 ± 0.02^{b}	5.61 ± 0.31^{c}
CH30	12.82 ± 1.63^{c}	1.27 ± 0.01^{c}	15.75 ± 0.86^{d}

[ad]Two means followed by the same letter in the same column are not significantly ($p > 0.05$) different through the Duncan´s multiple range test.

CONCLUSIONS

β-Chitin was successfully extracted from squid pens employing a simple treatment with NaOH (1 M) at room temperature. This method was sufficient to deproteinize the gladii without the degradation and deacetylation of the native chitin. The decrease of UV absorbance capacity demonstrated that only protein was removed from the squid pen, recovering 41.23% of β-chitin. Moreover, as the demineralization and decolouration steps were avoided, the chitin production cost and the environmental impact were reduced. Regarding SPI/CH films, it was concluded that chitin directly affected the degree of crystallinity of the SPI-based films. Thus, tensile strength and elastic modulus were improved. Additionally, a reduction of the water uptake was observed as well as a decrease in the film solubility, enhancing the stability of the samples.

9

chapter

ANTIOXIDANTS EXTRACTION USING MICROWAVE TECHNOLOGY

Garrido T., Gizdavic-Nikolaidis M., Leceta I., Urdanpilleta M., Guerrero P., de la Caba K., Kilmartin P. (2019)

Optimizing the extraction process of natural antioxidants from chardonnay grape marc using microwave-assisted extraction. Waste Management, 88, 110-117

SUMMARY

The wine industry involves the production of a large amount of residues that must be discarded, with some being destined to the distilleries to produce spirits such as grappa, or used in the production of tartaric acid or compost. Additionally, it is estimated that 3% of grape marc is used as animal feed. However, this biowaste is characterized by high contents of grape stalks, wine lees and grape marc, known to contain a high level of polyphenols that possess antioxidant and radical scavenging activities, with potential health benefits.

During winemaking, only a small part of the phytochemicals is transferred from grapes to wine, thus, a large quantity of valuable compounds remains in the waste. In the case of red wine, the juice is macerated along with skin and seeds to extract not only colour but also tannins, which contribute to the structure and body of the final wine. However, white wine fabrication requires the juice to be separated from the grape solids as soon as possible before the temperature-controlled fermentation, so many potential bioactives still remain in the grape marc.

Phenolic compounds vary depending on the type of grape, climatic factors, winemaking techniques and soil type, among others, and they can be classified in two main groups based on their carbon skeleton: flavonoids and non-flavonoids. The former group includes anthocyanidins (malvidin, delphinidin, petunidin, peonidin, and cyanidin), flavonols (quercetin, myricetin, and kaempferol), flavan-3-ols (catechin, epicatechin, epicathecin 3-gallate, and gallocatechin - both as monomers and within larger tannin structures), flavones (luteolin and apigenin), and flavanones (naringenin); and the latter

group includes hydroxycinnamic acids (caffeic, p-coumaric, and ferulic acids), benzoic acids (gallic, vanillic, and syringic acids), and stilbenes (resveratrol).

In recent years, efficient techniques for the extraction of these bioactive compounds have been assessed. Traditionally, solid-liquid extraction by mechanical agitation and Soxhlet extraction have been employed for polyphenols recovery from grape waste. Nevertheless, the high temperatures used, along with the long times and hazardous solvents, can cause hydrolysis and oxidation of the targeted compounds as well as a high environmental impact. Therefore, other techniques have been evaluated for the extraction of bioactive compounds. Among them, microwave-assisted extraction (MAE) has been employed for the extraction of a wide variety of bioactive compounds and one of its main advantages is a significant reduction of the extraction times. Despite the great potential of MAE for bioactive extraction, the use of high temperatures and/or hard conditions can be a drawback for developing a sustainable process in terms of energy consumption as well as for scaling up the process. Since the use of high temperatures in a process lowers the commercial potential of the technology, in this chapter the extraction process was undertaken at room temperature in order to increase the opportunities of designing a more sustainable extraction process.

When MAE is employed, multiple parameters can affect the extraction process and they should be taken into consideration due to their individual or combined effects on the yield of the extract and its composition. Therefore, the choice of solvent, solvent to solid ratio, power applied and extraction temperatures and times are key factors to maximize the extraction process. In order to optimize complex experimental processes that consider many factors, response surface methodology (RSM) is one of the most

relevant multivariate techniques, which allows a lower number of trials to be undertaken and an efficient interpretation of the optimization.

Taking all the above into consideration, the aim of this chapter was to analyse the feasibility of employing MAE at room temperature as an efficient technique to recover polyphenols from Chardonnay grape marc. For that purpose, firstly, the optimization of the extraction was carried out using RSM and secondly, the characterization of the extract was accomplished.

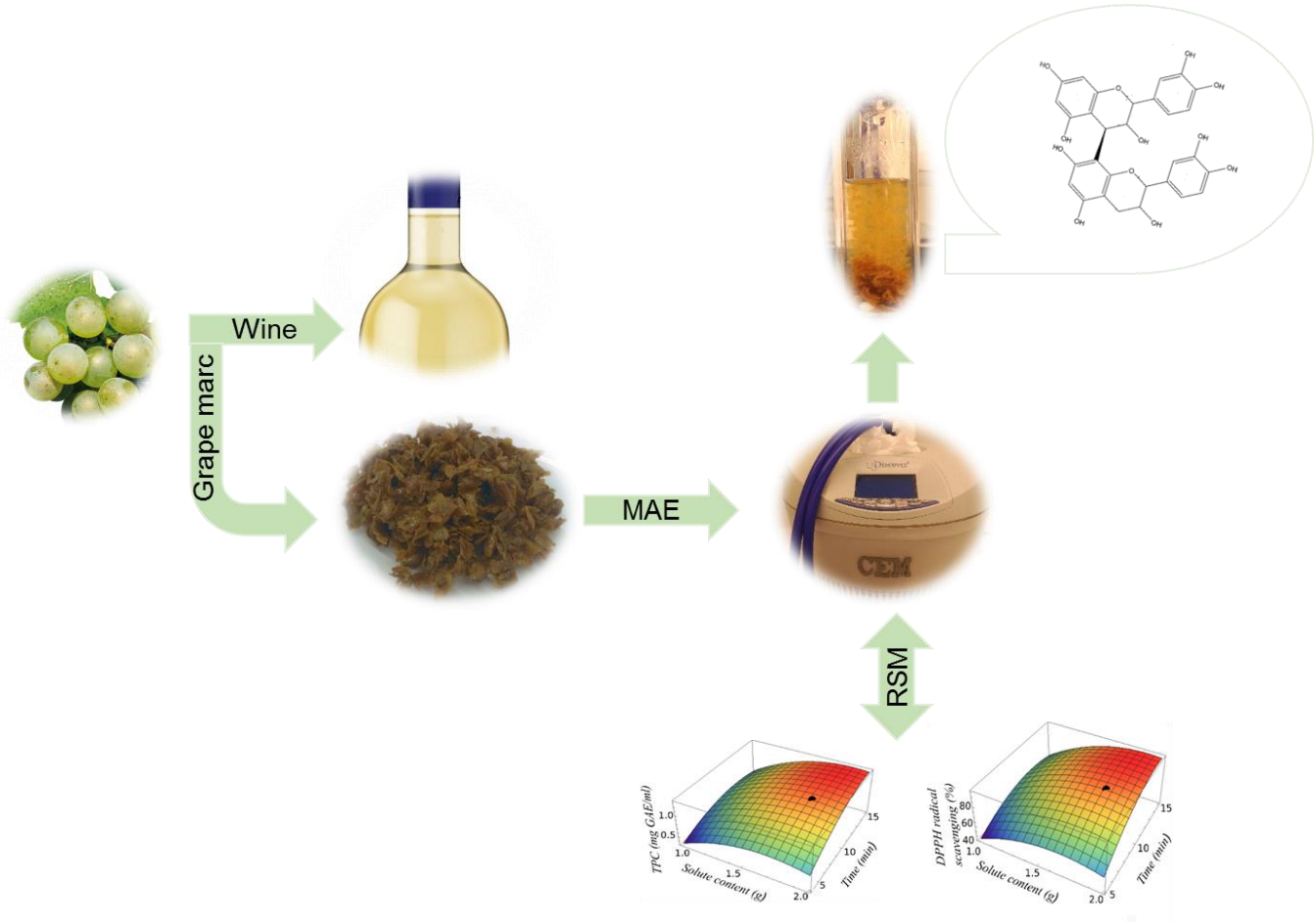

Figure I. Graphical abstract of Chapter 9.

9.1 RESULTS AND DISCUSSION

9.1.1 Optimization of MAE parameters

The effects of ethanol concentration, solid mass, and extraction time on TPC and DPPH radical scavenging capacity were studied, and the resulting experimental values are presented in **Table 9.1**. For each response variable, a quadratic polynomial model was developed by multiple regression. The regression equation coefficients of the obtained models are shown in **Table 9.2**. The results in **Table 9.3** revealed that *F* values of the models were significant ($p < 0.05$) for both responses. Furthermore, lack of fit values were non-significant ($p \geq 0.05$), as needed to validate the models.

The following second order polynomial equation was fitted between the non-coded independent factors, ethanol concentration (x_1), solid mass (x_2), and extraction time (x_3), and TPC response variable:

$$\text{TPC} = -3.30 + 0.0311\,x_1 + 2.64\,x_2 + 0.234\,x_3 - 0.000295\,x_1^2 - 0.982\,x_2^2 - 0.00736\,x_3^2 + 0.0094\,x_1x_2 - 0.00201\,x_1x_3 + 0.0374\,x_2x_3$$

As far as TPC is concerned, R^2 amounted to 0.87, while the adjusted R^2 value was 0.68.

In reference to DPPH radical scavenging capacity, the second order equation presented below showed the relation between the studied non-coded independent factors and the inhibition. The corresponding R^2 was 0.96 and the adjusted R^2 value was found to be 0.91.

$$\text{DPPH} = -127.6 + 1.72\,x_1 + 120.0\,x_2 + 10.89\,x_3 - 0.0175\,x_1^2 - 44.26\,x_2^2 - 0.4184\,x_3^2 + 0.349\,x_1x_2 - 0.0610\,x_1x_3 + 1.920\;x_2x_3$$

Table 9.1. Box-Behnken experimental design and responses for total phenolic content (TPC) and DPPH radical scavenging capacity.

Runs	Factors			Coded factors			Responses	
	Ethanol (%)	Solute (g)	Time (min)	Ethanol	Solute	Time	TPC (mg GAE/mL)	DPPH radical scavenging (%)
1	60	1.5	5	1	0	-1	0.581	62.1
2	45	1	5	0	-1	-1	0.322	47.5
3	60	1	10	1	-1	0	0.675	59.7
4	60	2	10	1	1	0	1.278	91.7
5	45	2	15	0	1	1	1.315	92.6
6	30	2	10	-1	1	0	0.869	78.7
7	45	2	5	0	1	-1	0.656	55.4
8	30	1.5	15	-1	0	1	1.528	91.8
9	45	1.5	10	0	0	0	1.192	89.2
10	45	1.5	10	0	0	0	1.268	89.1
11	60	1,5	15	1	0	1	0.870	78.5
12	45	1.5	10	0	0	0	1.071	84.5
13	30	1.5	5	-1	0	-1	0.637	57.1
14	45	1.5	10	0	0	0	1.087	84.4
15	45	1	15	0	-1	1	0.607	65.5
16	30	1	10	-1	-1	0	0.548	57.1

Table 9.2. Regression analysis for the full quadratic model of total phenolic content (TPC) and DPPH radical scavenging capacity.

	TPC				DPPH radical scavenging			
	Coef.	**Std. Δ**	***t*-value**	***p*-value**	**Coef.**	**Std. Δ**	***t*-value**	***p*-value**
b_0 (constant)	1.1545	0.0978	11.80	0.000*	86.78	2.40	36.12	0.000*
b_1 (Etha)	-0.0223	0.0692	-0.32	0.758	0.89	1.70	0.53	0.617
b_2 (Sol)	0.2457	0.0692	3.55	0.012*	11.06	1.70	6.51	0.001*
b_3 (Time)	0.2655	0.0692	3.84	0.009*	13.31	1.70	7.83	0.000*
b_{11} (Etha*Etha)	-0.0665	0.0978	-0.68	0.522	-3.94	2.40	-1.64	0.152
b_{22} (Sol*Sol)	-0.2455	0.0978	-2.51	0.046*	-11.07	2.40	-4.61	0.004*
b_{33} (Time*Time)	-0.1840	0.0978	-1.88	0.109	-10.46	2.40	-4.35	0.005*
b_{12} (Etha*Sol)	0.0706	0.0978	0.72	0.498	2.62	2.40	1.09	0.317
b_{13} (Etha*Time)	-0.1505	0.0978	-1.54	0.175	-4.58	2.40	-1.90	0.106
b_{23} (Sol*Time)	0.0935	0.0978	0.96	0.376	4.80	2.40	2.00	0.093

Coef.: Standardized regression coefficients; Std. Δ: standard error of the coefficients; *t*-value: statistic of the *t*-test; *p*-value: significance value of the *t*-test (*) significant at $p < 0.05$.

Table 9.3. Analysis of variance (ANOVA) of the full quadratic model.

	TPC					DPPH radical scavenging			
	DF	**SS (adj)**	**MS (adj)**	***F*-value**	***p*-value**	**SS (adj)**	**MS (adj)**	***F*-value**	***p*-value**
Model	9	1.59070	0.176744	4.62	0.038*	3593.56	399.28	17.29	0.001*
Linear	3	1.05106	0.350352	9.15	0.012*	2400.74	800.25	34.66	0.000*
Ethanol	1	0.00398	0.003977	0.10	0.758	6.41	6.41	0.28	0.617
Solid	1	0.48308	0.483085	12.62	0.012*	978.15	978.15	42.37	0.001*
Time	1	0.56399	0.563995	14.73	0.009*	1416.18	1416.18	61.34	0.000*
Quadratic	3	0.39411	0.131370	3.43	0.093	989.48	329.83	14.29	0.004*
Etha*Etha	1	0.01768	0.017681	0.46	0.522	62.09	62.09	2.69	0.152
Sol*Sol	1	0.24098	0.240984	6.29	0.046*	489.74	489.74	21.21	0.004*
Time*Time	1	0.13545	0.135446	3.54	0.109	437.65	437.65	18.96	0.005*
Interaction	3	0.14553	0.048509	1.27	0.367	203.34	67.78	2.94	0.121
Etha*Sol	1	0.01993	0.019933	0.52	0.498	27.46	27.46	1.19	0.317
Etha*Time	1	0.09060	0.090601	2.37	0.175	83.72	83.72	3.63	0.106
Sol*Time	1	0.03499	0.034995	0.91	0.376	92.16	92.16	3.99	0.093
Error	6	0.22972	0.038287			138.53	23.09		
Lack of fit	3	0.20390	0.067968	7.90	0.062	116.24	38.75	5.21	0.104
Pure error	3	0.02582	0.008606			22.29	7.43		
Total	15	1.82042				3732.09			
		R^2 (%)		R^2 (adj) (%)		R^2 (%)		R^2 (adj) (%)	
		87.38%		68.45		96.29		90.72	

DF: degrees of freedom; SS: sum of squares; SS (adj): adjusted sum of squares; *F*-value: statistics of the *F*-test; *p*-value: significance value of the *F*-test (*) significant at $p < 0.05$; R^2: coefficient of determination; R^2 (adj): adjusted coefficient of determination.

In this study, the extraction of phenolic compounds and the inhibition responses were optimized by maximizing TPC and DPPH inhibition simultaneously, taking into consideration that there is a strong correlation between TPC and scavenging antioxidant capacity from the DPPH assay, as reported by Tournour et al. (2015). Without any precondition or constraint, the obtained results for the optimal values of factors were $x_1 = 30$; $x_2 = 1.78$; $x_3 = 15$. As can be seen in **Figure 9.1** for TPC and in **Figure 9.2** for DPPH radical scavenging, the longer the time, the better the obtained response.

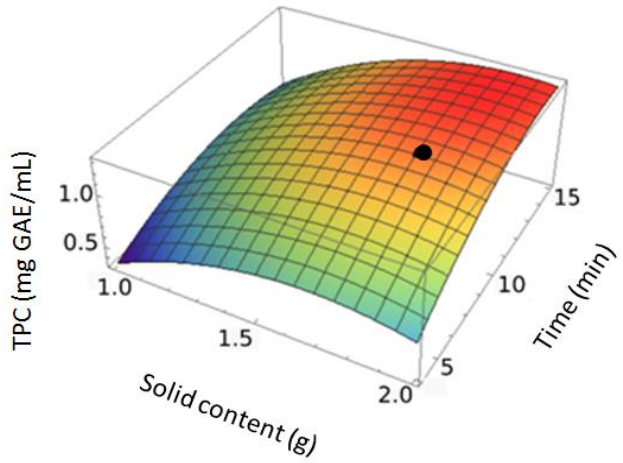

Figure 9.1. Three-dimensional response plot for TPC model including the combined optimal response with time restriction (black dot).

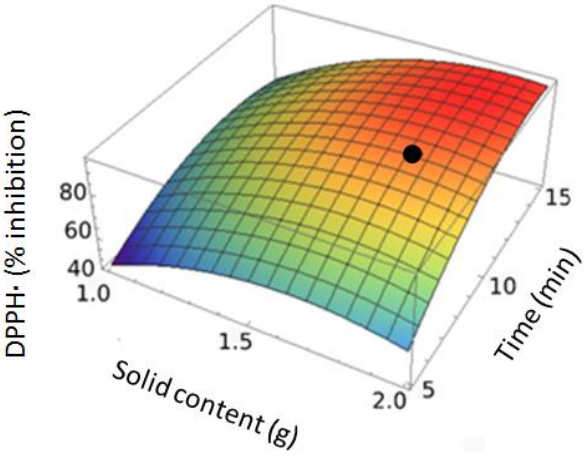

Figure 9.2. Three-dimensional response plot for DPPH radical scavenging model including the combined optimal response with time restriction (black dot).

With this combination, the expected theoretical responses were TPC_t^{opt1} = 1.42 mg GAE/mL and $DPPH_t^{opt1}$ = 93.3%. Nevertheless, with the potential of the industrial scale-up extraction in mind, a maximum time of 10 min was set as a constraint in a second optimization. With this new condition, the values of the factors that allowed a maximum in the responses were x_1 = 48, x_2 = 1.77, x_3 = 10, with predicted optimal responses of TPC_t^{opt2} = 1.22 mg GAE/mL and $DPPH_t^{opt2}$ = 89.8%. This optimal value was represented with a black dot in **Figure 9.1** and **Figure 9.2**. These new values were lower than those without any constraint, and the necessary reduction in time is compensated mainly by an increase in ethanol content. In order to verify the reliability of model and optimization, experiments following the optimum conditions were conducted in the lab. The obtained experimental values were in good agreement with the theoretical ones, with TPC_e^{opt2} = (1.21 ± 0.04) mg GAE/mL and $DPPH_e^{opt2}$ = (87 ± 5) %.

9.1.2 Grape marc extract characterization

Based on the results obtained using RSM for a maximum value of TPC and DPPH with the restriction of time and temperature, 48% ethanol, 10 min and 1.77 g of sample were found to be the optimal parameters. Consequently, the final extraction was carried out employing the selected conditions. The obtained grape marc extract was characterized by different experimental techniques. Among them, FTIR analysis was performed in order to examine the presence of phenolic compounds in the grape marc extract, and the FTIR spectrum is shown in **Figure 9.3**. As can be seen, a main band is shown at 3290 cm^{-1} associated with the stretching vibration of O-H group or O-H wagging of phenolic compounds (Alara et al., 2018). The band at 1723 cm^{-1} is related to the carboxyl group and indicates the presence of some phenolic acids (Lu and Hsieh, 2012). The absorption band at 1675 cm^{-1} could be due to aromatic ring deformations and C=C bonds, which

suggested the presence of polyphenols, flavonoids and amino acids (Zhao et al., 2015). The band at 1453 cm^{-1} shows the presence of CH_2, CH_3, aromatic rings and flavonoids. The band around 1261 cm^{-1} is characteristic of the flavonoid-based tannins (De Souza et al., 2015). Meanwhile, the sharp band at around 1020 cm^{-1} corresponds to C-O-H in phenolic compounds and sugar monomers (Saha et al., 2016). Finally, bands at wavenumbers below 919 cm^{-1} are related to C-H bonds in aromatic structures (Sardella et al., 2015).

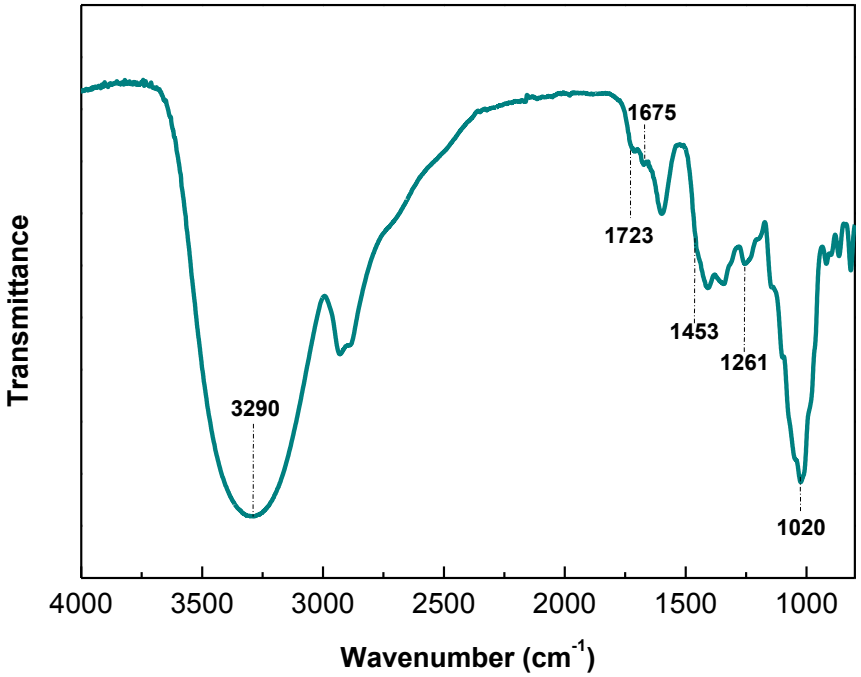

Figure 9.3. FTIR spectrum of the grape marc extract.

It is well known that grapes present a high amount of sugars in their composition, as demonstrated by the sharp peak shown in the infrared spectrum, and this was indeed confirmed by the Rebelein sugar method and HPLC results. The extracted sample had around 66% (w/v) of sugars, which consisted mainly of glucose (313.1 g/L) and mannose (112.6 g/L). This sugar fraction depends more on the winemaking extraction degree rather than on the grape variety (Llobera and Cañellas, 2007).

Besides sugars, phenolic compounds are also abundant constituents in grape marc. The composition varies depending on the extraction and on the subsequent reactions taking place during the vinification and postfermentation treatments and the wine aging. Normally, white wines are made without aeration to avoid large periods of contact with oxygen, which can cause browning of the wine and deterioration of quality (Salacha et al., 2008). Therefore, the maceration step lasts only few hours and sulphur dioxide is immediately added in order to protect against enzymatic oxidation. A higher amount of sulphur dioxide affects the content of total phenolics, flavonoids and flavan-3-ols in wines (Ivanova et al., 2011a). The polyphenols are primarily located in seeds and skins of grape (García-Esparza et al., 2018; Nogales-Bueno et al., 2017; Toaldo et al., 2013). In this chapter, the quantification of individual phenolic compounds was based on the employment of a calibration curve of specific standards and the combination of the retention times using chromatographic analysis by UHPLC (**Figure 9.4**). Full details on the resulting MS data and their assignments are provided in **Table 9.4**. The analysis presented a wide variety of polyphenols, mainly belonging to flavanols, flavonols, dihydroflavonols, hydroxycinnamic acids and hydroxybenzoic acids. 37 peaks were identified in the grape marc extract. Among the flavanols, procyanidins can be highlighted; in fact, the most abundant polyphenol in the sample was a procyanidin trimer, while monomeric catechin and epicatechin were also identified. Specifically, a total of 16 flavanols were determined and procyanidin was the most abundant with 9 of the 37 peaks observed in the grape marc; additionally, quercetin, kaempferol, and gallic acid were identified. Furthermore, glucuronide derivatives, quercetin-3-O-glucuronide and kaempferol-3-O-glucuronide, appeared due to the presence of grape skin in the sample (Ivanova et al., 2011b). Kaempferol derivatives were also observed, since they are usually found in Chardonnay grapes (Ragusa et al., 2017). Among the hydroxycinnamic acids

detected, p-coumaroyl-tartaric acid, usually located in the skin of white grapes, was found. Regarding the hydroxybenzoic acids, their content is strongly dependant on the grapevine variety. In this case, gallic acid was mainly identified, which is one of the most frequent hydroxybenzoic acids present in wines.

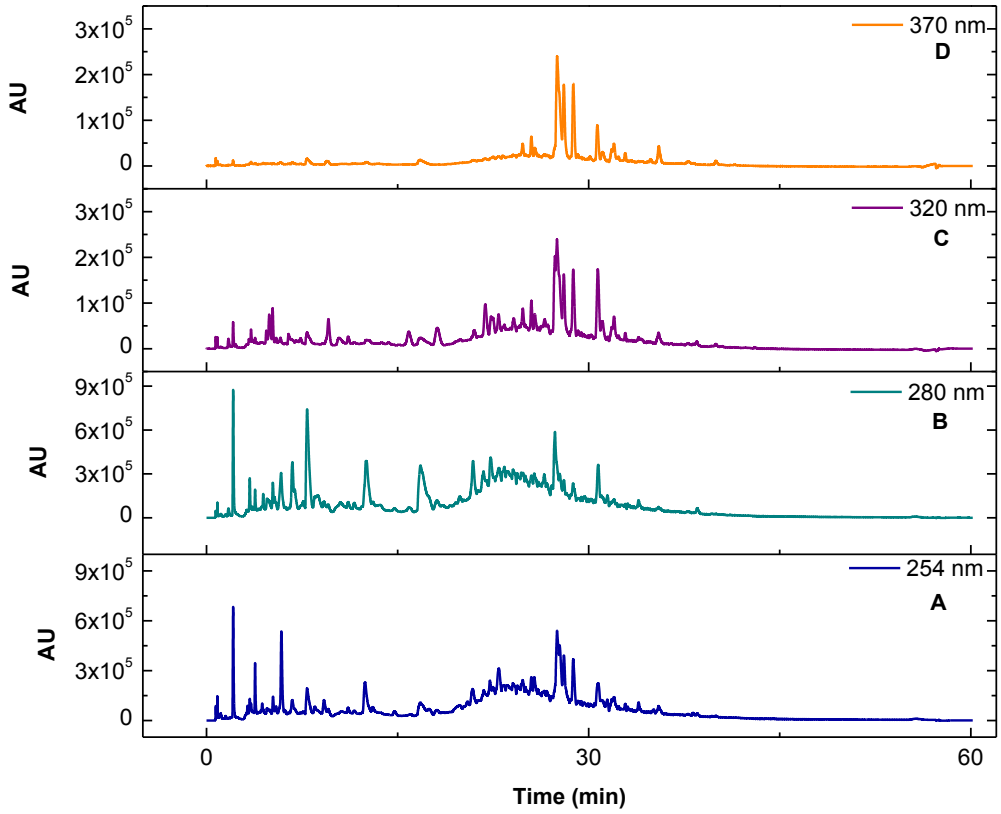

Figure 9.4. Diode-Array Detection (DAD) chromatogram of grape marc extract at 254 nm (A), 280 nm (B), 320 nm (C) and 370 nm (D).

Table 9.4. Characterization of polyphenols from grape marc extract determined by UHPLC-Q-TOF-MS/MS analysis.

Cmp. No	Tentative identification	LC tR (min)	DAD UV Bands (nm)	ESI(+)-Q-ToF			ESI(-)-Q-ToF		
				Exp. Acc. Mass $[M+H]^+$ Error (mDa)	Formula for the detected $[M+H]^+$	Adducts and Fragment ions of $[M+H]^+$	Exp. Acc. Mass $[M-H]^-$ Error (mDa)	Formula for the detected $[M-H]^-$	Adducts and Fragment ions of $[M-H]^-$
						Flavanols			
1	((Epi)cat)3 (1)	3.43	283	867.2144	C45H39O18	715.1664 [U(1,3A)MD]+	865.1988	C45H37O18	713.1519 [U(1,3A)MD]-
				0.8		579.1500 [MD]+	0.8		577.1306 [MD]-
						409.0916 [M(1,3A-H2O)D]+			407.0772 [M(1,3A-H2O)D]-
						289.0709 [D]+			289.0709 [U]-
						247.0605 [U-C2H2O]+			125.0257 [D(1,4A+2H)]-
						127.0391 [D(1,4A+2H)]+			
						123.0445 [D(1,2B)]+			
2	PBI	5.82	280	579.1508	C30H27O12	427.1021 [U(1,3A)D]+	577.1351	C30H25O12	425.0869 [U(1,3A)D]-
				0.5		409.0920[U(1,3A-H2O)D]+	0.5		407.0766 [U(1,3A-H2O)D]-
						291.0871[D]+			289.0713 [D]-
						289.0709[U]+			245.0803 [U-C2H2O]+
						287.0553[U(1,3A)D(1,2A-H2O)]+			125.0238 [D(1,4A+2H)]-
						247.0602[U-C2H2O]+			
						139.0391[D(1,3A)]+			
						127.0390[D(1,4A+2H)]+			
						123.0440[D(1,2B)]+			
3	((Epi)cat)3 (2)	6.09	283	867.2133	C45H39O18	715.1648 [U(1,3A)MD]+	865.1988	C45H37O18	713.1402 [U(1,3A)MD]-
				-0.3		579.1478 [MD]+	0.8		577.1306 [MD]-
						409.0924[M(1,3A-H2O)D]+			407.0772 [M(1,3A-H2O)D]-
						291.0863[D]+			289.0681 [U]-
						289.0708 [U]+			125.0257 [D(1,4A+2H)]-

						247.0600 [U-C2H2O]+ 139.0391 [D(1,3A)]+ 127.0389 [D(1,4A+2H)]+ 123.0438 [D(1,2B)]+			
4	PBII	6.77	280	579.1496 -0.7	C30H27O12	427.1020 [U(1,3A)D]+ 409.0923 [U(1,3-H2O)D]+ 291.0867 [D]+ 289.0709 [U]+ 287.0555 [U(1,3A)D(1,2A-H2O)]+ 247.0603 [U-C2H2O]+ 139.0393 [D(1,3A)]+ 127.0394 [U(1,4A+2H)D]+ 123.0444 [D(1,2B)]+	577.1358 1.2	C30H25O12	425.0875 [U(1,3A)D]- 407.0774[U(1,3A-H2O)D]- 289.0717 [D]- 245.0807 [U-C2H2O]+ 125.0240 [D(1,4A+2H)]-
5	((Epi)cat)3 (3)	8.02	283	867.2121 -1.5	C45H39O18	715.1641 [U(1,3A)MD]+ 579.1495 [MD]+ 409.0925[M(1,3A-H2O)D]+ 291.0865[D]+ 289.0710 [U]+ 247.0604 [U-C2H2O]+ 139.0391 [D(1,3A)]+ 127.0393 [D(1,4A+2H)]+ 123.0447 [D(1,2B)]+	865.1988 0.8	C45H37O18	713.1519 [U(1,3A)MD]- 577.1306 [MD]- 407.0772 [M(1,3A-H2O)D]- 289.0681 [U]- 125.0257 [D(1,4A+2H)]-
6	Cat	8.06	278	291.0873 0.4	C15H15O6	207.0655[Rup(A)]+ 147.0442 [0,4B-2H2O]+ 139.0392 [1,3A]+ 123.0442 [1,2B]+ 119.0493 [0,4B-2H2O-CO]+	289.0717 0.5	C15H13O6	205.0506 [Rup(A)]- 137.0243 [1,3A]- 123.0452 [1,3B-CO]- 109.0296 [1,3A-CO]-
7	PBIII	8.81	280	579.1500	C30H27O12	427.1022 [U(1,3A)D]+	577.1349	C30H25O12	425.0872[U(1,3A)D]-

				-0.3		409.0917 [U(1,3-H2O)D]+ 291.0865[D]+ 289.0706 [U]+ 287.0551 [U(1,3A)D(1,2A-H2O)]+ 247.0602 [U-C2H2O]+ 139.0390 [D(1,3A)]+ 127.0390[U(1,4A+2H)D]+ 123.0439 [D(1,2B)]+	0.3		407.0769[U(1,3A-H2O)D]- 289.0718 [D]- 245.0810[U-C2H2O]+ 125.0244 [D(1,4A+2H)]-
8	((Epi)cat)3 (4)	9.29	283	867.2141 0.5	C45H39O18	715.1628 [U(1,3A)MD]+ 579.1478 [MD]+ 409.0907[M(1,3A-H2O)D]+ 289.0701 [U]+ 247.0605 [U-C2H2O]+ 139.0391 [D(1,3A)]+ 127.0389 D(1,4A+2H)]+ 123.0443 [D(1,2B)]+	865.1988 0.8	C45H37O18	713.1519 [U(1,3A)MD]- 577.1306 [MD]- 407.0772 [M(1,3A-H2O)D]- 287.0561 [D]- 125.0257 [D(1,4A+2H)]-
9	((Epi)cat)3 (5)	10.21	283	867.2099 -3.7	C45H39O18	715.1667 [U(1,3A)MD]+ 579.1466 [MD]+ 409.0914[M(1,3A-H2O)D]+ 291.0852[D]+ 289.0702 [U]+ 247.0598 [U-C2H2O]+ 139.0388 [D(1,3A)]+ 127.0393 [D(1,4A+2H)]+ 123.0436 [D(1,2B)]+	865.1988 0.8	C45H37O18	713.1519 [U(1,3A)MD]- 577.1306 [MD]- 407.0772 [M(1,3A-H2O)D]- 289.0681 [U]- 287.6561 [D]- 125.0257 [D(1,4A+2H)]-
10	((Epi)cat)3 (6)	10.56	283	867.2144 0.8	C45H39O18	715.1671 [U(1,3A)MD]+ 579.1489 [MD]+ 409.0907 [M(1,3A-H2O)D]+	865.1988 0.8	C45H37O18	713.1519 [U(1,3A)MD]- 577.1306 [MD]- 407.0772 [M(1,3A-H2O)D]-

						291.0861[D]+ 289.0708 [U]+ 247.0607 [U-C2H2O]+ 139.0388 [D(1,3A)]+ 127.0392 [D(1,4A+2H)]+ 123.0446 [D(1,2B)]+			289.0681 [U]- 287.6561 [D]- 125.0257 [D(1,4A+2H)]-
11	PBIV	12.62	280	579.1509 0.6	C30H27O12	427.1030[U(1,3A)D]+ 409.0926[U(1,3-H2O)D]+ 291.0869[D]+ 289.0711 [U]+ 287.0555 [U(1,3A)D(1,2A-H2O)]+ 247.0606 [U-C2H2O]+ 139.0390 [D(1,3A)]+ 127.0390[U(1,4A+2H)D]+ 123.0439 [D(1,2B)]+	577.1349 0.3	C30H25O12	425.0871 [U(1,3A)D]- 407.0768[U(1,3A-H2O)D]- 289.0715 [D]- 245.0807 [U-C2H2O]+ 125.0240 [D(1,4A+2H)]-
12	((Epi)cat)3 (7)	13.70	283	867.2142 0.6	C45H39O18	715.1674 [U(1,3A)MD]+ 579.1492 [MD]+ 409.0910 [M(1,3A-H2O)D]+ 291.0855 [D]+ 289.0711 [U]+ 247.0602 [U-C2H2O]+ 139.0388 [D(1,3A)]+ 127.0390 [D(1,4A+2H)]+ 123.0435[D(1,2B)]+	865.1988 0.8	C45H37O18	713.1519 [U(1,3A)MD]- 577.1306 [MD]- 407.0772 [M(1,3A-H2O)D]- 289.0681 [U]- 287.6561 [D]- 125.0257 [D(1,4A+2H)]-
13	Epi	17.22	278	291.0869 0.0	C15H15O6	207.0656 [Rup(A)]+ 147.0444 [0,4B-2H2O]+ 139.0394[1,3A]+ 123.0444[1,2B]+	289.0719 0.7	C15H13O6	205.0505 [Rup(A)]- 137.0241 [1,3A]- 123.0449 [1,3B-CO]- 109.0293 [1,3A-CO]-

						119.0494 [0,4B-2H2O-CO]+			
14	((Epi)cat)3 (8)	18.17	283	867.2164 2.8	C45H39O18	715.1653 [U(1,3A)MD]+ 579.1487 [MD]+ 409.0922 [M(1,3A-H2O)D]+ 291.0874 [D]+ 289.0710 [U]+ 247.0605 [U-C2H2O]+ 139.0388 [D(1,3A)]+ 127.0393 [D(1,4A+2H)]+ 123.0441[D(1,2B)]+	865.1988 0.8	C45H37O18	713.1519 [U(1,3A)MD]- 577.1306 [MD]- 407.0772 [M(1,3A-H2O)D]- 289.0681 [U]- 287.6561 [D]- 125.0257 [D(1,4A+2H)]-
15	PB-gallate	19.90	280	731.1599 -1.3	C37H31O16	579.1130 [PB+H-Gallic acid]+ 427.1011 [U(1,3A)D]+ 409.0907 [U(1,3-H2O)D]+ 289.0711 [U]+ 287.0546 [U(1,3A)D(1,2A-H2O)]+ 247.0601 [U-C2H2O]+ 139.0390 [D(1,3A)]+ 127.0391[U(1,4A+2H)D]+ 123.0441 [D(1,2B)]+	729.1398 -5.8	C37H29O16	577.1201 [PB-H-Gallic acid]+ 425.0831 [U(1,3A)D]- 407.0772 [U(1,3A-H2O)D]- 289.0681 [D]- 245.0407 [U-C2H2O]+ 125.0257 [D(1,4A+2H)]-
16	((Epi)cat)3 (9)	20.96	283	867.2164 2.8	C45H39O18	715.1653 [U(1,3A)MD]+ 579.1487 [MD]+ 409.0922 [M(1,3A-H2O)D]+ 291.0874 [D]+ 289.0710 [U]+ 247.0605 [U-C2H2O]+ 139.0388 [D(1,3A)]+ 127.0393 [D(1,4A+2H)]+ 123.0441[D(1,2B)]+	865.1988 0.8	C45H37O18	713.1519 [U(1,3A)MD]- 577.1306 [MD]- 407.0772 [M(1,3A-H2O)D]- 289.0681 [U]- 287.6561 [D]- 125.0257 [D(1,4A+2H)]-

					Flavonols				
17	Que-hex-hex-1	24.81	264, 344	627.1572 1.1	C27H31O17	465.1021[Y1]+ 303.0497[Y0]+	625.137 -3.5	C27H29O17	463.0860 [Y1]- 301.0338 [Y0]-
18	Que-hex-hex-2	25.53	264, 344	627.1562 0.1	C27H31O17	465.1028[Y1]+ 303.0508[Y0]+	625.1401 -0.4	C27H29O17	463.0874 [Y1]- 301.0343 [Y0]-
19	Que-3-O-glucoronide	27.56	255, 352	479.0824 -0.2	C21H19O13	303.0513[Y0]+ 257.0451 [Y0-CHO-OH]+ 229.0501 [Y0-CHO-OH-CO]+ 153.0186 [1,3A]+	477.0667 -0.2	C21H17O13	301.0355 [Y0]- 151.0038 [1,3A]-
20	Que-3-O-gal	28.12	255, 353	n.d.	C21H21O12	487.0852 [M+Na]+ 303.0492 [Y0]+	463.0824 -5.3	C21H19O12	301.0300 [Y0]- 271.0252 [Y0-CHO-H]- 255.0287 [Y0-CHO-OH]- 151.0009 [1,3A]-
21	Que-3-O-glc	28.81	255, 352	n.d.	C21H21O12	487.0850[M+Na]+ 303.0525 [Y0]+	463.0918 4.1	C21H19O12	301.0375 [Y0]- 271.0252 [Y0-CHO-H]- 255.0287 [Y0-CHO-OH]- 151.0062[1,3A]-
22	Kaem-3-O-gal	30.70	265, 345	449.1081 -0.3	C21H21O11	471.0898[M+Na]+ 287.0559[Y0]+	447.0929 0.2	C21H19O11	285.0380 [Y0]- 151.0035 [1,3A]-
23	Kaem-3-O-Glucoronide	31.10	265, 345	463.0878 0.1	C21H19O12	n.d. [M+Na]+ n.d. [Y0]+	461.0701 -1.9	C21H17O12	285.0362 [Y0]- 151.0009 [1,3A]-
24	Kaem-3-O-glc	32.00	265, 348	449.1080 -0.4	C21H21O11	471.0910 [M+Na]+ 287.0569[Y0]+	447.0934 0.7	C21H19O11	285.0385 [Y0]- 151.0038 [1,3A]-
25	Iso-3-O-gal	32.35	254, 352	479.1192 0.2	C22H23O12	501.1008 [M+Na]+ 317.0668 [Y0]+ 301.1624 [Y0-CH3]+	477.1033 0.0	C22H21O12	315.0482 [Y0]- 151.0035 [1,3A]-

26	Iso-3-O-glc	32.91	254, 352	479.1188 -0.2	C22H23O12	501.1002[M+Na]+ 317.0664[Y0]+	477.1042 0.9	C22H21O12	315.0485 [Y0]- 151.0047 [1,3A]-
27	Kaem-3-O-rham	35.43	265, 359	433.1130 -0.5	C21H21O10	455.0955[M+Na]+ 287.0558[Y0]+	431.0961 -1.7	C21H19O10	285.0400 [Y0]- 151.0043 [1,3A]-
28	Kaem derivative	39.93	266, 364	Unknown		287.0563 [M+H]+ 258.0536 [M+CHO]+ 241.0506 [M+H-CHO-OH]+ 213.0549 [M+H+CHO-OH-CO]+ 185.0601 [M+H-CHO-OH-2CO]+ 165.0186 [0,2A]+ 153.0187 [1,3A]+ 137.0236 [0,2A-CO]+ 121.0285 [0,2B]+	285.0436 3.7		
						Dihydroflavonols			
29	DihydroQue-3-O-rham	27.40	255, 352	451.1241 0.1	C21H23O11	473.1060 [M+Na]+ 305.0673[Y0]+	449.1086 0.2	C21H21O11	303.0511[Y0]- 285.0408 [Y0-H2O]- 151.0042 [1,3A]-
						Hydroxycinnamic acids			
30	Ac *trans-p*Coumtar	4.73	310	n.d.			295.0450 -0.4	C13H11O8	163.0395 [pCoum acid-H]- 149.0088 [Tartaric acid-H]-
31	Ac *cis-p*Coumtar	5.04	310	n.d.			295.0451 -0.3	C13H11O8	163.0401 [pCoum acid-H]- 149.0089[Tartaric acid-H]-
32	pCumhex	11.16	313	n.d.			325.0925 0.2	C15H17O8	163.0418 [Y0]- 119.0483 [Y0-CO2]-
						Hydroxybenzoic acid			
33	Gal acid	2.13	271	171.0301		153.0186 [M+H-H2O]+ 125.0233 [M+H-H2O-CO]+	169.0107 -3.0	C7H5O5	125.0257 [M-H-CO2]- 107.0116 [M-H-H2O-CO2]-

					109.0280 [M+H-H2O-CO2]+ 107.0127 [M+H-2H2O-CO]+ 81.0337 [M+H-CO2-H2O-CO]+			79.0186 [M+H-CO2-H2O-CO]-
34	Galloyl Rhamnoside	3.26	279	n.d.		315.0717 0.1	C13H15O9	169.0164 [Y0]- 151.0009 [Y0-H2O]- 125.0257 [Y0-CO2]- 107.0116 [Y0-H2O-CO2]- 83.0148 [Y0-CO2-H2O-CO]-
35	Gal acid derivative-1	22.97	271	n.d.		Unknown		169.0164 [Y0]- 151.0009 [Y0-H2O]- 125.0257 [Y0-CO2]- 107.0116 [Y0-H2O-CO2]- 83.0148 [Y0-CO2-H2O-CO]-
36	Gal acid derivative-2	27.87	271	n.d.		Unknown		169.0164 [Y0]- 151.0009 [Y0-H2O]- 125.0257 [Y0-CO2]- 107.0116 [Y0-H2O-CO2]- 83.0148 [Y0-CO2-H2O-CO]-
37	Gal acid deivarive-3	35.63	271	n.d		Unknown		169.0107[Y0]- 151.0009 [Y0-H2O]- 125.0257 [Y0-CO2]- 107.0116 [Y0-H2O-CO2]- 83.0148 [Y0-CO2-H2O-CO]-

As the grape marc contains polyphenols, which possess antioxidant activity, as demonstrated by the DPPH assay results shown above, the incorporation of these compounds into film forming formulations could be of interest for active packaging applications. A grape marc extract has already shown promising properties when included in ethyl cellulose films (Olejar et al. 2014). The incorporation of the grape marc extract into protein-based materials in order to improve antioxidant properties to develop sustainable active films could be also a promising alternative to synthetic films. For that reason, the analysis of the degradation temperature of these compounds is of great relevance in order to select the appropriate processing temperatures. The TGA and DTG curves for the grape marc extract are shown in **Figure 9.5**.

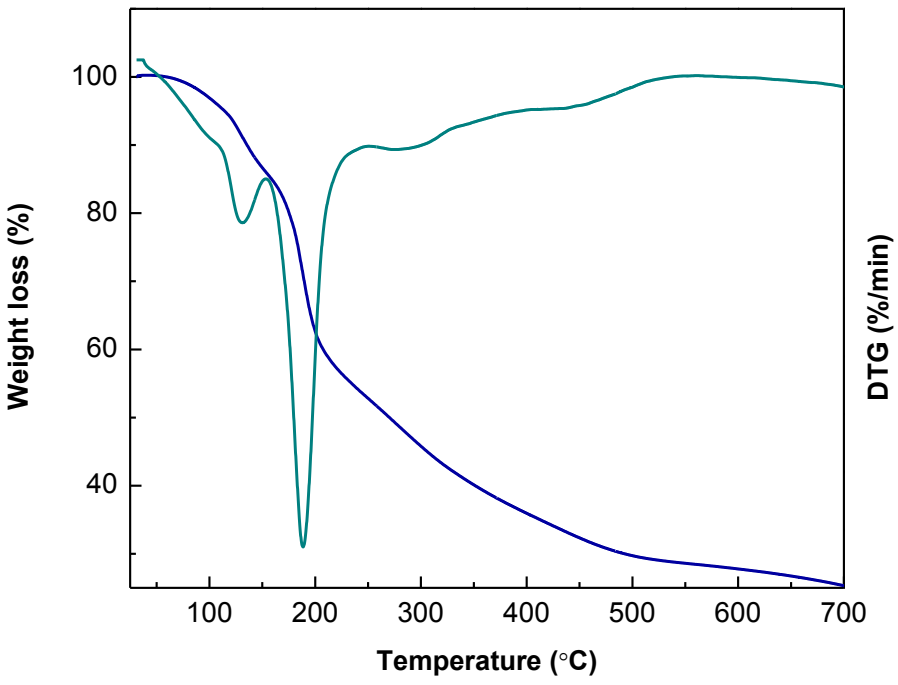

Figure 9.5. TGA and DTG curves of grape marc extract.

It can be noticed that the DTG curve of grape marc was composed of two major weight loss steps. The first mass loss between 30-105 ºC and the peak around 125 ºC were

related to the loss of adsorbed and structural water, respectively, accounting approximately 20% weight loss; the second peak around 200 ºC, when the major part of the mass is lost, was related to the thermo-degradation of organic compounds present in grape marc (Basso et al., 2016). The presence of tannins could promote the rapid degradation between 200 ºC and 300 ºC (Anwer et al., 2015). In previous works, it was shown that soy protein-based films can be manufactured at temperatures below 200 ºC when compression-moulding is employed as the processing method (Garrido et al., 2017; Garrido et al., 2019); thus, grape marc extract could be a promising bioactive for improving antioxidant properties of films based on proteins.

CONCLUSIONS

The microwave-assisted extraction allowed to recover natural antioxidants from grape marc at room temperature in a rapid way, thus, highlighting the potential of this technology for the extraction of bioactive compounds. RSM was successfully employed to determine the optimal parameters of solvent, solid mass and extraction time in order to obtain the highest values of TPC and DPPH radical scavenging capacity. Using those parameters, phenolic compounds were extracted from grape marc and analysed by UHPLC, which showed that flavanols were the most abundant phenolic compounds in the extract. Since these polyphenols do not degrade thermally up to 200 ºC, this thermal stability facilitates the incorporation of these compounds into biopolymeric formulations to manufacture bioactive products.

10

chapter

GENERAL CONCLUSIONS

The main conclusions of this doctoral thesis are summarised as follows:

1. Soy protein-based films are successfully prepared and transparent films with excellent UV barrier properties are obtained.

2. The best results are obtained at pH 10, at which the protein unfolding is better to promote interactions between compounds.

3. Films moulded by compression show a lower environmental impact than those processed by solution casting due to a lower energy consumption, associated with a lower processing time.

4. The employment of alkaline treatment at room temperature is an appropriate method to obtain hydrolysed feather keratin, valorising this agro-industrial waste.

5. The incorporation of hydrolysed keratin into SPI-based films increases the strength of the films, since keratin promotes disulphide bonds.

6. Agar/soy protein films are successfully manufactured by extrusion and compression moulding.

7. Extrusion and injection moulding are employed for manufacturing SPI-based biocomposites using algae waste as a filler.

8. β-Chitin is successfully extracted from squid pens employing a simple alkaline treatment at room temperature, which reduces chitin production cost and environmental impact.

9. Chitin directly affects the degree of crystallinity of the SPI-based films, thus, tensile strength and elastic modulus are improved.

10. Microwave-assisted technique allows to extract natural antioxidants from grape marc in a fast and environmentally friendly way due to the fact that high temperatures and long times are avoided.

11

chapter

REFERENCES

Abad-García B., Berrueta L.A., Garmón-Lobato S., Gallo B., Vicente F. (2009). A general analytical strategy for the characterization of phenolic compounds in fruit juices by high-performance liquid chromatography with diode array detection coupled to electrospray ionization and triple quadrupole mass spectrometry. Journal of Chromatography A, 1216(28), 5398-5415.

Acosta-Domínguez L., Hernández-Sánchez H., Gutiérrez-López G.F., Alamilla-Beltrán L., Azuara E. (2016). Modification of the soy protein isolate Surface at nanometric scale and its effect on physicochemical properties. Journal of Food Engineering, 168, 105-112.

Adilah Z.A.M., Jamilah B., Nur Hanani Z.A. (2018). Functional and antioxidant properties of protein-based films incorporated with mango kernel extract for active packaging. Food Hydrocolloids, 74, 207-218.

Aguiló-Aguayo I., Walton J., Viñas I., Tiwari B.K. (2017). Ultrasound assisted extraction of polysaccharides from mushroom by-products. LWT- Food Science and Technology, 77, 92-99.

Alara O.R., Abdurahman N.H., Ukaegbu C.I., Azhari N.H. (2018). *Vernonia cinerea* leaves as the source of phenolic compounds, antioxidants, and anti-diabetic activity using microwave-assisted extraction technique. Industrial Crops and Products, 122, 533-544.

Al-Bulushi K., Attard T.M., North M., Hunt A.J. (2018). Optimisation and economic evaluation of the supercritical carbon dioxide extraction of waxes from waste date palm (Phoenix dactylifera) leaves. Journal of Cleaner Production, 186, 988-996.

Albuquerque B.R., Prieto M., Barreiro M.F., Rodrigues A., Curran T.P., Barros L., Ferreira I.C. (2017). Catechin-based extract optimization obtained from *Arbutus unedo* L. fruits using maceration/microwave/ultrasound extraction techniques. Industrial Crops and Products, 95, 404-415.

Al-Dhabi N.A., Ponmurugan K., Jeganathan P.M. (2017). Development and validation of ultrasound-assisted solid-liquid extraction of phenolic compounds from waste spent coffee grounds. Ultrasonic Sonochemistry, 34, 206-213.

Alfaro A.T., Balbinot E., Weber C.I., Tonial I.B., Machado-Lunkes A. (2015). Fish gelatin: characteristics, functional properties, applications and future potentials. Food Engineering Reviews, 7(1), 33-44.

Al-Hamimi S., Abellan Mayoral A.C, Cunico L.P., Turner C. (2016). Carbon dioxide expanded ethanol extraction: Solubility and extraction kinetics of α-pinene and cis-verbenol. Analytical Chemistry, 88(8), 4336-4345.

Alkan D., Yemenicioğlu A. (2016). Potential application of natural phenolic antimicrobials and edible films technology against bacterial plant pathogens. Food Hydrocolloids, 55, 1-10.

Alonso-Carrillo N., de los Ángeles M.A., Vernon-Carter E.J., Jiménez-Alvarado R., Cruz-Sosa F., Román-Guerrero A. (2017). Extraction of phenolic compounds from Satureja macrostema using microwave-ultrasound assisted and reflux methods and evaluation of their antioxidant activity and cytotoxicity. Industrial Crops and Products, 103, 213-221.

Aloui H., Khwaldia K. (2016). Natural antimicrobial edible coatings for microbial safety and food quality enhancement. Comprehensive Reviews in Food Science and Food Safety, 15(6), 1080-1103.

Alparslan Y., Baygar T. (2017). Effect of chitosan film coating combined with orange peel essential oil on the shelf life of deepwater pink shrimp. Food and Bioprocess Technology, 10(5), 842-853.

Al-Saadi J.S., Shaker K.A., Ustunol Z. (2014). Effect of heat and transglutaminase on solubility of goat milk protein-based films. International Journal of Dairy Technology, 67(3), 420-426.

Álvarez K., Famá L., Gutiérrez T.J. (2017). Physicochemical, antimicrobial and mechanical properties of thermoplastic materials based on biopolymers with application in the food industry. In: Masuelli M., Renard D. (eds.). Advances in physicochemical properties of biopolymers (Part 1). Bentham science publishers, pp 358-400.

Álvarez A., Poejo J., Matias A.A., Duarte C.M.M., Cocero M.J., Mato R.B. (2017). Microwave pretreatment to improve extraction efficiency and polyphenol extract richness from grape pomace. Effect on antioxidant bioactivity. Food and Bioproducts Processing, 106, 162-170.

Alves M.M., Gonçalves M.P., Rocha C.M.R. (2017). Effect of ferulic acid on the performance of soy protein isolate-based edible coatings applied to fresh-cut apples. LWT- Food Science and Technology, 80, 409-415.

Ameer K., Shahbaz H.M., Kwon J.H. (2017). Green extraction methods for polyphenols from plant matrices and their byproducts: A review. Comprehensive Reviews in Food Science and Food Safety, 16(2), 295-315.

Ansorena M.R., Zubeldía F., Marcovich N.E. (2016). Active wheat gluten films obtained by thermoplastic processing. LWT- Food Science and Technology, 69: 47-54.

Anwer M.A.S., Naguib H. E., Celzard A., Fierro V. (2015). Comparison of the thermal, dynamic mechanical and morphological properties of PLA-Lignin and PLA-Tannin particulate green composites. Composites Part B: Engineering, 82, 92-99.

Arabestani A., Kadivar M., Shahedi M., Goli S.A.H., Porta R. (2013). Properties of a new protein film from bitter vetch (*Vicia ervilia*) and effect of $CaCl_2$ on its hydrophobicity. International Journal of Biological Macromolecules, 57, 118-123.

Arabestani A., Kadivar M., Shahedi M., Goli S.A.H., Porta R. (2016a). The effect of oxidized ferulic acid on physicochemical properties of bitter vetch (*Vicia ervilia*) protein-based films. Journal of Applied Polymer Science, 133(2), 42894-42901.

Arabestani A., Kadivar M., Shahedi M., Goli S.A.H., Porta R. (2016b).Characterization and antioxidant activity of bitter vetch protein-based films containing pomegranate juice. LWT- Food Science and Technology, 74, 77-83.

Aragui M., Moslehi Z. (2014). Chemical modification of cold water fish gelatin using phenolic cross-linker caffeic acid. Research Journal of Pharmaceutical, Biological and Chemical Sciences, 5(6), 674-679.

Arancibia M.Y., López-Caballero M.E., Gómez-Guillén C., Montero P. (2014). Release of volatile compounds and biodegradability of active soy protein lignin blend films with added citronella essential oil. Food Control, 44, 7-15.

Arfat Y.A., Benjakul S., Prodpran T., Sumpavapol P., Songtipya P. (2014). Properties and antimicrobial activity of fish protein isolate/fish skin gelatin film containing basil leaf essential oil and zinc oxide nanoparticles. Food Hydrocolloids, 41, 265-273.

ASTM D 3985-10. (2010). Standard test method for oxygen gas transmission rate through plastic film and sheeting using a Coulometric Sensor. In: Annual Book of ASTM Standards, American Society for testing and materials, Philadelphia.

ASTM D 523-14. (2014). Standard test method for specular gloss. In: Annual Book of ASTM Standards, American Society for testing and materials, Philadelphia.

ASTM D 638-03. (2003). Standard test method for tensile properties of plastics. In: Annual Book of ASTM Standards, American Society for testing and materials, Philadelphia.

ASTM E 96-00. (2000). Standard test method for water vapour transmission of materials. In: Annual Book of ASTM Standards, American Society for testing and materials, Philadelphia.

Atarés L., Chiralt A. (2016). Essential oils as additives in biodegradable films and coatings for active food packaging. Trends in Food Science and Technology, 48, 51-62.

Aydemir L.Y., Gökbulut A.A., Baran Y., Yemenicioğlu A. (2014). Bioactive, functional and edible film-forming properties of isolated hazelnut (*Corylus avellana* L.) meal proteins. Food Hydrocolloids, 36, 130-142.

Bai H., Xu J., Liao P., Liu X. (2013). Mechanical and water properties of soy protein isolate film incorporated with gelatin. Journal of Plastic Film and Sheeting, 29(2), 174-188.

Balakrishnan P., Geethamma V., Sreekala M.S., Thomas S. (2018). Polymeric biomaterials: State-of-the-art and new challenges, Fundamental Biomaterials: Polymers, Elsevier, pp 1-20.

Balestrieri C., Colonna G., Giovane A., Irace G., Servillo L. (1978). Second-derivative spectroscopy of proteins. A method for the quantitative determination of aromatic amino acids in proteins. European Journal of Biochemistry, 90, 433-440.

Ballesteros L.F., Teixeira J.A., Mussatto S.I. (2014). Selection of the solvent and extraction conditions for maximum recovery of antioxidant phenolic compounds from coffee silverskin. Food and Bioprocess Technology, 7(5), 1322-1332.

Barazi A., Osman E. (2017). Antimicrobial activity of a novel biodegradable edible film produced from Pistacia vera resin and *Origanum vulgare* essential oil. Research Journal of Biotechnology, 12(9), 15-21.

Barkay-Olami H., Zilberman M. (2016). Novel porous soy protein-based blend structures for biomedical applications: Microstructure, mechanical and physical properties. Journal of Biomedical Materials Research: Part B, 104, 1109-1120.

Barros F.C.N., da Silva D.C., Sombra V.G., Maciel J.S., Feitosa J.P.A., Freitas A.L.P., de Paula R.M.C. (2013). Structural characterization of polysaccharide obtained from red seaweed *Gracilaria caudata* (*J. Agardh*). Carbohydrate Polymers, 92, 598-603.

Basiak E., Galus S., Lenart A. (2015). Characterisation of composite edible films based on wheat starch and whey-protein isolate. International Journal of Food Science and Technology, 50(2), 372-380.

Basiak E., Lenart A., Debeaufort F. (2017). Effects of carbohydrate/protein ratio on the microstructure and the barrier and sorption properties of wheat starch-whey protein blend edible films. Journal of the Science of Food and Agriculture, 97(3), 858-867.

Basso D., Patuzzi F., Castello D., Baratieri M., Rada E.C., Weiss-Hortala E., Fiori L. (2016). Agro-industrial waste to solid biofuel through hydrothermal carbonization. Waste Management, 47, 114-121.

Basu S., Shivhare U.S., Singh T.V., Beniwal V.S. (2011). Rheological, textural and spectral characteristics of sorbitol substituted mango jam. Journal of Food Engineering, 105, 503-512.

Bengoechea C., Arrachid A., Guerrero A., Hill S.E., Mitchell J.R. (2007). Relationship between the glass transition temperature and the melt flow behavior for gluten, casein and soya. Journal of Cereal Science, 45, 275-284.

Benito-Román O., Rodríguez-Perrino M., Sanz M.T., Melgosa R., Beltrán S. (2018). Supercritical carbon dioxide extraction of quinoa oil: Study of the influence of process parameters on the extraction yield and oil quality. Journal of Supercritical Fluids, 139, 62-71.

Bertuzzi M.A., Slavutsky A.M. (2016). Standard and new processing techniques used in the preparation of films and coatings at the lab level and scale-up. In: Garcia M.P.M., Gómez-Guillén M.C., López-Caballero M.E., Barbosa-Cánovas G.V. (eds.). Edible films and coatings: fundamentals and applications. Chapter 1.CRC Press, USA.

Bezerra M.A., Santelli R.E, Oliveira E.P., Villar L.S., Escaleira L.A. (2008). Response Surface Methodology (RSM) as a tool for optimization in analytical chemistry. Talanta. 76(5), 965-977.

Bibi F., Guillaume C., Gontard N., Sorli B. (2017). Wheat gluten, a biopolymer to monitor carbon dioxide in food packaging: Electric and dielectric characterization. Sensors and Actuators B, 250, 76-84.

Bibi F., Guillaume C., Vena A., Gontard N., Sorli B. (2016). Wheat gluten, a bio-polymer layer to monitor relative humidity in food packaging: Electric and dielectric characterization. Sensors and Actuators B, 247, 355-367.

Biji K.B., Ravishankar C.N., Mohan C.O., Gopal T.K.S. (2015). Smart packaging systems for food applications: A review. Journal of Food Science and Technology, 52(10), 6125-6135.

Bodoira R., Rossi Y., Montenegro M., Maestri D., Velez A. (2017). Extraction of antioxidant polyphenolic compounds from peanut skin using water-ethanol at high pressure and temperature conditions. Journal of Supercritical Fluids, 128, 57-65.

Bonfante A., Alfieri S.M., Albrizio R., Basile A., de Mascellis R., Gambuti A., Giorio P., Langella G., Manna P., Monaco E., Terribile F. (2017). Evaluation of the effects of future climate change on grape quality through a physically based model application: a case study for the Aglianico grapevine in Campania region, Italy. Agricultural System, 152, 100-109.

Bonwell E., Wetzel D. (2009). Innovative FT-IR imaging of protein films secondary structure before and after heat treatment. Journal of Agricultural and Food Chemistry, 57, 10067-10072.

Boukroufa M., Boutekedjiret C., Petigny L., Rakotomanomana N., Chemat F. (2015). Bio-refinery of orange peels waste: a new concept based on integrated green and solvent

free extraction processes using ultrasound and microwave techniques to obtain essential oil, polyphenols and pectin. Ultrasonic Sonochemistry, 24, 72-79.

Bourny V., Perez-Puyana V., Felix M., Romero A., Guerrero A. (2017). Evaluation of the injection moulding conditions in soy/nanoclay based composites. European Polymer Journal, 95, 539-546.

Bourtoom T. (2008). Edible films and coatings: characteristics and properties. International Food Research Journal, 15(3), 237-248.

Boutaoui N., Zaiter L., Benayache F., Benayache S., Carradori S., Cesa S., Giusti A.M., Campestre C., Menghini L., Innosa D. (2018). Qualitative and quantitative phytochemical analysis of different extracts from thymus algeriensis aerial parts. Molecules, 23(2), 463-474.

Bouvier J., Campanella O.H. (2014). Extrusion processing technology: Food and non-food biomaterials. Wiley-Blackwell.

Božič M., Majerič M., Denac M., Kokol V. (2015). Mechanical and barrier properties of soy protein isolate films plasticized with a mixture of glycerol and dendritic polyglycerol. Journal of Applied Polymer Science, 132(17), 41837-41849.

Bubalo M.C., Vidović S., Redovniković I.R., Jokić S. (2018). New perspective in extraction of plant biologically active compounds by green solvents. Food and Bioproducts Processing, 109, 52-73.

Bucić-Kojić A., Sovová H., Planinić M., Tomas S. (2013). Temperature-dependent kinetics of grape seed phenolic compounds extraction: Experiment and model. Food Chemistry, 136(3-4), 1136-1140.

Bustamante M.A., Moral R., Paredes C., Pérez-Espinosa A., Moreno-Caselles J., Pérez-Murcia M.D. (2008). Agrochemical characterization of the solid by-products and residues from the winery and distillery industry. Waste Manage. 28(2), 372-380.

Caldas T.W., Mazza K.E.L., Teles A.S.C., Mattos G.N., Brígida A.I.S., Conte-Junior C.A., Borguini R.G., Godoy R.L.O., Cabral L.M.C., Tonon R.V. (2018). Phenolic compounds recovery from grape skin using conventional and nonconventional extraction methods. Industrial Crops and Products, 111, 86-91.

Carpiné D., Andreotti J.L., Canhadas L., Rogério M. (2015). Development and characterization of soy protein isolate emulsion-based edible films with added coconut oil for olive oil packaging: barrier, mechanical, and thermal properties. Food and Bioprocess Technology, 8, 1811-1823.

Casazza A.A., Aliakbarian B., De Faveri D., Fiori L., Perego P. (2012). Antioxidants from winemaking wastes: A study on extraction parameters using response surface methodology. Journal of Food Biochemistry, 36(1), 28-37.

Cecchini J.P., Spotti M.J., Piagentini A.M., Milt V.G., Carraca C.R. (2017). Development of edible films obtained from submicron emulsions based on whey protein concentrate, oil/beeswax and brea gum. Food Science and Technology International, 23(4), 371-381.

Cerqueira M.A.P.R., Pereira R.N.C., da Silva Ramos O.L., Teixeira J.A.C., Vicente A.A. (2016). Edible Food Packaging: Materials and Processing Technologies, CRC Press.

Chan C.-H., See T.-Y., Yusoff R., Ngoh G.-C., Kow K.-W. (2017). Extraction of bioactives from *Orthosiphon stamineus* using microwave and ultrasound-assisted techniques: Process optimization and scale up. Food Chemistry, 221, 1382-1387.

Chandumpai A., Singhpibulporn N., Faroongsarng D., Sornprasit P. (2004). Preparation and physic-chemical characterization of chitin and chitosan from the pens of the squid species, *Loligo lessoniana* and *Loligo formosana*. Carbohydrate Polymers, 58, 467-474.

Chang C., Nickerson M.T. (2014). Effect of plasticizer type and genipin on the mechanical, optical, and water vapour barrier properties of canola protein isolate-based edible films. European Food Research and Technology, 238(1), 35-46.

Chang C., Nickerson M.T. (2015). Effect of protein and glycerol concentration on the mechanical, optical, and water vapour barrier properties of canola protein isolate-based edible films. Food Science and Technology International, 21(1), 33-44.

Chaussard G., Domand A. (2004). New aspects of the extraction of chitin from squid pens. Biomacromolecules, 5, 559-564.

Chemat F., Rombaut N., Sicaire A.-G., Meullemiestre A., Fabiano-Tixier A.-S., Abert-Vian M. (2017). Ultrasound assisted extraction of food and natural products. Mechanisms, techniques, combinations, protocols and applications: A review. Ultrasonic Sonochemistry, 34, 540-560.

Chen B.J., Zhou Y.J., Wei X.Y., Xie H.J., Hider R.C., Zhou T. (2016). Edible antimicrobial coating incorporating a polymeric iron chelator and its application in the preservation of surimi product. Food and Bioprocess Technology, 9(6), 1031-1039.

Chen F., Monnier X., Gällstedt M., Gedde U.W., Hedenqvist M.S. (2014). Wheat gluten/chitosan blends: a new biobased material. European Polymer Journal, 60, 186-197.

Chen M., Liu F., Chiou B.-S., Sharif H.R., Xu J., Zhong F. (2017). Characterization of film-forming solutions and films incorporating free and nanoencapsulated tea polyphenol prepared by gelatins with different Bloom values. Food Hydrocolloids, 72, 381-388.

Chen P., Zhang L. (2005). New evidences of glass transitions and microstructures of soy protein plasticized with glycerol. Macromolecular Bioscience, 5, 237-245.

Chen P., Zhang L., Cao F. (2005). Effects of moisture on glass transition and microstructure of glycerol-plasticized soy protein. Macromolecular Bioscience, 5, 872-880.

Cheng S.Y., Wang B.J., Weng Y.M. (2015). Antioxidant and antimicrobial edible zein/chitosan composite films fabricated by incorporation of phenolic compounds and dicarboxylic acids. LWT- Food Science and Technology, 63(1), 115-121.

Cheung H., Ho M., Lau K., Cardona F., Hui D. (2009). Natural fibre-reinforced composites for bioengineering and environmental engineering applications. Composites Part B, 40, 655-663.

Chinma C.E., Ariahu C.C., Abu J.O. (2012). Development and characterization of cassava starch and soy protein concentrate based edible films. International Journal of Food Science and Technology, 47(2), 383-389.

Ciannamea E.M., Espinosa J.P., Stefani P.M., Ruseckaite R.A. (2017). Long-term stability of compression-molded soybean protein concentrate films stored under specific conditions. Food Chemistry, 243, 448-452.

Ciannamea E.M., Stefani P.M., Ruseckaite R.A. (2014). Physical and mechanical properties of compression moulded and solution casting soybean protein concentrate based films. Food Hydrocolloids, 38, 193-204.

Ciannamea E.M., Stefani P.M., Ruseckaite R.A. (2016). Properties and antioxidant activity of soy protein concentrate films incorporated with red grape extract processed by casting and compression molding. LWT- Food Science and Technology, 74, 353-362.

Cordeiro de Azeredo H.M. (2012). Edible coatings. In: Rodrigues S., Fernandes F.A.N. (eds.). Advances in fruit processing technologies. CRC Press Inc, USA, pp 345-361.

Córdoba L.J.P., Sobral P.J.A. (2017). Physical and antioxidant properties of films based on gelatin, gelatin-chitosan or gelatin-sodium caseinate blends loaded with nanoemulsified active compounds. Journal of Food Engineering, 213, 47-53.

Cortizo M.S., Berghoff C.F., Alessandrini J.L. (2008). Characterization of chitin from Illex argentinus squid pen. Carbohydrate Polymers, 74, 10-15.

Coşkun B.K., Çalikoğlu E., Emiroğlu Z.K., Candoğan K. (2014). Antioxidant active packaging with soy edible films and oregano or thyme essential oils for oxidative stability of ground beef patties. Journal of Food Quality, 37(3), 203-212.

Coughlan K., Shaw N.B., Kerry J.F., Kerry J.P. (2004). Combined effects of proteins and polysaccharides on physical properties of whey protein concentrate-based edible films. Food Engineering and Physical Properties, 69, 271-275.

Cuadri A.A., Bengoechea C., Romero A., Guerrero A. (2016). A natural-based polymeric hydrogel based on functionalized soy protein. European Polymer Journal, 95, 164-174.

Da Porto C., Natolino A. (2017). Supercritical fluid extraction of polyphenols from grape seed (*Vitis vinifera*): Study on process variables and kinetics. Journal of Supercritical Fluids, 130, 239-245.

da Silva B.G., Fileti A.M.F., Foglio M.A., Ruiz A.L.T.G, e Rosa P.d.T.V. (2017). Supercritical carbon dioxide extraction of compounds from *Schinus terebinthifolius Raddi* fruits: Effects of operating conditions on global yield, volatile compounds, and antiproliferative activity against human tumor cell lines. Journal of Supercritical Fluids, 130, 10-16.

da Silva Haas I.C., Toaldo I.M., Burin V.M., Bordignon-Luiz M.T. (2018). Extraction optimization for polyphenolic profiling and bioactive enrichment of extractives of non-pomace residue from grape processing. Industrial Crops and Products, 112, 593-601.

da Silva R.P., Rocha-Santos T.A., Duarte A.C. (2016). Supercritical fluid extraction of bioactive compounds. TrAC- Trends in Analytical Chemistry, 76, 40-51.

Dahesh M., Banc A., Duri A., Morel M.H., Ramos L. (2016). Spontaneous gelation of wheat gluten proteins in a food grade solvent. Food Hydrocolloids, 52, 1-10.

Dahmoune F., Nayak B., Moussi K., Remini H., Madani K. (2015). Optimization of microwave-assisted extraction of polyphenols from *Myrtus communis* L. leaves. Food Chemistry, 166, 585-595.

Damodaran S. (2007). Amino acids, peptides and proteins. In: Damodaran S., Parkin K.L., Fennema O.R. (eds.). Fennema´s food chemistry (4th edition). CRC Press, USA, pp 219-323.

Darmanto Y.S. (2002). The effect of chitin and chitosan of crab shell on water sorption of isotherm and denaturation of myofibrils during dehydration process. Journal of Coastal Development, 5, 75-83.

Daso A.P., Okonkwo O.J. (2015). Chapter 3: Conventional extraction techniques: soxhlet and liquid-liquid extractions and evaporation. Analytical Separation Science, 1437-1468.

Day L. (2011) Wheat gluten: production, properties and applications. In: Phillips G.O., Williams P.A. (eds.). Handbook of proteins. Woodhead publishing, UK, pp 267-288.

de Aguiar A.C., Osorio-Tobón J.F., Silva L.P.S., Barbero G.F., Martínez J. (2018). Economic analysis of oleoresin production from malagueta peppers (*Capsicum frutescens*) by supercritical fluid extraction. Journal of Supercritical Fluids, 133, 86-93.

de Moraes Crizel T., de Oliveira Rios A., Alves V.D., Bandarra N., Moldão-Martins M., Hickmann Flôres S. (2018). Active food packaging prepared with chitosan and olive pomace. Food Hydrocolloids, 74, 139-150.

de Moraes J.O., Scheibe A.S., Sereno A., Laurindo J.B. (2013). Scale-up of the production of cassava starch based films using tape-casting. Journal of Food Engineering, 119(4), 800-808.

de Oliveira N.A., Cornelio-Santiago H.P., Fukumasu H., de Oliveira A.L. (2018). Green coffee extracts rich in diterpenes-Process optimization of pressurized liquid extraction using ethanol as solvent. Journal of Food Engineering, 224, 148-155.

de Souza V.B., Thomazini M., Balieiro J.C.C., Fávaro-Trindade C.S. (2015). Effect of spray drying on the physicochemical properties and color stability of the powdered pigment obtained from vinification byproducts of the Bordo grape (*Vitis labrusca*). Food and Bioproducts Processing, 93, 39-50.

de Zordi N., Cortesi A., Kikic I., Moneghini M., Baldan V., Sut S., Solinas D., Dall'Acqua S. (2017). The Supercritical carbon dioxide extraction of ω-3, ω-6 lipids and β-sitosterol from Italian walnuts: a central composite design approach. Journal of Supercritical Fluids, 127, 223-228.

del Pilar Sánchez-Camargo A., Pleite N., Herrero M., Cifuentes A., Ibáñez E., Gilbert-López B. (2017). New approaches for the selective extraction of bioactive compounds employing bio-based solvents and pressurized green processes. Journal of Supercritical Fluids, 128, 112-120.

Denavi G., Tapia-Blácido D.R., Añón M.C., Sobral P.J.A, Mauri A.N., Menegalli F.C. (2009). Effects of drying conditions on some physical properties of soy protein films. Journal of Food Engineering, 90, 341-349.

Department of environment and regional planning of the Basque Government. (2008). Standards for urban solid waste management in the Basque Country. Ihobe, sociedad pública de gestión ambiental, Bilbao, Spain (in Spanish).

Derringer G., Suich R. (1980). Simultaneous optimization of several response variables. Journal of Quality Technology, 12(4), 214-219.

Derringer G., Suich R. (1980). Simultaneous optimization of several response variables. Journal of Quality Technology, 12(4), 214-219.

Devesa-Rey R., Vecino X., Varela-Alende J.L, Barral M.T, Cruz J.M., Moldes A.B. (2011). Valorization of winery waste vs. the costs of not recycling. Waste Management, 31, 2327-2335.

Di Lorenzo A., Bloise N., Meneghini S., Sureda A., Tenore G.C., Visai L., Arciola C.R., Daglia M. (2016). Effect of winemaking on the composition of red wine as a source of polyphenols for anti-infective biomaterials. Materials, 9(5), 316-335.

Díaz-Calderón P., Flores E., González-Muñoz A., Pepczynska M., Quero F., Enrione J. (2017). Influence of extraction variables on the structure and physical properties of salmon gelatin. Food Hydrocolloids, 71, 118-128.

Díaz-de-Cerio E., Arráez-Román D., Segura-Carretero A., Ferranti P., Nicoletti R., Perrotta G.M., Gómez-Caravaca A.M. (2018). Establishment of pressurized-liquid extraction by response surface methodology approach coupled to HPLC-DAD-TOF-MS for the determination of phenolic compounds of myrtle leaves. Analytical and Bioanalytical Chemistry, 410(15), 3547-3557.

Dou Y., Zhang B., He M., Yin G., Cui Y. (2016). The structure, tensile properties and water resistance of hydrolyzed feather keratin-based bioplastics. Chinese Journal of Chemical Engineering, 24, 415-420.

Drosou C., Kyriakopoulou K., Bimpilas A., Tsimogiannis D., Krokida M. (2015). A comparative study on different extraction techniques to recover red grape pomace polyphenols from vinification byproducts. Industrial Crops and Products, Part B, 75, 141-149.

Duconseille A., Wien F., Audonnet F., Traore A., Refregiers M., Astruc T., Santé-Lhoutellier V. (2017). The effect of origin of the gelatin and ageing on the secondary structure and water dissolution. Food Hydrocolloids, 66, 378-388.

Duval A., Molina-Boisseau S., Chirat C., Morel M.H. (2015). Dynamic mechanical analysis of the multiple glass transitions of plasticized wheat gluten biopolymer. Journal of Applied Polymer Science, 133(14), 43254-43265.

Echeverría I., López-Caballero M.E., Gómez-Guillén M.C., Mauri A.N., Montero M.P. (2016). Structure, functionality and active release of nanoclay-soy protein films affected by clove essential oil. Food and Bioprocess Technology, 9(11), 1937-1950.

Echeverría I., López-Caballero M.E., Gómez-Guillén M.C., Mauri A.N., Montero M.P. (2017). Active nanocomposite films based on soy proteins-montmorillonite-clove essential oil for the preservation of refrigerated bluefin tuna (*Thunnus thynnus*) fillets. International Journal of Food Microbiology, DOI: 10.1016/j.ijfoodmicro.2017.10.003.

El-Hefian E.A., Nasef M.M., Yahaya A.H. (2012). Preparation and characterization of chitosan/agar blended films: Part 2. Thermal, mechanical, and surface properties. E-Journal of Chemistry, 9, 510-516.

Emin M.A., Quevedo M., Wilhelm M., Karbstein H.P. (2017). Analysis of the reaction behavior of highly concentrated plant proteins in extrusion-like conditions. Innovative Food Science and Emerging Technologies, 44, 15-20.

Erşan S., Üstündağ Ö.G., Carle R., Schweiggert R.M.. (2018). Subcritical water extraction of phenolic and antioxidant constituents from pistachio (*Pistacia vera* L.) hulls. Food Chemistry, 253, 46-54.

Esquivel-Hernández D.A., Rodrígiez-Rodríguez J., Rostro-Alanis M., Cuéllar-Bermúdez S.P., Mancera-Andrade E.I., Nuñez-Echeverria J., García-Pérez J.S., Chandra R., Parra-Saldivar R. (2017). Advancement of green process through microwave-assisted extraction of bioactive metabolites from *Arthrospira Platensis* and bioactivity evaluation. Bioresources Technology, 224, 618-629.

Etxabide A., Uranga J., Guerrero P., de la Caba K. (2017). Development of active films by means of valorisation of food processing waste: A review. Food Hydrocolloids, 68, 192-198.

Etxabide A., Urdanpilleta M.., Guerrero P, de la Caba K. (2015). Effect of cross-linking in nanostructure and physicochemical properties of fish gelatins for bio-applications. Reactive and Functional Polymers, 94, 55-62.

Falguera V., Quintero J.P., Jiménez A., Muñoz J.A., Ibarz A. (2011). Edible films and coatings: Structures, active functions and trends in their use. Trends in Food Science and Technology, 22(6), 292-303.

Fang Y., Zhang B., Wei Y. (2014). Effects of the specific mechanical energy on the physicochemical properties of texturized soy protein during high-moisture extrusion cooking. Journal of Food Engineering, 121, 32-38.

Fernández-Espada L., Bengoechea C., Cordobés F., Guerrero A. (2016). Protein/glycerol blends and injection-molded bioplastic matrices: Soybean versus egg albumen. Journal of Applied Polymer Science, 133, 43524-43534.

Feuereisen M.M., Barraza M.G., Zimmermann B.F., Schieber A., Schulze-Kaysers N. (2017). Pressurized liquid extraction of anthocyanins and biflavonoids from Schinus terebinthifolius Raddi: A multivariate optimization. Food Chemistry, 214, 564-571.

Fiore V., Botta L., Scaffaro R., Valenza A., Pirrotta A. (2014). PLA based biocomposites reinforced with *Arundo donax* fillers. Composites Science and Technology, 105, 110-117.

Focher B., Naggi A., Torri G., Cosani A., Terbojevich M. (1992). Structural differences between chitin polymorphs and their precipitates from solutions- evidence from CP-MAS ^{13}C-NMR, FT-IR and FT-Raman spectroscopy. Carbohydrate Polymers, 17(2), 97-102.

Francis F.J., Clydesdale F.M. (1975). Food Colorimetry: Theory and Applications. The AVI Publishing Company, Westport.

Freile-Pelegrín Y., Madera-Santana T., Robledo D., Veleva L., Quintana P., Azamar J.A. (2007). Degradation of agar films in humid tropical climate: Thermal, mechanical, morphological and structural changes. Polymer Degradation and Stability, 92, 244-252.

Friesen K., Chang C., Nickerson M. (2015). Incorporation of phenolic compounds, rutin and epicatechin, into soy protein isolate films: mechanical, barrier and cross-linking properties. Food Chemistry, 172, 18-23.

Galanakis C.M. (2015). Food waste recovery: processing technologies and industrial techniques, Academic Press.

Galus S., Lenart A., Voilley A., Debeaufort F. (2013). Effect of oxidized potato starch on the physicochemical properties of soy protein isolate-based edible films. Food Technology and Biotechnology, 51(3), 403-409.

Galus S., Mathieu H., Lenart A., Debeaufort F. (2012). Effect of modified starch or maltodextrin incorporation on the barrier and mechanical properties, moisture sensitivity and appearance of soy protein isolate-based edible films. Innovative Food Science and Emerging Technologies, 16, 148-154.

Ganiari S., Choulitoudi E., Oreopoulou V. (2017). Edible and active films and coatings as carriers of natural antioxidants for lipid food. Trends in Food Science and Technology, 68, 70-82.

Garavand F., Rouhi M., Hadi Razavi S., Cacciotti I., Mohammadi R. (2017). Improving the integrity of natural biopolymer films used in food packaging by crosslinking approach: A review. International Journal of Biological Macromolecules, 104, 687-707.

García-Esparza M. J., Abrisqueta I., Escriche I., Intrigliolo D.S., Álvarez I., Lizama V. (2018). Volatile compounds and phenolic composition of skins and seeds of 'Cabernet Sauvignon' grapes under different deficit irrigation regimes. Vitis, 57, 83-91.

Garrido T., Etxabide A., Leceta I., Cabezudo S., de la Caba K., Guerrero P. (2014). Valorization of soya by-products for sustainable packaging. Journal of Cleaner Production, 64, 228-233.

Garrido T., Etxabide A., de la Caba K., Guerrero P. (2017). Versatile soy protein films and hydrogels by the incorporation of β-chitin from squid pens (*Loligo* sp.). Green Chemistry, 19, 5923-5931.

Garrido T., Peñalba M., de la Caba K., Guerrero P. (2019). A more efficient process to develop protein films derived from agro-industrial by-products. Food Hydrocolloids, 86, 11-17.

Ghaani M., Cozzolino C.A., Castelli G., Farris S. (2016). An overview of the intelligent packaging technologies in the food sector. Trends in Food Science and Technology, 51, 1-11.

Ghanbarzadeh B., Oromiehi A.R. (2008). Studies on glass transition temperature of mono and bilayer protein films plasticized by glycerol and olive oil. Journal of Applied Polymer Science, 109(5), 2848-2854.

Ghidelli C., Mateos M., Rojas-Argudo C., Pérez-Gago M.B. (2014). Extending the shelf life of fresh-cut eggplant with a soy protein-cysteine based edible coating and modified atmosphere packaging. Postharvest Biology and Technology, 95, 81-87.

Ghidelli C., Mateos M., Rojas-Argudo C., Pérez-Gago M.B. (2015). Novel approaches to control browning of fresh-cut artichoke: effect of soy protein-based coating and modifies atmosphere packaging. Postharvest Biology and Technology, 99, 105-113.

Gizdavic-Nikolaidis M.R., Stanisavljev D.R., Easteal A.J., Zujovic Z.D. (2010). Microwave-assisted synthesis of functionalized polyaniline nanostructures with advanced antioxidant properties. The Journal of Physical Chemistry, C, 114, 18790-18796.

Goedkoop M., Spriensma R. (2001). The ecoindicator 99: A damage oriented method for life cycle impact assessment. Pré Consultants, Amersfoort.

Golmakani M.T., Moayyedi M. (2015). Comparison of heat and mass transfer of different microwave-assisted extraction methods of essential oil from Citrus limon (Lisbon variety) peel. Food Science and Nutrition, 3(6), 506-518.

Gómez-Estaca J., López de Dicastillo C., Hérnández-Muñoz P., Catalá R., Gavara R. (2014). Advances in antioxidant active food packaging. Trends in Food Science and Technology, 35(1), 42-51.

Gómez-Guillén M.C., Pérez-Mateos M., Gómez-Estaca J., López-Caballero E., Giménez B, Montero P. (2009). Fish gelatin: a renewable material for developing active biodegradable films. Trends in Food Science and Technology, 20(1), 3-16.

Gómez-Heincke D., Martínez I., Partal P., Guerrero A., Gallegos C. (2016). Development of antimicrobial active packaging materials based on gluten proteins. Journal of the Science of Food and Agriculture, 96(10), 3432-343.

González A., Igarzabal C.I.A. (2013). Soy protein-Poly (lactic acid) bilayer films as biodegradable material for active food packaging. Food Hydrocolloids, 33(2), 289-296.

González A., Igarzabal C.I.A. (2015). Nanocrystal-reinforced soy protein films and their applications as active packaging. Food Hydrocolloids, 43, 777-784.

González-Estrada R.R., Chalier P., Ragazzo-Sánchez J.A., Konuk D., Calderón-Santoyo M. (2017). Antimicrobial soy protein based coatings: Application to Persian lime (*Citrus latifolia* Tanaka) for protection and preservation. Postharvest Biology and Technology, 132, 138-144.

Gorgani L., Mohammadi M., Najafpour G.D., Nikzad M. (2017). Sequential microwave-ultrasound-assisted extraction for isolation of piperine from black pepper (*Piper nigrum* L.). Food and Bioprocess Technology, 10(12), 2199-2207.

Granato D., Katayama F.C.U., de Castro I.A. (2011). Phenolic composition of South American red wines classified according to their antioxidant activity, retail price and sensory quality. Food Chemistry, 129(2), 366-373.

Granda H., de Pascual-Teresa S. (2018). Polyphenols interactions with other food components as a mean for their neurological health benefits. Journal of Agricultural and Food Chemistry, DOI: 10.1021/acs.jafc.8b02839.

Gu L., Wang M., Zhou J. (2013). Effects of protein interactions on properties and microstructure of zein-gliadin composite films. Journal of Food Engineering, 119(2), 288-298.

Guerrero P., Beatty E., Kerry J.P., de la Caba K. (2012). Extrusion of soy protein with gelatin and sugars at low moisture content. Journal of Food Engineering, 110, 53-59.

Guerrero P., de la Caba K. (2010). Thermal and mechanical properties of soy protein films processed at different pH by compression. Journal of Food Engineering, 100, 261-269.

Guerrero P., Etxabide A., Leceta I., Peñalba M., de la Caba K. (2014). Extraction of agar from *Gelidium sesquipedale* (*Rodhopyta*) and surface characterization of agar based films. Carbohydrate Polymers, 99, 491-498.

Guerrero P., Garrido T., Leceta I., de la Caba K. (2013). Films based on proteins and polysaccharides: Preparation and physical-chemical characterization. European Polymer Journal, 49, 3713-3721.

Guerrero P., Kerry J.P., de la Caba K. (2014). FTIR characterization of protein-polysaccharide interactions in extruded blends. Carbohydrate Polymers, 111, 598-605.

Guerrero P., Nur Hanani Z.A., Kerry J.P., de la Caba K. (2011). Characterization of soy protein-based films prepared with acids and oils by compression. Journal of Food Engineering, 107, 41-49.

Guerrero P., O´Sullivan M.G., Kerry J.P., de la Caba K. (2015). Application of soy protein coatings and their effect on the quality and shelf life stability of beef patties. RSC Advances, 5(11), 8182-8189.

Guerrero P., Stefani P.M., Ruseckaite R.A., de la Caba K. (2011b). Functional properties of films based on soy protein isolate and gelatin processed by compression molding. Journal of Food Engineering, 105, 65-72.

Gullón B., Gullón P., Lú-Chau T.A., Moreira M.T., Lema J.M., Eibes G. (2017). Optimization of solvent extraction of antioxidants from *Eucalyptus globulus* leaves by response surface methodology: Characterization and assessment of their bioactive properties. Industrial Crops and Products, 108, 649-659.

Gupta P., Nayak K.K. (2015). Characteristics of protein-based biopolymers and its applications. Polymer Engineering and Science, 55(3), 485-498.

Hamman F., Schmid M. (2014). Determination and quantification of molecular interactions in protein films: A review. Materials, 7, 7975-7996.

Han J., Shin S.H., Park K.M., Kim K.M. (2015). Characterization of physical, mechanical and antioxidant properties of soy protein-based bioplastics films containing carboxymethylcellulose and catechin. Food Science and Biotechnology, 24(3), 939-945.

Han Y., Yu M., Wang L. (2018). Preparation and characterization of antioxidant soy protein isolate films incorporating licorice residue extract. Food Hydrocolloids, 75, 13-21.

Harper J.M. (1989). Food extruders and their applications. In: Mercier C., Linko P., Harper J.M. Extrusion Cooking. American Association of Cereal Chemists, Minnesota.

Hernandez-Izquierdo V.M., Krochta J.M. (2008). Thermoplastic processing of proteins for film formation: A review. Journal of Food Science, 73(2), 30-39.

Herrero M., del Pilar Sanchez-Camargo A., Cifuentes A., Ibanez E. (2015). Plants, seaweeds, microalgae and food by-products as natural sources of functional ingredients obtained using pressurized liquid extraction and supercritical fluid extraction. TrAC-Trends in Analytical Chemistry, 71, 26-38.

Hill P., Brantley H., Van Dyke M. (2010). Some properties of keratin biomaterials: Kerateines. Biomaterials, 31, 585-593.

Ho K., Ferruzzi M., Liceaga A., San Martín-González M. (2015). Microwave-assisted extraction of lycopene in tomato peels: effect of extraction conditions on all-trans and cis-isomer yields. LWT- Food Science and Technology, 62(1), 160-168.

Hopkins E.J., Chang C., Lam R.S.H., Nickerson M.T. (2015). Effect of flaxseed oil concentration on the performance of a soy protein isolated-based emulsion type film. Food Research International, 67, 418-425.

Hu L., Hsieh F., Huff H.E. (1993). Corn meal extrusion with emulsifier and soybean fiber. Food Science and Technology, 26, 544-55.

Ianiro A., Di Giosia M., Fermani S., Samori C., Barbalinardo M., Valle F., Pellegrini G., Biscarini F., Zerbetto F., Calvaresi M., Falini G. (2014). Customizing properties of β-Chitin in squid pen (*Gladius*) by chemical treatments. Marine drugs, 12, 5979-5992.

Ince A.E., Sahin S., Sumnu G. (2014). Comparison of microwave and ultrasound-assisted extraction techniques for leaching of phenolic compounds from nettle. Journal of Food Science and Technology, 51(10), 2776-2782.

Insaward A., Duangmal K., Mahawanich T. (2015). Mechanical, optical and barrier properties of soy protein film as affected by phenolic acid addition. Journal of Agricultural and Food Chemistry, 63(43), 9421-9426.

Irkin R., Esmer O.K. (2015). Novel food packaging systems with natural antimicrobial agents. Journal of Food Science and Technology, 52(10), 6095-6111.

ISO 14040. (2006). Environmental Management e Life Cycle Assessment e Principals and Framework.

Ivanova V., Stefova M., Vojnoski B., Dörnyei Á., Márk L., Dimovska V., Stafilov T., Kilár F. (2011b). Identification of polyphenolic compounds in red and white grape varieties grown in R. Macedonia and changes of their content during ripening. Food Research International, 44(9), 2851-2860.

Ivanova V., Vojnoski B., Stefova M. (2011a). Effect of the winemaking practices and aging on phenolic content of Smederevka and Chardonnay wines. Food and Bioprocess Technology, 4, 1512-1518.

Jakobsen M., Jespersen L., Juncher D., Becker E.M., Risbo J. (2005). Oxygen- and light-barrier properties of thermoformed packaging materials used for modified atmosphere packaging. Evaluation of performance under realistic storage conditions. Packaging Technology and Science, 18, 265-272.

Jang M.-K., Kong B.-G., Jeong Y.-I., Lee C.H., Nah J.-W. (2004). Physicochemical characterization of α-chitin, β-chitin and γ-chitin separated from natural resources. Journal of Polymer Science: Part A: Polymer Chemistry, 42, 3423-3432.

Jansens K.J.A., Vo Hong N., Telen L., Brijs K., Lagrain B., Van Vuure A.W., Van Acker K., Verpoest I., Van Puyvelde P., Goderis B., Smet M., Delcour J.A. (2013). Effect of molding conditions and moisture content on the mechanical properties of compression molded glassy, wheat gluten bioplastics. Industrial Crops and Products, 44, 480-487.

Jerez A., Partal P., Martinez I., Gallego C., Guerrero A. (2007). Protein-based bioplastics: effect of thermo-mechanical processing. Rheological Acta, 46, 711-720.

Jeyaratnam N., Nour A.H., Kanthasamy R., Nour A.H., Yuvaraj A., Akindoyo J.O. Essential oil from Cinnamomum cassia bark through hydrodistillation and advanced microwave assisted hydrodistillation. Industrial Crops and Products, 92, 57-66.

Ji Y., Chen J., Lv J., Li Z., Xing L., Ding S. (2014). Extraction of keratin with ionic liquids from poultry feather. Separation and Purification Technology, 132, 577-583.

Jiang P., Liu H.F., Zhao X.H., Ding Q. (2017). Physicochemical properties of soybean protein isolate affected by the cross-linking with horseradish peroxidase, glucose oxidase and glucose. Journal of Food Measurement and Characterization, 11(3), 1196-1202.

Jindal M., Kumar V., Rana V., Tiwary A.K. (2013). Physico-chemical, mechanical and electrical performance of bael fruit gum-chitosan IPN films. Food Hydrocolloids, 30, 192-199.

Jung J., Zhao Y. (2014). Alkali- or acid-induced changes in structure, moisture absorption ability and deacetylating reaction of β-chitin extracted from jumbo squid (*Dosidicus gigas*) pens. Food Chemistry, 152, 355-362.

Junqueira-Gonçalves M.P., Salinas G.E., Bruna J.E., Niranjan K. (2017). An assessment of lactobiopolymer-montmorillonite composites for dip coating applications on fresh strawberries. Journal of the Science of Food and Agriculture, 97(6), 1846-1853.

Kakaei S., Shahbazi Y. (2016). Effect of chitosan-gelatin film incorporated with ethanolic red grape seed extract and *Ziziphora clinopodioides* essential oil on survival of *Listeria monocytogenes* and chemical, microbial and sensory properties of minced trout fillet. LWT-Food Science and Technology, 72, 432-438.

Kalman D.S. (2014). Amino acid composition of an organic brown rice protein concentrate and isolate compared to soy and whey concentrates and isolates. Foods, 3(3), 394-402.

Kang H.J., Kim S.J., You Y.S., Lacroix M., Han J. (2013). Inhibitory effect of soy protein coating formulations on walnut (*Junglans regia* L.) kernels against lipid oxidation. LWT- Food Science and Technology, 51(1), 393-396.

Karbowiak T., Debeaufort F., Champion D., Voilley A. (2006). Wetting properties at the surface of iota-carrageenan-based edible films. Journal of Colloid and Interface Science, 294, 400-410.

Kashiri M., Cerisuelo J.P., Domínguez I., López-Carballo G., Muriel-Gallet V., Gavara R., Hernández-Muñoz P. (2017a). Zein films and coatings as carriers and release systems of *Zataria multiflora* Boiss. essential oil for antimicrobial food packaging. Food Hydrocolloids, 70, 260-268.

Kashiri M., Maghsoudlo Y., Khomeiri M. (2017b). Incorporating *Zataria multiflora* Boiss. essential oil and sodium bentonite nano-clay open a new perspective to use zein films as bioactive packaging materials. Food Science and Technology International, 23(7), 582-596.

Kerton F.M., Marriot R. (2013). Green solvents-Legislation and certification, in: Kerton F.M., Marriot R. (eds.). Alternative Solvents for Green Chemistry. RSC Publishing, 20, pp 31-50.

Kessel A., Ben-Tal N. (2010). Introduction to proteins: structure, function and motion. CRS Press, USA.

Khalil A.A., Deraz S.F., Elrahman S.A., El-Fawal G. (2015). Enhancement of mechanical properties, microstructure, and antimicrobial activities of zein films cross-linked using succinic anhydride, eugenol, and citric acid. Preparative Biochemistry and Biotechnology, 45(6), 551-567.

Khuwijitjaru P., Suaylam B., Adachi S. (2014). Degradation of caffeic acid in subcritical water and online HPLC-DPPH assay of degradation products. Journal of Agricultural and Food Chemistry, 62(8), 1945-1949.

Kible-Boeckler G. (1996). Measuring gloss and reflection properties of surfaces. TAPPI Journal, 79, 194-198.

Koch L., Emin M.A., Schuchmann H.P. (2017). Influence of processing conditions on the formation of whey protein-citrus pectin conjugates in extrusion. Journal of Food Engineering, 193, 1-9.

Koshy R.R., Mary S.K., Pothan L.A., Thomas S. (2015). Soy protein-and starch-based green composites/nanocomposites: Preparation, properties, and applications. In: Thakur V.K., Thakur M.K. (ed.). Eco-friendly polymer nanocomposites. Springer, India, 75, 433-467.

Kovačević D.B., Barba F.J., Granato D., Galanakis C.M., Herceg Z., Dragović-Uzelac V., Putnik P. (2018). Pressurized hot water extraction (PHWE) for the green recovery of bioactive compounds and steviol glycosides from Stevia rebaudiana Bertoni leaves. Food Chemistry, 254, 150-157.

Kowalczyk D., Gustaw W., Zieba E., Lisiecki S., Stadnik J., Baraniak B. (2016). Microstructure and functional properties of sorbitol-plasticized pea protein isolate emulsion films: Effect of lipid type and concentration. Food Hydrocolloids, 60, 353-363.

Kumar M.N.V.R. (2000). A review of chitin and chitosan applications. Reactive and Functional Polymer, 46, 1-27.

Kumar R., Choundhary V., Mishra S., Varma I.K., Mattiason Bo. (2002). Adhesives and plastics based on soy protein products. Industrial Crops and Products, 16, 155-172.

Kumari M., Mahajan H., Joshi R., Gupta M. (2017). Development and structural characterization of edible films for improving fruit quality. Food Packaging and Shelf Life, 12, 42-50.

Kurita K. (2001). Controlled functionalisation of the polysaccharide chitin. Progress in Polymer Science, 26, 1921-1971.

Kusuma H.S., Altway A., Mahfud M. (2018). Solvent-free microwave extraction of essential oil from dried patchouli (*Pogostemon cablin Benth*) leaves. Journal of Industrial and Engineering Chemistry, 58, 343-348.

Laemmli U.K. (1970). Cleavage of structural proteins during the assembly of the head of Bacteriophage T4. Nature, 227, 680-685.

Lassoued I., Jridi M., Nasri R., Dammak A., Hajji M., Nasri M., Barkia A. (2014). Characteristics and functional properties of gelatin from thornback ray skin obtained by pepsin-aided process in comparison with commercial halal bovine gelatin. Food Hydrocolloids, 41, 309-318.

Lau H.H., Murney R., Yakovlev N.L., Noselova M.V., Lim S.H., Roy N., Singh H., Sukhorukov G.B., Haigh B., Kiryukhin M.V. (2017). Protein-tannic acid multilayer films: A multifunctional material for microencapsulation of food-derived bioactives. Journal of Colloid and Interface Science, 505, 332-340.

Lavall R.L., Assis O.B., Campana-Filho S.P. (2007). β-Chitin from the pens of *Loligo sp*.: Extraction and characterization. Bioresource Technology, 98, 2465-2472.

Leceta I., Guerrero P., Cabezudo S., de la Caba K. (2013). Environmental assessment of chitosan-based films. Journal of Cleaner Production, 41, 312-318.

Lee J.E., Kim K.M. (2010). Characteristics of soy protein isolate-montmorillonite composite films. Journal of Applied Polymer Science, 118, 2257-2263.

Leyva-Jiménez F.J., Lozano-Sánchez J., Borrás-Linares I., Arráez-Román D., Segura-Carretero A. (2018). Comparative study of conventional and pressurized liquid extraction for recovering bioactive compounds from Lippia citriodora leaves. Food Research International, 109, 213-222.

Li H., Liu, B.L., Gao L.Z., Chen H.L. (2004). Studies on bullfrog skin collagen. Food Chemistry, 84, 65-69.

Li Y., Chen F., Zhan L., Yao Y. (2015). Effect of surface changes of soy protein materials on water resistance. Material Letters, 149, 120-122.

Liew S.Q., Ngoh G.C., Yusoff R., Teoh W.H. (2016). Sequential ultrasound-microwave assisted acid extraction (UMAE) of pectin from pomelo peels. International Journal of Biological Macromolecules, 93, 426-435.

Lin D., Zhao Y. (2007). Innovations in the development and application of edible coatings for fresh and minimally processed fruits and vegetables. Comprehensive Reviews in Food Science and Food Safety, 6(3), 60-75.

Liu C., Wang H., Cui Z., He X., Wang X., Zeng X., Ma H. (2007). Optimization of extraction and isolation for 11S and 7S globulins of soybean seed storage protein. Food Chemistry, 102, 1310-1316.

Liu, F., Antoniou, J., Yue, L., Y, J., Yokoyama, W., Ma, J., Zhong, F. (2015). Preparation of gelatin films incorporated with tea polyphenol nanoparticles for enhancing controlled-release antioxidant properties. *Journal of Agriculture and Food Chemistry*, 63(15), 3987-3995.

Liu F., Chiou B., Avena-Bustillos R.J., Zhang Y., Li Y., McHugh T.H., Zhong F. (2017a). Study of combined effects of glycerol and transglutaminase on properties of gelatin films. Food Hydrocolloids, 65, 1-9.

Liu F., Majeed H., Antoniou J., Li Y., Ma Y., Yokoyama W., Ma J., Zhong F. (2016). Tailoring physical properties of transglutaminase-modified gelatin films by varying drying temperature. Food Hydrocolloids, 58, 20-28.

Liu H., Li J., Zhu D., Wang Y., Zhao Y., Li J. (2014). Preparation of soy protein isolate (SPI)-pectin complex film containing cinnamon oil and its effects on microbial growth of dehydrated soybean curd (dry tofu). Journal of Food Processing and Preservation, 38(3), 1371-1376.

Liu H., Zhang L. (2006). Structure and properties of soy protein plastics plasticized with acetamide. Macromolecular Materials and Engineering, 91, 509-515.

Liu Y., Zhang H., Xu L., Chi Y., Wu Y., Cao W., Li T. (2017b). Properties of soy protein isolate antimicrobial films and its application in preservation of meat. Emirates Journal of Food and Agriculture, 29(8), 589-600.

Llobera A., Cañellas J. (2007). Dietary fibre content and antioxidant activity of Manto Negro red grape (*Vitis vinifera*): pomace and stem. Food Chemistry, 101(2), 659-666.

Lodha P., Netravali A.N. (2005). Thermal and mechanical properties of environment friendly ‘green’ plastics from stearic acid modified-soy protein isolate. Industrial Crops and Products, 21, 49-64.

Lončarić A., Lamas J.P., Guerra E., Kopjar M., Lores M. (2018). Thermal stability of catechin and epicatechin upon disaccharides addition. International Journal of Food Science and Technology, 53, 1195-1202.

López-Simeon R., Campos-Terán J., Beltrán H.I., Hernández-Guerrero M. (2012). Free-lignin cellulose obtained from agar industry residues using a continuous and minimal solvent reaction/extraction methodology. RSC Advances, 2, 12286-12297.

Lores M., Pájaro M., Álvarez-Casas M., Domínguez J., García-Jares C. (2015). Use of ethyl lactate to extract bioactive compounds from *Cytisus scoparius*: Comparison of pressurized liquid extraction and medium scale ambient temperature systems. Talanta, 140, 134-142.

Lu X., Zheng Z., Li H., Cao R., Zheng Y., Yu H., Xiao J., Miao S., Zheng B. (2017) Optimization of ultrasonic-microwave assisted extraction of oligosaccharides from lotus (*Nelumbo nucifera Gaertn*.) seeds. Industrial Crops and Products, 107, 546-557.

Lu P., Hsieh Y-L. (2012). Cellulose isolation and core-shell nanostructures of cellulose nanocrystals from chardonnay grape skins. Carbohydrate Polymers, 87(4), 2546-2553.

Luchese C.L., Garrido T., Spada J.C., Tessaro I.C., de la Caba K. (2018). Development and characterization of cassava starch films incorporated with blueberry pomace. International Journal of Biological Macromolecules, 106, 834-839.

Luo X., Cui J., Zhang H., Duan Y. (2018a). Subcritical water extraction of polyphenolic compounds from sorghum (*Sorghum bicolor* L.) bran and their biological activities. Food Chemistry, 262, 14-20.

Luo X., Cui J., Zhang H., Duan Y., Zhang D., Cai M., Chen G. (2018b). Ultrasound assisted extraction of polyphenolic compounds from red sorghum (*Sorghum bicolor* L.) bran and their biological activities and polyphenolic compositions. Industrial Crops and Products, 112, 296-304.

Ma L., Zhang M., Bhandari B., Gao Z. (2017). Recent developments in novel shelf life extension technologies of fresh-cut fruits and vegetables. Trends in Food Science and Technology, 64, 23-38.

Ma Q., Wang L. (2016). Preparation of a visual pH-sensing film based on tara gum incorporating cellulose and extracts from grape skins. Sensors and Actuators, B, 235, 401-407.

Ma W., Tang C.H., Yang X.Q., Yin S.W. (2013). Fabrication and characterization of kidney bean (*Phaseolus vulgaris* L.) protein isolate-chitosan composite films at acidic pH. Food Hydrocolloids, 31, 237-247.

Machado A.P.D.F., Pasquel-Reátegui J.L., Barbero G.F., Martínez J. (2015). Pressurized liquid extraction of bioactive compounds from blackberry (*Rubus fruticosus* L.) residues: a comparison with conventional methods. Food Research International,77, 675-683.

Machado A.P.D.F., Pereira A.L.D., Barbero G.F., Martínez J. (2017). Recovery of anthocyanins from residues of *Rubus fruticosus*, *Vaccinium myrtillus* and *Eugenia brasiliensis* by ultrasound assisted extraction, pressurized liquid extraction and their combination. Food Chemistry, 231, 1-10.

Madera-Santana T.J., Freile-Pelegrín Y., Azamar-Barrios J.A. (2014). Physicochemical and morphological properties of plasticized poly(vinyl alcohol)-agar biodegradable films. International Journal of Biological Macromolecules, 60, 176-184.

Majtán J., Bíliková K., Markovič O., Gróf J., Kogan G., Šimúth J. (2007). Isolation and characterization of chitin from bumblebee (*Bombus terrestris*). International Journal of Biological Macromolecules, 40, 237-241.

Maniglia B., Domingos J., De Paula R., Tapia-Blácido D. (2014). Development of bioactive edible film from turmeric dye solvent extraction residue. LWT- Food Science and Technology, 56(2), 269-277.

Martínez I., Partal P., García-Morales M., Guerrero A., Gallegos C. (2013). Development of protein-based bioplastics with antimicrobial activity by thermo-mechanical processing. Journal of Food Engineering, 117(2), 247-254.

Massani M.B., Botana A., Eisenberg P., Vignolo G. (2014). Development of an active wheat gluten film with *Lactobacillus curvatus* CRL705 bacteriocins and a study of its antimicrobial performance during ageing. Food Additives and Contaminants, Part A 31(1), 164-171.

Mathew A.P., Dufresne A. (2002). Plasticized Waxy Maize Starch: Effect of polyols and relative humidity on material properties. Biomacromolecules, 3, 1101-1108.

Mazzutti S., Rodrigues L.G.G., Mezzomo N., Venturi V., Ferreira S.R.S. (2018). Integrated green-based processes using supercritical CO_2 and pressurized ethanol applied to recover antioxidant compouds from cocoa (*Theobroma cacao*) bean hulls. Journal of Supercritical Fluids, 135, 52-59.

Mehyar G.F., El Assi N.M., Alsmairat N.G., Holley R.A. (2014). Effect of edible coatings on fruit maturity and fungal growth on Berhi dates. International Journal of Food Science and Technology, 49(11), 2409-2417.

Meinlschmidt P., Sussmann D., Schweiggert-Weisz U., Eisner P. (2015). Enzymatic treatment of soy protein isolates: effects on the potential allergenicity, technofuncionality and sensory properties. Food Science and Nutrition, 4(1), 11-23.

Mo X., Sun X. (2002). Plasticization of soy protein polymer by polyol-based plasticizers. Journal of the American Oil Chemists' Society. 79, 197-202.

Mojumdar S.C., Moresoli C., Simon L.C., Legge R.L. (2011). Edible wheat gluten protein films: Preparation, thermal, mechanical and spectral properties. Journal of Thermal Analysis and Calorimetry, 104(3), 929-936.

Molinaro S., Cruz-Romero M., Sensidoni A., Morris M., Lagazio C., Kerry J.P. (2015). Combination of high-pressure treatment, mild heating and holding time effects as a means of improving the barrier properties of gelatin-based packaging films using response surface modeling. Innovative Food Science and Emerging Technologies, 30, 15-23.

Monedero F.M., Fabra M.J., Talens P., Chiralt A. (2009). Effect of oleic acid-beeswax mixtures on mechanical, optical and water barrier properties of soy protein isolate based films. Journal of Food Engineering, 91, 509-515.

Monteiro A., Paquincha D., Martins F., Queirós R.P., Saraiva J.A., Švarc-Gajić J., Nastić N., Delerue-Matos C., Carvalho A.P. (2018). Liquid by-products from fish canning industry as sustainable sources of ω3 lipids. Journal of Environmental Management, 219, 9-17.

Moore G.P.R, Martelli S.M., Gandolfo C., Sobral P.J.A., Laurindo J.B. (2006). Influence of the glycerol concentration on some physical properties of feather keratin films. Food Hydrocolloids, 20, 975-982.

Moradi M., Tajik H., Rohani S.M.R., Mahmoudian A. (2016). Antioxidant and antimicrobial effects of zein edible film impregnated with *Zataria multiflora* Boiss. essential oil and monolaurin. LWT- Food Science and Technology, 72, 37-43.

Moreira M.M., Barroso M.F., Boeykens A., Withouck H., Morais S., Delerue-Matos C. (2017). Valorization of apple tree wood residues by polyphenols extraction: Comparison between conventional and microwave-assisted extraction. Industrial Crops and Products, 104, 210-220.

Moreira M.M., Barroso M.F., Porto J.V., Ramalhosa M.J., Švarc-Gajić J., Estevinho L., Morais S., Delerue-Matos C. (2018). Potential of Portuguese vine shoot wastes as natural resources of bioactive compounds. Science of the Total Environment, 634, 831-842.

Muhamad I.I., Hassan N.D., Mamat S.N.H., Nawi N.M., Rashid W.A., Tan N.A. (2017). Extraction technologies and solvents of phytocompounds from plant materials: physicochemical characterization and identification of ingredients and bioactive compounds from plant extract using various instrumentations. In: Grumezescu A.M., Holban A.M. (eds.). Handbook of food bioengineering. Academic Press, pp 523-560.

Muhamad I.I., Hassan N.D., Mamat S.N.H., Nawi N.M., Rashid W.A., Tan N.A. (2017). Extraction technologies and solvents of phytocompounds from plant materials: physicochemical characterization and identification of ingredients and bioactive

compounds from plant extract using various instrumentations. In: Grumezescu A.M. Holban A.M. (eds.). Handbook of food bioengineering. Academic Press, pp 523-560.

Murano E., Toffanin R., Zanetti F., Knutsen S. H., Paoletti S., Rizzo R. (1992). Chemical and macromolecular characterization of agar polymers from Gracilaria dura (*C agardh*) J agardh (*Gracilariaceae, Rhodophyta*). Carbohydrate Polymers, 18, 171-178.

Nata I.F., Wang S.S., Wu T., Lee C. (2012). Chitin nanofibrils for self-sustaining hydrogels preparation via hydrothermal treatment. Carbohydrate Polymers, 90, 1509-1514.

Nawab A., Alam F., Haq M.A., Lutfi Z., Hasnain A. (2017). Mango kernel starch-gum composite films: Physical, mechanical and barrier properties. International Journal of Biological Macromolecules, 98, 869-876.

Nayak A., Bhushan B., Rosales A., Turienzo L.R., Cortina J.L. (2018). Valorisation potential of Cabernet grape pomace for the recovery of polyphenols: Process intensification, optimisation and study of kinetics. Food and Bioproducts Processing, 109, 74-85.

Nayak B., Dahmoune F., Moussi K., Remini H., Dairi S., Aoun O., Khodir M. (2015). Comparison of microwave, ultrasound and accelerated-assisted solvent extraction for recovery of polyphenols from *Citrus sinensis* peels. Food Chemistry, 187, 507-516.

Niaounakis M. (2015). Biopolymers: Applications and trends, William Andrew.

Nogales-Bueno J., Baca-Bocanegra B., Rooney A., Hernández-Hierro J. M., Byrne H. J., Heredia F.J. (2017). Study of phenolic extractability in grape seeds by means of ATR-FTIR and Raman spectroscopy. Food Chemistry, 232, 602-609.

Noishiki Y., Takami H., Nishiyama Y., Wada M., Okada S., Kuga S. (2003). Inclusion Complex of β-Chitin and Aliphatic Amines. Biomacromolecules, 4, 896-899.

Norrahim M.N.F., Ariffin H., Hassan M.A., Ibrahim N.A., Nishida H. (2013). Performance evaluation and chemical recyclability of a polyethyelene(poly(3-hydroxybutyrate-co-3-hydroxyvalerate) blend for sustainable packaging. RSC Advance, 3, 24378-24388.

Nur Hanani Z.A., Beatty E., Roos Y.H., Morris M.A., Kerry J.P. (2012). Manufacture and characterization of gelatin films derived from beef, pork and fish sources using twin screw extrusion. Journal of Food Engineering, 113, 606-614.

Nur Hanani Z.A., McNamara J., Roos Y.H., Kerry J.P. (2013). Effect of plasticizer content on the functional properties of extruded gelatin-based composite films. Food Hydrocolloids, 31(2), 264-269.

Ogale A.A., Cunningham P., Dawson P.L., Acton J.C. (2000). Viscoelastic, thermal, and microstructural characterization of soy protein isolate films. Food Science, 65, 672-679.

Olejar K.J., Ray S., Kilmartin P.A. (2017). Utilisation of agro-waste extract in thermoplastics. International Journal of Nanotechnology, 14(1-6), 304-312.

Olejar K. J., Ray S., Ricci A., Kilmartin P.A. (2014). Superior antioxidant polymer films created through the incorporation of grape tannins in ethyl cellulose. Cellulose. 21, 4545-4556.

Olejar K.J., Vandermeer C., Kilmartin P.A. (2016). Grape tannins: Structure, antioxidant and antimicrobial activity. In: Combs, C.A. (ed.). Tannins. Biochemistry, food sources and nutritional properties. Nova Science Publishers, New York, pp 59-85.

Olivas G.I., Mattinson D.S., Barbosa-Cánovas G.V. (2007). Alginate coatings for preservation of minimally processed 'Gala' apples. Postharvest Biology and Technology, 45(1), 89-96.

Ortiz C.M., de Moraes J.O., Vicente A.R., Laurindo J.B., Mauri A.N. (2017) Scale-up of the production of soy (*Glycine max* L.) protein films using tape casting: Formulation of film-forming suspension and drying conditions. Food Hydrocolloids, 66, 110-117.

Otero P., Quintana S.E., Reglero G., Fornari T., García-Risco M.R. (2018). Pressurized Liquid Extraction (PLE) as an innovative green technology for the effective enrichment of galician algae extracts with high quality fatty acids and antimicrobial and antioxidant properties. Marine Drugs, 16(5), 156-170.

Otoni C.G., Avena-Bustillos J., Azeredo H.M.C., Lorevide M.V., Moura M.R., Mattoso L.H.C., McHugh T.H. (2017). Recent advances on edible films based on fruits and vegetables: A review. Comprehensive Reviews in Food Science and Food Safety, 16(5), 1151-1169.

Otoni C.G., Avena-Bustillos R.J., Olsen C.W., Bilbao-Sainz C., McHugh T.H. (2016). Mechanical and water barrier properties of isolated soy protein composite edible films

as affected by carvacrol and cinnamaldehyde micro and nanoemulsions. Food Hydrocolloids, 57, 72-79.

Ozcalik O., Tihminlioglu F. (2013). Barrier properties of corn zein nanocomposite coated polypropylene films for food packaging applications. Journal of Food Engineering, 114(4), 505-513.

Pan H., Jiang B., Chen J., Jin Z. (2014). Blend-modification of soy protein/lauric acid edible films using polysaccharides. Food Chemistry, 151, 1-6.

Park H.J., Byun Y.J., Kim Y.T., Whiteside W.S., Bae H.J. (2014). Processes and applications for edible coating and film materials from agropolymers. In: Han J.H. (ed.). Innovation in food packaging. Academic Press, UK, pp 257-275.

Patel S., Srivastava S., Singh M.R., Singh D. (2018). Preparation and optimization of chitosan-gelatin films for sustained delivery of lupeol for wound healing. International Journal of Biological Macromolecules, 107, 1888-1897.

Pena-Pereira F., Tobiszewski M. (2017). The application of green solvents in separation processes, Elsevier.

Pena-Serna C., Penna A.L.B., Lopes Filho J.F. (2016). Zein-based blend coating: Impact on the quality of a model cheese of short ripening period. Journal of Food Engineering, 171, 208-213.

Périno S., Pierson J.T., Ruiz K., Cravotto G., Chemat F. (2016). Laboratory to pilot scale: Microwave extraction for polyphenols lettuce. Food Chemistry, 204, 108-114.

Phan The D., Debeaufort F., Voilley A., Luu D. (2009). Biopolymer interactions affect the functional properties of edible films based on agar, cassava starch and arabinoxylan blends. Journal of Food Engineering, 90, 548-558.

Pinheiro J.C., Alegria C.S., Abreu M.M., Gonçalves E.M., Silva C.L. (2016). Evaluation of alternative preservation treatments (water heat treatment, ultrasounds, thermosonication and UV-c radiation) to improve safety and quality of whole tomato. Food and Bioprocess Technology, 9(6), 924-935.

Pommet M., Redl A., Guilbert S., Morel M.H. (2005). Intrinsic influence of various plasticizers on functional properties and reactivity of wheat gluten thermoplastic materials. Journal of Cereal Science, 42(1), 81-91.

Pongmalai P., Devahastin S., Chiewchan N., Soponronnarit S. (2015). Enhancement of microwave-assisted extraction of bioactive compounds from cabbage outer leaves via the application of ultrasonic pretreatment. Separation and Purification Technology, 144, 37-45.

Preece K.E., Hooshyar N., Zuidam N.J. (2017). Whole soybean protein extraction processes: A review. Innovative Food Science and Emerging Technologies, 43, 163-172.

Prietto L., Mirapalhete T.C., Pinto V.Z., Hoffmann J.F., Vanier N.L., Lim L.T., Dias A.R.G., da Rosa Zavareze E. (2017). pH-sensitive films containing anthocyanins extracted from black bean seed coat and red cabbage. LWT- Food Science and Technology, 80, 492-500.

Pudziuvelyte L., Jakštas V., Ivanauskas L., Laukevičienė A.,. Ibe C.F.D, Kursvietiene L., Bernatoniene J. (2018). Different extraction methods for phenolic and volatile

compounds recovery from Elsholtzia ciliata fresh and dried herbal materials. Industrial Crops and Products, 120, 286-294.

Qazanfarzadeh Z., Kadivar M. (2016). Properties of whey protein isolate nanocomposite films reinforced with nanocellulose isolated from oat husk. International Journal of Biological Macromolecules, 91, 1134-1140.

Qu P., Huang H., Wu G., Sun E., Chang Z. (2015). Effects of hydrolysis degree of soy protein isolate on the structure and performance of hydrolyzed soy protein isolate/urea/formaldehyde copolymer resin. Journal of Applied Polymer Science, 132, 41469-41477.

Ragusa A., Centonze C., Grasso M.E., Latronico M.F., Mastrangelo P.F., Sparascio F.,Fanizzi F.P., Maffia M. (2017). A comparative study of phenols in Apulian Italian Wines. Food. 6(4), 24-34.

Raja I.S., Fathima N.N. (2015). A gelatin based antioxidant enriched biomaterial by grafting and saturation: Towards sustained drug delivery from antioxidant matrix. Colloids and Surfaces B: Biointerfaces, 128, 537-543.

Rasines-Perea Z., Teissedre P.-L. (2017). Grape polyphenols' effects in human cardiovascular diseases and diabetes. Molecules. 22(1), 68-87.

Reddy N. (2015). Non-food industrial applications of poultry feathers. Waste Management, 45, 91-107.

Ren H.M., Cai C., Leng C.B., Pang S.F., Zhang Y.H. (2016). Nucleation kinetics in mixed $NaNO_3$/glycerol droplets investigated with the FTIR-ATR technique. Journal of Physical Chemistry B, 120, 2913-2920.

Rezaei M., Motamedzadegan A. (2015). The effect of plasticizers on mechanical properties and water vapor permeability of gelatin-based edible films containing clay nanoparticles. World Journal of Nanoscience and Engineering, 5(04), 178-193.

Rhim J.W., Mohanty K.A., Singh S.P., Ng P.K.W. (2006). Preparation and properties of biodegradable multilayer films based on soy protein isolate and poly(lactide). Industrial and Engineering Chemistry Research, 45, 3059-3066.

Rhim J.W., Wang L.F., Hong S.I. (2013). Preparation and characterization of agar/silver nanoparticles composite films with antimicrobial activity. Food Hydrocolloids, 33, 327-335.

Rocha C.M.R., Souza H.K.S., Magalhães N.F., Andrade C.T., Gonçalves M.P. (2014). Rheological and structural characterization of agar/whey proteins insoluble complexes. Carbohydrate Polymers, 110, 345-353.

Rodrigues I.M., Coelho J.F.J., Carvalho M.G.V.S. (2012). Isolation and valorisation of vegetable proteins from oilseed plants: Methods, limitations and potential. Journal of Food Engineering, 109(3), 337-346.

Rombouts I., Lamberts L., Celus I., Lagrain B., Brijis K., Delcour J.A. (2009). Wheat gluten amino acid composition analysis by high-performance anion-exchange chromatography with integrated pulsed amperometric detection. Journal of Chromatography A, 1216(29), 5557-5562.

Ruiz-Aceituno L., García-Sarrió M.J., Alonso-Rodriguez B., Ramos L., Sanz M.L. (2016). Extraction of bioactive carbohydrates from artichoke (*Cynara scolymus* L.) external bracts using microwave assisted extraction and pressurized liquid extraction. Food Chemistry, 196, 1156-1162.

Ruiz-Ruiz F., Mancera-Andrade E.I., Iqbal H.M.N. (2017). Marine-derived bioactive peptides for biomedical sectors: A review. Protein and Peptide Letters, 24(2), 109-117.

Saberi B., Vuong Q.V., Chockchaisawasdee S., Golding J.B., Scarlett C.J., Stathopoulos C.E. (2017). Physical, barrier and antioxidant properties of pea starch-guar gum biocomposite edible films by incorporation of natural plant extracts. Food and Bioprocess Technology, 10(12), 2240-2250.

Saha S., Kurade M.B., El-Dalatony M.M., Chatterjee P.K., Lee D.S., Jeon B.H. (2016). Improving bioavailability of fruit wastes using organic acid: An exploratory study of biomass pretreatment for fermentation. Energy Conversion and Management, 127, 256-264.

Sahraee S., Milani J.M., Ghanbarzadeh B., Hamishehkar H. (2017). Effect of corn oil on physical, thermal, and antifungal properties of gelatin-based nanocomposite films containing nano chitin. LWT - Food Science and Technology, 76, 33-39.

Salacha M.I., Kallithraka S., Tzourou I. (2008). Browning of white wines: correlation with antioxidant characteristics, total polyphenolic composition and flavanol content. International Journal of Food Science and Technology, 43, 1073-1077.

Salazar M., Costa J.V., Urbina G.R.O., Cunha V.M.B., Silva M., do Nascimento Bezerra P., Pinheiro W., Gomes-Leal W., Lopes A.S., Junior R.C. (2018). Chemical composition, antioxidant activity, neuroprotective and anti-inflammatory effects of cipó-pucá (*Cissus sicyoides* L.) extracts obtained from supercritical extraction. Journal of Supercritical Fluids, 138, 36-45.

Samsalee N., Sothornvit R. (2017). Modification and characterization of porcine plasma protein with natural agents as potential cross-linkers. International Journal of Food Science and Technology, 52(4), 964-971.

Sánchez-Camargo A., Mendiola J., Valdés A., Castro-Puyana M., García-Cañas V., Cifuentes A., Herrero M., Ibáñez E. (2016). Supercritical antisolvent fractionation of rosemary extracts obtained by pressurized liquid extraction to enhance their antiproliferative activity. Journal of Supercritical Fluids, 107, 581-589.

Sandoval-Ventura O., Olguin-Contreras L.F., Cañizares-Macias M.P. (2017). Total polyphenols content in white wines on a microfluidic flow injection analyzer with embedded optical fibers. Food Chemistry, 221, 1062-1068.

Santos Ê.R., Oliveira H.N., Oliveira E.J., Azevedo S.H., Jesus A.A., Medeiros A.M., Dariva C., Sousa E.M. (2017). Supercritical fluid extraction of *Rumex Acetosa* L. roots: Yield, composition, kinetics, bioactive evaluation and comparison with conventional techniques. Journal of Supercritical Fluids, 122, 1-9.

Santos T.M., Souza Filho M.D.S.M., Muniz C.R., Morais J.P.S., Kotzebue L.R.V., Pereira A.L.S., Azeredo H.M.C. (2017). Zein films with unoxidized or oxidized tannic acid. Journal of the Science of Food and Agriculture, 97(13), 4580-4587.

Sardella F., Gimenez M., Navas C., Morandi C., Deiana C., Sapang K. (2015). Conversion of viticultural industry wastes into activated carbons for removal of lead and cadmium. Journal of Environmental Chemistry Engineering, 3(1), 253-260.

Schaefer J., Kramer K.J., Garbow J.R., Jacob G.S., Stejskal E.O., Hopkins T.L., Speirs R.D. (1987). Aromatic cross-links in insects cuticle: Detection by solid-state ^{13}C and ^{15}N NMR. Science, 235, 1200-1204.

Schmid M., Krimmel B., Grupa U., Noller K. (2014). Effects of thermally induced denaturation on technological-functional properties of whey protein isolate-based films. Journal of Dairy Science, 97(9), 5315-5327.

Schmidt V., Giacomelli C., Soldi V. (2005). Thermal stability of films formed by soy protein isolate-sodium dodecyl sulfate. Polymer Degradation and Stability, 87, 25-31.

Setyaningsih W., Saputro I., Palma M., Barroso C. (2015). Optimisation and validation of the microwave-assisted extraction of phenolic compounds from rice grains. Food Chemistry, 169, 141-149.

Sharma K., Jain R., Bhargava N., Sharma R., Sharma K.S. (2010). Dielectric studies of wheat in powder from at microwave frequencies. Indian Journal of Experimental Biology, 47, 1002-1007.

Sharma L., Singh C. (2016). Sesame protein based edible films: Development and characterization. Food Hydrocolloids, 61, 139-147.

Sharma N., Khatkar B.S., Kaushik R., Sharma P., Sharma R. (2017). Isolation and development of wheat based gluten edible film and its physicochemical properties. International Food Research Journal, 24(1), 94-101.

Shirsath S., Sable S., Gaikwad S., Sonawane S., Saini D., Gogate P. (2017). Intensification of extraction of curcumin from Curcuma amada using ultrasound assisted approach: Effect of different operating parameters. Ultrasonic Sonochemistry, 38, 437-445.

Shukla R., Cheryan M. (2001). Zein: the industrial protein from corn. Industrial Crops and Products, 13(3), 171-192.

Siró I., Plackett D., Sommer-Larsen P. (2010). A comparative study of oxygen transmission rates through polymer films base on fluorescence quenching. Packaging Technology and Science, 23, 301-315

Smiderle F.R., Morales D., Gil-Ramírez A., de Jesus L.I., Gilbert-López B., Iacomini M., Soler-Rivas C. (2017). Evaluation of microwave-assisted and pressurized liquid extractions to obtain β-d-glucans from mushrooms. Carbohydrate Polymers, 156, 165-174.

Snyder Y., Strauss H.L., Elllger C.A. (1982). Carbon-hydrogen stretching modes and the structure of n-alkyl chains. 1. Long, disordered chains. Journal of Physical Chemistry, 86, 5145-5150.

Socaci S.A., Rugină D.O., Diaconeasa Z.M., Pop O.L., Fărcaş A.C., Păucean A., Tofană M., Pintea A. (2017). Antioxidant compounds recovered from food wastes. In: Chavarri M. (ed). Functional food-improve health through adequate food, DOI: 10.5772/intechopen.69124.

Song C.L., Zhao X.H. (2014). Structure and property modification of an oligochitosan-glycosylated and crosslinked soybean protein generated by microbial transglutaminase. Food Chemistry, 16, 114-119.

Song Y., Zheng Q. (2014). Ecomaterials based on food proteins and polysaccharides. Polymer Reviews, 54, 514-571.

Sousa-Gallagher M.J., Tank A., Sousa R. (2016). Emerging technologies to extend the shelf life and stability. In: Subramaniam P., Wareing P. (eds). The stability and shelf life of food. Woodhead Publishing, UK, pp 399-424.

Spigno G., Marinoni L., Garrido G.D. (2017). State of the art in grape processing by-products. In: Galanakis C.M. (ed.). Handbook of grape processing by-products: Sustainable solutions, Academic Press, pp 1-28.

Su J.F., Huang Z., Yang C.M. and Yuan X.Y. (2008). Properties of soy protein isolate/poly(vinyl alcohol) blend "green" films: compatibility, mechanical properties, and thermal stability. Journal of Applied Polymer Science, 110, 3706-3716.

Su J.F., Huang Z., Yang C.M., Yuan X.Y. (2008). Properties of soy protein isolate/ poly(vinyl alcohol) blend ''green'' films: compatibility, mechanical properties, and thermal stability. Journal of Applied Polymer Science, 110, 3706-3716.

Su J.F., Yuan X.Y., Huang Z., Wang X.Y., Lu X.Z., Zhang L.D., Wang S.B. (2012). Physicochemical properties of soy protein isolate/carboxymethyl cellulose blend films crosslinked by Maillard reactions: Color, transparency and heat-sealing ability. Materials Science and Engineering Part C, 32, 40-46.

Sui C., Zhang W., Ye F., Liu X., Yu G. (2016). Preparation, physical and mechanical properties of soy protein isolate/guar gum composite films prepared by solution casting. Journal of Applied Polymer Science, 133(18), 43375-43381.

Sumere B.R., de Souza M.C., dos Santos M.P., Bezerra R.M.N., da Cunha D.T., Martinez J., Rostagno M.A. (2018). Combining pressurized liquids with ultrasound to improve the extraction of phenolic compounds from pomegranate peel (Punica granatum L.). Ultrasonic Sonochemistry, 48, 151-162.

Tanada-Palmu P., Helén H., Hyvönen L. (2000). Preparation, properties and applications of wheat gluten edible films. Agricultural and Food Science, 9, 23-35.

Tanase C.E., Spiridon, I. (2014). PLA/chitosan/keratin composites for biomedical applications. Materials Science and Engineering: C, 40, 242-247.

Tansaz S., Boccaccini A.R. (2016). Biomedical applications of soy protein: A brief overview. Journal of Biomedical Materials Research Part A, 104, 553-569.

TAPPI 211 om-02. (2002). Ash in wood, pulp, paper and paperboard: Combustion at 525 °C. In: TAPPI Standard methods. Atlanta, Tappi press.

Tatara R.A. (2017). Compression molding. In: Kutz M. (ed.). Applied plastics engineering handbook, processing, materials, and applications (2nd edition). William Andrew, USA, pp 291-320.

Thammahiwes S., Riyajan S.A., Kaewtatip K. (2017). Preparation and properties of wheat gluten based bioplastics with fish scale. Journal of Cereal Science, 75, 186-191.

Tian H., Wu W., Guo G., Gaolum B., Jia Q., Xiang A. (2012). Microstructure and properties of glycerol plasticized soy protein plastics containing castor oil. Journal of Food Engineering 109, 496-500.

Tian H., Xu G., Yang B., Guo G. (2011). Microstructure and mechanical properties of soy protein/agar blend films: Effect of composition and processing methods. Journal of Food Engineering, 107, 21-26.

Tian H., Xu G., Yang B., Guo G. (2011). Microstructure and mechanical properties of soy protein/agar blend films: Effect of composition and processing methods. Journal of Food Engineering, 107, 21-26.

Tian H., Xu G., Yang B., Guo G. (2011). Microstructure and mechanical properties of soy protein/agar blend films: Effect of composition and processing methods. Journal of Food Engineering, 107, 21-26

Timilsena Y.P., Adhikari R., Barrow C.J., Adhikari B. (2016). Physicochemical and functional properties of protein isolate produced from Australian chia seeds. Food Chemistry, 212, 648-656.

Tirado D.F., Tenorio M.J., Cabañas A., Calvo L. (2018). Prediction of the best cosolvents to solubilise fatty acids in supercritical CO_2 using the Hansen solubility theory. Chemical Engineering Science, 190, 14-20.

Tiwari B.K. (2015). Ultrasound: A clean, green extraction technology. TrAC- Trends in Analytical Chemistry, 71, 100-109.

Toaldo I.M., Fogolari O., Pimentel G. C., de Gois J.S., Borges D.L.G., Caliari V., Bordignon-Luiz M. (2013). Effect of grape seeds on the polyphenol bioactive content and elemental composition by ICP-MS of grape juices from *Vitis labrusca* L. LWT-Food Science and Technology, 53(1), 1-8.

Tongnuanchan P., Benjakul S., Prodpran T. (2012). Properties and antioxidant activity of fish skin gelatin film incorporated with citrus essential oils. Food Chemistry, 134(3), 1571-1579.

Tongnuanchan P., Benjakul S., Prodpran T., Pisuchpen S., Kazufumi O. (2016). Mechanical, thermal and heat sealing properties of fish skin gelatin film containing palm oil and basil essential oil with different surfactants. Food Hydrocolloids, 56, 93-107.

Tournour H.H., Segundo M.A., Magalhães L.M., Barreiros L., Queiroz J., Cunha L.M. (2015). Valorization of grape pomace: Extraction of bioactive phenolics with antioxidant properties. Industrial Crops and Products, 74, 397-406.

Trezza T.A., Krochta J.M. (2000). The gloss of edible coatings as affected by surfactants, lipids, relative humidity, and time. Journal of Food Science, 65, 658-662.

Tsuda Y., Nomura Y. (2014). Properties of alkaline-hydrolyzed waterfowl feather keratin. Animal Science Journal, 85, 180-185.

Türe H., Gällstedt M., Hedenqvist M.S. (2012). Antimicrobial compression-moulded wheat gluten films containing potassium sorbate. Food Research International, 45(1), 109-115.

Ünalan I.U., Arcan I., Korel F., Yemenicioğlu A. (2013). Application of active zein-based films with controlled release properties to control *Listeria monocytogenes* growth and lipid oxidation in fresh Kashar cheese. Innovative Food Science and Emerging Technologies, 20, 208-214.

USDA, 2018. United States Department of Agriculture. World agricultural production Available at: https://www.fas.usda.gov/data/world-agricultural-production. Accessed 26 November 2018.

Usov A.I., Ivaniva E.G., Shashkov A.S. (1983). Polysaccharides of algae XXXIII: Isolation and ^{13}C-NMR spectral study of some new gel forming polysaccharides from japan sea red seaweeds. Botanica Marina, 26, 285-294.

Ustunol Z. (2009). Edible films and coatings for meat and poultry. In: Huber K.C., Embuscado M.E. (eds.). Edible films and coatings for food applications. Springer, USA, pp 245-268.

Vajic U.J., Grujic-Milanovic J., Zivkovic J., Savikin K., Godevac D., Miloradovic Z., Bugarski B., Mihailovic-Stanojevic N. (2015). Optimization of extraction of stinging nettle leaf phenolic compounds using response surface methodology. Industrial Crops and Products, 74, 912-917.

Valdés A., Vidal L., Beltran A., Canals A., Garrigós M.C. (2015). Microwave-assisted extraction of phenolic compounds from almond skin byproducts (*prunus amygdalus*): A multivariate analysis approach. Journal of Agricultural and Food Chemistry, 63(22), 5395-5402.

Vardanega R., Carvalho P.I., Santos D.T., Meireles M.A.A. (2017). Obtaining prebiotic carbohydrates and beta-ecdysone from Brazilian ginseng by subcritical water extraction, Innov. Food Science and Emerging Technologies, 42, 73-82.

Verbeek C.J.R., van den Berg L.E. (2010). Extrusion processing and properties of protein-based thermoplastics. Macromolecular Materials and Engineering, 295(1), 10-21.

Viganó J., Zabot G.L., Martínez J. (2017). Supercritical fluid and pressurized liquid extractions of phytonutrients from passion fruit by-products: economic evaluation of sequential multi-stage and single-stage processes. Journal of Supercritical Fluids, 122, 88-98.

Vignon M.R., Rochas C., Vuong R., Tekely P., Chanzy H. (1994). Gelidium sesquipedale (*Gelidiales, Rhodophyta*) II. An ultrastructural and morphological study. Botanica Marina, 37, 331-340.

Villalobos R., Chanona J., Hernández P., Gutiérrez G., Chiralt A. (2005). Gloss and transparency of hydroxypropyl methylcellulose films containing surfactants as affected by their microstructure. Food Hydrocolloids, 19, 53-61.

Visakh P.M., Nazarenko O. (eds.). (2017). Soy Protein-Based Blends, Composites and Nanocomposites. John Wiley & Sons, UK.

Visschers R.W., de Jongh H.H.J. (2005). Disulphide bond formation in food protein aggregation and gelation. Biotechnology Advances, 23, 75-80.

Vogles E. (1998). Structure and reactivity of water at biomaterial surfaces. Advances in Colloid and Interface Science, 74, 69-117.

Wang H., Hu D., Ma Q., Wang L. (2016). Physical and antioxidant properties of flexible soy protein isolate films by incorporating chestnut (*Castanea mollissima*) bur extracts. LWT- Food Science and Technology, 71, 33-39.

Wang H., Wang L. (2017). Developing a bio-based packaging film from soya by-products incorporated with valonea tannin. Journal of Cleaner Production, 143, 624-633.

Wang J., Qian W., He Y., Xiong Y., Song P., Wang R.-M. (2017a). Reutilization of discarded biomass for preparing functional polymer materials. Waste Management, 65, 11-21.

Wang K., Li M., Wen X., Chen X., He Z., Ni Y. (2018a). Optimization of ultrasound-assisted extraction of okra (Abelmoschus esculentus (L.) Moench) polysaccharides based on response surface methodology and antioxidant activity. Intustrial Journal of Biological Macromolecules, 114, 1056-1063.

Wang K., Xie X., Zhang Y., Huang Y., Zhou S., Zhang W., Lin Y., Fan H. (2018c). Combination of microwave-assisted extraction and ultrasonic-assisted dispersive liquid-liquid microextraction for separation and enrichment of pyrethroids residues in Litchi fruit prior to HPLC determination. Food Chemistry, 240, 1233-1242.

Wang L., Boussetta N., Lebovka N., Vorobiev E. (2018b). Selectivity of ultrasound-assisted aqueous extraction of valuable compounds from flesh and peel of apple tissues. LWT- Food Science and Technology, 93, 511-516.

Wang S., Marcone M., Barbut S., Lim L.T. (2012). The impact of anthocyanin-rich red raspberry extract (ARRE) on the properties of edible soy protein isolate (SPI) film. Journal of Food Science, 77(4), 497-505.

Wang S.Y., Zhu B.B., Li D.Z., Fu X.Z., Shi L. (2012). Preparation and characterization of TiO_2/SPI composite film. Material Letters, 83, 42-45.

Wang X.J., Zheng X.Q., Liu X.L., Kopparapu N.K., Cong W.S., Deng Y.P. (2017c) Preparation of glycosylated zein and retarding effect on lipid oxidation of ground pork. Food Chemistry, 227, 335-341.

Wang Z., Hu S., Gao Y., Ye C., Wang H. (2017b). Effect of collagen-lysozyme coating on fresh-salmon fillets preservation. LWT-Food Science and Technology, 75, 59-64.

Wang Z., Zhou J., Wang X., Zhang N., Sun X., Ma Z. (2014). The effects of ultrasonic/microwave assisted treatment on the water vapor barrier properties of soybean protein isolate-based oleic acid/stearic acid blend edible films. Food Hydrocolloids, 35, 51-58.

Ward G., Nussinovitch A. (1997). Characterizing the gloss properties of hydrocolloid films. Food Hydrocolloids, 11, 357-365.

Ward G., Nussinovitch A. (2017). Characterizing the gloss properties of hydrocolloid films. Food Hydrocolloids, 11, 357-365.

Wihodo M., Moraru C.I. (2013). Physical and chemical methods used to enhance the structure and mechanical properties of protein films: A review. Journal of Food Engineering, 114, 292-302.

Wu T., Dai S., Cong X., Liu R., Zhang M. (2017c). Succinylated soy protein film coating extended the shelf life of apple fruit. Journal of Food Processing and Preservation, 41(4), 13024-13034.

Xia C., Wang L., Dong Y., Zhang S., Shi S.Q., Cai L., Li J. (2015). Soy protein isolate-based films cross-linked by epoxidized soybean oil. RSC Advances, 5(101), 82765-82771.

Xu D.-P., Zheng J., Zhou Y., Li Y., Li S., Li H.-B. (2017). Ultrasound-assisted extraction of natural antioxidants from the flower of Limonium sinuatum: Optimization and comparison with conventional methods. Food Chemistry, 217, 552-559.

Xu F., Dong Y., Zhang W., Zhang S., Li L., Li J. (2015). Preparation of cross-linked soy protein isolate-based environmentally-friendly films enhanced by PTGE and PAM. Industrial Crops and Products, 67, 373-380.

Xu H., Chai Y., Zhang G. (2012). Synergistic effect of oleic acid and glycerol on zein film plasticization. Journal of Agricultural and Food Chemistry, 60(40), 10075-10081.

Xu J., McCarthy S.P., David R.A.G, Kaplan L. (1996). Chitosan film acylation and effects on biodegradability. Macromolecules, 29, 3436-3440.

Yan W., Zhou J., Sun M., Chen J., Hu J., Shen B. (2014). The construction of an amino acid network for understanding protein structure and function. Amino acids, 46(6), 1419-1439.

Yemenicioğlu A. (2016). Zein and its composites and blends with natural active compounds: development of antimicrobial films for food packaging. In: Barros-Velazquez J (ed.). Antimicrobial food packaging. Elsevier Inc, Netherlands, pp 503-513.

Yemiş G.P., Candoğan K. (2017). Antibacterial activity of soy edible coatings incorporated with thyme and oregano essential oils on beef against pathogenic bacteria. Food Science and Biotechnology, 26(4), 1113-1121.

Yin X.C., Li F.Y., He Y.F., Wang Y., Wang R.M. (2013). Study on effective extraction of chicken feather keratins and their films for controlling drug release. Biomaterial Science, 1, 528-536.

Younes I., Rinaudo M. (2015). Chitin and chitosan preparation from marine sources. Structure, properties and applications. Marine Drugs, 13, 1133-1174.

Yu Z., Sun L., Wang W., Wang W., Zeng W., Mustapha A., Li M. (2018). Soy protein-based films incorporated with cellulose nanocrystals and pine needle extract for active packaging. Industrial Crops and Products, 112, 412-419.

Zárate-Ramírez L.S., Romero A., Bengoechea C., Partal P., Guerrero A. (2014). Thermo-mechanical and hydrophilic properties of polysaccharide/gluten-based bioplastics. Carbohydrate Polymers, 112, 24-31.

Zárate-Ramírez L.S., Romero A., Bengoechea C., Partal P., Guerrero A. (2014). Thermo-mechanical and hydrophilic properties of polysaccharide/gluten-based bioplastics. Carbohydrate Polymers, 112, 24-31.

Zema L., Loreti G., Melocchi A., Maroni A., Gazzaniga A. (2012). Injection molding and its application to drug delivery. Journal of Controlled Release, 159(3), 324-331.

Zeng X., Duan Y., Zhe W., Jiang J., He L., Wang S., Wang M. (2013). Edible coating based on soy protein to improve shelf life and overall quality of minimally processed jujubes. Journal of Food, Agriculture and Environment, 11(3-4), 263-269.

Zhang B., Zhang Y., Dreisoerner J., Wei Y. (2015). The effects of screw configuration on the screw fill degree and special mechanical energy in twin-screw extruder for high-moisture texturised defatted soybean meal. Journal of Food Engineering, 157, 77-83.

Zhang Y., Cui L., Che X., Zhang H., Shi N., Li C., Chen Y., Kong W. (2015b). Zein-based films and their usage for controlled delivery: Origin, classes and current landscape. Journal of Controlled Release, 206, 206-219.

Zhang Y.B., Wang J.W., Jiang J., Li Y.X. (2013). Antimicrobial activity of soy protein isolate-essential oil monomers edible composite films for chilled pork preservation. Advanced Materials Research,726, 638-641.

Zhang B., Yang, R., Liu C.-Z. (2008). Microwave-assisted extraction of chlorogenic acid from flower buds of *Lonicera japonica Thunb*. Separation and Purification Technology, 62(2), 480-483.

Zhao X., Chen J., Zhu Q., Du F., Ao Q., Liu J. (2011). Surface characterization of 7S and 11S globulin by X-ray photoelectron spectroscopy and scanning electron microscopy. Colloids and Surfaces B: Biointerfaces, 86, 260-266.

Zhao X., Zhu H., Zhang G., Tang W. (2015). Effect of superfine grinding on the physicochemical properties and antioxidant activity of red grape pomace powders. Powder Technology, 286, 838-844.

Zhong Y., Cavender G., Zhao Y. (2014). Investigation of different coating application methods on the performance of edible coatings on Mozzarella cheese. LWT-Food Science and Technology, 56(1), 1-8.

Zink J., Wyrobnik T., Prinz T., Schmid M. (2016). Physical, chemical and biochemical modifications of protein-based films and coating: An extensive review. International journal of Molecular Science, 17(9), 1376-1421.

Zoecklein B.W., Fugelsang K.C., Gump B.H., Nury F.S. (1995). Wine analysis and production, Chapman and Hall, New York.

Zubeldía F., Ansorena M.R., Marcovich N.E. (2015). Wheat gluten films obtained by compression molding. Polymer Testing, 43, 68-77.

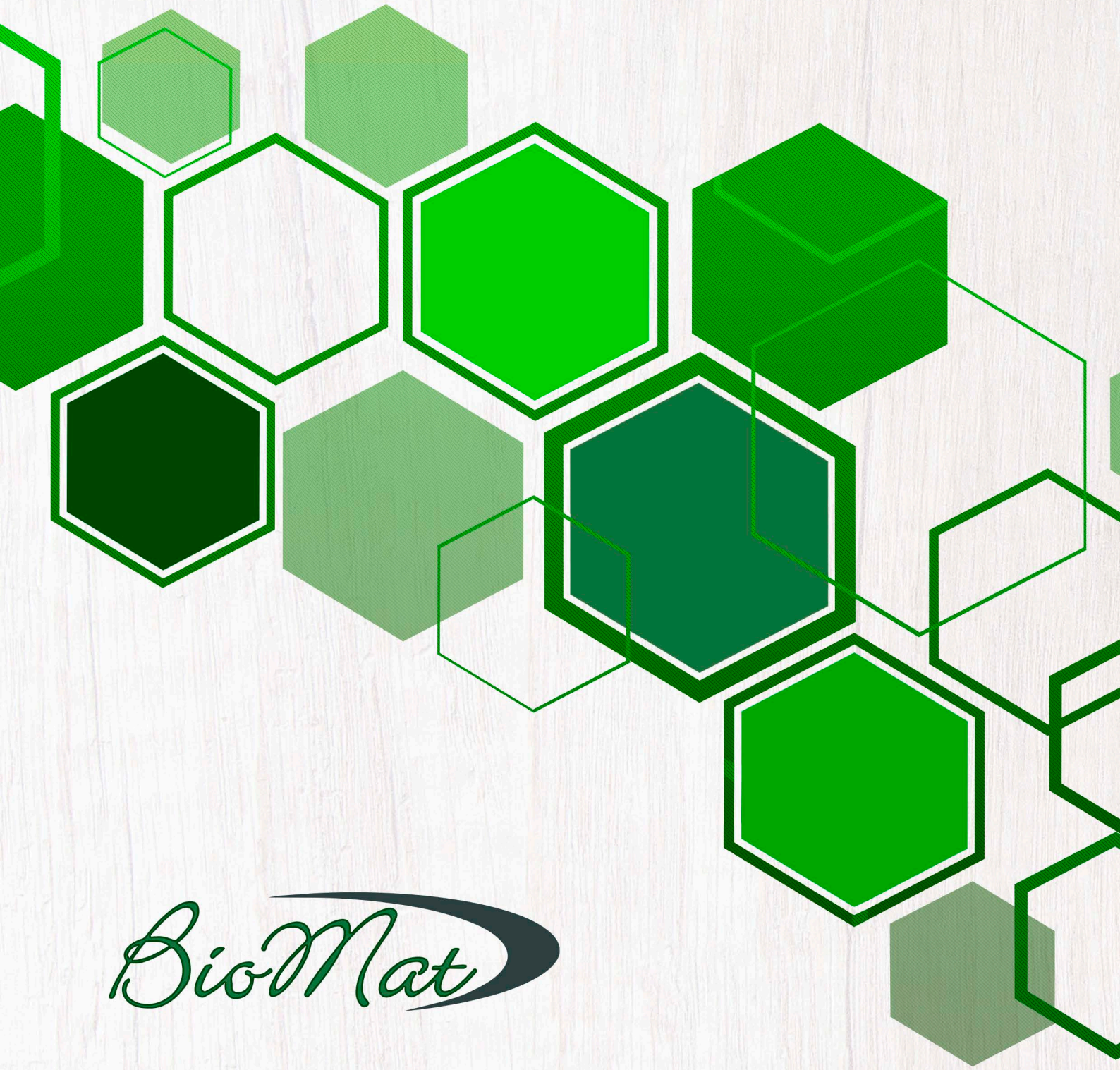
BioMat